Signalling pathways involved in cancer cell migration towards CXCL8 and CXCL10

Enana Alassaf

A thesis presented for the degree of Doctor of Philosophy at the University of East Anglia, School of Pharmacy

July 2020

Abstract

Aim: Chemokines are signalling molecules that mediate the migration of immune cells and are involved in tumour progression, invasion, and metastasis. CXCL8 and CXCL10 are responsible for the recruitment and activation of leukocytes to the site of inflammation. The aberrant expression of CXCL8 or CXCL10 and their receptors was identified in multiple cancer types where they contribute towards cancer progression. The aim of this thesis was to characterise the role of these two chemokines in cancer cell migration and associated cellular morphological changes, as well as identifying the main signalling pathways involved in these processes, which could be utilized as desirable targets for therapeutic intervention to prevent cancer progression.

Methodology: To investigate the migratory effect of CXCL8 and CXCL10 on cancer cell lines, several migration assays were used, such as time-lapse imaging, chemotaxis, wound healing, and Boyden chamber. The expression of the correspondent receptors of both chemokines was observed using immunofluorescence assay. To investigate the downstream signalling pathways involved in the chemokine-induced migration and cytoskeleton rearrangement, a number of small molecule inhibitors were used. The effect on the release of intracellular calcium was also assessed for some of the inhibitors.

Results: We identified a role of CXCL8 and CXCL10 signalling in the migration of THP-1, MDA-MB231, PC3 and MCF-7 cells. Using small molecule inhibitors to target signalling molecules revealed a difference in the pathways utilised by CXCL8 to induce migration in the two cell lines: PC3 and MDA-MB231 cells. The major signalling pathways investigated are Pi3K/AKT, Raf/Rac/MEK/ERK, DOCK1/2/5, FAK/Src, Arp2/3, PKA, PKC, PKD, and β-catenin. Inhibitors like LY294002, AKTi, ZM336372, SL327, PD89059, BS203580, EHT1864, CPYPP, PF562271, Bosutinib, CK666, CID755673 can inhibit the migration of both MDA-MB231 and PC3 cells which could be further investigated as universal inhibitors. Other inhibitors like L779450, FH535, and H89 were cell-type specific. Furthermore, the effect of PKC on the migration and cytoskeleton rearrangement was cell-type and chemokine specific.

Conclusion: In this thesis we confirmed the migratory effect both CXCL8 and CXCL10 have on different cancer cell lines. The signalling pathways involved in the chemokine-induced migration varied between the cell lines. These potential signalling molecules that were identified require further investigation to establish their vitality as potential cancer treatment.

Acknowledgments

I would like to express my gratitude to my Ph.D. supervisor Prof Anja Mueller for her guidance, encouragement, and continuous pat on the back. I would also like to acknowledge my second supervisor, Dr Derek Warren, for his input and his enthusiastic ideas for my research. In addition, Dr Monica Malik is warmly thanked for funding part of my research, and for always having great conversations. Likewise thank you to UEA for providing me with a scholarship to carry on my Ph.D.

My sincere wishes are extended to Dr Gerald Keil, Dr Poh Hui Goh, Dr Isabel Hamshaw, Dr Nursabah Atli, Dr Sultan Ahmed, and Wing Yee Lai for their help during my time in the lab, and for their knowledge, friendliness, and inspiration. Special thanks to Dr Stefan Bidula, Dr Isabel Hamshaw, Dr Gerald Keil, and Dr Saurabh Prabhu for the time and effort they put to proofread my thesis. Furthermore, my dearest friends at UEA and in Norwich, thank you for helping me settle in the UK and for always being there.

The fulfilment of this research would have not been possible without my very amazing family who not only supported me through every step in my life but also fully believed in me. Thank you so incredibly much for your love and care baba, mama, Farah, Marah, Yazen and Soumar.

Publication

Alassaf, E. and Mueller, A., 2020. The role of PKC in CXCL8 and CXCL10 directed prostate, breast and leukemic cancer cell migration. *European Journal of Pharmacology*, 886, p.173453.

Abbreviations

7TMR	Seven transmembrane receptors
AC	Adenylyl cyclase
ADP	Adenosine diphosphate
ANOVA	Analysis of variance
Arp2/3	Actin-related proteins-2/3
AP-1	Activator protein 1
ATCC	American Type Culture Collection
ATP	Adenosine triphosphate
BSA	Bovine serum albumin
Ca^{2+}	Calcium ions
CHO	Chinese hamster ovary cells
CO_2	Carbon dioxide
c-Src	Cellular sarcoma non-receptor tyrosine kinase
CTX	Chemotaxis
CXCL	C-X-C motif chemokine ligand
CXCR	C-X-C motif chemokine receptor
DAPI	4',6-diamidino-2-phenylindole
DAG	Diacylglycerol
DMEM	Dulbecco's modified Eagle's medium
DMSO	Dimethyl sulfoxide
DOCK	Dedicator of cytokinesis
DPX	*p*-xylene-bis-pyridinium bromide
EC_{50}	Concentration at which 50% of an effect occurs
EDTA	Ethylenediaminetetraacetic acid
EGF	Epidermal growth factor
EGFP	Enhanced green fluorescent protein
EGFP	Epidermal growth factor receptor
ECM	Extracellular matrix
EMT	Epithelial to mesenchymal transition
ER	Endoplasmic reticulum
ERK	Extracellular signal-regulated kinase
FAK	Focal adhesion kinase
FCS	Foetal calf serum

FDA	Food and Drug Administration
G_{α}	G-Protein α subunit
$G_{\beta\gamma}$	G-Protein βγ subunit Guanosine
GAG	Glycosaminoglycan
GAP	GTPase activating protein
GDP	Guanosine diphosphate
GEF	Guanine nucleotide exchange factors
GRO	Growth-regulated oncogene
GTP	Guanosine triphosphate
GPCR	G-Protein coupled receptor
GRK	G-protein couple receptor kinase
HEK293	Human embryonic kidney 293 cells
HIV	Human immunodeficiency virus
IC_{50}	Concentration at which 50% inhibition occurs
IP_3	Inositol triphosphate
IKK	Inhibitor of NF-κB kinase
IL	Interleukin
JAK	Janus kinase
JNK	c-Jun N-terminal kinase
mAB	Monoclonal antibody
MAPK	Mitogen activated protein kinase
MCF-7	Michigan Cancer Foundation-7 (breast cancer cells)
MAPK/MEK	Mitogen-activated protein kinase
MMP	Matrix metalloproteinases Messenger
mRNA	Messenger ribonucleic acid
NAP	Neutrophil activating protein
NF-κB	Nuclear factor kappa-light-chain-enhancer of activated B cells
NK	Natural killer
p38 MAPK	p38 mitogen activated protein kinase
PBS	Phosphate buffered saline
PDGF	Platelet-derived growth factor
PI	Phosphoinositide
Pi3K	Phosphoinositide 3-kinase
PIP2	Phosphatidylinositol 4,5-biphosphate
PKA	Protein kinase A

PKB	Protein kinase B
PKC	Protein kinase C
PLC	Phospholipase C
PLD	Phospholipase D
PTEN	Phosphatase and tensin homolog
PTX	Pertussis toxin
Rac	Ras-related C3 botulinum toxin substrate
RAF	Rapidly accelerated fibrosarcoma
Ras	Rat sarcoma GTPase
Rho	Ras homolog gene family
RhoA	Ras homolog gene family-member A
RPMI	Roswell Park memorial institute medium
ROCK	Ras homolog gene family kinase
RT-PCR	Reverse transcription polymerase chain reaction
SDF	Stromal cell-derived factor
SD	Standard deviation
SEM	Standard error of the mean
siRNA	Small interfering ribonucleic acid
STAT	Signal transducer and activator of transcription
TK	Tyrosine kinase
TNFα	Tumour necrosis factor alpha
VEGF	Vascular endothelial growth factor
WASP	Wiskott–Aldrich Syndrome protein
WAVE	WASP-family verprolin-homologous

Table of contents

List of Figures

List of Tables

Chapter 1: Introduction

1.1 Cell migration and cancer metastasis

Metastasis is the spread of cancer cells from the primary tumour site to distant organs, and is considered the main reason for cancer morbidity and mortality [2]. The molecular mechanisms involved in the process of cancer cells metastasizing are not well understood due to their complexity. Mainly it includes the tumour detaching from the primary site, intravasating into the vascular or lymphatic circulations, escaping immune attack, invading the vascular basement membrane and extracellular matrix (ECM) to extravasate at distal capillaries, invading and proliferating by gaining epithelial characteristics in distant organs [3]. Several hypotheses aimed to explain the process and origin of metastasizing cancer cells. One of which addressed the Go or Grow hypothesis, stating that cell division and migration are temporally exclusive phenomena, and cancer cells defer proliferation for cell migration [4]. It is proposed that cells cannot undergo cytoskeletal changes and genetical modulation to perform both cell division and migration simultaneously [4], [5]. In other words, proliferating cells have less migratory attitude, and migrating cells have less proliferative behaviour. However, with their heterogeneous properties, cancer cells tend to have a mixed phenotype of moderate levels of migration and proliferation concurrently [6], [7]. As for the ability of primary tumour cells to gain migratory abilities brings up the epithelial-mesenchymal transition (EMT) phenomena.

EMT is characterized by the phenotypic and morphological changes encountering epithelial cancer cells leading to their transformation into mesenchymal cells during tumour metastasis [8]. During EMT, tumour cells surrounding the epithelial cells and matrix lose their polarity and adhesive features to give a more elongated, spindle-like, fibroblastic-like shape, thus improving the ability of cells to migrate and invade [9]. EMT undergoes differential expression of several epithelial and mesenchymal molecular cancer markers, such as the activation of transcriptional repressors of E-cadherin gene in the downstream signalling, including down-regulation of epithelial markers such as α-catenin, β-catenin and γ-catenin leading to the loss of the epithelial phenotype, while an upregulation of mesenchymal molecular markers such as N-cadherin, vimentin, and fibronectin [10]. Therefore, EMT has been considered as a potential drug target with inhibitors of receptor tyrosine kinases reaching to Phase III clinical trials [11].

Moreover, whereas EMT requires prolonged and extensive gene transcription changes, mesenchymal-amoeboid transition (MAT) or amoeboid-mesenchymal transition (AMT) undergo a rapid alternation to the motility behaviour that suppress or enhance the activity of certain pathways involved in the metastasis process [12].

The mechanism of migration recruited by cells after EMT can be categorized into one of the two categories: single and collective migration [13]. The classic opinion about metastasis seeding begin with a single colonial growth tumour cell from the primary tumour, that goes through a sequence of complicated events compromising the basic tumour transmission models, such as EMT and migratory cancer stem cells to arrive to its distant site [14]. However, the current paradigm is suggesting that seeding requires collective migration which is probably one of the main modes of migration during metastasis of many solid tumours [15]. Indeed, emerging evidence showed a significant difference in the mechanics between the two types of migration [15]. Single cells can circulate as individual circulating tumour cells (CTCs) and use two main modes of migration, amoeboid and mesenchymal. Amoeboid migration is described by blebbing, rounding, weak adhesions, and rapid migration, while mesenchymal migration is described by strong fibres, polarization, and actin meshwork including leading and trailing edge [16], [17]. Amoeboid migration is a more flexible and squeezing-into-gaps kind of pattern that does not involve degrading the ECM. The amoeboid tumours usually have hematopoietic or neuroectodermal origins, involving leukaemia, lymphoma, and small cell lung carcinoma, and most other tumour types [18], [19]. In contrast, the migration of mesenchymal cells generates the path as cells degrade the surrounding ECM using proteolysis to allow them to move through [12]. This migration pattern is also adopted by collective CTC and not limited to single CTCs [20]. The mesenchymal migrating tumours are often from tumours of the connective tissues, including fibrosarcoma or breast cancer cells [21]. Certain cell types may alternate between migration types at different points in time obtaining hybrid phenotypes as they circulate the microenvironment [20], [22]. Moreover, collective cells migration are detected in early stage cancer patients, have high invasive capacity, associated with worse clinical outcomes and have high survival response to chemotherapeutics than the single CTCs migration [23]. Collective CTCs can migrate in a verity of modes including sheets, strands, tubes, and clusters (**Figure 1**). They differ to single CTCs mainly by maintaining connection via cell-cell junctions during movement and exhibiting collective polarization, mechanical coupling, and cytoskeletal kinetics [14]. Therefore, tumour cells undergo EMT, MAT, and AMT assuming different migration modes depending on the environment [12], [24].

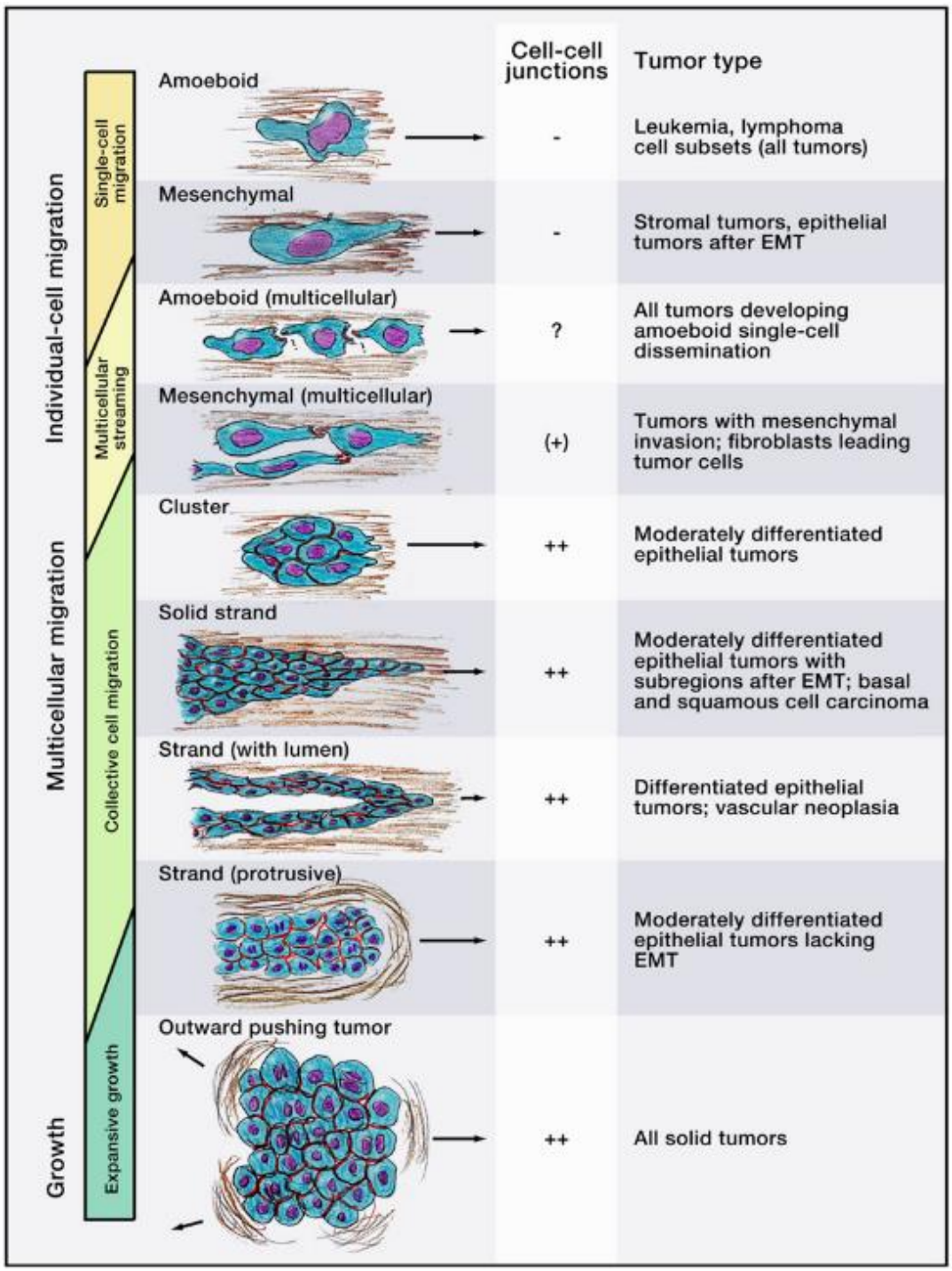

Figure 1. The different motility modes adopted by tumour cells upon detachment from the primary tumour. Cells can spread individually, or collectively as multicellular groups based on specific cell-cell junctions. During the process, cells change morphology to adjust to the environment between an amoeboid and mesenchymal phenotype. Image is taken from [20].

Cell migration is initiated and maintained by signalling pathways that regulate cytoskeletal dynamics [25]. In general, cytoskeleton dynamics interact with cell surface receptors that engage with the surrounding environment; consequently, the cytoskeleton operates as an engine, and the receptors behave as its transmission [20], [25]. The process starts with a migratory signal that causes the cell to polarize. During polarization, the front and rear ends of the cells change in structure [26]. Some of the vital regulators of this process are Rac and Cdc42, which reside at the leading edge of the cell, while Rho gathers at the sides and rear end of the cell [27] (**Figure 2**). The polarization of elongated mesenchymal migrating cells starts with assembling actin-rich protrusion like lamellipodia and filopodia at the leading edge [28]. Lamellipodia form a dendritic-like endings, branched and cross-linked actin network that sway across a broader stretch of the membrane, while filopodia are formed of parallel bundles of actin filaments that can sense signals from the surrounding environment [28]. During protrusion formation, lamellipodia are made by the Arp2/3 complex, which resides near pre-existing filaments, responsible for forming new actin filaments that branch off [29]. Rho GTPases modulate WASP/WAVE, which in turn regulate the action of Arp2/3 complex [30], [31]. Rac is necessary for lamellipodia extension, promoted by growth factors, cytokines and ECM components [32]. Although actin reorganisation is regulated by Rho GTPases, Pi3K are considered crucial for cell polarity and defining the leading edge of the cell [33]. This is suggested to be controlled by a positive feedback loop between Rho and Pi3K, which are required for efficient cell migration [34]. Extension of protrusions happens alongside the assembly of focal adhesions that attach the actin cytoskeleton to the ECM [35]. This process is mediated by adhesion molecules, such as integrins, Arp2/3, formins, cofilin and cortactin [16]. These molecular structures along with contractile actin stress fibres serve as traction areas to push the cell, and as sensors to translate signals from the ECM to the inside of the cell [12]. Assembled integrins give rise to the focal adhesions that then recruits EMC proteolytical enzymes such as metalloproteinases (MMPs) to perform pericellular ECM remodelling to lay out the path for migrating cells [36], [37]. The disassembly of adhesions is modulated by Src, FAK and phosphatases [38]. It is thought that this pathway stimulates Rac and Erk which are responsible for adhesion turnover [39]. In contrast, as mentioned before, in the amoeboid migration style, cells assume a rounded shape with ability to squeeze and glide through matrix barriers having contractility abilities, without involving MMPs and integrins [24]. Thus, with metastasis being a multistage process during which cells pass through different migration styles, it is vital to have a full understanding of the signalling molecules orchestrating the migration process to manage tumours spreading.

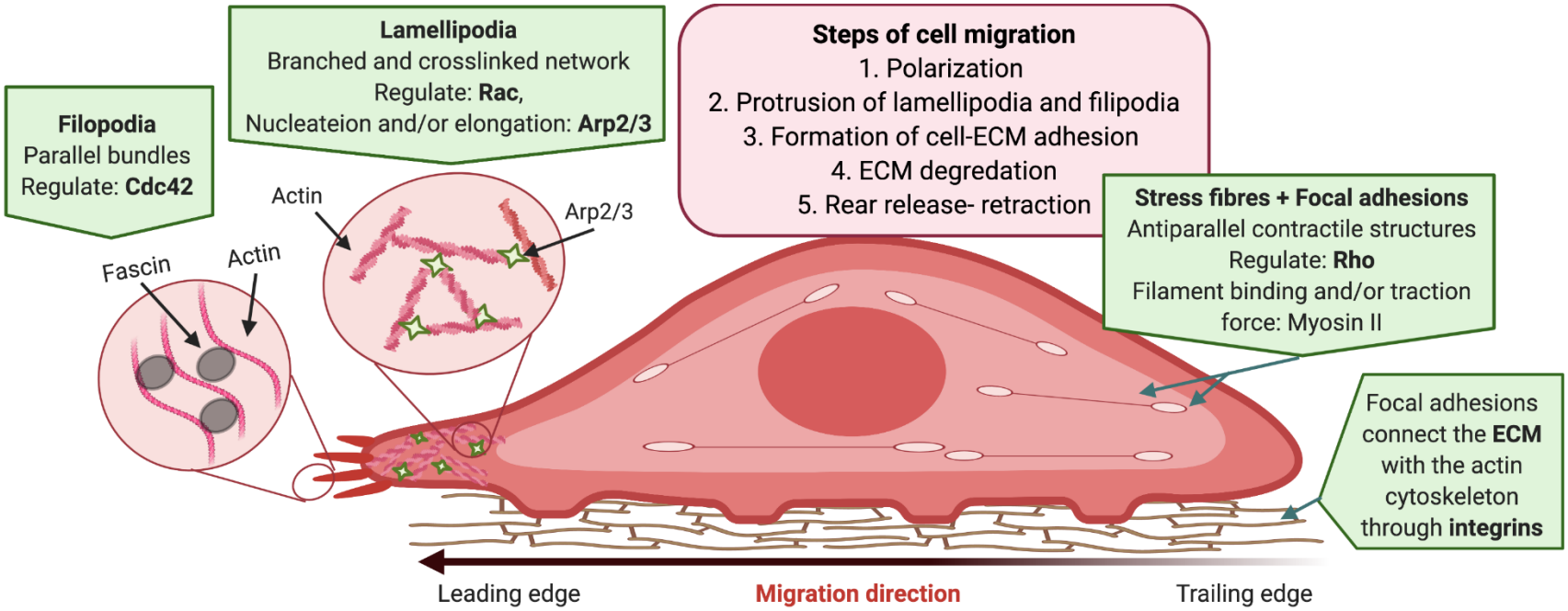

Figure 2. Assembly of actin filament network. Cell migration comprises cell polarization and protrusion of the leading edge (driven by lamellipodia and filopodia). Lamellipodium requires Rac for its assembly and stimulation of membrane ruffling, and it is comprised of a branched actin filament network, which are nucleated by Arp2/3 complex [29]. Filopodium are highly regulated by Cdc42 and is constructed of parallel bundles of Fascin cross-linking in the filopodia [40]. The cell will then attach the leading edge to the substrate with focal complexes, which develop into focal adhesions. Focal adhesions are integrin-based structures that anchor the ends of stress fibres [41]. Stress fibres are composed of thick antiparallel contractile actin filaments. They mediate strong attachments to the substrates and require Rho for their assembly [41]. Cell body contraction is driven by forces generated by actomyosin interactions [42]. Myosin II creates contractile forces implicated in driving actin network translocation [43]. RhoA is capable of stimulating myosin II through ROCK [25]. Rho activates tail retraction and forward sliding of cell rear [44].

1.2 Chemokines and chemokines receptors

1.2.1 Chemokines

Chemokines are a family of small secreted proteins that are structurally related to cytokines and are distinguished from other chemoattractants by their specificity to leukocytes subsets [45]. The chemokine system is a large one that is currently known to include more than 50 chemokines and 20 chemokine receptors [46] (**Figure 3**).

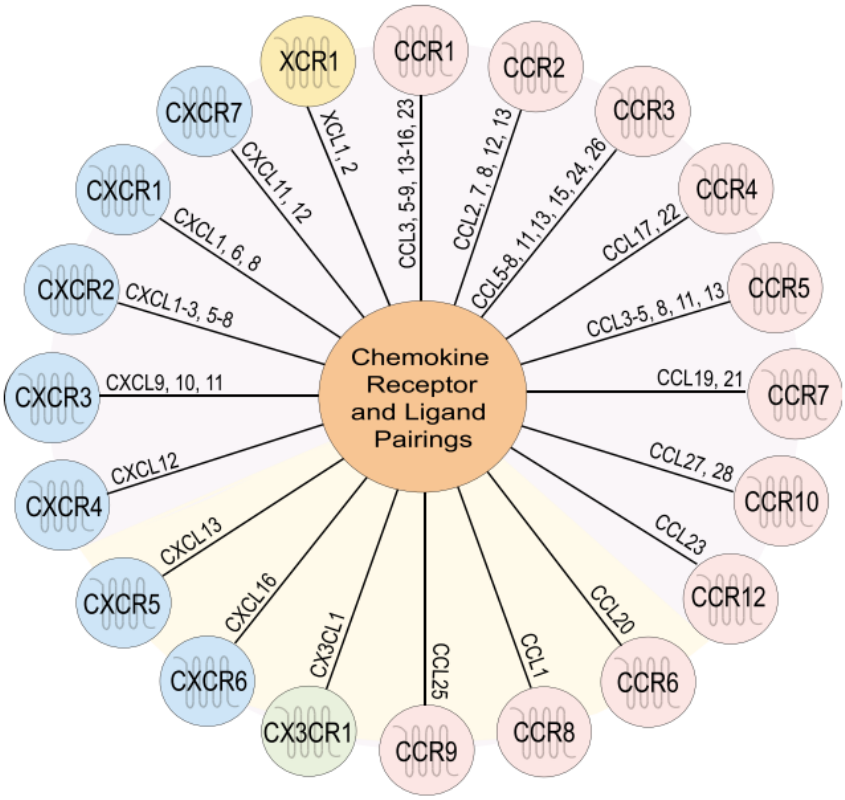

Figure 3. Illustration of chemokines and their respective cognate receptors. Multiple chemokines can bind to one receptor Image taken from [47].

They are small (6-14 kDa) molecular chemoattractants comprising structurally related and secreted proteins of 67-127 amino acids in length [48]. NMR and X-ray crystallography studies have revealed a lot about their structures. All chemokines feature a remarkably conserved tertiary structure containing a disordered N-terminus (signalling domain) of 6-10 amino acids which functions as an important domain in all characterised chemokines [49]. This region is followed by a structured core domain of a long N-loop, a 3_{10} helix, a three stranded antiparallel β-sheet, an α-sheet at the C-terminal tail, and disulfide bonds for the stabilisation of the structure of the chemokine monomers [49]. Chemokines are classified into four subgroups based on the location of the two initial cysteine residues attached to the N terminal of each chemokine: CXC, CC, CX_3C, and C chemokines (C represents the cysteine and X represents the non-cysteine amino acids) [50]. CXC chemokines are further subdivided into ELR- and ELR+ according to the presence or absences of the three motif amino acids: Glutamic acid-Leucine-Arginine, that proceed the first cysteine residue on the N-terminus [51] (**Figure 4**).

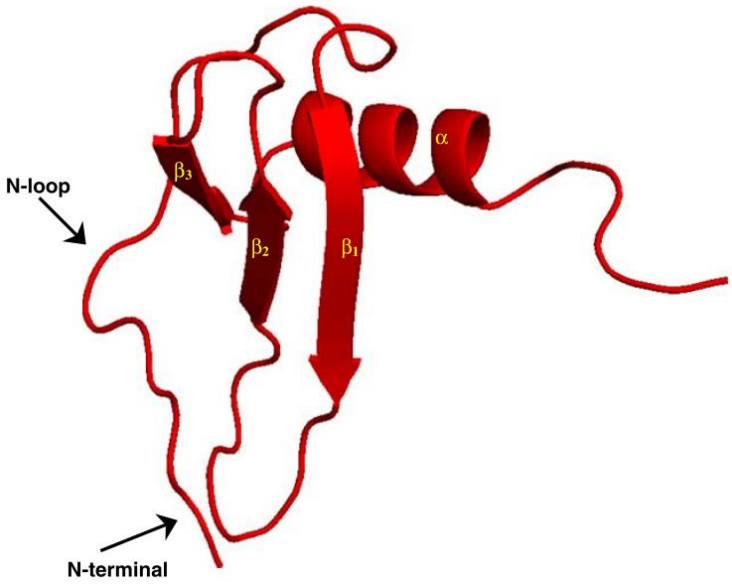

Figure 4. A schematic of a chemokine structure. Representation of an N-terminal, N-loop residues, three stranded antiparallel β-sheet, and an α-sheet at the C-terminal tail. Image taken from [52].

Chemokines are known to form dimers and oligomers, alone, in solution or when interacting with glycosaminoglycans (GAGs). CC dimerization occurs through the N-terminus where this domain becomes buried in the β-sheet of the other protomer [53]. While CXC ligands, for example CXCL8, form dimers by the interaction of residues from the first β-strand from one subunit to the same region of a second subunit, giving one extended six-stranded β-sheet which binds to the α-helix at the end of the C-terminus [54]. The different dimers motifs of CC and CXC ligands were primarily thought to define the affinity of interaction with the respective chemokine receptor [55], however, it is hypothesized that chemokines bind with their receptors as monomers, at least when directing cells motility [49], [56], [57]. For example, monomeric mutants of CXCL8 were found to recruit and stimulate neutrophils *in vitro* as efficiently as wild type, consistent with the data suggesting receptor interaction as a monomer [58], [59]. The monomeric form of CCL2 was also found to be sufficient for receptor binding and activation [60]. Nonetheless, oligomerization was still found to be involved in some crucial cellular functions independent of direct receptor interaction, such as binding to GAGs [61]. The latter interaction facilitates the secretion of chemokines from cancer cells, T cells, maintaining chemokine stability and signalling [62]. Notably, binding to GAGs appeared to be important in establishing a cell surface gradient to facilitate directional migration, *in vivo*, although this is not necessarily the case *in vitro* [63], [49]. Hoogewerf and colleagues confirmed that cell surface GAGs promote polymerization of chemokines, resulting in their elevated concentration which promotes their effect on their receptors [64]. Loss of GAGs significantly reduce the affinity of cells to chemokines [65]. Furthermore, binding to GAGs can protect some chemokines against processing by specific proteases [66]. For instance, Metzemaekers *et al*. [67] found that NH_2 proteolytic cleavage of CXCL9, CXCL10 and CXCL11 mediated by dipeptidyl peptidase IV/CD26 is protected by CXCR3 binding to GAGs, while this GAGs interaction also interferes with the receptor signalling. Consequently, the two states of monomers or oligomers share the significance in enabling chemokines function either by binding to the respective cognate receptor or with GAGs, accordingly.

Indeed, It is suggested that chemokines can promote each other's functions by forming heterodimers [68], [69], a process referred to as "chemokine cooperativity" [70]. Cooperative chemokines compete for binding with GAGs, thus elevating the effective free chemokines concentration that can bind their receptors [64]. Indeed, heterodimers formation is found to be thermodynamically favoured among various chemokines such as CXCL4, CXCL8, CXCL1 and CXCL7, CCL5, CCL2, and CCL8 [69]. For instance, CXCL4 binds to CXCL8 which attenuates CXCL8-stimulated signalling in $CD34^+$ human hematopoietic progenitor cells, promote CXCL8-stimulated chemotaxis, and induce the

anti-proliferative effect of CXCL4 on endothelial cells [71], [72]. Therefore, the function of chemokines can be influenced by the formation of heterodimers which can have substantial biological implications.

Although one of the main characteristics of chemokines is their ability to induce direct migration in a process called chemotaxis, they also have shown more complex physiological functions; having homeostatic roles in haematopoiesis, stimulating adaptive immune responses and immune surveillance [73], [74]. The expression of chemokine receptors was reported in the skin, intestinal mucosa, and lungs for their role in continuously invigilating any abnormal activity [49]. Chemokines are classified into inflammatory or homeostatic chemokines, although, few of them were identified to have dual-functions [75]. Inflammatory chemokines are expressed by leukocytes, and regulate the recruitment of monocytes, neutrophils, and other effector leukocytes from the circulation to the infected and damaged tissue [48]. The expression of inflammatory receptors is reported to be temporary within the inflammation area until the situation is resolved [49]. The other class of chemokines are homeostatic chemokines which are constitutively expressed [76]. They are needed for the constant regulation of cell migration required by the immune system and processes that are involved in the progressive movement and patterning of cells, such as in T and B cells development to particular secondary sites of the lymph nodes [48]. Lymphocytes also require haemostatic chemokines for regular immune monitoring [76]. Dual-function chemokines engage in immune defence by being activated in inflammatory conditions and target non-effector leukocytes at sites of leukocyte development and immune surveillance [74]. This type of chemokine was identified to have a role in T-cell development in the thymus and recruitment to inflamed tissue [74].

Furthermore, chemokine expression has been associated with many pathologies including cancer. Indeed, malicious cancer cells take advantage of the chemokine system in order to survive, progress, metastasize and colonise at distance areas, as well as promote the immune suppression [77]. Moreover, the aberrant expression of chemokines and their receptors has been documented to correlate to different pathologies [78] such as: autoimmune, vascular, pulmonary disorders relating to psoriasis, atherosclerosis, rheumatoid arthritis, multiple sclerosis, asthma, sepsis, inflammatory bowel disease, transplant rejection or HIV (as reviewed by [49]).

1.2.2 Chemokine receptors

Chemokine receptor structure: Chemokine receptors belong to class A rhodopsin-like family of G-protein coupled receptors (GPCRs) or seven-transmembrane (7TM) receptors, with three intracellular and three extracellular hydrophilic loops [79]. They are close in size (about 250 amino acids in length), have an acidic N-terminal end exposed outside the cell and an intracellular C-terminus containing serine and threonine residues facing the cytosolic side. The first two extracellular loops of the receptor have a pair of conserved cysteines that allow the formation of a disulphide bridge between these loops [80]. The extra disulphide bond is expected to keep the membrane-spanning segments arranged in a circle to maintain the 3D structure of the receptor [81]. G-proteins are coupled to the C-terminal domain of the receptor which, when activated, signal to multiple distinct intracellular signalling cascades, while the N-terminal determines ligand binding affinity [82].

1.2.3 Ligand-receptor activation

Ligand binding structure: Structural and functional studies indicate that all chemokines bind to their receptors using the same two sites, N-terminal and N-loop (binding domain) residues of the ligand to the N-terminal and one or more extracellular loops of the receptors [52]. The first step of ligand-receptor binding involve the core domain of the ligand, including the N-loop, binding with the N-terminus (site I) and the extracellular loops of its receptor, this binding area is referred to as the “chemokine recognition sites” [83] and triggers receptor activation. Notably, the term “chemokine redundancy” [84] has been associated with the ability or “promiscuity” of one chemokine to bind to multiple types of its receptors, both canonical and atypical ones, to exert similar or different actions based on the context [85], [85]. In the second step, the flexible N-terminus (triggering domain) of the ligand binds with the second recognition site buried in the cavity formed by the extracellular loops of the transmembranes domains III to VII (**Figure 5**). This process induces a change to the receptor conformation that initiates receptor activation followed by signal transduction [86]. Consequently, the N-loop residue is important for receptor selectivity and binding affinity, and N-terminal residues are significant for binding affinity and receptor activation [52]. Truncation of the N-terminus often leads to the chemokine losing its agonist activity, where the chemokine still binds to the receptor in high affinity but acts as an antagonist [61], [83], [87], [88]. On the other hand, some chemokines that are highly present in the plasma membrane [89] possessing long N-terminal extensions could demonstrate elevated agonist activity levels by sequential N-terminal proteolytic processing [87].

G-proteins in receptor activation: G-proteins consists of three subunits α, β and γ. Upon receptor stimulation, GPCR undergo conformational changes that expose

the intracellular sites involved in the interaction with heterotrimeric G-proteins. The Gα subunit is bound directly to the receptor intracellular loops, while Gβ subunit bind to Gγ in a tight complex. Ligand-receptor interaction leads the dissociation of GDP-bound Gα subunit to be exchanged and replaced with GTP [90]. Gα-GTP then separates from the receptor and the Gβγ heterodimer. The two G-protein complexes then stimulate various downstream effectors that ultimately lead to cellular responses such as cytoskeleton rearrangement, cell migration, integrin upregulation, release of oxidative species and phagocytosis [91]–[94].

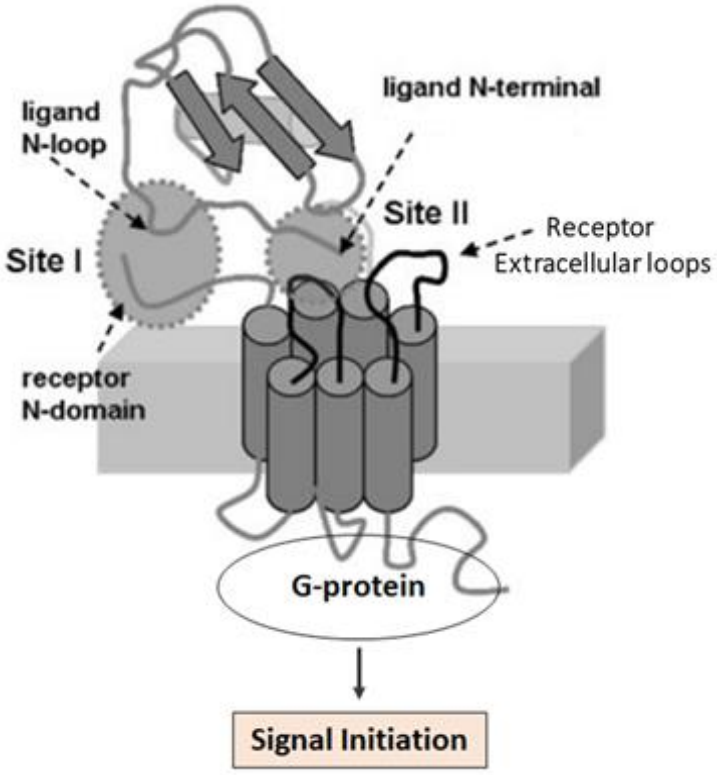

Figure 5. A model of chemokine ligand-receptor binding. The N-loop of the ligand interacts with the N-terminus of the receptor (site I), and the N-terminal of the ligand interact with the receptor extracellular loops and transmembrane residues (Site II). Image adapted from [48], [95].

1.2.4 Receptor desensitization and internalisation

Internalisation and desensitisation are two regulatory methods cells use to regulate the level of the receptor expression and to prevent continuous signalling. Indeed, stimulation with elevated amounts of the chemokine may exhibit receptor internalisation rather than the initiation of $G\alpha_i$ activation as well as, prolonged exposure to chemokines could lead to the downregulation of the receptor from the cell surface [96]–[99]. In desensitization, the receptor becomes refractory to the constant stimuli signalling. Moreover, endocytosis is a cellular activity mainly responsible for membrane receptor internalisation, where the receptor is physically removed from the cell surface and form an endosome. Notably, endocytosis could lead to total cellular receptor reduction through receptor downregulation [100]. Three families of regulatory molecules are involved in tightly controlling receptor desensitization: second messenger dependent protein kinases, G protein-coupled receptor kinases (GRKs) and β-arrestins. GRKs along with protein kinase (A) and protein kinase C (PKC) specifically phosphorylate the activated receptor which in turn recruit β-arrestins that are ubiquitously expressed and lead receptor desensitization, endocytosis and signalling [101], [102].

Activated chemokine receptor binds to β-arrestins which are adaptor proteins that act by interacting with phosphorylated serine/threonine residues on the C-terminal tail of the receptor [103]–[105]. Recruited β-arrestins block any further G-protein coupling by sterically inhibiting the receptor and G-protein interaction. The conformational changes of the receptor due to interaction with β-arrestins promotes endocytosis which is generated by the coordinated contact of β-arrestins with clathrin, adaptor protein (AP-2) and phosphoinositides [106], [107]. The complex ultimately leads the receptor to be recycled or degraded via lysosomes formation (**Figure 6**).

Accumulating evidence suggest that along with the β-arrestins being an adaptor protein binding to endocytosis machinery to terminate signals, they could also function as scaffolding proteins that activate several signalling pathways such as Src [102], and components of MAPK, ERK, JNK, and p38 cascades [108]–[111]. β-arrestins can confer different enzymatic activities upon the receptor, which may results in signals that modulate different cellular responses such as being involved in the regulation of the actin cytoskeleton [112]–[115]. For example, Luttrell *et al*. [116] found that β-arrestins can interact with GRKs and cytosolic tyrosine kinase c-Src, resulting in Src recruitment to the β-arrestins-clathrin-coated pit complex, thus initiating mitogenic signals from the activated receptor. Further studies showed the involvement of Src recruitment by β-arrestins to be associated with tyrosine phosphorylation of dynamin [117], stimulation of ERK/MAPK pathway [109], [116], and activation of neutrophil degranulation [118]. Serving as a scaffold, β-arrestins can trigger the activation of JNK3 pathway [119].

As for the role of β-arrestins in chemotaxis, receptor desensitization and recycling are important for maintenance of cellular polarity required by chemotaxis [111], [120]. β-arrestins can serve as scaffolds to localize molecules involved in cytoskeleton rearrangement associated with chemokines-induced cell migration [121]. In a review by DeFea [121], it was argued that β-arrestins may prefer terminating the coupling of the receptor with G-proteins in the back of the cell while the front of the cell being heavily polarized in the direction of the chemoattractant gradient. Additionally, the importance of β-arrestins in chemotaxis downstream of multiple receptors was linked to apoptosis, inflammation as well as cell migration [111], [122]–[125].

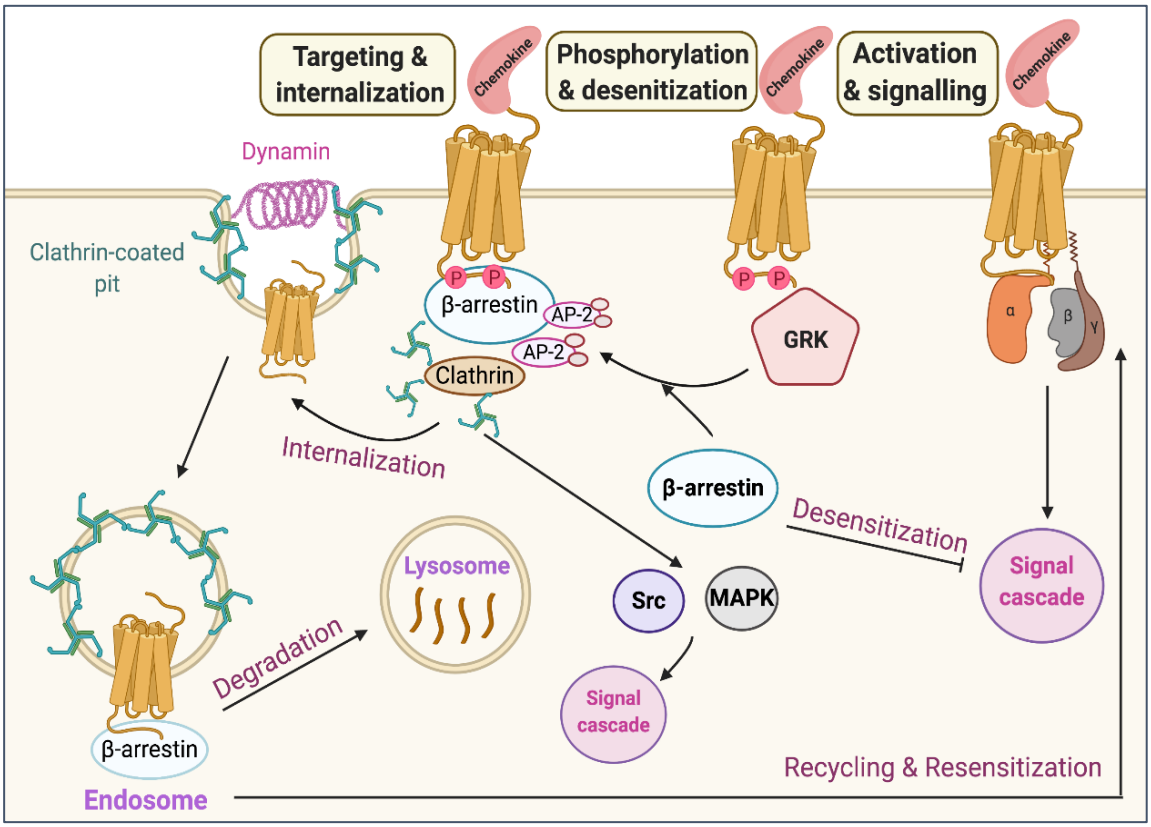

Figure 6. β-arrestin-dependent desensitization and internalisation of GPCRs. Chemokine activation of the GPCR leads to G-protein dissociation and stimulation of downstream signalling cascades. GPCRs are phosphorylated by GRKs leading to the recruitment of β-arrestins [126]. β-arrestins act together with clathrin and AP-2 complex, which associate the receptor to clathrin-coated pits. The GTPase, dynamin, regulates the release of the clathrin-coated pits. Clathrin-coated vesicles are formed, and the receptor is then internalized into endosomes. Dephosphorylation of the receptors leads to their degradation through formation of lysosomes or resensitization and recycling moving back to the cell surface. Beyond the function of β-arrestins in regulating receptor endocytosis, they can recruit c-Src and initiate mitogenic signals from activated receptors [116]. Recruitment of Src kinases might also modulate receptor endocytosis, trigger ERK1/2 stimulation, and regulate exocytosis [102]. β-arrestins can also serve as scaffold for JNK3 pathway [119] or trigger the assembly of MAPK activation and subsequently ERK1/2 signalling [102], [109].

1.3 CXCL8 and CXCR1-CXCR2 axis

CXCL8, also known as interleukin (IL-8), is a proinflammatory CXC chemokine that was first reported in 1987 for its activation and recruitment of neutrophils and granulocytes to sites of inflammation [127], [128]. Its history goes back to Peveri *et al.* [129] who showed that LPS-activated monocytes produce a protein called neutrophil activating factor (NAF), which leads to the stimulation of neutrophil exocytosis and respiratory burst by binding to specific cell surface receptors. NAF was purified and sequenced and later called IL-8 or CXCL8 [128]–[130].

CXCL8 acts by binding to its cognate receptors CXCR1 and CXCR2. This chemokine is barely detected in normal tissues or unstimulated cells [131]–[133]. However, CXCL8 receptors are expressed on the surface of leukocytes including neutrophils, monocytes, macrophages, basophils and T-lymphocytes and endothelial cells [134]. The expression of CXCL8 is rapidly induced by hypoxia, cytokines (such as tumour necrosis factor α (TNF-α), IL-1β, and IL-6), growth factors, and pathophysiological stresses mediated by transcription factors (such as nuclear factor-κB (NF-κB) and activator-protein-1 (AP-1)) [135]–[137]. Hypoxia and stressed tumour microenvironments use NF-κB to induce macrophages to secrete CXC chemokines [138]. Indeed, cytokine-mediated stimulation of NF-κB is considered the leading mechanism for transcriptional induction of chemokines. Specifically for CXCL8, transcription is regulated through NF-κB as well as other transcription factors including API and NF-IL-6 [139]–[141].

Moreover, the effect of autocrine/paracrine signalling of CXCL8 on the elevated expression levels of CXCR1 and CXCR2 has been reported in many cancer cells, suggesting a positive role of this chemokine on the cancer microenvironment [142], [143]. For instance, CXCL8 induces the angiogenic responses in CXCR1 and CXCR2 expressing endothelial cells [144], and the recruitment of neutrophils to the tumour microenvironment through its paracrine activity [137]. Simultaneously, in melanoma cells, stimulation with CXCL8 promotes cancer cell proliferation, survival, and migration via an autocrine activity [145]. Indeed, CXCL8 acts as an autocrine growth factor in liver, pancreas, and colorectum cancer [146]–[149]. Autocrine signalling according to Oladipo *et al*. [150] may have adverse prognostic effects in breast cancer, on the other hand, the positive role of CXCL8 in immune infiltrate may have good prognostic implications. Taking it together, the aberrant expression of CXCL8 have been noted to be associated with advanced stages of cancer and a poor prognostic marker for malignant disease, however, its complex role in the tumour microenvironment and its role as a prognostic and/or predictive cancer biomarker requires further investigation.

1.3.1 Activation of CXCR1 and CXCR2

CXCR1 and CXCR2 belong to the vast family of GPCRs, which bind extracellular ligands and consequently initiate intracellular signalling. Both CXCR1 and CXCR2 are highly homologous, sharing 76% sequence and bind to CXCL8 with similar affinities [151], [152]. The most divergent regions between the two receptors are the N-terminal (extracellular) and C-terminal (intracellular) regions [151]–[154]. CXCR1 is stimulated upon the interaction with CXCL8 or granulocyte chemotactic protein-2, whereas CXCR2 is stimulated by CXCL1, CXCL2, CXCL3, CXCL5, CXCL6, CXCL7, CXCL8, granulocyte chemotactic protein-2, and growth-regulated oncogenes [143], [155], [156]. Both receptors internalize through the recruitment of arrestins, with CXCR2 showing an extra phosphorylation-independent internalizing mechanism [102], [157]. Notably, CXCR2 undergoes internalisation rapidly (~95% after 5-10 min) with slower recovery (~35% after 90 min) relative to CXCR1 which internalizes slowly (~45% after 1 hr) and recovers rapidly (~100% after 1hr and 30 min) [98], [103], [158]. Indeed, a study by Richardson *et al.* [103] found that the C-tail of phosphoryl-deficient and C-terminus deleted mutants of CXCR1 and CXCR2 is crucial for receptor phosphorylation and arrestin recruitment, yet, it is not sufficient to account for the differences in receptor internalisation and recycling. These difference in receptor trafficking seem to be substantial for determining the ability of the receptors to stimulate specific leukocyte responses, including respiratory burst and cross-regulatory and exocytotic signals [158].

Furthermore, CXCL8 can exist in monomer or dimer forms that could bind with CXCR1 and CXCR2 with different affinities and potencies to regulate various cellular events [159]. CXCL8 forms dimers at micromolar concentrations ($K_d \approx 10$ μM) and binds to its receptors at a nanomolar concentration ($K_d \approx 1$ nM), proposing that monomers are sufficient for receptor activation [59], [160]. Existing in a monomer form was found to be more active than dimers for events like intracellular calcium mobilization, phosphoinositide hydrolysis, chemotaxis, and exocytosis [161]. The rate of monomer-mediated regulation of CXCR1 was greater for these intracellular events, whilst for CXCR2, both monomeric and dimeric CXCL8 can potentiate these events at a similar rate [161]. Therefore, it is worth considering the distinct properties of the monomer and dimer forms of CXCL8 and its receptors, and their role in orchestrating immune cells recruitment during different physiological conditions.

Inhibitors of CXCR1 and CXCR2: because of the therapeutic potential associated with the inhibition of CXCR1 and CXCR2, several small molecule inhibitors have been developed to target these receptors. Amongst some of CXCR1 and CXCR2 antagonists are Reparixin, SCH527123, and SB225002. Reparixin is a non-competitive allosteric blocker of CXCR1 and CXCR2 activation. Mutation analysis and molecular modelling revealed that this antagonist binds to a pocket in the transmembrane allosteric region of CXCR1 and blocks CXCL8-induced intracellular signal transduction without affecting receptor bindings [162]. SCH527123 is another CXCR1 and CXCR2 antagonist that is highly potent and features non-competitive allosteric properties with a K_d= 49 pM towards CXCR2, and K_d= 3.9 nM towards CXCR1 [163]. Moreover, SB225002 is a potent antagonist that inhibits CXCL8 binding to CXCR2 with an IC_{50}= 22 nM and binding to CXCR1 with IC_{50} > 150-fold higher than CXCR2. Further details about the effect of these antagonists are discussed in chapter 3.

1.3.2 CXCL8 involvement in cancer

As mentioned earlier, an increased expression of CXCL8 and/or its receptors has been characterized in cancer cells, tumour-associated macrophages, infiltrating neutrophils, and endothelial cells, indicating the vital role this axis plays in the tumour microenvironment. CXCL8 was the first chemokine detected to stimulate melanoma cancer cells chemotaxis and hepatotactic migration [164]. Following this, it was reported that the binding of CXCL8 to its receptors promotes the proliferation and migration of melanoma cells and MCF-7 breast cancer cells [147], [165]. Additionally, Zuccari *et al*. [166] reported elevated expression levels of CXCL8 in neoplastic mammary tissues compared to normal tissues. Other cancers that demonstrated association with elevated levels of CXCL8 are melanoma [137], breast [167], thyroid [168], gastric carcinoma [169], ovarian [165], prostate [170], and lung cancer [146]. Consequently, there is strong correlation between high levels of CXCL8 and invasive metastasis with an increased risk of recurrence [171], [172].

1.3.3 CXCL8 involvement in angiogenesis

In the 1990s, Folkman demonstrated that certain activated signalling cascades within tumour cells could promote surrounding blood vessels to grow [173]. A tumour could acquire its own blood supply by forming a network of blood vessels around itself and then growing around those vessels, a phenomenon that Folkman referred to as angiogenesis [173]. Angiogenesis is involved in multiple conditions such as wound healing, embryonic development, chronic inflammation, and the progression of cancer [173]. During wound healing, endothelial cells undergo ECM proteolysis, increased local migration, proliferation, and the development of new capillary all while maintaining the equilibrium of angiogenic and anti-angiogenic regulators [174]. Tumour angiogenesis

exploits the same signalling cascades used by wounds to form new blood vessels, which unlike the balanced state of wound healing, favours the upregulation of angiogenic factors and downregulation of anti-angiogenic factors [175]. Upon ligand-receptor binding, angiogenesis starts by secreting matric metalloproteinases (MMP2 and MMP9) to break down the ECM where it will begin initiating and growing the capillaries. Studies found that CXCL8 promotes the proliferation of endothelial cells and capillary tube organisation, whereas neutralizing antibodies against CXCR1 and CXCR2 inhibited this process [142], [176]. CXCL8 mimics vascular endothelial growth factor (VEGF), transactivates VEGF-R2, and induce angiogenesis [177]. Moreover, CXCL8 promote $a_v\beta_3$ upregulation that has a role in endothelial cell survival and tumour migration during angiogenesis [178]. *In vivo* cancer models with depleted CXCL8 or its receptors showed a reduction of tumour growth associated with decreased microvessel density [179]. For example, depleted CXCR2 in mouse models with prostate or pancreatic cancer had lower tumour angiogenesis and less tumour growth [180]. A similar study found that *in vivo* $CXCR2^{-/-}$ mice with lung cancer had decreased the angiogenic activity presented by lower vascular density [179], [181]. Moreover, blocking CXCL8 and its receptors could reduce angiogenesis of metastatic melanoma [137], [143].

1.3.4 CXCL8 involvement in metastasis

In addition to the local effects of chemokines on leukocytes and tumour, it is confirmed that cancer cells can utilise chemokines, such as CXCL8, to enable metastases [143]. For example, CXCL8 serum level could be a helpful prognostic marker for metastatic breast cancer [182]. Indeed, several studies suggest that tumour metastasis is facilitated by the binding of CXCL8 to its receptors enabling EMT, cell migration, and cell seeding at secondary sites [183], [184] (**Figure 7**). CXCL8 produced in the inflammatory microenvironment, exasperates the inflammatory state, and enables cancer cells to proliferate and migrate to secondary tumour sites. Notably, CXCR1 and CXCR2-expressing neutrophils are attracted to the cancer site following a CXCL8 gradient produced by cancer cells. Neutrophils release enzymes that enable ECM remodelling which facilitate cancer cells migration and entry to the vascular bed, leading them to metastatic sites [185]. Furthermore, it was also established by Christiansen and Rajasekaran. [186] that cells which lose their epithelial differentiation and assume mesenchymal features become more invasive, motile, gain cancer-stem like features, and have more resistance to chemotherapeutics. In addition, the effect of stress on stromal cells leads to the secretion of CXCL8 which could be involved in the invasiveness and/or metastasis of tumour cells [187].

Thereafter, guidance and direction of organ-specific metastasis to the lymph nodes and to other sites will be mediated by the cells expressing CXCL8 and/or its cognate receptors [133]. For example, the liver was found to be amongst the primary sites of breast cancer recurrence where Khazali *et al*. [188] found that hepatic stellate cells and their derived CXCL8 could stimulate breast cancer growth and proliferation. Further data show that CXCL8 is implicated in osteolysis and the stimulation of osteoclastogenesis correlated with metastatic breast cancer [189], [190]. High levels of CXCL8 mRNAs were reported in association with distant lymph node metastasis, poor survival and quick relapse of NSCLC [191], [192]. Also, implantation of pancreatic adenocarcinoma cells into the pancreas of nude mice led to the formation of liver metastasis correlated with elevated expression of CXCL8 [193]. Taken together, developing therapeutic approaches to inhibit metastasis requires a full understanding of the mechanism by which primary tumours utilize CXCL8 to migrate to metastatic sites and the importance of further expression of these chemokines at the new site.

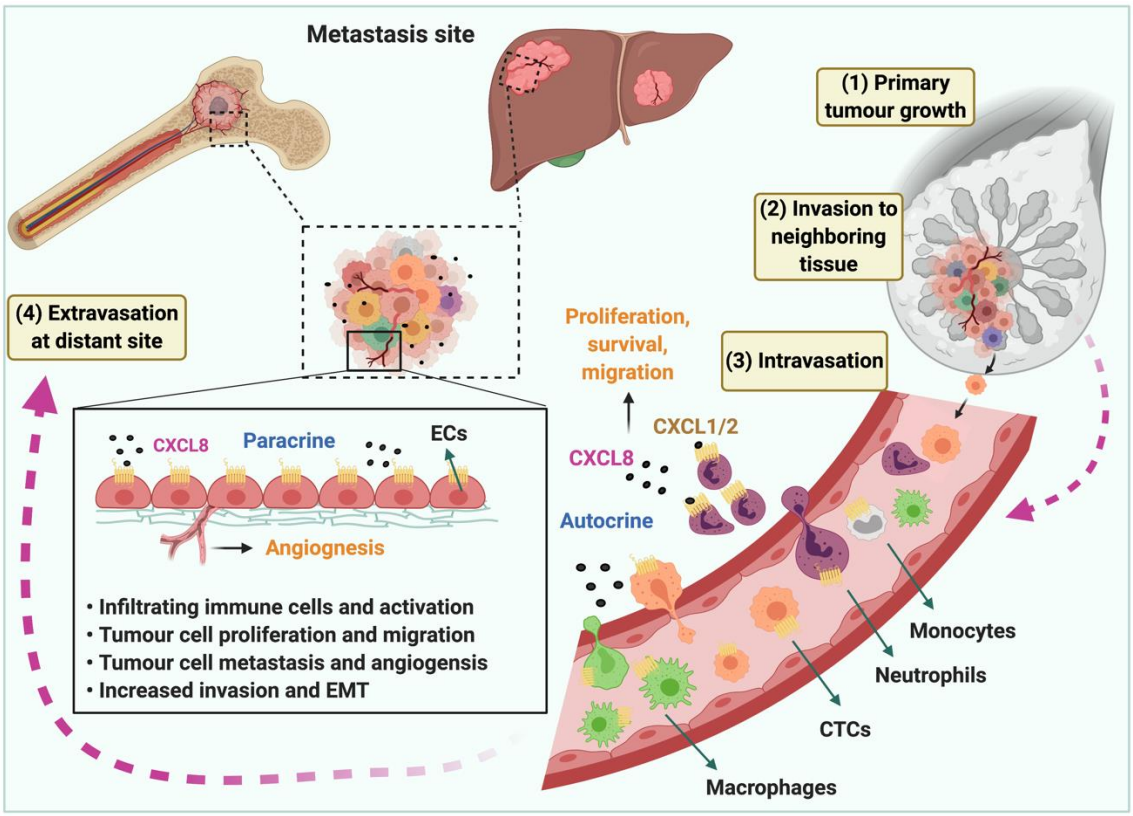

Figure 7. Involvement of CXCL8 in cancer metastasis. (**1**) Primary tumour growth initiated in the breast (**2**) gain invasion and migratory properties to intravasate the blood stream. (**3**) CXCL8 exerts a chemotactic action on CXCR1 and CXCR2-expressing immune cells which further produce CXCL8 and guide their infiltration to the blood stream. (**4**) Circulating tumour cells (CTCs) expressing the receptors as well as the immune cells will extravasate the blood stream to distant organs, such as the liver [188] or bones [190], [194]. Moreover, CXCL8 may also promote angiogenesis by inducing endothelial cells' (ECs) migration or chemotaxis [142], [195]. CXCL8 promotes epithelial-mesenchymal transition (EMT) of tumour cells which enhance the metastatic dissemination and secretion of angiogenic factors [196], [197]. Endothelial cells expressing CXCL8 receptors are thought to stimulate the angiogenic effect in a paracrine manner [144], whereas the proliferation, survival and migration of tumour cells is mediated through an autocrine activity [145].

1.4 CXCL10 and CXCR3 axis

CXCL10, also known as interferon “gamma-induced (IFN- γ) and protein of 10 kDa” (IP-10), is one of the first identified chemokines that is secreted by multiple cell types [198]. ELR^+ CXC chemokines such as CXCL8 mediate neutrophil attraction and angiogenesis as discussed earlier, however, CXCL10 is an ELR^- CXC chemokine that attracts lymphocytes and exert anti-angiogenic effects by binding to its receptor, CXCR3 [199], [200]. Indeed, CXCL10 together with CXCL9 and CXCL11 share the property of being predominantly induced by IFN-γ, which is itself mediated by IL-12 cytokines [201]. IFN-γ is produced by a wide range of cells, such as endothelial cells, fibroblasts, keratinocytes, monocytes, and T lymphocytes [202], [203]. T helper-1 cells recruitment could mediate IFN-γ and TNF-α secretion, which promotes the production of CXCL10 from various cell types creating an amplified feedback loop which sustains the autoimmune process [201]. Secretion of CXCL9, CXCL10, and CXCL11 can also be induced by LPS, TNF-α, proinflammatory cytokines, IFN-α and IFN-β, depending on the cell type [204].

1.4.1 Activation of CXCR3

CXCR3 has three splice variants generated by the alternative gene splicing of three different exons: CXCR3-A, CXCR3-B, and CXCR3-Alt. Although CXCR3 expression is linked to cancer progression as mentioned earlier, some studies did not account for the different isoforms of CXCR3, which were reported to have opposite effects [205]. Each of these variant CXCR3 receptors were found to stimulate distinct intracellular signalling cascades proposing that they have non-redundant roles in immune responses [206]. The term biased agonism is associated with CXCR3 due to the ability of different ligands to bind CXCR3 and preferentially stimulate some signalling cascades while inhibiting others [207]. Former studies claimed that the specificity of each CXCR3 splice variant to induce particular downstream signalling pathways is cell-type specific [205], [206].

CXCR3-A is a 368 amino acid protein that is considered to be the most abundant variant in cells [208]. Notably, CXCR3-A is the predominant form expressed on T cells [209]. This form activates $G\alpha_i$, induce arrestin recruitment, and initiate phosphorylation of ERK1/2, p38 MAPK, JNK, and Pi3K/AKT signalling cascades [208], [210]–[214]. CXCR3-A stimulate intracellular calcium release, DNA synthesis, actin polymerization, promote endothelial cells proliferation, and mediate Th1 cell chemotaxis [205], [215], [216]. Indeed, CXCL9 and CXCL10 use the C-terminal and the third intracellular loop of CXCR3 to induce chemotaxis, calcium flux, and the internalisation of CXCR3-A, processes that are identified to be mediated by arrestins [217] (**Figure 8**),while CXCL11 predominantly induces a C-terminal independent cascade [218]. Upon stimulation, β-arrestin form a core scaffolding complex that is thought to stimulate the phosphorylation of ERK1/2 [219].

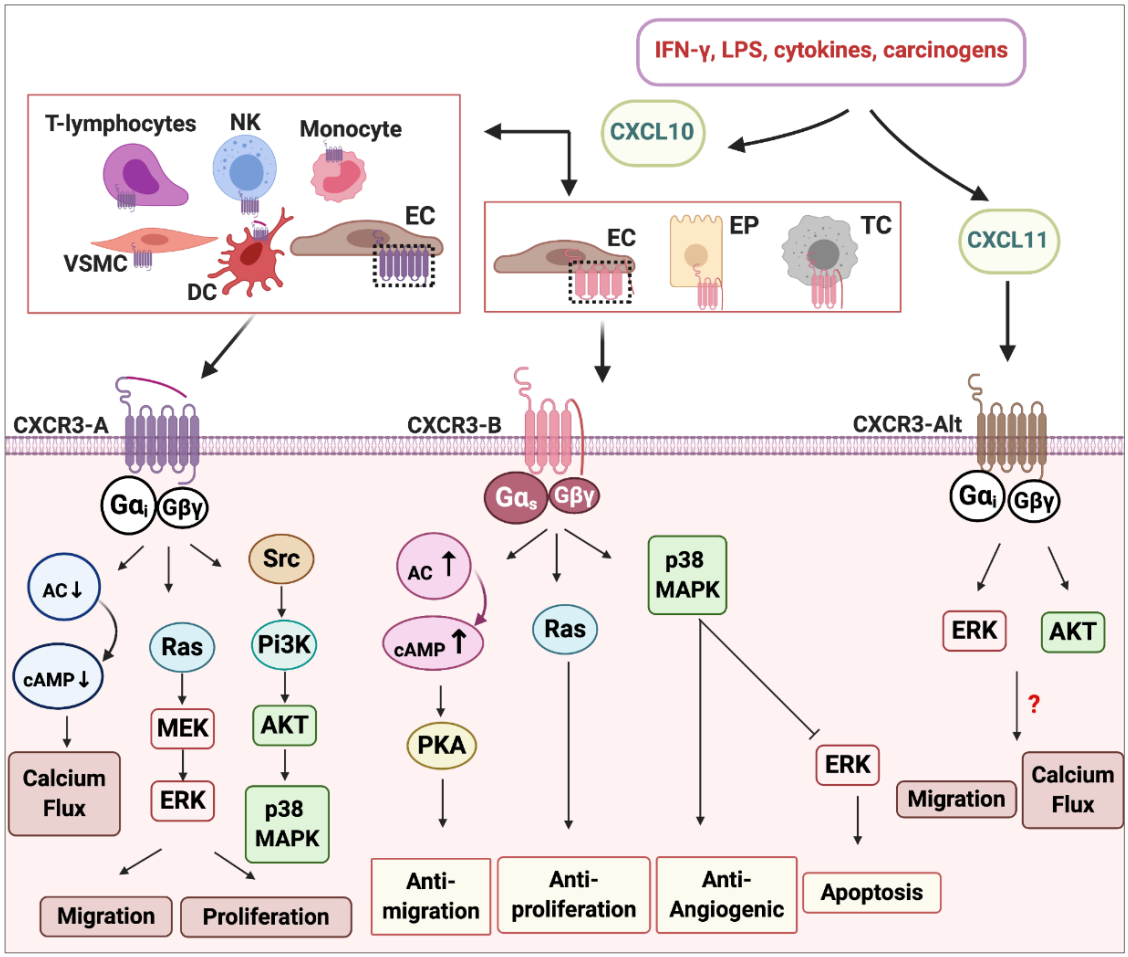

Figure 8. Schematic representation of CXCR3-mediated signalling pathways. CXCR3 is expressed on T-lymphocytes, natural killer (NK) cells, monocytes, vascular smooth muscle cells (VSMC), endothelial cells (EC), dendritic cells (DC), epithelial cells (EP), and tumour cells (TC) [198], [205], [220]–[223]. The coupling of CXCL10 to CXCR3-A activates $G\alpha_i$ that inhibits adenylyl cyclase and decrease cAMP, which induce calcium flux. CXCR3-induced chemotaxis is mediated by Src, Pi3K/AKT, and p38 MAPK which is also linked to cell migration, invasion, proliferation and metastasis [210]–[212], [216]. Activation of CXCR3-B leads to $G\alpha_s$ coupling enabling the activation of p38 MAPK that promotes apoptosis by inhibiting ERK [224]. This pathway mediate the anti-angiogenic effect of CXCR3-B [225]. The anti-proliferative effect of CXCR3-B is due to Ras activation [222]. CXCR3-B signalling also triggers PKA (cAMP-dependent), which inhibits m-calpain activation (not shown in figure) and blocks cell migration [226]. CXCR3-Alt specifically binds to CXCL11 and has a moderate effect on inducing chemotaxis and calcium flux [227]. It has shown that it activates signalling such as ERK1/2 and AKT phosphorylation [227], [228], with no specified role in cells proliferation [208]. Nonetheless, very little is known about CXCR3-Alt signal transduction pathways.

On the other hand, CXCR3-B, a 415 amino acid protein, has a longer N-terminal tail consisting of 51 amino acid that replaces the four most N-terminal residues of CXCR3-A [229], [230]. CXCR3-B expression is debated in the literature regarding which G-proteins it interacts with. For example, CXCR3-B interacts with $G\alpha_s$ to activate adenylyl cyclase and increase cAMP concentration leading to the inhibition of cell proliferation, migration, chemotaxis, and apoptosis induction [212], [223], [231], [232] (**Figure 8**). Nonetheless, a study reported that CXCL11 (but not CXCL9 or CXCL10) interact with CXCR3-B and activate $G\alpha_i$ at a concentration of 100 nM, while all three chemokines failed to signal through $G\alpha_s$ in receptor-transfected HEK293T cells [206]. Another study found that CXCR3-B demonstrated no measurable $G\alpha_i$ or $G\alpha_s$ activity [233]. Furthermore, Campanella *et al*. [234] argued that CXCL10 induce its anti-proliferative effect on endothelial cells independent of CXCR3, instead it binds to GAGs. Moreover, it has been previously demonstrated that CXCL10 has a higher binding affinity to CXCR3-B relative to CXCL9 and CXCL11, whereas the affinity is similar between these ligands towards CXCR3-A [205]. Endothelial [205], epithelial [221] and tumour cells [222], [223] showed expression of CXCR3-B, which has led to the assumption that this variant is preferentially expressed on these cells [234]. Alongside CXCL9, CXCL10, and CXCL11, platelet induced chemokines CXCL4 and CXCL4L1 also bind to CXCR3-A and CXCR3-B [235].

The third CXCR3 splice variant, CXCR3-Alt, consists of 267 amino acids and is a result of posttranscriptional exon skipping which misses several transmembrane domains that are characteristic of GPCR [227]. It is identified to be co-expressed with CXCR3-A at very low levels [203], [215], [227]. The biological role of CXCR3-Alt is not well known, although expression of CXCR3-Alt coincided with the upregulation of CXCL11 [236]. In addition, CXCR3-Alt was reported to have elicit the signalling of ERK1/2 and AKT phosphorylation [227], [228]. The binding of CXCL11 to CXCR3-Alt demonstrates a moderate induction of chemotaxis and calcium flux, suggesting involvement of pertussis toxin sensitive $G\alpha_i$ [227], however no effect on cell proliferation was reported [237].

Taken together, an additional layer of complexity is added to the chemokine system defined by the biased agonism emphasizing the importance of considering the context when targeting CXCR3 with small molecules.

1.4.2 CXCL10 involvement in cancer

Several studies have reported that CXCL10 is overexpressed in multiple human diseases such as infectious diseases, chronic inflammation, and tumour progression [237]. Specifically, CXCL10 is involved in the recruitment of leukocyte to inflamed sites, exacerbating inflammation and leading to substantial tissue damage [201]. CXCL10 binds to the CXCR3 chemokine receptor and exert signalling effects in both a paracrine and autocrine fashion [203], [238], [239]. CXCL10 induction is predominantly based on the C-terminus of CXCR3, which is vital for receptor internalisation, chemotaxis and calcium flux [217]. CXCR3 is present on normal plasma cells and multiple myeloma cells enabling migration/chemotaxis to the bone marrow [223]. Moreover, CXCL10 is found in significant amounts in cancer like melanoma [240], [241] and malignant B lymphocytes, where it triggers chemotaxis and contribute to cell proliferation and survival [242]. On the other hand, CXCL10 appear to have a dual role in cell proliferation, because when bound to CXCR3 it acted as an efficient inhibitor of endothelial cell proliferation and this effect is counteracted with anti-CXCR3 antibodies [205].

Moreover, CXCR3 ligands promote the migration and invasion of MDA-MB231 breast cancer cells, with neutralizing anti-CXCR3 antibody inhibiting this effect [243]. Additionally, the invasiveness of breast (MCF-7, T47D) and lung (A549) cancer cells were also stimulated by CXCR3 ligands [244]. Studies found that CXCL10 can activate T-lymphocytes tumorigenesis and metastasis [245]–[248]. Furthermore, CXCR3 expression is associated with breast [249], osteosarcoma [250], ovarian carcinoma [228], B-cell lymphoma [251], and colon metastasis [252], [253], having a role in the tumour progression or acting as a useful diagnostic marker. Simultaneously, endothelial cell production of CXCL10 along with VEGF can promote cancer metastasis, within the tumour microenvironment or via autocrine interaction of CXCL10 axis on tumour cells [238], [254].

In contrast, elevated production of CXCL10 was reported in tumours that presented spontaneous regression and impaired angiogenesis [255]. Thus, CXCL10 has been identified as an anti-angiogenic factor that inhibits human NSCLC [245] and human microvascular endothelial cells [205], this is potentially mediated via CXCR3-B interaction [222]. Previous studies have debated whether the anti-angiogenic effect CXCL10 exerted is through binding to CXCR3 or GAGs. Indeed, it was confirmed that the tumour anti-angiogenic activity induced by CXCL10 or CXCL11 is CXCR3-dependent [256], [257]. Altogether, the role of CXCL10 in tumour progression is rather complex and relies on the cell type and the CXCR3 isoform expressed.

1.5 Signalling pathways involved in chemokine signalling

Cascades with aberrant signals in the context of cancer could be the driving force for sustaining the life of tumour cells [258]. The human genome has about 500 kinases which can attach phosphate tags, for example γ-phosphate of ATP, to serine, threonine or tyrosine residues in a process called phosphorylation [258]. Phosphorylation is required for intracellular and extracellular signals transmission throughout the cells and to the nucleus thus, works as a 'molecular master switch' [259]. Indeed, researchers have considered kinases to be pivotal in coordinating signals responsible for cellular responses and hypothesized that signal transduction therapy may be valid for targeting cancer [260].

Kinases phosphorylation is carried out when they target specific amino acids in the destined proteins. For instant, tyrosine kinase phosphorylates tyrosine, and serine/threonine kinases phosphorylate serine and threonine. Both kinases have a catalytic core with a glycine-rich N-terminal ATP-binding pocket and a central conserved aspartic acid residue required for its catalytic activity [261]. Tyrosine kinases are classified into receptor and non-receptor tyrosine kinases. Receptor tyrosine kinases are transmembrane proteins that have a ligand binding extracellular domain, and a catalytic intracellular kinase domain [261]. Non-receptor tyrosine kinases are located in the cytosol, nucleus, and in the inside surface of the plasma membrane. Therefore, kinases can behave as receptors on the membrane of the cell or as an intracellular signal regulator to launch a chain of cellular responses [262].

Tremendous effort have been invested in developing specific protein kinase inhibitors as therapeutic agents for perturbed cellular behaviour [263]. The US FDA approved 52 small molecule protein kinase inhibitors, so far [264]. Kinase inhibitors are classified based on their targeting of the ATP-binding site, with the kinase adopting a conformation mimicking the ATP binding ability. The ATP-binding pocket lies in the protein kinase domain. This domain is positioned in a deep cleft and held in place via hydrogen bonds formed between the ATP adenine ring and the kinase hinge ring. This kinase hinge ring is bound by the N-terminal lobe, and C-terminal lobe [262]. The enzyme activity is controlled by a conserved activation loop which is tagged by a conserved DFG motif at the start of the loop and ending with an Ala-Pro-Glu motif [265]. Protein kinase inhibitors possess a high ATP-competitive affinity to compete with the elevated intracellular concentration of ATP and efficiently block kinase function [266].

Tyrosine kinase inhibitors are a class of anticancer medications that inhibit the action of one or more of the tyrosine kinases. They can operate in four different mechanisms. Type I and type II inhibitors compete with the ATP pocket of the kinase in its active or inactive state, respectively [267]. Indeed, type I kinase inhibitors bind in and around the binding site of the adenine ring of the ATP and mimic its interaction with the hinge site of the protein [268]. This type targets the ATP-binding site of the kinase in the active form, which is recognized by its open conformation of the activation loop. This is associated with the "DFG-in" conformation of the activation loop which is characterized by its positioning of the aspartate-phenylalanine-glycine at the beginning of the activation loop [269]. Type II inhibitors bind to the DFG-out inactive kinase conformation and target the allosteric site of the ATP pocket [270] (**Figure 9**). The allosteric site is formed of an additional hydrophobic pocket presented by the DFG-out adjunct to the adenine region [269]. The amino acids in the allosteric site are less conserved relative to those in the ATP binding site, which proposes that it may be easier to achieve kinase selectivity with type II inhibitors [271], [272]. Moreover, Type III inhibitors occupy an adjacent allosteric pocket residing on the outside the ATP pocket without competing with it. Type IV inhibitors interfere with the surfaces that are important for protein-protein interactions [273].

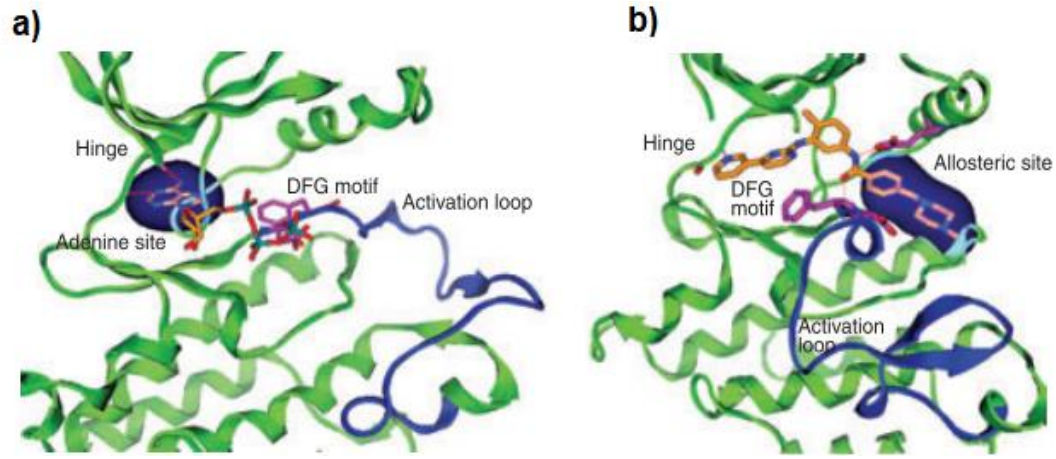

Figure 9. Binding sites of type I and II protein kinase inhibitors. Ribbon diagram of **a)** type I inhibitor binding to the adenine site with DFG-in conformation, whereas **b)** is type II inhibitor shows binding to the DFG-out inactive kinase conformation and target the allosteric site of the ATP pocket. Image taken from [270].

Although, the ATP active site possess a highly conserved nature making it challenging to selectively target type I and II inhibitors, the pharmaceutical industry field have encountered big advances in the progression of selective protein kinase inhibitors [272], [274], [275]. Indeed, development of small molecule kinase inhibitors that can activate or inhibit specific kinase signalling cascades propose new opportunities for pharmacological manipulation of protein kinase function (**Table 1**).

Table 1. List of some FDA-approved tyrosine kinase inhibitors. Table taken from [267].

Approved Inhibitors	Approved Date	Primary Targets	Inhibitor of Type
Imatinib	2001/05	ABL/PDGFR/c-KIT	II
Gefitinib	2003/05	EGFR	I
Erlotinib	2004/11	EGFR	I
Sorafenib	2005/12	VEGFR/PDGFR etc	II
Sunitinib	2006/01	KIT/PDGFR etc	I
Dasatinib	2006/06	ABL/SRC etc	I
Lapatinib	2007/03	EGFR/Her2	I
Nilotinib	2007/10	ABL/KIT etc	II
Pazopanib	2009/10	c-KIT/FGFR etc	I
Vandetanib	2011/04	VEGFR/EGFR etc	I
Crizotinib	2011/08	ALK/ROS1	I
Vemurafenib	2011/08	BRAF	I
Ruxolitinib	2011/11	JAK1/JAK2	I
Axitinib	2012/01	VEGFR etc	I
Bosutinib	2012/09	ABL/SRC	I
Regorafenib	2012/09	VEGFR etc	II
Tofacitinib	2012/11	JAK1/JAK3	I
Cabozantinib	2012/11	c-MET/VEGFR2 etc	II
Ponatinib	2012/12	ABL	II
Trametinib	2013/05	MEK1	III
Dabrafenib	2013/05	BRAF	I
Afatinib	2013/07	EGFR	I
Ibrutinib	2013/11	BTK	I
Ceritinib	2014/04	ALK	I
Idelalisib	2014/07	PI3Kd	I
Nintedanib	2014/10	VEGFR etc	I
Palbociclib	2015/02	CDK4/CDK6	I
Lenvatinib	2015/02	VEGFR1/2/3	I
Cobimetinib	2015/11	MEK	III
Osimertinib	2015/11	EGFR	I
Alectinib	2015/12	ALK	I
Ribociclib	2017/03	CDK4/CDK6	I
Brigatinib	2017/04	ALK/EGFR	I
Midostaurin	2017/04	FLT3 etc	I
Neratinib	2017/06	EGFR/HER2	I
Abemaciclib	2017/09	CDK4/CDK6	I
Copanlisib	2017/09	PI3Ka/PI3Kd	I
Acalabrutinib	2017/10	BTK	I
Fostamatinib	2018/04	SYK	I
Baricitinib	2018/05	JAK1/2	I
Binimetinib	2018/06	MEK	III
Encorafenib	2018/06	BRAF	I

1.5.1 Pi3K/AKT pathway

Activation of GPCRs by extracellular stimuli transmit the signal across the plasma membrane into intracellular signalling events [276]. The binding of the chemokine to its receptor induces a conformational change in the receptor that activates various small G proteins that regulate downstream effector pathways. The active conformational change facilitates the exchange of bound GDP to GTP of the Gα subunit, which are grouped into $G\alpha_{q/11}$, $G\alpha_{i/o}$, $G\alpha_{s}$ and $G\alpha_{12/13}$, and dissociate from Gβγ subunits [277]. Chemokine receptor activation promote intracellular signalling through both Gα and Gβγ subunits, which can stimulate distinct, complementary, or antagonistic cascades [278]. One of the pathways that gets activated through either Gα or Gβγ subunits is the Pi3K/AKT signalling pathway (**Error! Reference source not found.**). Gβγ can directly bind and activate Pi3K. Direct activation of Pi3K/AKT cascade through Gα has not been precisely measured but this activation is made via transactivating integrins, receptor tyrosine kinase and other growth factor receptors [279].

CXCL8 signalling has attracted a lot of attention because of its involvement in cancer angiogenesis, survival, proliferation, and tumorigenesis [280]. One of the widely studied signalling pathways is the Pi3K-associated pathway. This pathway has been proven to be significant for the cells ability to sense a chemokine gradient and guide the directed migration in response to chemokine receptor activation in multiple cell types [281] (**Error! Reference source not found.**). Pi3K works on maintaining cell polarity and defining the leading edge of cell migration [34]. Indeed, this lipid/protein kinase was reported to be crucial for CXCL8-induced chemotaxis of neutrophils, causing an increase of phosphorylation of its substrate serine/threonine kinase AKT [282].

AKT activation is involved in modulating cell survival, growth, angiogenesis, and migration [283]. Jiang and colleague found that CXCL8 stimulated the invasion of osteosarcoma cells by regulating the Pi3K/AKT signalling cascade [284]. Furthermore, studies have shown that CXCL8 promoted the migration of chondrosarcoma cells by elevating integrin β3 expression via Pi3K/AKT signalling [285]. In oestrogen receptor-negative breast cancer, CXCL8 is involved in leptin-mediated EMT, increased integrin β3 expression and promotes cell invasion all through the activation of Pi3K/AKT signalling [94], [286].

NF-κB is a transcription factor that is involved in stimulating the expression of CXCL8 [155]. Indeed, Pi3K/AKT signalling promotes CXCL8 expression in human lung epithelial cells by stimulating IKK and NF-κB proteins [287]. Also, CXCL8 potentiate NF-κB activation through EGFR-transactivated AKT signalling in human ovarian cancer cells [288]. The production of CXCL8 was elevated through the betacellulin-EGFR-Pi3K-AKT

and ERK pathway in NSCLC A549 cells, which was involved in the development of an inflammatory microenvironment with consequences on lung cancer proliferation and migration [289].

Accumulating evidence have used LY294002, the well-established potent pharmacological inhibitor of Pi3K to advance our knowledge in the importance of this signalling pathway [290]–[292]. LY294002 significantly reduced CXCL8-induced cell migration in neutrophils and L1.2 cells overexpressing CXCR2 [282], [293]. In androgen-independent prostate cancer cells, CXCL8 induced the activation of mammalian target of rapamycin (mTOR) via PLD-dependent and Pi3K/AKT and MAPK-dependent pathways, and using Pi3K inhibitor, LY294002, attenuated the rate of cells proliferation [294]. Moreover, treatment of colorectal adenocarcinoma HT-29 cells with LY294002 downregulated LPS-induced CXCL8 expression [295]. Due to the inhibitory effect of Pi3K inhibitor, LY294002, on MAPK signalling in CXCL8-induced neutrophils, Takami *et al.* [296] suggested a model of Pi3K being upstream of MAPK. Another study using NSCLC cells found that Pi3K/AKT and c-Jun (a member of MAPKs) were involved in human papillomavirus-16 oncoprotein induced VEGF and CXCL8 expression in the cells, leading to angiogenesis *in vitro* [291]. Additionally, a study found that since Pi3K/AKT and MAPK are implicated in inducing the angiogenic effect of CXCL8 and VEGF in breast cancer cells, blocking these dominant signalling pathways rather than the chemokine might be more tumour-specific, eliminating potential side effects [297]. This study also reported that LY294002 treatment inhibited the expression of CXCL8 and VEGF in breast cancer cells with constitutively stimulated AKT. Simultaneously, Pi3K can induce VEGF expression by activating HIF-1, ERK1/2, and NF-κB to induce tumour angiogenesis [298], [299]. Indeed, Pi3K/AKT, mTOR and their effectors HIF-1α and VEGF function in controlling angiogenesis, where PTEN, a Pi3K inhibitor, mediate the inhibition of angiogenesis by regulating these effectors [300], [301].

In all, these studies demonstrate that CXCL8 utilizes the Pi3K/AKT signal transduction pathway to induce a range of effects favouring cancer progression.

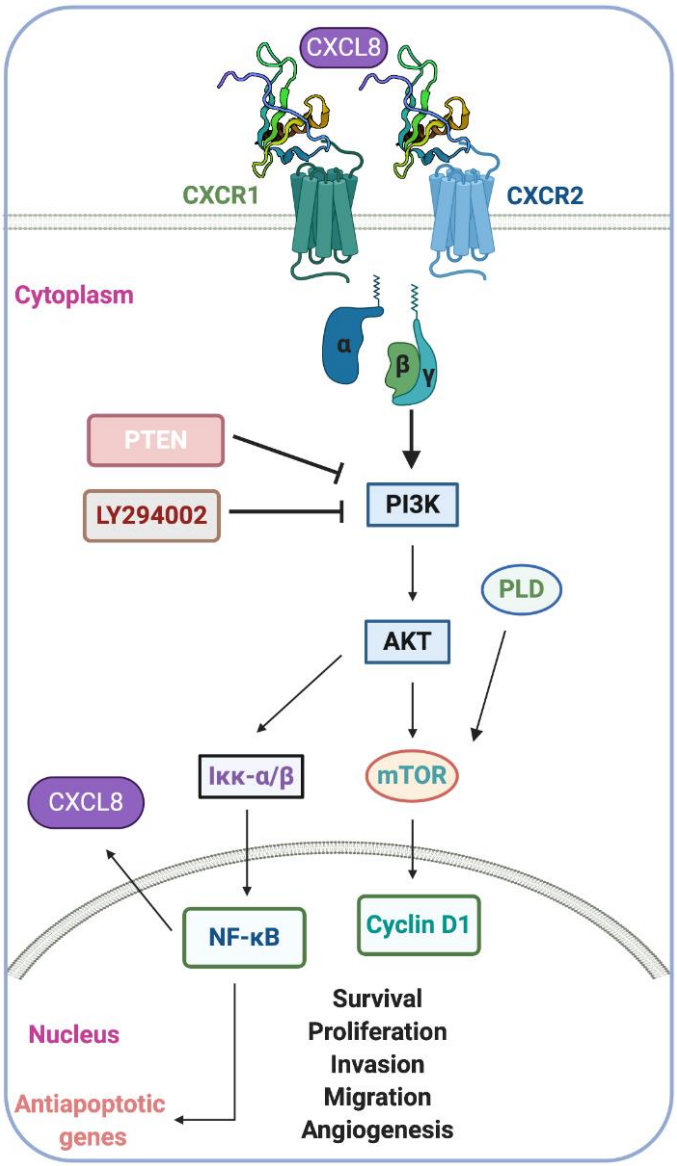

Figure 10. Induction of Pi3K/AKT signalling upon CXCL8 binding to CXCR1 and CXCR2. CXCL8 activates mTOR via Pi3K/AKT and PLD which produce an effect on cyclin D1 that regulates proliferation in androgen-independent prostate cancer cells [294]. Pi3K and c-Jun were found to be involved in inducing angiogenesis in CXCL8-induced NSCLC cells [291]. Pi3K was reported to be crucial for neutrophil migration in response to CXCL8 gradient [282]. Moreover, IKK and NF-κB stimulation via Pi3K/AKT leads to the expression and release of CXCL8 in lung epithelial cells [287]. Potentiation of NF-κB mediates transcription of antiapoptotic genes and also activates Pi3K/AKT and MAPK [294] that is crucial for cell survival [296], a response that is elevated in hypoxic cells [302]. In addition, NF-κB is involved in CXCL8 and VEGF-induced angiogenic effect that is mediated through Pi3K/AKT and MAPK [297]. Pi3K inhibitor, LY294002, blocks signals associated with survival, proliferation, migration, and angiogenesis [282], [293]–[297]. Moreover, loss of Pi3K/AKT inhibitor, the tumour suppress gene PTEN, leads to a selective upregulation of CXCL8 signalling *in vitro* and *in vivo* [303].

1.5.2 The Ras/Raf/MEK/ERK, and p38 MAPK pathway

CXCL8 signalling modulates the activity of MAPK signalling pathway that comprise several serine/threonine kinases [143]. MAPKs are evolutionarily conserved protein kinases that link and transmit extracellular signals responsible for regulating major cellular responses such as, survival, growth, differentiation, migration, and apoptosis [304], [305]. Aberrant MAPK signalling has been associated with cancer progression. For example, many MAPK cascades are involved in stress signalling related to hypoxia, substrate detachment, inflammation, and metabolic stress [306]–[308]. Therefore, the importance of this protein kinase in sensing and processing stress signals is established [304]. These characteristics associated with stress-induced kinases are linked to cancer, inflammation, DNA damage response and apoptosis [305], [307], [308]. The best characterized pathway of these kinases is the Ras/Raf/MEK/ERK pathway (**Figure 11**). Pi3K has been identified as a mediator for coupling CXCL8 to MAPK signalling in neutrophils [309]. The Ras/Raf/MEK/ERK and Ras/Pi3K/PTEN/AKT cascades interact with each other to regulate growth and often tumorigenesis [310].

The Ras/Raf/MEK/ERK pathway pairs signals from the cell surface and transmit them to transcription factors, which sequentially regulate gene expression [311]. Upon stimulus binding, Ras exchange GDP for GTP which induce conformational change causing its activation. This in turn enables Raf to be recruited to the cell membrane. Indeed, Ras is a small GTP-binding protein that is considered a common upstream molecule in many signalling pathways such as Raf/MEK/ERK, Pi3K/AKT, and RalEGF/Ral [312]. Studies have shown that different mutation frequencies in Ras that cause its constitutive stimulation is often linked to human cancer (as reviewed [310]).

The Raf family have a role in modulating cell proliferation, differentiation, and apoptosis upon induction with cytokines [313]–[316]. This family consists of A-Raf, B-Raf, and C-Raf (also known as Raf-1). The A-Raf member has a weak effect on ERK activation [316] and yet was a crucial stimulus for hematopoietic cells growth [311]. The role of C-Raf has been questioned since the discovery of B-Raf, where the latter appeared to be a much potent activator of MEK relative to C-Raf and A-Raf [314], [317]. C-Raf may have a function in blocking the activity of apoptosis promoters and could itself be activated by B-Raf [317]. Indeed, B-Raf gene mutation seemed to be involved in inducing proliferation and transformation [318]. Therapeutic intervention by targeting B-Raf with RNA interference have shown that depleted oncogenic B-Raf in cancer cells abrogate ERK activity, inhibit proliferation and induce apoptosis [319], [320]. Knall *et al*. [309] found that Pi3K inhibition block CXCL8-induced stimulation of C-Raf and B-Raf, causing an inhibition of MAPK stimulation. Conversely, another study found that the inhibition of Pi3K with LY294002 led to an upregulation of B-Raf activity

[321]. Thus, it is suggested that there could be more than one mechanism controlling the activation of Raf. Simultaneously, other signalling molecules interact with the Ras/Raf/MEK/ERK cascade to enhance or inhibit their activity with a potential crosstalk between the Raf/MEK/ERK and Pi3K/AKT. Notably, the growth of hematopoietic cells was inhibited by targeting both signalling pathways [322], with further interactions between the two pathways being reviewed in [312]. Therefore, the abnormal signalling in cancer could be due to mutations in upstream membrane receptors, Ras and B-Raf as well as genes in other pathways such as, Pi3K, PTEN and AKT, which can control Raf activity [310].

ERK1/2 induction in response to extracellular signals is suggested to have a dual effect on cancer cells by either enhancing or inhibiting their progression depending on the context and strength of stimulation [304]. CXCL8 induces rapid and transient phosphorylation of ERK1/2 and Pi3K in neutrophils [323]. The role of ERK1/2 activation by CXCL8 in neutrophil migration is not well understood [282], [309], [324]. CXCL8 signalling activates the MAPK pathway which in turn enables the downstream phosphorylation of ERK1/2 that has been detected in cancer cells. For example, this pathway promotes cell proliferation and survival in prostate [294], ovarian [165], NSCLC [325], pancreas [326], and colon [149] cancer cells. The activation of ERK-MAPK proposes that there is a pathway connecting CXCL8 signalling to the stimulation of E2F and activator protein transcription factors, whose main role is to regulate the transcription of genes involved with cell proliferation [299], [327], [328]. Moreover, MEK inhibitors PD98059 and U0126 inhibit the release of adenovirus serotype 7 upon stimulation with CXCL8 via inhibition of ERK pathway in a dose-dependent manner [131]. Another study found that PD98059 and p38 MAPK inhibitor, SB203580, block CXCL8 expression, whereas JNK inhibition only partially inhibit CXCL8 secretion/expression in human oesophageal epithelial cells [329]. This study also added that MAPK and PKC signalling are important for regulating acid-mediated CXCL8 expression through NF-κB, where the inhibition of the NF-κB may exhibit a potential therapeutic target for oesophageal inflammation. In addition, reported data had suggested that ERK inhibition in lung cancer stimulates glycogen synthase kinase 3β, possibly leading to β-catenin degradation, which causes inhibition of cancer progression and migration [330].

The p38 MAPK pathway is identified as a regulator for inflammation and modulating stress responses and can be stimulated by CXCL8 [331]. For instance, the p38 MAPK inhibitor, SB203580, inhibits IL-1β-stimulated CXCL8 mRNA expression and protein production in Caco-2 and HT-29 cells [332]. Another p38 MAPK inhibitor, SB202190, blocks TNFα and LPS-stimulated CXCL8 mRNA expression in monocytes [333]. Furthermore, using RWJ 67657, which is also a p38 MAPK inhibitor, caused the

abrogation of transcription and production of CXCL8 in monocyte-derived macrophages in a dose-dependent manner [334]. Moreover, p38 MAPK, plays an important role in the post-translational regulation of CXCL8, and its inhibition with SB203580 blocks TNFα-induced CXCL8 secretion [332]. CXCL8 was also found to have induced the migration and invasion of head and neck squamous cell carcinoma by stimulating p38 MAPK/ERK-NF-κB pathway and reducing JNK [335].

Overall, this highlights the link between CXCL8 activation of the Ras/Raf/MEK/ERK as well as p38 and JNK (MAPKs) and their involvement in cancer. This makes these kinases desirable targets for therapeutic intervention to prevent cancer progression.

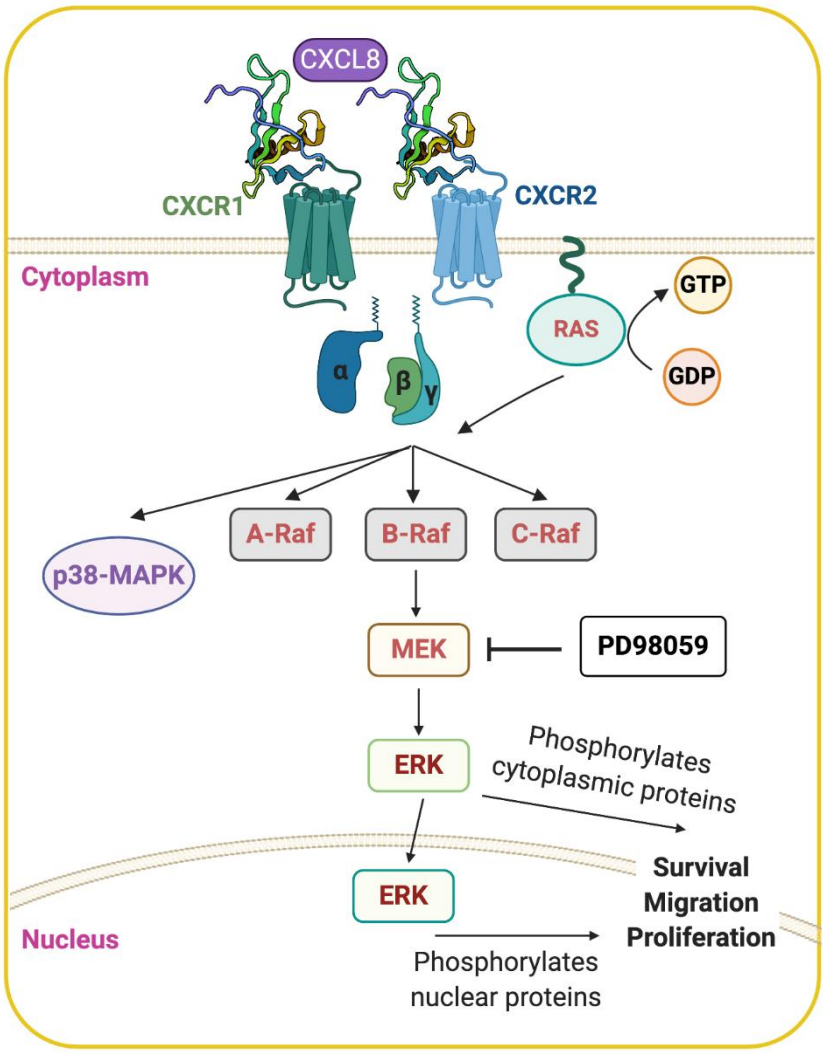

Figure 11. The Ras/Raf/MEK/ERK pathway and intracellular signalling. The pathway is initiated with receptor activation upon ligand binding, such as CXCL8. Ras resides in the plasma membrane and facilitates the exchange of GDP to GTP. Ras recruits the Raf family to the cell membrane. Raf phosphorylation activated MEK which subsequently phosphorylated ERK1/2. In turn, activated ERK1/2 produce a wide range of cytosolic and nuclear responses resulting in migration, proliferation, and survival [131], [336]. For example, MEK inhibition with PD98059 supressed CXCL8-activated neutrophil chemotaxis [324]. Moreover, PC3 cells stimulated with CXCL8 promote the proliferation via induction of ERK1/2 and p38 MAPK [331].

1.5.3 Rho GTPases and DOCK1/2/5 pathway

Amongst other signalling pathways is the Rho family GTPases that are key regulators of the actin cytoskeleton [337]–[341]. This family belongs to Ras superfamily of small GTPases and among its well-characterized molecules are Rho (A, B, C isoforms), Rac (1, 2, 3 isoforms) and Cdc42 (Cdc42Hs, G25K isoforms) [341]. These proteins play a role in regulating the actin cytoskeleton by modulating the formation of lamellipodia, filopodia, and stress fibres, respectively [341] (**Figure 12**). Rho GTPases regulate cellular processes by working as a switch based on their GDP or GTP-bounding form. Guanine nucleotide exchange factors (GEFs) catalyse the exchange of GDP with GTP, while GTPase-activated proteins (GAPs) conversely hydrolyses GTP to GDP [338]. In their GTP-bound conformation, Rho GTPases activate downstream effector proteins involved in the cytoskeleton rearrangement, migration, proliferation, transformation and differentiation [338]. CXCL8 binding to CXCR1 induce rapid stimulation of Rho resulting in a cytoskeleton response in microvascular endothelial cells, whereas binding to CXCR2 cause a retraction of endothelial cells mediated by Rac [342]. Thus, signalling of CXCL8 induces the polymerization and subsequently the retraction of the actin cytoskeleton. Further evidence demonstrate the dynamic, time-dependent regulation of Rho, Rac, and Cdc42 activity upon application of exogenous CXCL8 on prostate cancer cells, proposing that all three proteins are significant mediators of CXCL8-driven cancer cell migration and invasion [143]. Moreover, a study confirmed that the chemotactic role of CXCL8 on endothelial cells is mediated by p38 MAPK, which is potentially a downstream activator of Rac1/Cdc42 and RhoA GTP binding proteins [343]. RhoA, Rac1 and Cdc42 showed elevated levels of expression in breast cancers [344].

The role of Rho GTPase in cancer development has been widely investigated. This family is involved in stimulating cell cycle progression and regulation of gene transcription, revealing its pro-oncogenic characters, such as inducing Ras-induced transformation [345], and promoting neovascularisation [346]. Since this family has a role in modulating cell body contraction by regulating actin-myosin contractility and forming stress fibres [340], their inhibition was found to block the migration of macrophages [339]. Indeed, Rho absence can cause an inhibition of the cell tail detachment through reduced actin-myosin contraction [347]. Furthermore, Rho activity can be blocked downstream of cadherins resulting in a more migratory phenotype [348]. The expression level of RhoA and RhoC is generally elevated in cancer, whilst RhoB is downregulated and so is inversely linked to cancer aggressiveness [349]. RhoA is involved in cancer cell proliferation and survival due to its constitutive activation which can promote transformation [350]. In fact, RhoA is a crucial regulator of amoeboid and mesenchymal motility [337]. This happens through the RhoA-ROCK pathway inducing

actomyosin-based cortical contractility resulting in amoeboid blebbing leading to its motility, and also causing tail retraction in mesenchymal migration [351]. RhoA and its downstream target ROCK are also involved in cancer extravasation, based on experimentation using chemical inhibitors [337], [352]. Indeed, Pi3K activating Rho leads to ROCK, Myc phosphorylation and thrombospondin-1 repression. The latter is an anti-angiogenic factor that when repressed through RhoA is implicated in promoting breast cancer angiogenesis [349].

The expression of Rac1, Rac2 and Rac3 is elevated in some tumours [349]. Accumulating evidence suggest that Rac1 is expressed in a vast number of cancer causing malignant transformations [349]. With this in mind, Rac1 appears to be mutated in some cancers, such as meningiomas, astrocytomas and pituitary adenomas, leading to its overexpression and further increasing the survival of the tumours [353]. Rac1 may promote cancer cell proliferation by regulating the cell cycle. For instance, Rac1 was shown to promotes the expression of cyclin D1, and stimulation of cell transformation *in vitro* [354]. Moreover, DOCK1/2/5 is characterized as a major regulator of Rac in neutrophils, thus, blocking it has inhibited chemotaxis migration of neutrophils [355]. DOCK2 binds to Rac and mediate GTP-GDP exchange reaction. Inhibition of DOCK2 is thought to be an attractive target for inflammatory-related pathologies [356].

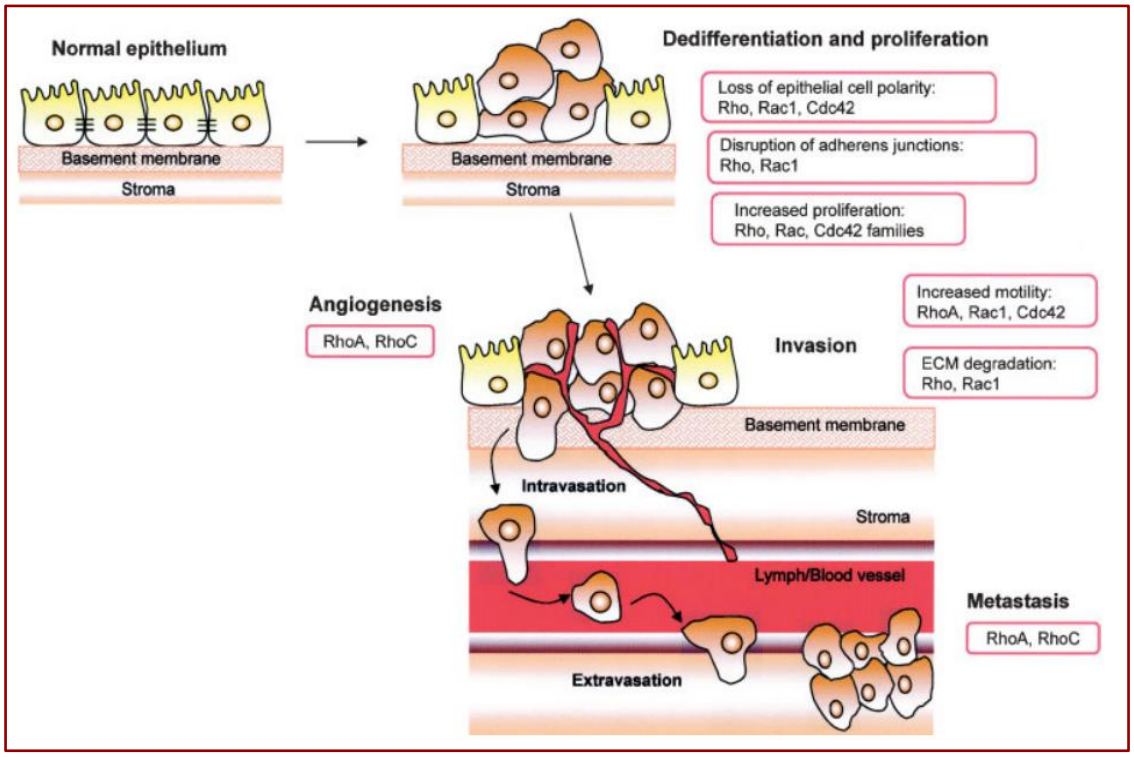

Figure 12. Illustration of the involvement of Rho GTPases in tumour progression. From the loss of the polarity and directionality to the disruption of the adherent junctions leading to tumour increased migration, proliferation and remodelling of the ECM, and induction of angiogenesis, the Rho protein family plays an important role in maintaining the integrity of the cells, and their abnormal expression is highly associated with tumour development (Image taken from [349]).

It is well documented that cells require Cdc42 for their polarity and directed migration, otherwise they would migrate randomly [357]. Cdc42 controls the polarity by relocating the microtubule-organising centre and Golgi apparatus at the front of the nucleus in the direction of the leading edge resulting in the growth of microtubules and transfer of vesicles towards this region [358]. The relation between Cdc42 and cancer appear to be tissue specific. For example, an elevated expression level of Cdc42 was found in breast cancers and hardly detected in corresponding normal tissue [344], [359], [360], whereas the absence of Cdc42 promoted the progression of liver cancer [360]. Indeed, Cdc42 was reported to induce the invasion and metastatic activity of breast cancer cells [361]. Moreover, Cdc42 inhibitor, ZCL278, was found to have inhibited the migration of PC3 cells [362] as well as suppressed the invasion and migration of pancreatic cancer cells [363].

The primary target for Cdc42 and Rac are the WASP/WAVE family of Arp2/3 complex activators [364]. Rac uses WAVE signalling to induce lamellipodia extension [365], and Cdc42 interacts with WASP causing the stimulation of Arp2/3 complex leading to dendritic actin polymerization [366]. The stimulated Arp2/3 complex allows the rapid

polymerization of actin and the formation of the branched filaments present in lamellipodia [366].

Overall, Rho GTPases are involved in the multiple stages of cancer progression, with a primary role in actin cytoskeleton rearrangement associated with cell migration and invasion, but also modulating other cellular responses, such as cell survival and proliferation. Small molecule inhibitors seem to be evolving in targeting these kinases and are considered valuable anti-cancer therapeutic approach.

1.5.4 Src and FAK signalling

The non-tyrosine kinases Src and FAK are crucial intermediates in the CXCL8 signalling pathway [367] (**Figure 13**). As previously discussed, CXCL8 stimulates members of Rho GTPases family which could lead to the stimulation of Src and FAK [143]. The induction of Src and FAK protein kinases is associated with cells proliferation and migration [368], as well as the development of metastatic phenotypes by Src [369]. Their chemotactic effect is facilitated by phosphorylating substrates involved in focal adhesion and migration [370]. FAK and Src play a crucial role in the development of solid tumours by stimulating EMT which correlates with metastatic phenotypes (review by [371]). Cells missing these two kinases appear to have greater adhesions and reduced mobility [372]. For example, fibroblasts lacking Src or FAK showed lower levels of spreading, decreased motility rates and seemingly elevated numbers of adhesions [373], [374]. Src stimulation appears to increase the growth and invasion of tumours and decrease apoptosis [369]. Moreover, CXCL8-activated rat basophilic (RBL) cells induces FAK phosphorylation and re-localization, which is linked to increased cell spreading and migration [143], [375], [376]. Further evidence suggest a role of FAK and Src in the growth of prostate cancer cells besides their chemotactic effect [367]. Actin cytoskeleton rearrangement downstream of Src contributes to growth factor and integrin signalling, for instant, cellular Src facilitate EGF-activated cellular motility, morphology, and stress fibres reorganisation [377]. Inhibition of the two kinases using anti-Src and anti-FAK antibodies have shown inhibited proliferation, angiogenesis and metastasis in human tumours [371]. Therefore, targeting Src and FAK for cancer therapy might produce promising outcomes by preventing tumour metastasis.

1.5.5 PKC and PKD signalling

The binding of chemokine to its receptor activates G protein which in turn activates PLC enzymes (**Figure 13**). Gα, particularly $G\alpha_q$ and $G\alpha_{11}$ activates PLCβ, while Gβγ activates PLCγ. PLCβ cleaves the membrane phospholipid phosphoatidylinositol-4,5-biphosphate (PIP_2) into 1, 3, 5- inositol triphosphate (IP_3) and diacylglycerol (DAG) [378]. IP_3 releases calcium from its intracellular stores, and DAG in the presence of calcium activates membrane-bound PKC [379], [380]. PKCs are a multifunctional proteins serine/threonine kinases. The family of PKC consists of 15 isoforms classified into three categories based on their second messenger requirements. Conventional PKCs (α, βI, βII, γ) requires DAG and calcium; novel PKCs (δ, ε, η, θ) requires DAG only and atypical PKCs (ζ, ι (λ)) are not directly activated by the PLCβ signalling pathway, therefore, does not require DAG or calcium for activation [381]. Instead, atypical PKCs can be stimulated by lipid components like PIP_3 [382], phosphatidic acids [383], arachidonic acid, and ceramide [384], [385]. PKCs are fundamental components in intercellular networks that mediate vast number of cellular processes. They can affect the morphology of cells thereby regulating processes such as cell migration [386]. PKC seem to also affect intracellular calcium release as reported in CCL3-induced CHO.CCR5 cells and THP-1 cells [387]. PKCα was significant for CXCL12-activated Jurkat and MCF-7 cells migration, while PKCζ is not important [388]. Conversely, PKCα was found to be crucial for PC3 cells migration according to data generated by using PKC inhibitor staurosporine [389].

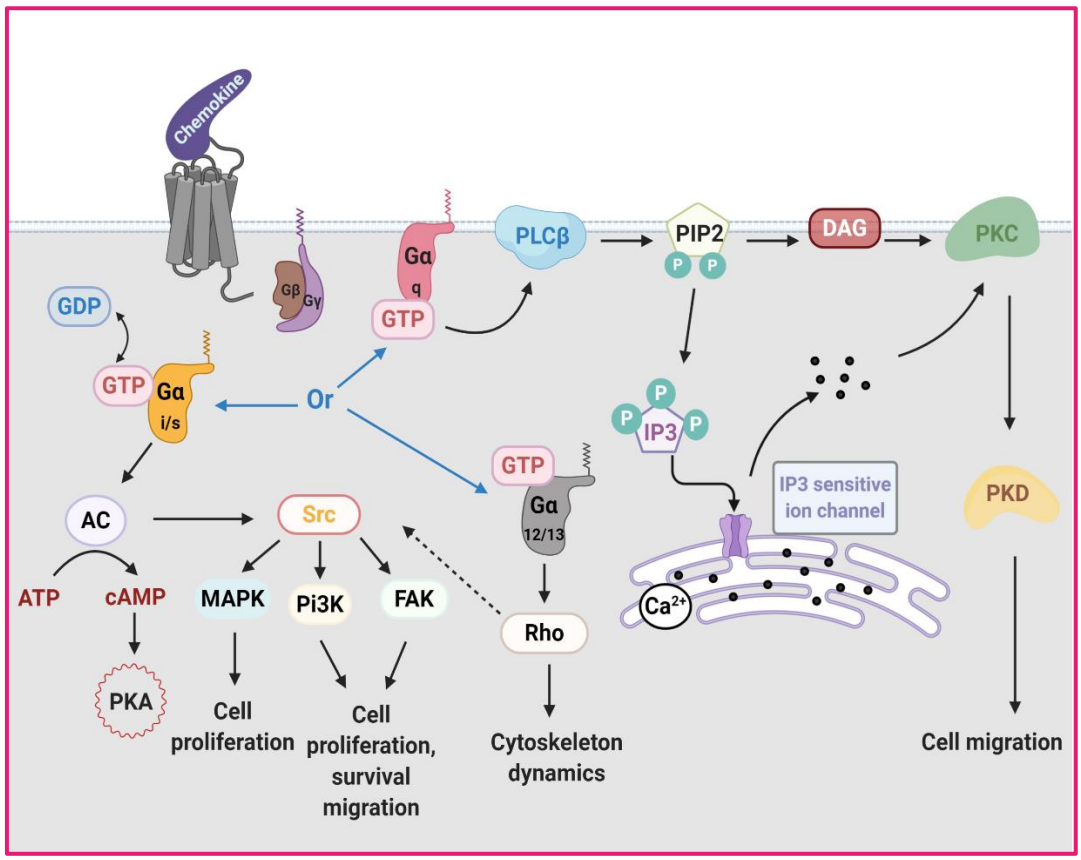

Figure 13. G protein-dependent pathways involved in chemokine intracellular signalling. Upon receptor activation, $G\alpha_q$ activates PLCβ, which hydrolyses PIP_2 to yield the two second messengers; IP_3 and DAG. IP_3 opens the IP_3 dependent Ca^{2+} channel on the endoplasmic reticulum realising Ca^{2+}. DAG, in the presence of Ca^{2+} activates membrane-bound PKC, which in turn can activate PKD [390]. The PLC/PKC/PKD signalling pathway contribute to neutrophil chemotaxis [391]. Additionally, PKC and PKD are important for the migration of CXCL12-activated PC3 cells [389]. Gβγ dimer could also activate PLCβ and IP_3 resulting in PKC activation [392]. $G\alpha_s$ and $G\alpha_i$ act through adenylyl cyclase (AC), which regulate the concentration of cAMP, thereby stimulating PKA. $G\alpha_{12/13}$ activates Rho dependent pathways [393], [394]. Rho GTPases could lead to the activation of Src and FAK upon CXCL8 binding [143]. The latter is involved in regulating the actin cytoskeleton and its interaction with the ECM [143]. In addition, $G\alpha_i$ could activate Src leading to MAPK, Pi3K and FAK [395], [396]. CXCL8 was reported to induce FAK-Src-cortactin signalling in prostate cancer cell lines [143] and was correlated with an elevated cell proliferation, survival, invasion, and migration [368], [397].

All PKCs consist of a regulatory and a catalytic domain joined together by a hinge region. The catalytic domain is highly conserved in the different PKC subsets, and the regulatory domain leads to the distinguished cellular responses between the isoforms, which are typically similar within the classes [381]. In cPKCs and nPKCs, the C1 domain sense phorbol 12-myrisate 13-acetate (PMA) and DAG, while in aPKC, the does not bind PMA and DAG [398]. The C2 domain serves as calcium-dependant phospholipid binding modules in cPKCs, whereas this domain does not bind calcium in nPKCs [381]. APKC lacks the C2 region and is activated, in part, by interaction with the Cdc42-GTP-Par6 complex through PB1 (Phox and Bem1) domain [399]. PKCs are regulated by two distinct mechanism: by phosphorylation which regulates the active site along with the subcellular localisation of the enzyme, and by second messengers, which induce the association of PKC membrane leading to pseudosubstrate exposure [398] (**Figure 14**).

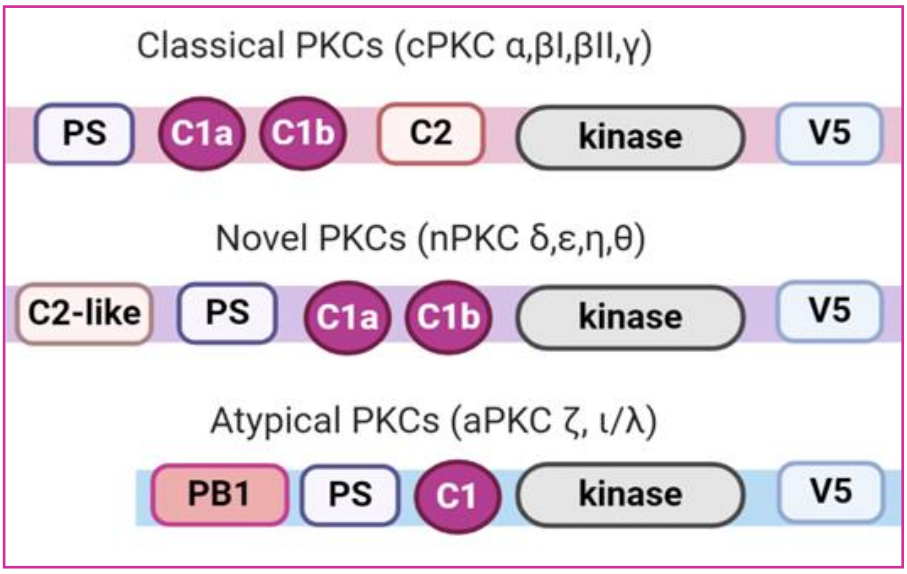

Figure 14. Structure of PKC isoforms. PKCs consist of an N-terminal regulatory domain comprising a pseudosubstrate (PS), two C1 domains (C1a and C1b) and a C2 domain. The C-terminal domain has a V5 region that is distinguished amongst the different PKC isoforms. The C2 site bind to calcium in the cPKCs, but not in nPKCs [381], [386].

The PKD family are serine/threonine kinases with a similar homology to PKC, and comprise of three isoforms: PKD1, PKD2, and PKD3. Similar to PKCs, DAG and IP3 are crucial activators of PKD, as well as growth factors and PKC isoforms [400] (**Figure 13**). Induction of PKD through oxidative stress is reported, where the activation is partly pursued through PKC-mediated activation loop phosphorylation and partly via Src-mediated PKD tyrosine phosphorylation, therefore, PKD has been identified as a sensor of oxidative stress [401], [402]. The family of kinases seem to have a vital role in regulating cellular processes including cell growth, protein trafficking, and lymphocyte biology [403]. Moreover, PKD isoforms are expressed in neutrophils, and they are important facilitators of their chemotaxis [404]. Accumulating evidence indicate the role CID755673 play in inhibiting all the three PKD isoforms and associated PKD cellular responses [405]. For example, this inhibitor reduced the migration speed of CXCL12-stimulated PC3 cells where cells also assumed an elongated appearance with PKD inhibition [389].

In all, although some studies have shed light on the importance of PKC and PKD in cancer progression, little is known about their role in chemokine-driven migration. This could be due to the complexity of the two protein kinases associated with their different isoforms which could exhibit different cellular responses (discussed further in chapter 5). To add to this complexity is the lack of specific inhibitors for the different isoforms of the two kinases.

1.6 Research objectives

Chemokines are a large family of small cytokines that are known for their essential role in mediating the directed migration of leukocytes and cancer cells [239]. Chemokine signalling contribute to cancer progression and metastasis, and their expression in both primary tumours and metastatic sites is associated with poor prognosis in cancer patient [85]. Pharmacological disruption of chemokine receptor mediated processes could be utilized for therapeutic intervention in cancer. However, the effort of targeting a chemokine or a chemokine receptor for the aim of limiting cancer cells from metastasizing has not been very promising in clinical trials [406]. This is mainly due to the redundancy of the chemokines generally binding to multiple receptors, subsequently yielding varied responses. It is also due to the inappropriate target and dosing selection [407]. Therefore, there is a need to further understand the role of chemokines and their receptors to find alternative strategies to manage their dysregulation in cancer.

The role of CXCL8 signalling in cancer progression has been widely studied. CXCL8 binds to CXCR1 and CXCR2 and is involved in various steps of cancer progression including growth, proliferation, and migration [408]. Likewise, elevated levels of CXCL10 have been reported in a range of diseases such as inflammatory, autoimmune disorders, and cancer [201], [237]. The expression of these chemokines and their effect could be cell-type specific [409], therefore, it is challenging to be conclusive with the outcomes they generate on cancer cells. The aim of this thesis is to expand our knowledge in the effect of these two chemokines in cancer cell migration. To accomplish this, the following experimentation will be undertaken:

Chapter 3: Characterise cancer cell response to CXCL8 and CXCL10. Primarily, the expression of the corresponding receptors of CXCL8 and CXCL10 will be explored. This will be followed by investigating the role of these two chemokines in inducing cancer cell migration in leukemic (THP-1 and Jurkat), breast (MCF-7 and MDA-MB231) and prostate (PC3) cancer cell lines.

Chapter 4: Examine the involvement of different signalling pathways in CXCL8-activated cancer cell migration. Small-molecule inhibitors will be used to target the different signal transduction molecules. The effect of these inhibitors for inducing cellular morphology changes will also be studied.

Chapter 5: The role of PKC in directing the migration of CXCL8 and CXCL10-activated cells was the aim of this chapter. PKC inhibitors were used to address the cytoskeletal rearrangement, cell migration, as well as the release of intracellular calcium in MDA-MB231 cells and PC3 cells.

Chapter 2: Materials and Methods

2.1 Cell lines and tissue culture

2.1.1 Acute monocytic leukaemia cell line THP-1

THP-1 cells are derived from the peripheral blood of a one-year old male donor diagnosed with acute monocytic leukaemia. THP-1 cells were purchased from the American Type Culture Collection (ATCC) (Teddington, UK). They were cultured in RPMI 1640 growth media (Corning, Biosera) supplemented with 10% v/v Foetal Calf Serum (FCS) (Invitrogen), 100 µM non-essential amino acids (Gibco) and 2 mM glutamine (Invitrogen). They were used at $60x10^4$ cell / mL.

2.1.2 Human breast adenocarcinoma cell line MCF-7

MCF-7 cells are a mammalian epithelial cancer cells that are derived from the pleural effusion of a 69-years old Caucasian woman with metastatic breast adenocarcinoma. This cell line is characterized as being non-invasive, with low metastatic ability, and are positive for oestrogen and progesterone (as reviewed by [410]). MCF-7 cells were cultured in DMEM (Corning, Biosera) supplemented with 10% v/v FCS (Invitrogen), 100 µM non-essential amino acids (Gibco) and 2 mM glutamine (Invitrogen).

2.1.3 Human breast cancer cell line MDA-MB231

MDA-MB231 cells are a human epithelial breast cancer cell line that is derived from a 51-years old Caucasian female with metastatic breast adenocarcinoma. This cell line is highly aggressive, invasive, negative for oestrogen and progesterone expression, and poorly differentiated triple-negative breast cancer cells. MDA-MB231 cells were cultured in DMEM (Corning, Biosera) supplemented with 10% v/v FCS (Invitrogen), 100 µM non-essential amino acids (Gibco) and 2 mM glutamine (Invitrogen).

2.1.4 Human Prostate cancer cell line PC3

PC3 cells are human epithelial cancer cells that are derived from a 62-years old Caucasian male suffering from bone metastasis of grade IV of prostate cancer. They are androgen insensitive and considered as a useful study model because of their aggressive migratory behaviour [411]. PC3 cells were obtained from ATCC (Teddington, UK) and were cultured using RPMI (Corning, Biosera) supplemented with 10% v/v Fetal Calf Serum (FCS) (Invitrogen), 100 µM non-essential amino acids (Gibco) and 2 mM glutamine (Invitrogen).

2.1.5 Leukemic T-lymphocyte Jurkat cell line

Jurkat cells are human T lymphocytes cells derived from the peripheral blood of a one-year-old male suffering from acute T cell leukaemia. Jurkat cells were obtained from the American Type Culture Collection (ATCC) (Teddington, UK) and were cultured using RPMI (Corning, Biosera) supplemented with 10% v/v Foetal Calf Serum (FCS) (Invitrogen), 100 μM non-essential amino acids (Gibco) and 2 mM glutamine (Invitrogen).

The previous cell lines were used to allow a comparison with different cancer types. They were used extensively for their migration ability [1], [388], [389].

2.1.6 Routine tissue culture procedures for cell lines

Both adherent and suspension cell lines were cultured in 75 cm^2 flasks (Corning) in a humidified incubator at a temperature of 37^oC with 5% CO_2. Adherent cell lines would be used when they are confluent enough, reaching around 80-90% confluency. Prior to using the cells, they would undergo detachment from the flask they are incubated in. For MDA-MB231 and PC3 cells, they would be washed with 4 mL PBS (1.5 mM potassium phosphate monobasic, 3 mM potassium phosphate dibasic, 150 mM NaCl; pH 7.2, at room temperature), then incubated with 2 mL 0.25% Trypsin/EDTA (Gibco). MCF-7 cells would be detached with PBS/EDTA. Cells would be incubated for around 10 mins at 37^oC with 5% CO_2. Flasks would then gently be tabbed to suspend the cells. To harvest the cells, they would be centrifuged at 800 g for 5 mins, discarding the supernatant, and the pellet resuspended in the relevant growth medium. Cells' wellbeing would be detected microscopically, and haemocytometer would be used for counting them.

Suspension Jurkat cells would be used after one day of passaging them or until they reach the density of 1 x 10^6 /mL, as they proliferate fast. THP-1 cells take around 2-3 days to be ready for performing experiments on them. Prior to the purpose of using the cells, they would be centrifuged at 800g for 5 mins and the pellet resuspended in relevant growth media.

For cells' freezing to be cryopreserved, 1 X 10^6 of cells would be centrifuged, pellet resuspended into 1 mL of 10% v/v DMSO in FCS and transferred into cryotubes. To slow down the sudden freezing process, cryotubes would be wrapped in multiple tissue layers and frozen at -80^oC for at least 24 hrs before long-term storage in liquid nitrogen at -196^oC.

2.2 Migration assays

2.2.1 Wound healing assay

The migratory potential of cells in the presence of CXCL8 was investigated by wound healing assay. 24 well plates were marked on its outside bottom surface with two parallel lines (with permanent marker) to form a reference point when analysing images of wound closure. Cells would be harvested, centrifuged, washed, and resuspended in growth media at a density of 6 x 10^5 cells per mL. Cells were seeded into the prepared 24 well plates, and 1 mL of cells would go in the wells, and incubated at 37°C, 5% CO_2 for 24 hrs till they form a monolayer with minimum gaps. Three scratches across the marked lines were introduced to each of the wells, with a sterile pipette tip. Afterwards, the media would be removed and very gentle washing with PBS to remove debris from scratch induction or any dead cells. Cells were then immersed with 200 µL serum deprived media and the scratches made were imaged with duplicates for each treatment using an inverted Leica DMII fluorescence microscope in bright field at 10X magnification. As a reference point, the parallel lines drawn on the bottom of the well were used to refer to the same spot across different time-points. Chemokines and inhibitors or antagonists were added to the wells at their working concentrations. After 24 hrs of incubation with the compounds, media would be removed and cells would be hydrated with PBS (100 µL), images were taken again. To quantify the effect of the treatments on the wound healing process, before and after images of 0 and 24 hrs time-points were analysed and compared using Microsoft PowerPoint by measuring the width of wounds. Results were presented in a ratio where 1 indicates no migration and any number lower indicates migration. The experiment was repeated four times.

2.2.2 Chemotaxis migration assay using ChemoTx® plate

Suspension cells were tested for their directed migration ability using ChemoTX 5 µm pore chemotaxis plates (ChemoTx® System from Neuro probe Inc, USA). The lower chambers of the chemotaxis well plate was blocked with 30 µL 1% BSA blocking buffer (in simple RPMI) for 30 mins at room temperature. Chemokines were diluted in 0.1% BSA working buffer (in simple RPMI) at 1 nM for CXCL10 and 5 nM for CXCL8, depending on the experiment. Then 31 µL of the diluted chemokine was loaded on the wells. THP-1 or Jurkat cells were collected, centrifuged and diluted in working buffer to a concentration of 25 x 10^4 cell /mL. Cells were incubated with the inhibitor treatment or vehicle for 30 mins at 37 °C before loading. 20 µL cells were then administrated on to the top chamber of the polyvinylpyrrolidone-free polycarbonate filter (5 µm pores). The chemotaxis plate was incubated at 37 °C, and 5% CO_2 for 5 hrs to allow cells to migrate. The filter was then removed and 10 µL from the wells was loaded onto a Neubauer

haemocytometer and counted, demonstrating the number of migrating cells. All the experiments were repeated at least three times.

2.2.3 Transwell migration assay using Boyden chamber

Transwell migration assay was conducted using Falcon 8.0 µm pore size cell culture inserts (Thermo Fisher Scientific). Initially, adherent MDA-MB231 cells were harvested, and resuspended in simple DMEM media containing 0.1% BSA to a density of $1x10^6$ per well. Inserts were positioned in a 24 well plate. Cells were treated with an equivalent amount of antagonists prior to loading for 30 mins at 37 °C and 5% CO_2. 200 µL of cell solution was poured on top of the filter membrane into the inserts and incubated for 10 mins at 37 °C and 5% CO_2, for cells to settle. 600 µL of simple media with 0.1% BSA was added to the lower chamber with equivalent amount of chemokine (10 nM for CXCL8) and incubated for 24 hrs at 37 °C and 5% CO_2. Culture media was removed and replaced with 300 µL DMEM with 0.1% BSA, in addition to 4 µM Calcein AM (Cambridge Biosciences) for 45 mins. Inserts were removed from the plate and with a cotton swab, the top remaining cell suspension was removed. Inserts were transferred into fresh wells containing 0.25% Trypsin/EDTA and incubated for 10 min at 37°C, and 5% CO_2. Cells that have migrated over the 24 hrs hour will be detached by the Trypsin/EDTA. 200 µL of the detached cells in the bottom chamber were transferred to opaque reader plate (Thermo Fisher Scientific) and measured at a ratio of the fluorescence detected at 530nm/ 410nm using BMG Labtech Fluorostar Optima plate reader (BMG Labtech, Germany).

2.2.4 Agarose Spot Migration Assay

The agarose spots solution was initially made by melting 0.5% of low-melting point agarose (Sigma- Aldrich, Germany) in PBS. The mixture was heated and stirred until complete dissolution, then cooled down to 40°C. The chemokine required was diluted in 0.1% BSA in PBS, then added into the agarose solution to give a stock concentration of 1 µM. The control sample contained 0.1% BSA in PBS added in equivalent volume to the agarose solution.

Prior to the addition of the spots, a 35 mm plate was marked across with a marker pen and labelled with the position of where the samples were going to be spotted (**Figure 15**). 2 mm was cut off a 200 µL pipette tip followed by the transfer of 10 µL of the viscous molten agarose solution with the chemokine into the position labelled and the control spot was added to the other side. The plate was then left to cool at 4°C for 5 min for the spots to settle. Adherent cells at a number of $1.7x10^5$ were suspended in 1 mL of complete media and gently placed over the agarose spots. The liquid tension will prevent the spots from crushing. After 4 hrs of incubation, the medium was replaced with 0.1% FCS in DMEM and incubated overnight at 37°C and 5% CO_2. Visualisation was performed using an inverted Leica DMII fluorescence microscope. Cells that invaded the agarose spot were analysed by imagining different fields of the spot to cover the whole circumference and cells were counted using Fiji/ImageJ.

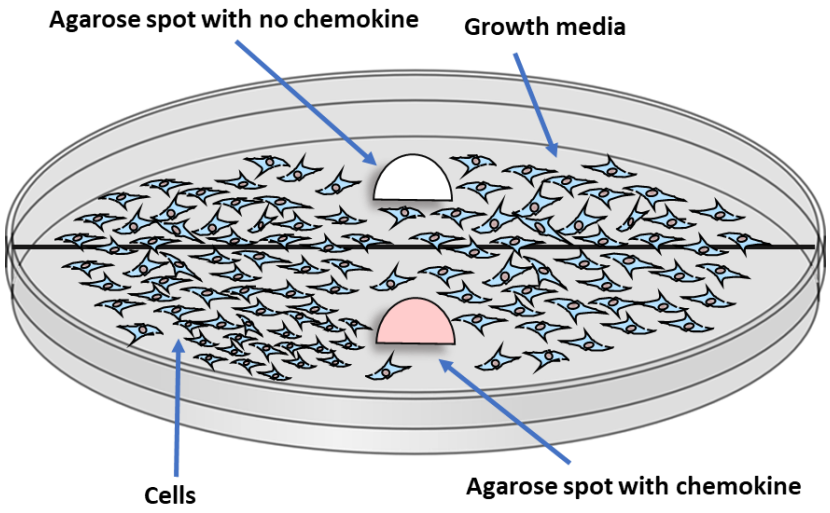

Figure 15. Schematic representation of agarose spot migration assay. Cells were seeded, and two agarose spots were loaded on a 35 mm petri dish, with or without the chemokine. After overnight incubation, migrating cells towards the agarose spot were visualised and images were taken of different fields of the circumference of the spots.

2.2.5 Oris migration assay

PC3 and MDA-MB231 cells were harvested using a relevant agent and resuspended in RMPI or DMEM growth media, respectively, to a density of $5x10^4$ /mL per well. Pipette 100 µL of the cell suspension into one side of the Oris™ Seeding Stopper (Platypus Technology). The cells were left to adhere overnight at 37°C and 5% CO_2. The role of the gel stoppers is to generate a detection empty area for the cells to settle around (**Figure 16**). Afterwards, the medium was removed, and the gel stopper was removed as well gently with a sterile tweezer. 100 µL of relevant fresh medium was added along with 10 nM CXCL8, CXCL9, CXCL10 or CXCL12 and incubated overnight at 37°C and 5% CO_2. Medium was removed and 100 µL of PBS was added with 4 µM calcein to stain the cells for 45 mins in the incubator at 37°C and 5% CO_2. Wells were then washed and replaced with 100 µL PBS. For imaging purposes, light field or fluorescence microscopy was used to take images of the cells migrating with inverted Leica DMII fluorescence microscope. However, for quantification, cells that migrated were measured by limiting the reading area to the detection zone by applying an Oris™ Detection Mask and the ratio of the fluorescence detected was measure at 530nm/ 410nm using BMG Labtech Fluorostar Optima plate reader (BMG Labtech, Germany).

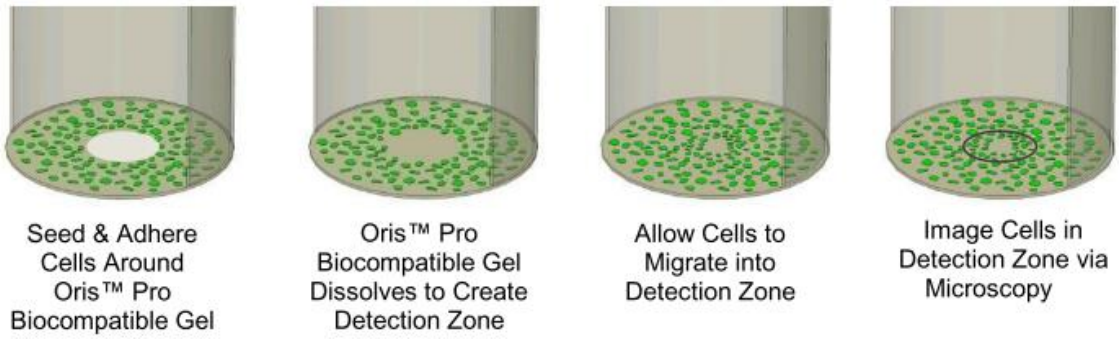

Figure 16. Steps of Oris™ Migration Assay. Cells grown around a gel stopper attached to the wells. After cells adherence, the chemoattractant was added with the removal of the gel stopper. Cells would migrate towards the centre of the detection zone. Images or quantification of the detection area using calcein was used for analyses of the migrating cell. Schematic is taken from [412].

2.2.6 Time-lapse cell migration assay

The effect of CXCL8 and CXCL10 on the migration speed of the cells was observed using time-lapse video microscopy. MDA-MB231 and PC3 cells were seeded out in a 24-well plate in complete RPMI and DMEM media, respectively, for 24 hrs at 37 °C. Equivalent concentrations of the inhibitors (as indicated in **Table 4**) were added to the cells followed by the addition of CXCL8 (10 nM) or CXCL10 (10 nM). Using Carl Zeiss AxioVision Rel. 4.8 software, time-lapse images were taken every 4 mins for 10 hrs at 10x objective in a controlled chamber of 37°C, and 5% CO_2. Time-lapse videos created were analysed using Fiji/ImageJ software where 10 cells in each video were tracked manually throughout the video frames. The speed sum of each individual cell was averaged over the course of experiments - sum of the distance of 10 cells/ time (10 hrs) = Speed All the experiments were repeated at least four times.

2.2.6.1 Cell morphology analysis

From the previous time-lapse migration assay experiments, the videos generated were reanalysed for the observation and quantification of the cellular morphology. Cell morphology was measured using Fiji/ImageJ. The last frame of the videos indicating 10 hr of cells migration was screenshotted. Using the free hand drawing option, cells were drawn around and measurements of area, aspect ratio and circularity were made using the Analyse and Set measurement options. Subsequently, these parameters were averaged for 70 cells per image per experiment and the experiments were repeated at least three times.

2.2.6.2 Cell proliferation analysis

Upon performing the time-lapse migration assay to test for the speed of migrating cells towards the CXCL8 or CXCL10, the videos generated were reanalysed for the observation of the mitotic behaviour of the cells. Two images were obtained by taking screenshots of 0 hr time-point and 10 hrs time-point from the time-lapse videos (section 0) using Fiji/ImageJ. Screenshots were obtained using the slice remover function from the tool's menu. Subsequently, the pointer clicker was customized to give a red cross mark on the cells counted and added to the region of interest manager to keep track of the number of cells. Thereafter, the number of cells in the picture frame were compared between the treated and control cells.

2.3 MTS cytotoxicity assay

MTS assay was performed using a CellTiter 96 AQ_{ueous} Non-Radioactive Cell Proliferation Assay (Promega). 100 µL cells were seeded at 1 x 10^5 mL^{-1} in complete RPMI medium for PC3 or THP-1 cells, and DMEM for MDA-MB231 and MCF-7 cells in a round (for suspension cells) or flat (for adherent cells) bottomed clear 96 well plate (Sterilin Ltd, UK). Treatment of antagonists or inhibitors were added to the cells and incubated at 37°C and 5% CO_2. To validate the toxicity of the treatments on the cells, 10 µL of the MTS reagent (3-(4,5-Dimethylthiazol-2-yl)-5-(3-carboxymethoxyphenyl)-2-(4-sulfophenyl)-2H-tetrazolium) was added to each well and incubated for 2 hrs. Cytotoxicity of the test compounds will be decided on the viability of the cells over the incubation period. The viability of cells is defined by the metabolism of the MTS reagent to formazan, which is read at 490 nm, and compared to the compound-tested cells.

2.4 Calcium flux

Cells were harvested and centrifuged at 800 g for 5 min. The supernatant would be removed, and cells would be washed twice with calcium flux buffer (148 mM NaCl, 5 mM KCl, 2.5 mM CaCl2, 10 mM HEPES, 1 mM glucose, pH 7.4, stored at 4°C), and re-suspended in 1 mL of the calcium flux buffer. Cells were treated with the required concentration of the antagonist or inhibitor and loaded with a final concentration of 4 µM Fura-2 dye (Invitrogen). They were then incubated at 37ºC and 5% CO_2 for 30 mins. Thereafter cells were centrifuged and washed twice to remove excess Fura-2, then re-suspended in 1 mL calcium flux buffer. 100 µL of cells were added to a 96 well black plate (ThermoFisher Scientific) before calcium flux assessment using BMG Labtech Fluorostar Optima plate reader. (BMG Labtech, Germany). The Fluorometer injection was previously washed with H_2O few times, then primed with the chemokine. The fluxes in intracellular calcium release were characterised by radiometric analysis of alterations in fluorescence sequentially stimulated at an excitation and emission wavelengths of 340 nm (bound Fura-2) and 380 nm (unbound Fura-2) and measured at 510 nM. Data was analysed as the difference of fluorescence before stimulation at 340 nM and after stimulation and after stimulation at 380 nM using BMG Optima software.

2.5 Imaging Techniques

2.5.1 Phalloidin actin stain

Cells were harvested after reaching around 90% confluency. MDA-MB231, PC3, and MCF-7 cells were seeded onto 12 well plate with glass coverslips and 1500 mL growth media. Inhibitors were added with or without CXCL8 or CXCL10 (10nM) to the wells and left to incubate for 10 hrs at 37°C and 5% CO_2. Afterwards, the media was removed, and cells were washed gently in PBS (stored at 4ºC). Cells were fixed with 500 µL of 4% paraformaldehyde for 10 mins. Cells were then washed again with 1 mL PBS (4ºC), and permeabilized with 200 µL 0.1% Triton x-100 solution (FischerBiotech) for 10 mins. They were then washed again with 1 mL PBS (4ºC) and stained with 1:100 Phalloidin-iFlour 488 Conjugate (Abcam) in PBS and left to incubate in the dark for 30 mins at 4 ºC. If required, nucleus stain of the cells happened after washing the wells twice with 1 mL PBS (4ºC) and stained with DAPI (4',6 diamidino-2-phenylindole) (Sigma Aldrich) at 1:5000 for 5 mins at 4 ºC. Final washing of excess stain with 1 mL PBS (4 ºC) followed by extracting the coverslips gently with tweezers and mounting on a glass slide with DPX (ThermoFisher Scientific). Coverslips were mounted onto glass slides with DPX mounting media (Fisher Scientific). Stained cells were then imaged using inverted Leica DMIL fluorescence microscope.

2.5.2 Immunofluorescence staining

MDA-MB231 and PC3 cells were harvested in a relevant agent after reaching around 90% confluency. MDA-MB231 and PC3 cells were seeded onto 12 well plate with glass coverslips and 1500 µL growth medium. Cells were fixed with 500 µL of 4% paraformaldehyde for 10 mins, while being incubated at 4 °C. After incubation cells were washed with 1 mL PBS (4ºC) and blocked with primary antibodies of IL-8RA (CXCR1) antibody (SC-7303, Santa Cruz); IL-8RB (CXCR2) antibody (SC-7304, Santa Cruz), or CXCR-3 (H-1) antibody (SC-133087, Santa Cruz) at 1:100 dilution. Well plate was incubated for 1 hr at 4°C in the dark. Afterwards, cells were washed with 1 mL PBS (4ºC) and incubated with the corresponding secondary antibodies of Alexa Fluor 488-conjugated goat anti-mouse IgG (Abcam, Cambridge, MA) at a ratio of 1:1000. Cells were further washed with 1 mL PBS (4ºC) and incubated with DAPI (Sigma Aldrich) at 1:5000 for 5 mins at 4 ºC. Coverslips were mounted onto glass slides with DPX mounting media (Fisher Scientific). Final washing of excess stain with 1 mL PBS (4 ºC) followed by extracting the coverslips gently with tweezers and mounting on a glass slide with DPX (ThermoFisher Scientific). Stained cells were then imaged using inverted Leica DMIL fluorescence microscope.

THP-1 cells were harvested and centrifuged and the same process was applied to them except they were stained in their eppendorfs instead of in a well plate. 40 µL of the stained cells were loaded on the mounting buffer DPX (ThermoFisher Scientific) on a glass slide, allowed to dry and imaged using Leica DMII fluorescence microscope.

2.6 Chemokines, antibodies, and small molecules

Table 2. List of chemokine and their cognate receptors. Chemokines were made up in purified water.

Chemokines	Supplier	Chemokine Receptor
CXCL8 (IL-8)	Gift from K. Schmitz (TU Darmstadt) [413]	CXCR1, CXCR2
CXCL9 (IP-9)	PeproTech	CXCR3
CXCL10 (IP-10)	PeproTech	CXCR3
CXCL11 (IP-11)	PeproTech	CXCR3
CXCL12 (SDF1-α)	PeproTech	CXCR4, CXCR7

Table 3. List of antibodies. For immunofluorescence assay

Primary Antibody	Protein Target	Dilution Factor	Supplier	Species raised in	Storage
IL-8RA sc-7303	Human CXCR1	1:100	Santa Cruz	Mouse	4°C
IL-8RB sc-7304	Human CXCR2	1:100	Santa Cruz	Mouse	4°C
CXCR3 (H-1) sc-133087	Human CXCR3	1:100	Santa Cruz	Mouse	4°C
Secondary Antibody	**Antibody specificity**	**Dilution Factor**	**Supplier**	**Species raised in**	**Storage**
Anti-mouse IgG (Alexa Fluor 488)	mouse	1:1000	Abcam, Cambridge, MA	Goat	-20°C

Table 4. List of small molecule inhibitors.

Inhibitor	Target	Supplier	Working conc
L779450	Raf	Abcam	100 nM
ZM336372	Raf	Santa Cruz	1 μM
PD98059	MEK	Abcam	25 μM
SL327	MEK	Abcam	1 μM
SB203580	p38 MAPK	Tocris	1 μM
FH535	B-catenin	Abcam	1 μM
Staurosporine	PKC	Tocris	10 nM
GF109203X	PKC	Tocris	5 μM
PKCζi	PKC	Calbiochem	10 μM
CID755673	PKD	Tocris	11 μM
PF562271	FAK	Abcam	10 nM
Bosutinib	Src	Shellek chemicals	1 μM
NSC23766	Rac1	Tocris	100 μM
EHT1864	Rac1	Cambridge Biosciences	100 nM
ZCL278	Cdc42	Tocris	20 μM
CCG 1432	RhoA	Tocris	1 μM
Y27632	ROCK	Tocris	20 μM
CPYPP	DOCK1/2/5	Tocris	100 μM
LY294002	Pi3K	Tocris	10 μM
AKTi	AKT	Abcam	20 μM
CK666	Arp2/3	Tocris	80 μM
H89 HCL	PKA	Tocris	10 nM

2.7 Statistical data analysis

Data analysis was performed using GraphPad Prism V6 software (La Jolla, CA). Unpaired t-test was used to analyse two-variables while One-way ANOVA with *post-hoc* Dunnett's multiple comparison was performed on three or more variables. Kruskal-Wallis non-parametric test with post Dunn's multiple comparison tests were applied for normalized values. 95% was considered a value for significance in all statistical tests performed with *p-value* indicating no significance $p > 0.05$, * = $p \leq 0.05$, ** = $p \leq 0.01$, *** = $p \leq 0.001$, and **** = $p \leq 0.0001$. Data represents the mean ± standard errors of means (SEM) at least three independent experiment repeats.

Chapter 3: Characterisation of cancer cell response to CXCL8 and CXCL10

3.1 Introduction

Chemokines were first described as chemoattractant cytokines, which play a key role in guiding the movement of leukocytes under basal and inflammatory conditions [79]. CXCL8 was identified as a neutrophil-activating factor and is produced by a plethora of cell types including keratinocytes, fibroblasts, neurons, endothelial cells, epithelial cells, smooth muscle cells, hepatocytes, and melanocytes (as reviewed by [280]). CXCL8 binding to the G-protein coupled receptors CXCR1 and CXCR2 expressed on these cells may participate in modulating various steps of cancer progression including growth, proliferation, and migration [408]. CXCL8 has been documented to stimulate angiogenic responses in endothelial cells, as well as increasing the growth, survival, and migration of both endothelial and cancer cells [143], [280], [414], [415]. Likewise, elevated levels of CXCL10 have been reported in a diverse range of human diseases such as infectious, inflammatory, autoimmune disorders, and cancer [237], [416], [417]. CXCL10 has a crucial role in the recruitment and homing of leukocytes to the inflamed area, but this recruitment can result in significant tissue damage [201]. CXCL10, together with CXCL9 and CXCL11, bind to CXCR3, which has been associated with malignant melanoma, ovarian carcinoma, multiple myeloma, B-cell lymphoma, and basal cell carcinoma (as reviewed by Liu *et al.* [237]). In this chapter, we investigated the expression of CXCL8 and CXCL10 receptors on cancer cells, the effect of activating these receptors on intracellular calcium release, along with their effect on the migratory behaviour of different cancer types.

Cell migration is crucial to many biological processes including, wound healing, embryogenic development, and immune defence. However, cell migration also significantly contributes to tumour progression. Therefore, the migratory capacity of a tumour cell is an important indicator of its potential to metastasize [418]. Three forms of locomotion can characterize cell migration: random, kinesis, and chemotaxis. Random motion happens in the absence of environmental stimuli. Kinesis, specifically chemokinesis, is a random motion that is influenced by a chemical stimulus. While chemotaxis is a directed movement of cells towards a gradient of a stimulus [282]. Here we present different *in vitro* migration assays to study the migratory behaviour of various cancer cell types. They are based on two-dimensional (2D) methods including the wound healing assay, chemotaxis, Boyden chamber assay, Oris migration assay, and agarose

spot assay. However, these protocols have temporal limitations and do not allow the acquisition of migratory information in real-time. Here, we tracked individual cells using *in vitro* 2D time-lapse real-time cell imaging. The suitable cell type for each of these protocols is presented, and all the data acquired by these protocols is accompanied by an explanation on the troubleshooting and analysis process.

Chapter Aims:

Investigate the response of various cancer cell types to CXCL8 and CXCL10.

Optimise migration assays for different cancer cell types to study the chemotactic effect of CXCL8 or CXCL10.

3.2 Results

3.2.1 Characterising the response of cancer cells to CXCL8

3.2.1.1 The response of THP-1 cells to CXCL8

3.2.1.1.1 Expression of CXCR1 and CXCR2 receptors on THP-1 cells

THP-1 cells are non-adherent, acute monocytic leukaemia cells that are a well-established model for studying the behaviour of monocytes [419]. They share common features with normal human monocytes, such as their morphology, expression of plasma membrane receptors and cytokines [420]. Using semi-quantitative analysis of receptor mRNA expression, THP-1 monocytes showed strong expression of CXCR2 mRNA but not CXCR1 [421]. These results by other research groups agree with our immunofluorescence observations whereby CXCR2 was detectable on THP-1 cells, but CXCR1 was not (**Figure 17**). Whilst CXCR1 expression was not visible in THP-1 cells, MDA-MB231 cells clearly express this receptor (**Figure 25**).

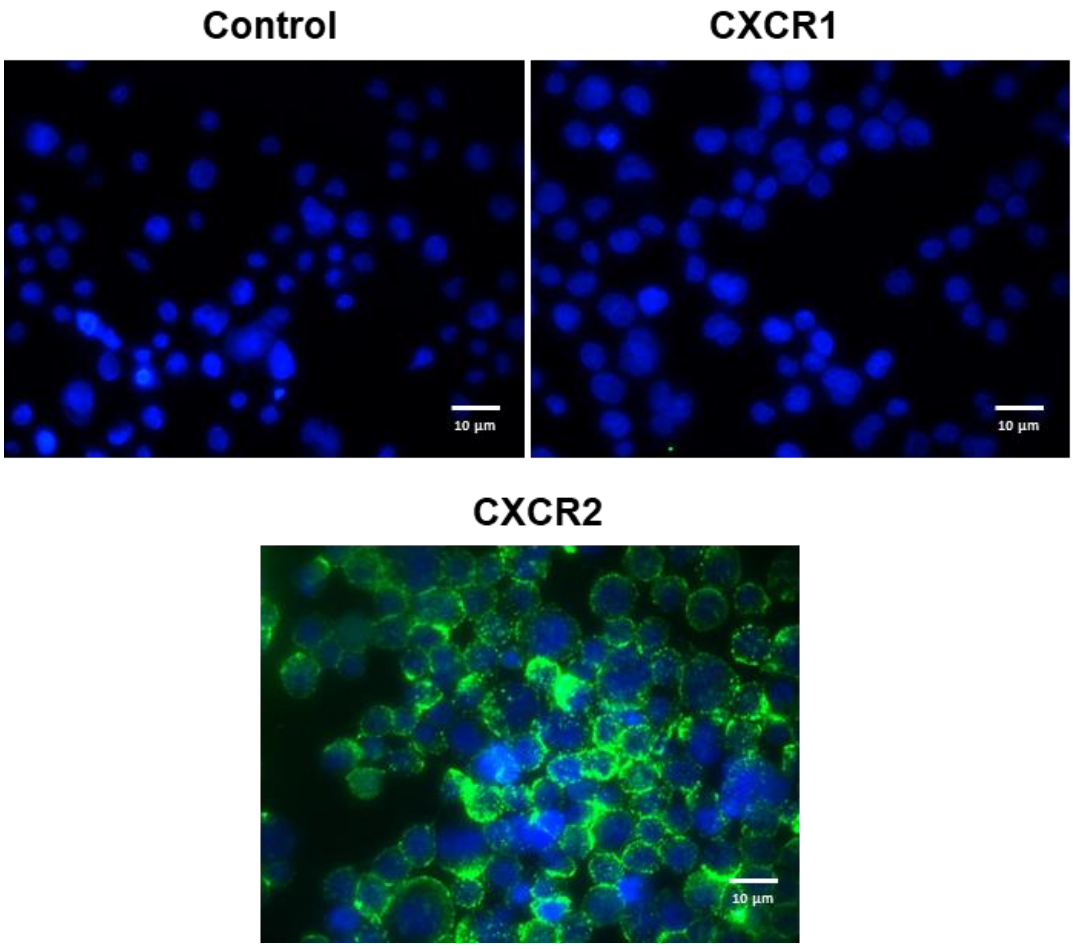

Figure 17. THP-1 cells express CXCR2 but not CXCR1. Immunofluorescence staining of the THP-1 cell line using anti-CXCR1, or anti-CXCR2 and their corresponding secondary anti-mouse Alexa-488 conjugated antibodies (green). Control represents anti-mouse Alexa-488 alone. The nucleus was stained with DAPI (blue). Images are representative of the cell population of one experiment from three independent experiments, acquired at 63x objective using a Leica DMII fluorescence microscope and Leica imaging suite.

3.2.1.1.2 THP-1 cells migrate towards CXCL8, and inhibiting CXCR1 and CXCR2 reduces the number of migrating cells

Tumour progression is determined by the interaction of cancer cells with the host microenvironment. Several reports have demonstrated the impact of chemokines not only on the motility of endothelial cells, and thus angiogenesis, but also chemotaxis of cancer cells [418]. Therefore, chemotaxis assay was used to identify the directed migration of THP-1 cells. Results showed that treating THP-1 cells with CXCL8 (5 nM) for five hrs resulted in an almost two-fold increase in the number of migrating cells when compared to un-treated basal cells (**Figure 18**).

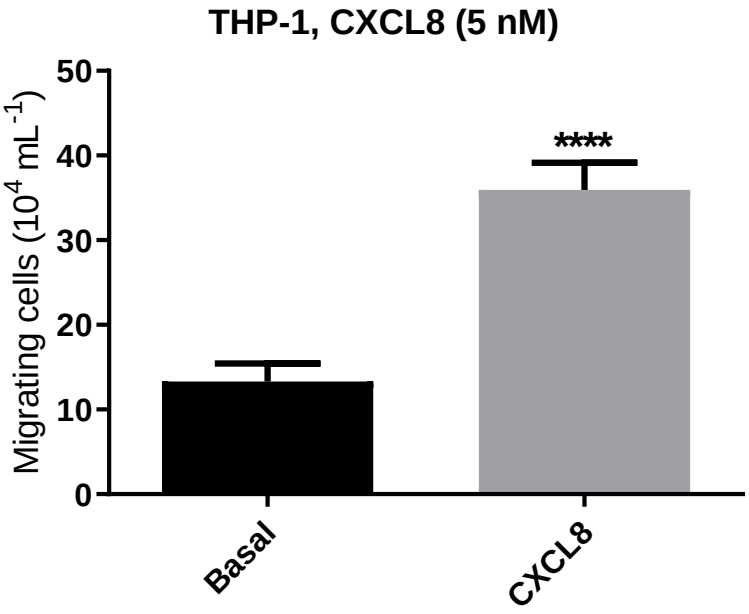

Figure 18. CXCL8 increases the migration of THP-1 cells in a chemotaxis assay. The number of migrating THP-1 cells increased significantly after 5 hrs incubation in the presence of CXCL8 (5 nM) in a ChemoTx® System relative to the unstimulated cells. Data shown are the mean ± SEM of six independent experiments. (Unpaired t-test, **** = $p \leq 0.0001$).

Reparixin is a low molecular weight inhibitor of human CXCL8 receptor activation [162]. It inhibits CXCL8-induced migration and calcium flux in human and rat neutrophils [422]. SCH527123 is a potent small molecule and allosteric antagonist of both CXCR1 and CXCR2. It was applied for the treatment of inflammation arising from neutrophil infiltration [163]. This compound has also been shown to inhibit colon cancer metastasis, decrease tumour neovascularization, and induce tumour cell death in mouse models [423]. Additionally, Reparixin and SCH527123 have been used in clinical trials to inhibit the development of breast, colon, and colorectal cancer [424]–[426]. Moreover, SB225002, the first non-peptide antagonist of CXCR2 has also been identified [427]. This compound blocked CXCL8 binding to recombinant and native CXCR2, as well as inhibited CXCL8-induced chemotaxis of neutrophils *in vitro* and *in vivo* [427]. The concentrations of these antagonists chosen took into consideration the IC_{50} for each compound, previously tested concentrations in other studies, and the toxicity on our cell lines.

To investigate the effect of CXCR1 and CXCR2 antagonists; Reparixin, SCH527123, and SB225002 on the migration of THP-1 cells. Cells were pre-treated with the antagonist for half an hour prior to loading onto the chemotaxis filter, while CXCL8 (5 nM) was present in the bottom chamber. There was a significant increase in the number of migrating cells upon stimulation with CXCL8 ($p \leq 0.05$) compared to untreated basal cells. All of the three antagonists were able to decrease the migration of THP-1 cells, but only SCH527123 and SB225002 could significantly impact the number of cells migrating towards the CXCL8 gradient (**Figure 19**).

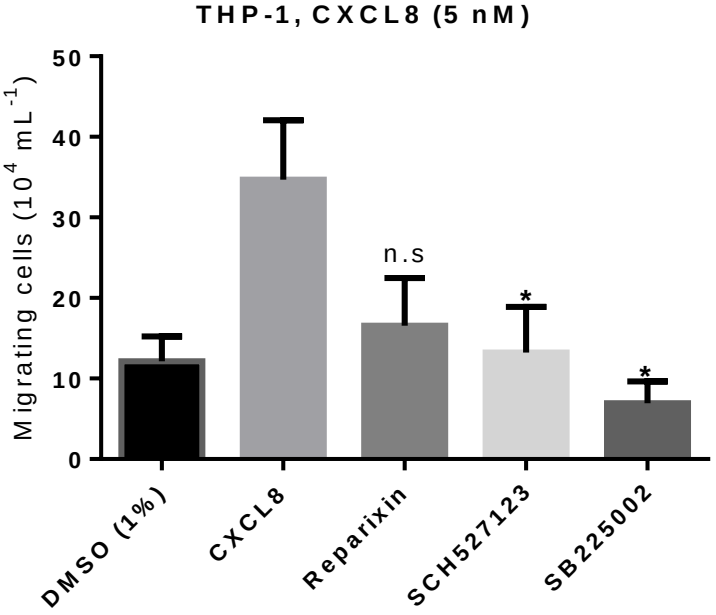

Figure 19. CXCR1 and CXCR2 antagonists reduce the migration of THP-1 cells towards CXCL8 in a chemotaxis assay. The multiple comparison test conducted after 5 hrs incubation with CXCL8 (5 nM) and inhibitors showed that SCH527123 (20 μM) or SB225002 (1 μM) significantly reduced the number of migrating CXCL8-stimulated THP-1 cells. Reparixin (15 μM) also impacted the migration of cells but not significantly. Comparison was made against CXCL8. 1% DMSO was added to the basal cells as a vehicle control. Data shown are the mean ± SEM of at least 3 independent experiments. (One-way ANOVA with a Dunnett's multiple comparisons test as post-test, n.s.= no significance $p > 0.05$, * = $p \leq 0.05$).

3.2.1.1.3 CXCL8 promotes intracellular calcium responses in THP-1 cells

Upon CXCL8 binding to CXCR1 or CXCR2, GPCR signalling pathways are stimulated which induces downstream events such as chemotaxis, intracellular calcium release, and/or receptor internalisation [130]. The downstream release of calcium has been used for many years as an indicator of chemokine receptor activation [386]. **Figure 20** shows the release of intracellular calcium upon the addition of CXCL8 in a concentration-dependent manner. The release of calcium increases with the elevation of the CXCL8 concentration, but the curve does not plateau because the maximum is not reached.

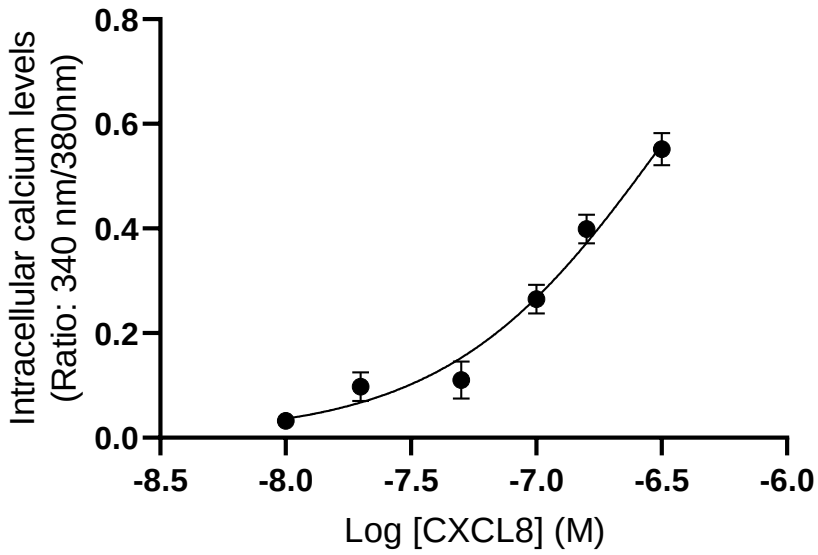

Figure 20. Intracellular calcium response of THP-1 cells following treatment with varying concentrations of CXCL8. Data is expressed as changes in fluorescence ratio (340 nm/380 nm) upon incubation with 4 µM Fura-2 for 30 min. The basal fluorescence, prior to the addition of CXCL8, is subtracted from the peak fluorescence following injection with CXCL8. Data represent mean ± SEM from four independent experiments. (Non-linear regression dose-concentration response curve assuming a Hill coefficient of 1).

3.2.1.1.4 CXCR1 and CXCR2 antagonists block intracellular calcium flux in CXCL8-treated THP-1 cells

We next determined the effect of blocking CXCL8 receptors on the intracellular calcium responses. We observed that inhibition with Reparixin (15 μM) could reduce the release of intracellular calcium upon activating the receptor with CXCL8 (200 nM; **Figure 21a**). Similarly, significant reductions in the ability of CXCL8 to stimulate intracellular calcium release were observed following inhibition with SCH527123 (20 μM; **Figure 21b**) and SB225002 (1 μM; **Figure 21c**).

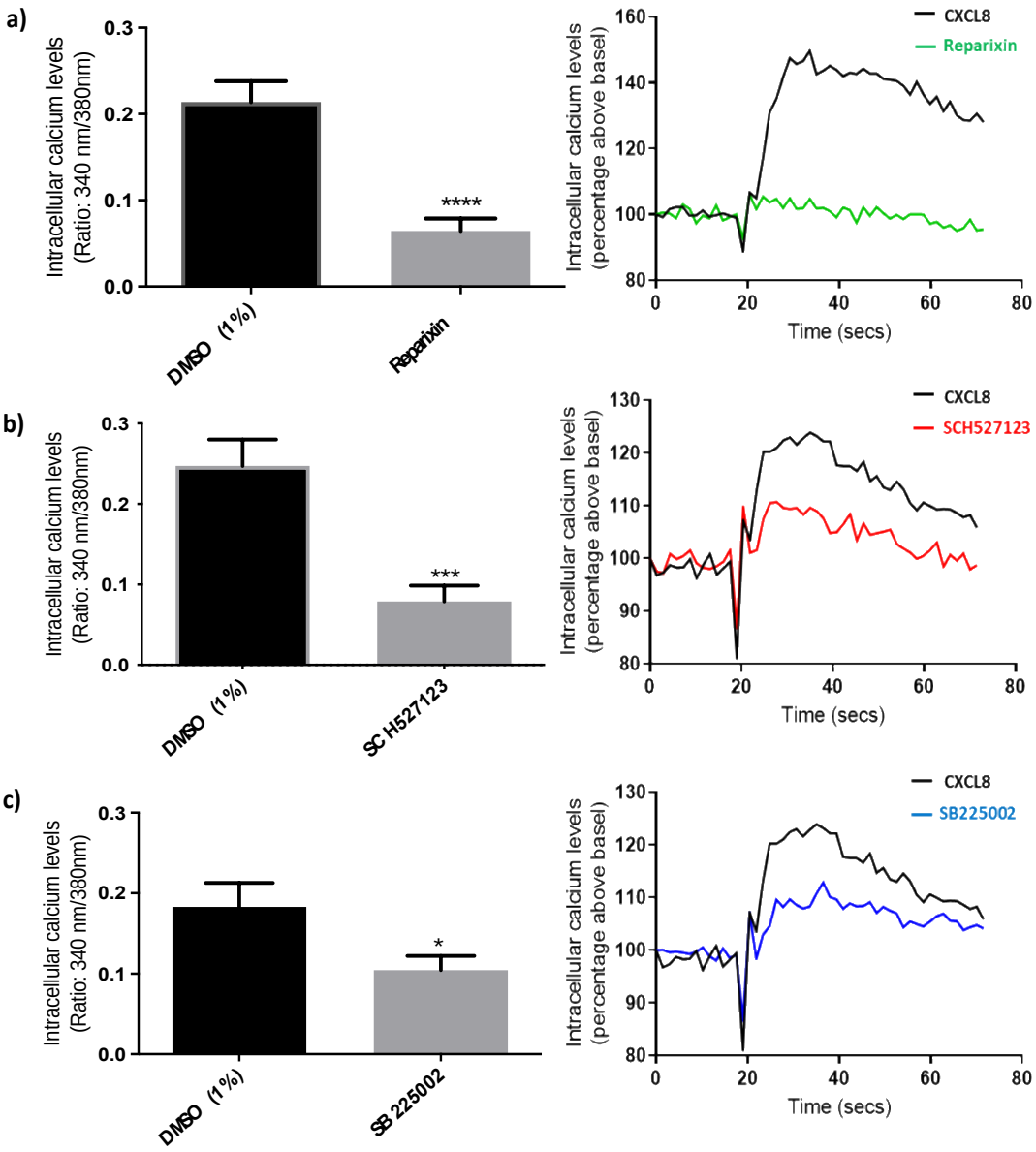

Figure 21. CXCR1 and CXCR2 antagonists reduce intracellular calcium release in CXCL8-stimulated THP-1 cells. Pre-treatment for 30 mins with **a)** Reparixin (15 μM), **b)** SCH527123 (20 μM), and **c)** SB225002 (1 μM) significantly reduce the release of calcium when activated with CXCL8 (200 nM). Intracellular calcium measurement traces are taken from a representative experiment. 1% DMSO was added to CXCL8. Data represents the mean ± SEM of nine independent experiments. (Unpaired t-test ** = $p \leq 0.01$, *** = $p \leq 0.001$, **** = $p \leq 0.0001$).

3.2.1.1.5 Toxicity of CXCR1 and CXCR2 antagonists towards THP-1 cells

An MTS assay was performed to test the cell toxicity of CXCR1 and CXCR2 antagonists on THP-1 cells. Treatment of THP-1 cells with increasing concentrations of SCH527123 and SB225002 resulted in a cytotoxic effect, while Reparixin up to 30 µM was not cytotoxic (**Figure 22**). The concentrations used in our experiments demonstrated no cytotoxicity because the IC_{50} and concentrations used in previous studies were taken into consideration [428], [429]. In this study, Reparixin concentrations up to 30 µM were tolerated, SCH527123 became toxic at 30 µM, and SB225002 demonstrated toxicity at concentrations of 2 µM onwards.

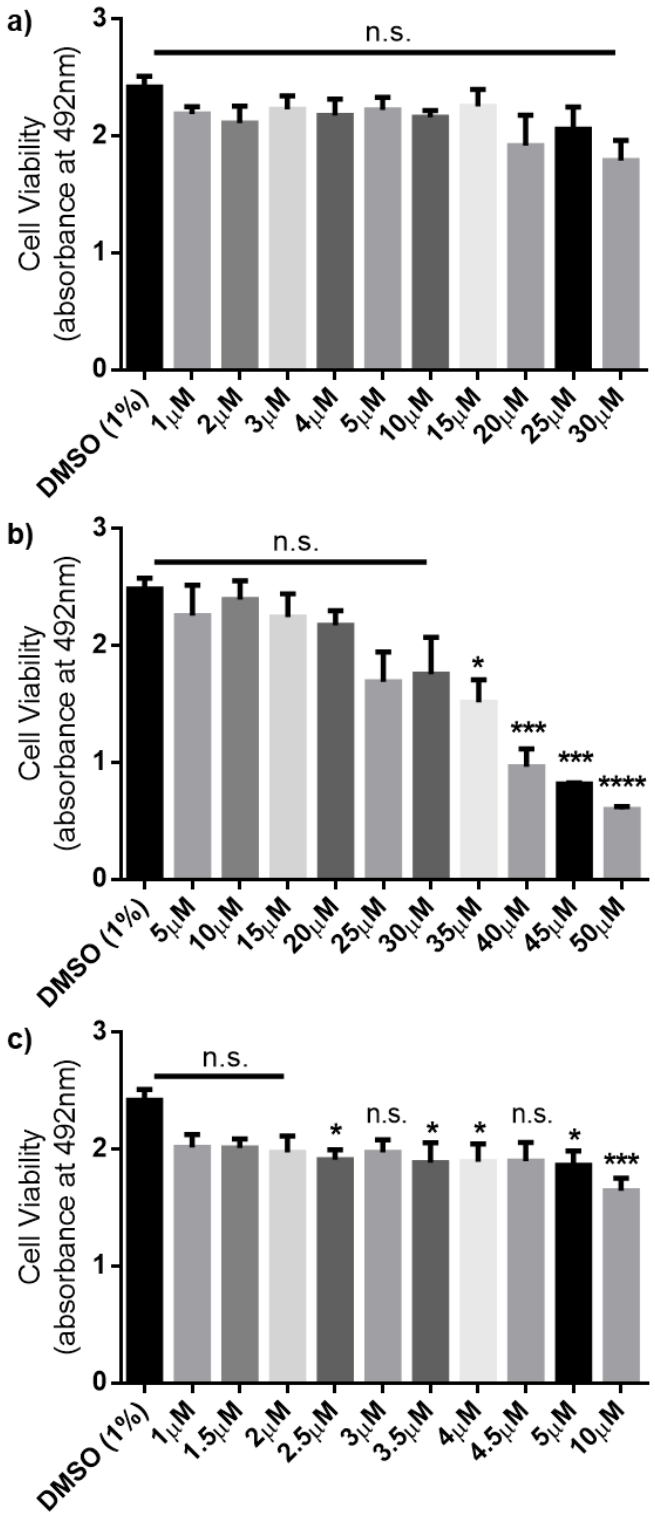

Figure 22. Toxicity of CXCR1 and CXCR2 antagonists towards THP-1 cells. The absorbance following incubation of THP-1 for 24 hrs with **a)** Reparixin, **b)** SCH527123, and **c)** SB225002 and treatment with MTS reagent for 2 hrs. 1% DMSO was added to the basal as a vehicle control. Data is representative of the mean ± SEM of three independent experiments (One-way ANOVA with a Dunnett's multiple comparisons test as post-test, n.s.= no significance $p>0.05$, * = $p \leq 0.05$, ** = $p \leq 0.01$, *** = $p \leq 0.001$, **** = $p \leq 0.0001$).

3.2.1.2 The response of Jurkat cells to CXCL8

3.2.1.2.1 Jurkat cells do not migrate towards CXCL8

Jurkat cells are immortalized T lymphocytes that were obtained from the peripheral blood of a one-year-old boy with acute T cell leukaemia. They have been widely used as they express multiple chemokine receptors, and they are prone to viral entry [430]–[432]. As for THP-1 cells, we investigated the effect of CXCL8 on the migration of Jurkat cells. Our lab have already reported that CXCL12 induces the migration of Jurkat cells [388], [433]–[435], so CXCL12 was used as a positive control. Indeed, Jurkat cells migrate significantly more in response to CXCL12, but no chemotactic activity was observed in the presence of CXCL8 (both 5 nM; **Figure 23**). To our knowledge, the activation of Jurkat cells by CXCL8 or native expression of the CXCL8 receptor have not been reported. However, they have been used as a model system for transfection with CXCL8 receptors [436], [437].

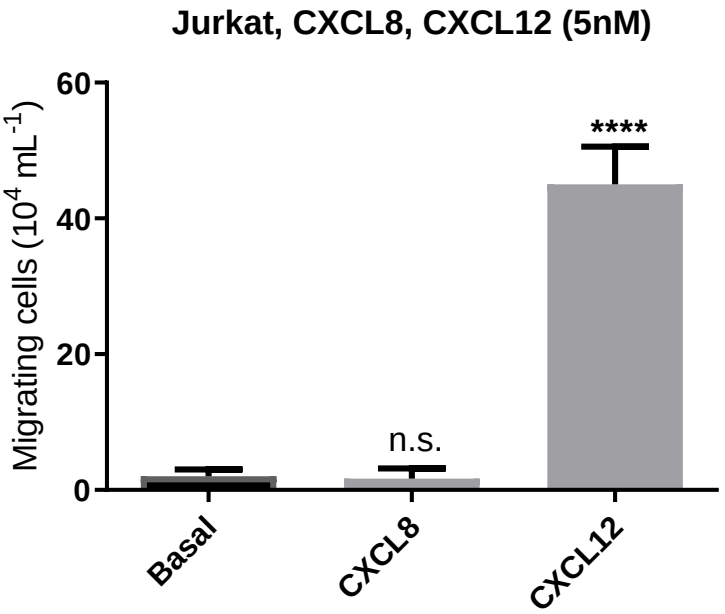

Figure 23. Jurkat cells do not migrate towards CXCL8 in a chemotaxis assay. After 5 hrs incubation, CXCL8 treatment (5 nM) did not induce migration in Jurkat cells, but cells migrated towards CXCL12 (5 nM). Data shown are the mean ± SEM of three independent experiments. (One-way ANOVA with a Dunnett's multiple comparisons test as post-test, n.s.= no significance $p > 0.05$, **** = $p \leq 0.0001$).

3.2.1.2.2 Weak intracellular calcium release in response to CXCL8 in Jurkat cells

The induction of intracellular calcium signalling was used to determine chemokine receptor activation. Injecting CXCL8 in a concentration-dependent manner gave fluctuating results, generally with very low responses from the cells (**Figure 24a**). It was difficult to determine a realistic EC_{50} considering there was hardly any calcium release. Neither the lowest (10 nM) or highest (300 nM) concentrations of CXCL8 could elicit significant intracellular calcium responses (**Figure 24b)**. No further experiments with Jurkat cells were performed, as they responded very poorly to CXCL8, suggesting their lack of CXCL8 receptors expression.

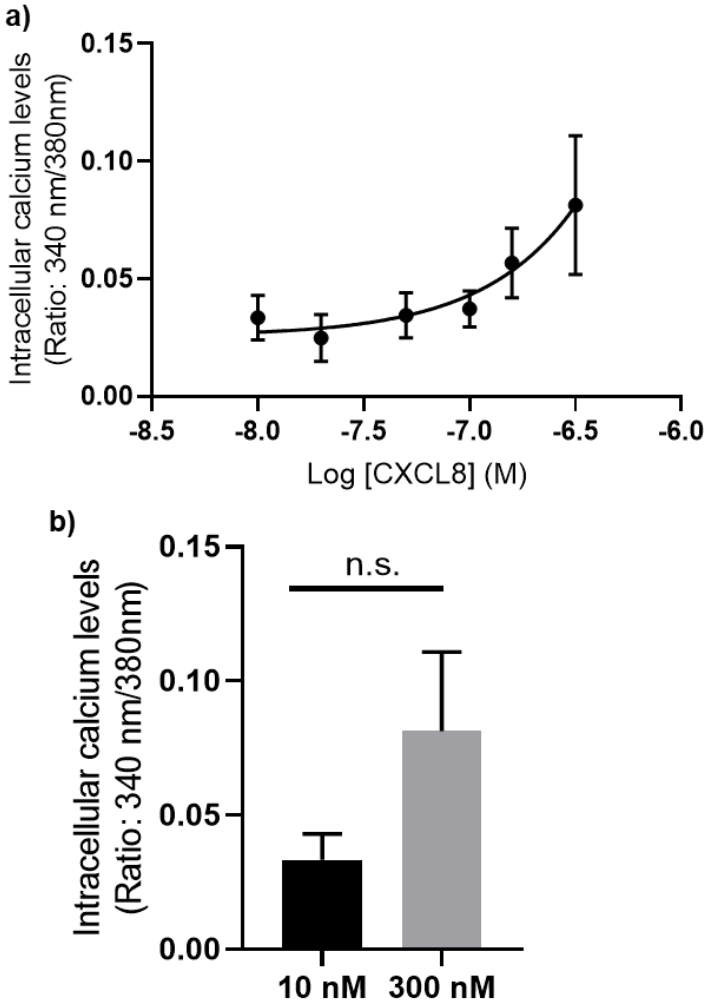

Figure 24. CXCL8 does not induce intracellular calcium release in Jurkat cells. **a)** Intracellular calcium responses upon CXCL8 injection. Data is expressed as changes in fluorescence ratio (340nm/380nm) where the basal fluorescence, prior to the injection of CXCL8, is subtracted from peak fluorescence following injection of CXCL8. **b)** Lowest and highest concentrations of CXCL8 showing no significant release of calcium (Unpaired t-test, n.s.=no significance). Data represent mean ± SEM from six independent experiments. (Non-linear regression dose-concentration response curve assuming a Hill coefficient of 1).

3.2.1.3 The response of MDA-MB231 to CXCL8

3.2.1.3.1 Expression of CXCR1 and CXCR2 receptors on MDA-MB231 cells

The cellular model MDA-MB231 is extensively used for studying breast cancer metastasis [438]. To estimate the biological effects of CXCL8 on MDA-MB231 cancer cells, it was important to check for receptor expression. MDA-MB231 stained positive for both CXCR1 and CXCR2 after staining with anti-CXCR1 (also known IL-8RA) mAB and anti-CXCR2 (also known IL-8RB) mAB, respectively (**Figure 25**). This comes in agreement with studies by other groups whereby high levels of CXCR1 expression were measured by flow cytometry and RT-PCR showing expression of CXCR2 in MDA-MB231 cells [243], [439].

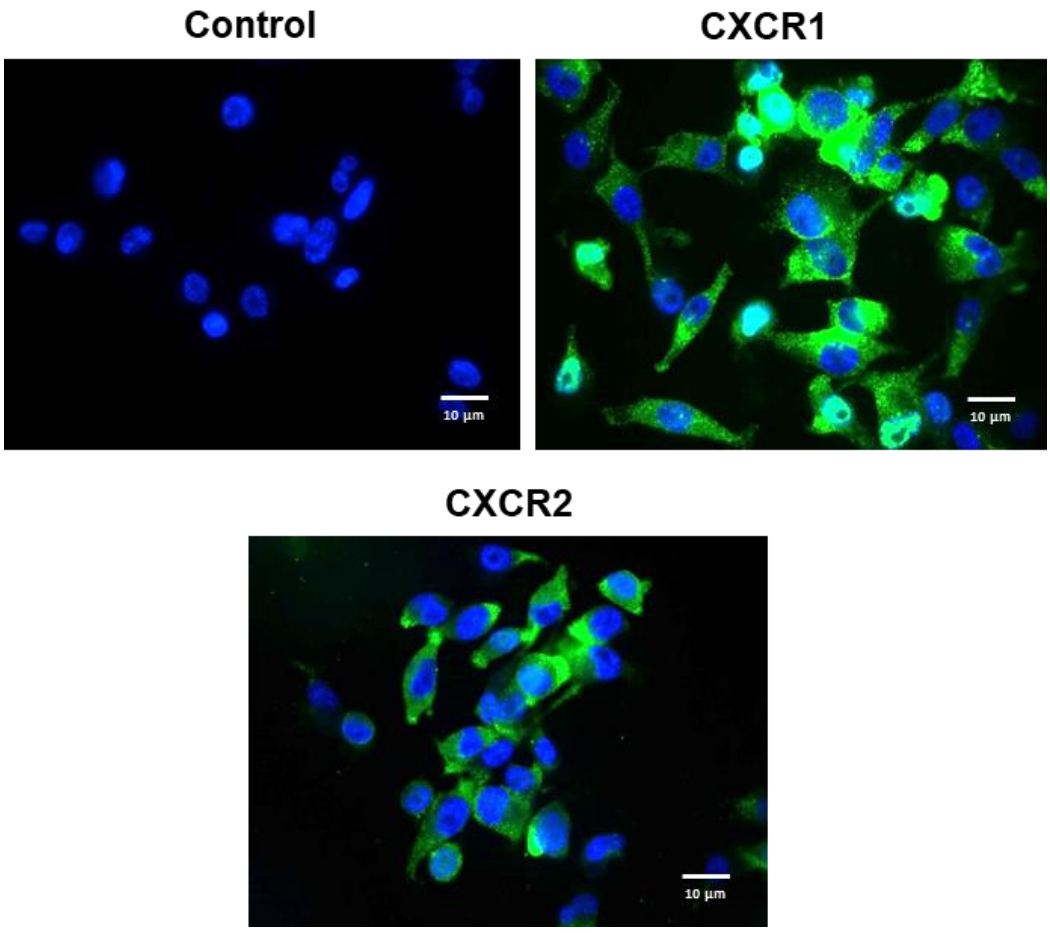

Figure 25. MDA-MB231 cells express CXCR1 and CXCR2. Immunofluorescence staining of MDA-MB231 cells using anti-CXCR1, anti-CXCR2 and their corresponding secondary Alexa-488 conjugated antibodies (green). Control was anti-mouse Alexa-488 alone. The nucleus was stained with DAPI (blue). Cells were fixed and images are representative of the cell population of one experiment out of three independent repeats, acquired at 63x objective using a Leica DMII fluorescence microscope and Leica imaging suite.

3.2.1.3.2 MDA-MB231 cells migrate towards CXCL8 in a Boyden chamber migration assay

Since MDA-MB231 cells showed expression of both CXCR1 and CXCR2, a Boyden chamber migration assay was performed to determine the migratory capacity of the cells in response to CXCL8. MDA-MB231 cells are a highly aggressive, invasive, and poorly differentiated triple-negative breast cancer cell line [440]. They obtain their invasiveness from their ability to degrade the extracellular matrix. A Boyden chamber migration assay is a widely used technique that creates a chemoattractant concentration gradient. In the upper chamber, cells were cultured in serum free media (to prevent cytokines and growth factors tampering with the stimulus effect). CXCL8 (10 nM) was added to the bottom chamber, separated through surface tension, which hinders the chemokine from readily dispersing into the cell chamber. Indeed, there was a significant increase in the number of MDA-MB231 cells migrating towards CXCL8 relative to the control (**Figure 26**).

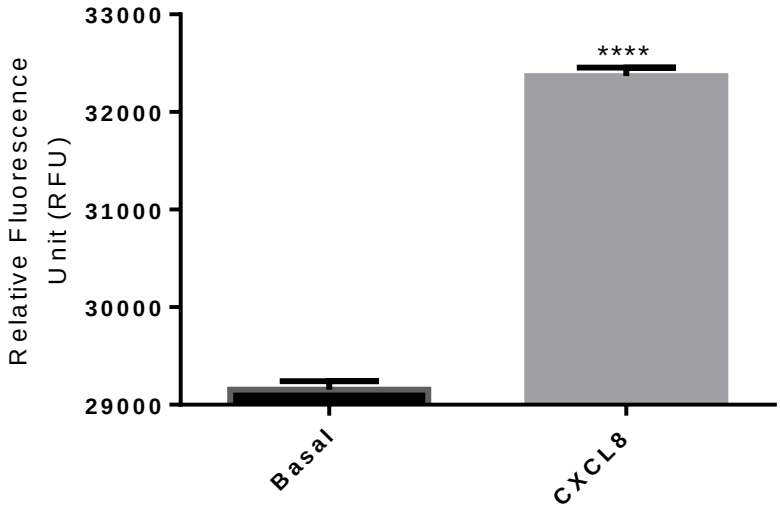

Figure 26. CXCL8 induces migration of MDA-MB231 cells in a Boyden chamber transwell assay. Cells were incubated with or without CXCL8 (10 nM) on a transwell insert to maintain a chemokine gradient for 24 hrs, they were then stained with calcein for 45 mins and fluorescence was measured at 530nm/ 410nm. All data shown are the mean ± SEM of seven independent experiments. (Unpaired t-test, **** = $p \leq 0.0001$).

3.2.1.3.3 Agarose spot assays are not suitable for measuring the migration of MDA-MB231 cells

Our results obtained with the Boyden chamber migration assay, which relies on a semi-permeable membrane to generate a concentration gradient, showed that MDA-MB231 cells migrate towards CXCL8. To confirm these results, an agarose spot assay was performed to increase the reliability. In this assay, the chemokine is contained in the middle of the well in a bubble formed of 0.5% agarose. Theoretically, cells seeded outside of this spot should travel towards the chemokine contained in the soft agarose. The protocol used for this experiment was inspired by work performed by Vinadar *et al*. [441] and Ahmed *et al*. [442]. They found that cells significantly migrated towards CXCL12 compared to the control. However, the reproducibility of this assay was challenging, and no meaningful results were generated with MDA-MB231 cells in response to CXCL8 (10 nM) or CXCL12 (10 nM). There were several different observations noted from repeating the experiments. i) A colony of cells would penetrate into the agarose spot (**Figure 27a**), ii) the agarose spot kept dislodging and moving from its intended position (**Figure 27b**). Although different conditions were attempted to maintain the agarose spot in one place, for example, switching between plastic and glass bottom plates, altering cooling and heating temperatures, or slightly changing the concentration of the agarose; the penetration of cells under the agarose spot was not successful. **Figure 27c, d** represents the expected number of migrating cells (in a well-contained agarose spot) to a chemokine-gradient. However, in order to generate randomized, unbiased data, the whole spot should be imaged. As mentioned before, some clusters of cells tended to migrate towards one position more than the other. Ahmed *et al.* [442] imaged the agarose spot of PC3 cells migration at different angles, however, we think that also imaging the spot circumference in full at a lower microscope objective would give a better representation of the migration patterns of the cells. Overall, this approach did not seem reproducible for measuring chemokine-induced chemotaxis and there are numerous challenges associated with the analysis process.

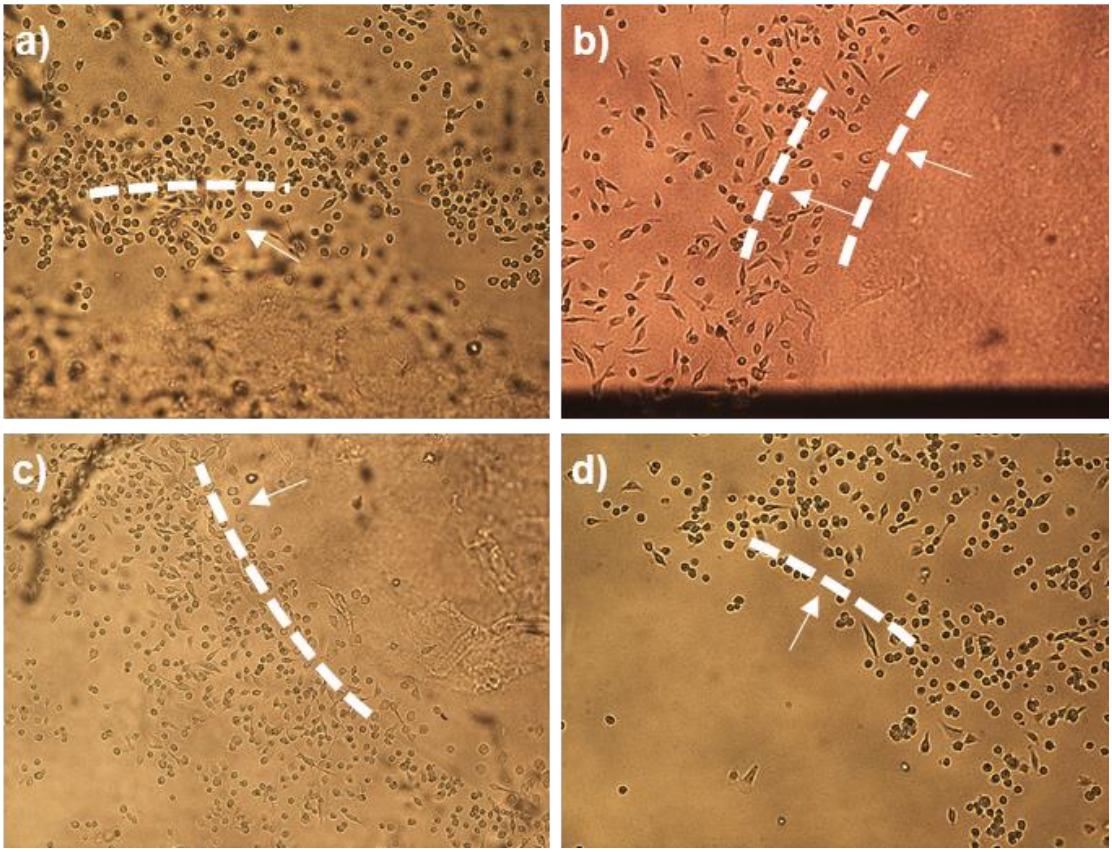

Figure 27. Agarose spot assays did not provide consistent data for MDA-MB231 cells. a) A colony of cells migrating under the agarose spot. The dash lines indicate the spot border. **b)** Agarose spot sliding as indicated with the position of the two arrows. **c, d)** Different angles of the agarose spot represents different sets of migrating cells. Data are representative of four different experiments. Cells images are representative of the cell population acquired at 10x objective using a Leica DMII inverted microscope and Leica imaging suite.

3.2.1.3.4 The migration speed of MDA-MB231 cells increases when activated with CXCL8

After testing CXCR1 and CXCR2 expression and the ability of CXCL8 to induce migration in MDA-MB231 cells, a time-lapse migration assay was performed to study the speed of the migrating cells. Following treatment of the cells with CXCL8 (10 nM), the speed of migration increased by almost two-fold. The basal speed of cells was 24.4 ± 5.8 µm/hr, whereas for CXCL8 treated cells this speed increased to 49.9 ± 11.6 µm/hr (**Figure 28***).*

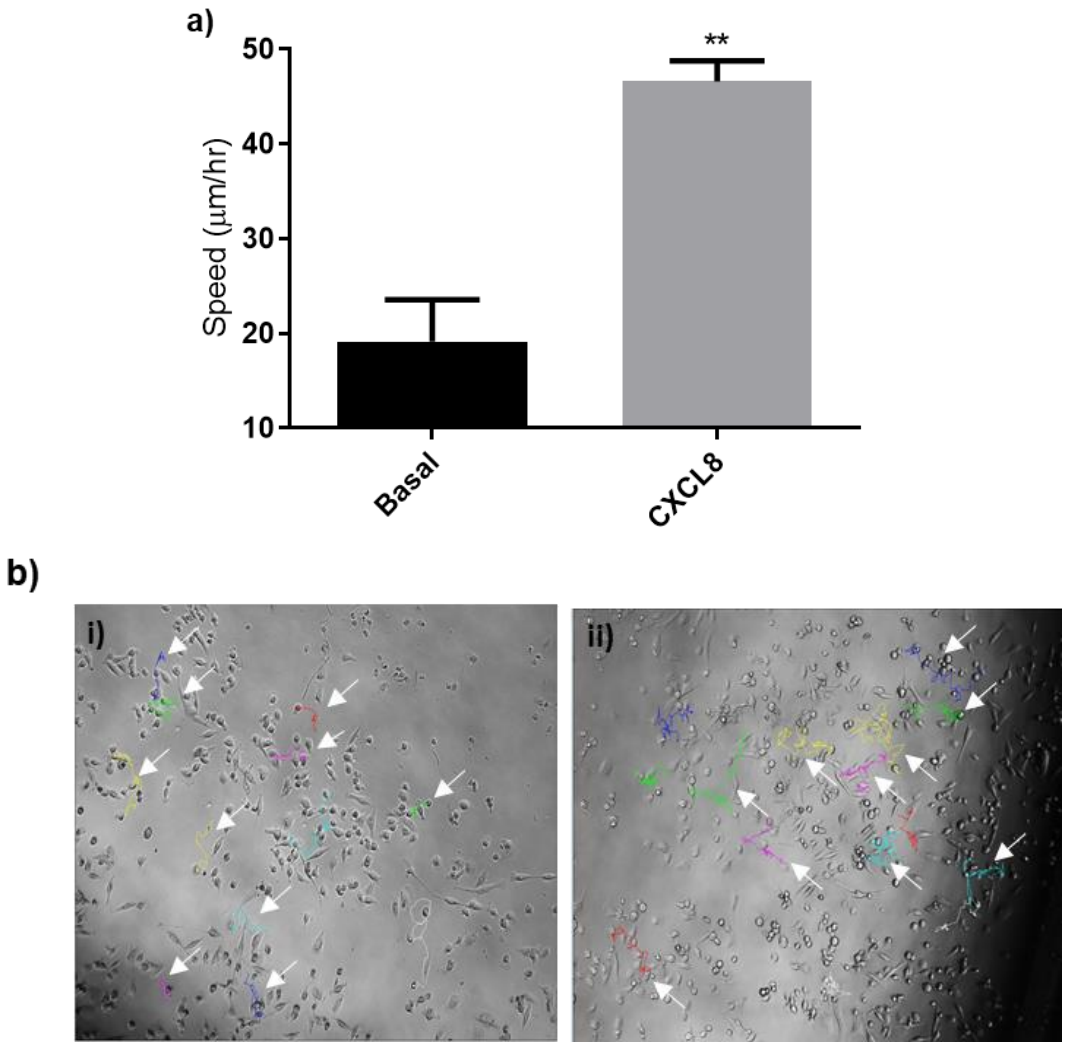

Figure 28. MDA-MB231 cells migrate faster in the presence of CXCL8. a) MDA-MB231 cells activated by CXCL8 (10 nM) demonstrated a significant increase in the migration speed upon analysing 10 cells from each experiment. Data representative of the mean ± SEM of four independent experiments (unpaired t-test, ** = $p \leq 0.01$) **b)** Endpoint images from individual cell tracking using Fiji/ImageJ after 10 hrs, i) Basal, ii) CXCL8 (10 nM). Images are a representation of the cell population and were taken at 10x objective with Zeiss Axiovert 200M microscope and processed using AxioVision Rel 4.8 software.

MDA-MB231 cells treated with Reparixin (10 μM), SCH527123 (10 μM) or SB225002 (1 μM), followed by activation with CXCL8 (10 nM) were significantly slowed down (32.2 ± 11.5 μm/hr, 29.5 ± 5.2 μm/hr and 15.4 ± 7.1 μm/hr, respectively), demonstrating full inhibition of the CXCL8 effect (**Figure 29)**. Fu *et al.* [443] found that Reparixin (40 or 60 μM/L) or SCH527123 (40 or 60 μM/L) did not inhibit cell viability, colony formation, or wound healing closure as significantly as the potent inhibition achieved by combining either of them with bazedoxifene (targeting IL-6).

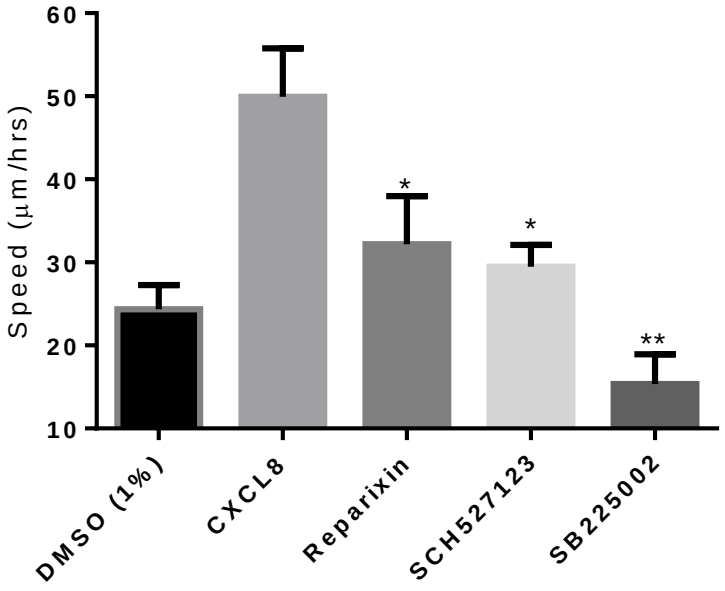

Figure 29. The migration speed of MDA-MB231 cells is reduced in the presence of CXCR1 and CXCR2 antagonists. Reparixin (10 μM), SCH527123 (10 μM), and SB225002 (1 μM) significantly reduce the migration of MDA-MB231 towards CXCL8 (10 nM) over 10 hrs. Comparison was made against CXCL8. 1% DMSO was added to the basal cells as a vehicle control. Data are representative of three independent experiments (One-way ANOVA with a Dunnett's multiple comparisons test as post-test, * = $p \leq 0.05$, ** = $p \leq 0.01$).

Another experiment was performed to investigate the migration speed of MDA-MB231 cells over a period of 30 hrs. This experiment was performed on a different more basic microscope (Celestron 44126-CGL Micro 360). On average, cells migrated up to 60 μm/hr (**Figure 30a**). The significant effect of CXCL8 on the enhanced migration of cells compared to control cells can be clearly observed from the images obtained after 30 hrs (**Figure 30b**)**.**

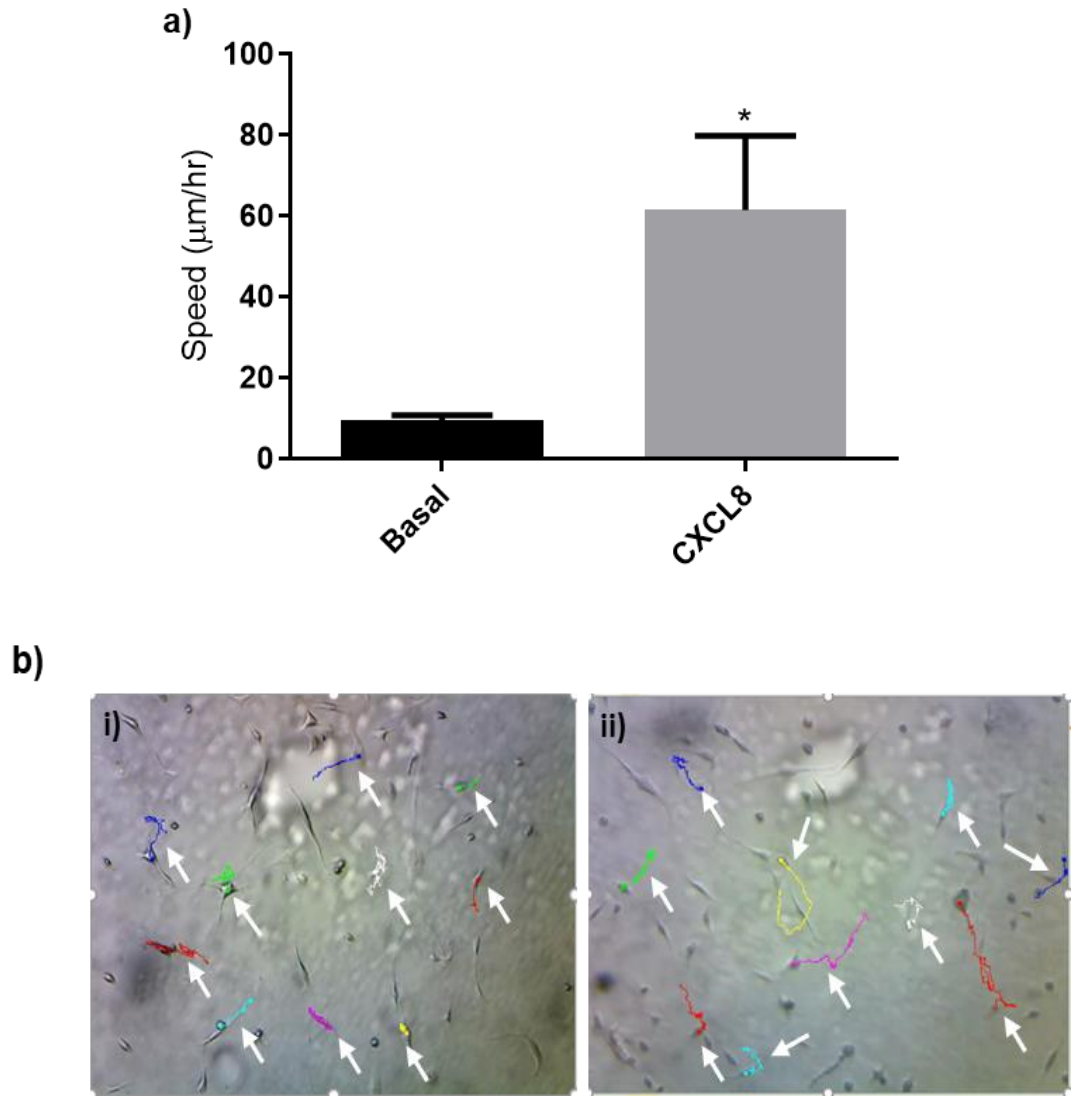

Figure 30. MDA-MB231 cells migrate faster in the presence of CXCL8 over 30 hrs. a) MDA-MB231 cells migrate faster in the presence of CXCL8 (10 nM). **b)** Arrows pointing at cell tracks that were randomly picked and analysed of the i) basal sample (image taken after 20 hrs), ii) followed by the addition of CXCL8 (10 nM) to the same well and imaged over 30 hrs. Data are representative of three independent experiments. Images are a representation of the cell population and were taken at 10x objective using a Celestron 44126-CGL Micro 360 and Celestron HD digital microscope imager, processed by Debut professionals-NCH software, decompressed videos with Camtasia studio 8.0, tracking and analysis with Fiji/ImageJ. (Unpaired t-test, * = $p \leq 0.05$).

3.2.1.3.5 CXCL8 induces proliferation in MDA-MB231 cells

CXCL8 and its receptors CXCR1 and CXCR2 are expressed by various cancer cell types and activate cancer cell proliferation and migration in an autocrine fashion (reviewed by [131]). Results obtained by the time-lapse migration assay indicated that treating cells with CXCL8 (10 nM) increased MDA-MB231 cell migration. Further analysis was performed on the videos generated by this experiment. Taking two screenshots of the cells at 0 hr-time point and 10 hrs-time-point, the number of cells were counted using Fiji/ImageJ. Analysis showed that cells treated with exogenous CXCL8 displayed enhanced proliferation compared to the control cells **Figure 31a**. The experiment was repeated three times and this increase was observed in all experiments. A number of studies have shown that several cell lines react in the same way when stimulated with CXCL8, including breast, lung, melanoma, and epithelial cells [142], [146], [325], [444]. However, we cannot specifically conclude that CXCL8 induce the proliferation in MDA-MB231 from this mere observation. That is because the screenshot was taken from a discrete location in the well, therefore cells could have migrated away from the field of view. Yet, we could still observe that within this limited area, cells exhibited more mitogenic activity in the presence of CXCL8 (**Figure 31b**).

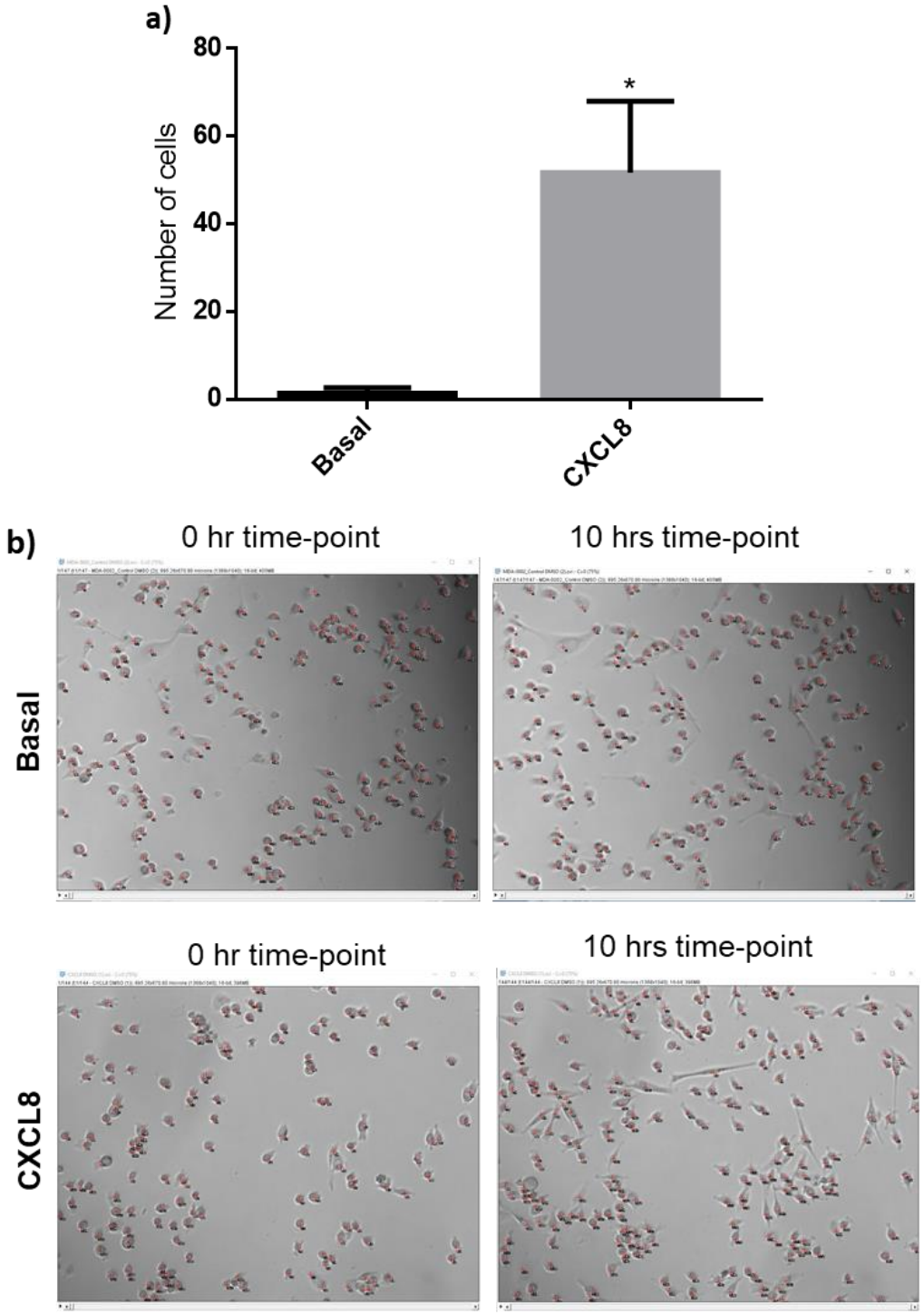

Figure 31. A significant increase in the proliferation of MDA-MB231 cells was observed in the presence of CXCL8. a) The number of cells were elevated significantly in the presence of CXCL8 (10 nM). **b)** Images from 0 hr and 10 hrs-timepoints obtained from the time-lapse migration assay with the red crosses indicating the number of cells in each frame analysed using Fiji/ImageJ. Data representative of three independent experiments (Unpaired t-test, * = $p \leq 0.05$). Images are a representation of the cell population and were taken at 10x objective with a Zeiss Axiovert 200M microscope and processed using AxioVision Rel 4.8 software.

3.2.1.3.6 Toxicity of CXCR1 and CXCR2 antagonists towards MDA-MB231 cells

An MTS assay was performed to test the cellular toxicity of the CXCR1 and CXCR2 antagonists on MDA-MB231 cells. A study conducted by Brandolini *et al*. [445] found that treating cells with 1 µM - 3 mM of Reparixin for 72 hrs resulted in a reduction of cell viability in a concentration-dependent manner, up to 60% of the control.

In our hands, Reparixin at concentrations of 5 to 30 µM, SCH527123 at 20 µM to 50 µM, and SB225002 at 1, 5 and 10 µM showed no toxicity after 24 hrs (**Figure 32**).

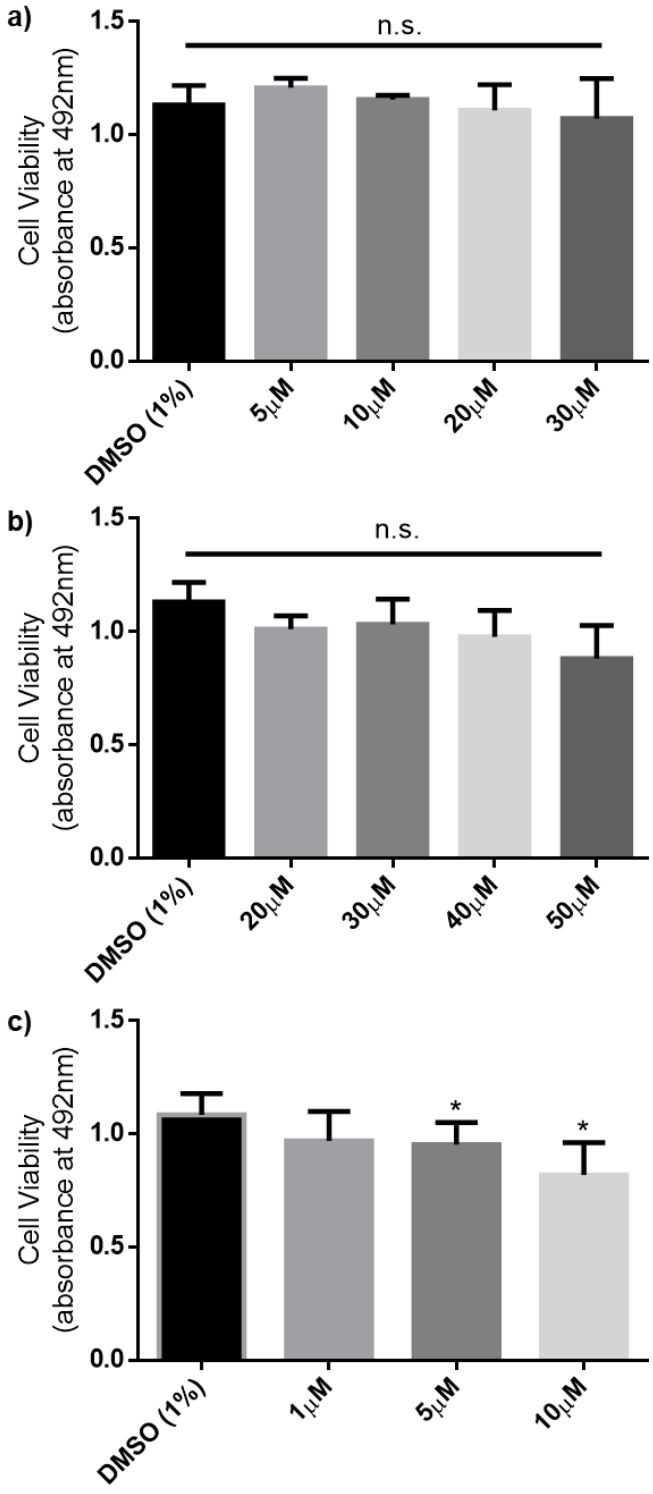

Figure 32. Toxicity of CXCR1 and CXCR2 antagonists towards MDA-MB231 cells. Toxicity of MDA-MB231 cells after treatment with **a)** Reparixin, **b)** SCH527123, and **c)** SB225002 for 24 hrs and MTS reagent for 2 hrs. Data are representative of the mean ± SEM of three independent experiments (One-way ANOVA with a Dunnett's multiple comparisons test as post-test, * = $p \leq 0.05$, n.s.= no significance $p > 0.05$).

3.2.1.4 The response of MCF-7 cells to CXCL8

3.2.1.4.1 Expression of CXCR1 and CXCR2 receptors on MCF-7 cells

MCF-7 cells are another mammary cell model used to study the expression of chemokine receptors. Xu *et al.* [446] reported that MCF-7 cells express CXCR2 at low levels. Conversely, Müller *et al*. [447] showed that CXCR2 was upregulated in MCF-7 cells through flow cytometric analyses and quantitative RT-PCR. Our findings show that MCF-7 cells expressed both CXCR1 and CXCR2 in an immunofluorescence assay (**Figure 33**).

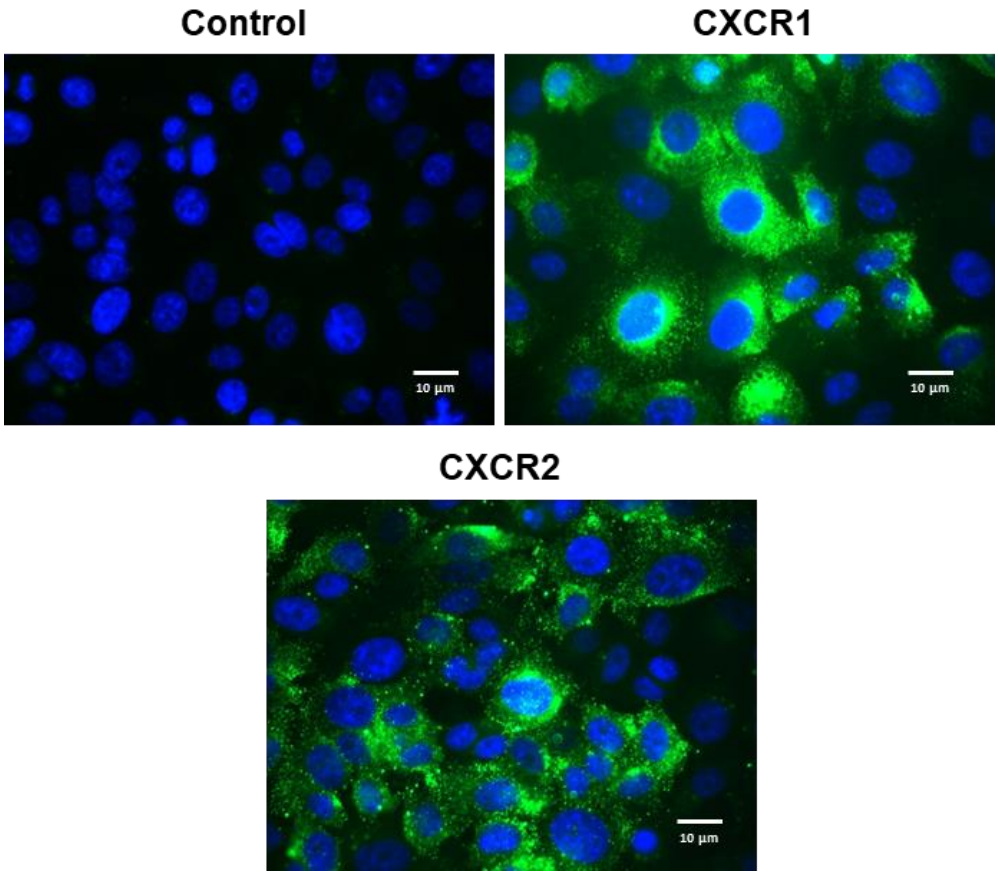

Figure 33. MCF-7 cells express CXCR1 and CXCR2. Immunofluorescence staining of the MCF-7 cells using anti-CXCR1, anti-CXCR2 and their corresponding secondary Alexa-488 conjugated antibodies (green). Control was anti-mouse Alexa-488 alone. The nucleus was stained with DAPI (blue). Cells were fixed, and images are representative of the cell population of one experiment out of three independent experiments, acquired at 63x objective using a Leica DMII fluorescence microscope and Leica imaging suite.

3.2.1.4.2 CXCL8 promotes MCF-7 wound closure

A wound healing assay is a well-known, simple, cheap, and useful technique for the analysis of cell migration *in vitro* in two dimensions. The assay steps are initiated by creating a scratch in an adhered monolayer of cells, then capturing images of the wound closure with different treatments at different time-points to monitor the scratch closure. After observing the expression of CXCR1 and CXCR2 on MCF-7 cells, a wound healing assay was performed to assess the migration potential of the cells in the presence of CXCL8 (10 nM). Indeed, after 24 hrs incubation with CXCL8, MCF-7 cells migrated significantly more towards closing the scratch compared to controls. The wound width ratio was 0.85 for CXCL8 whilst it was 0.95 for the control (**Figure 34**). Here, 0 denotes complete migration and 1 denoted no migration.

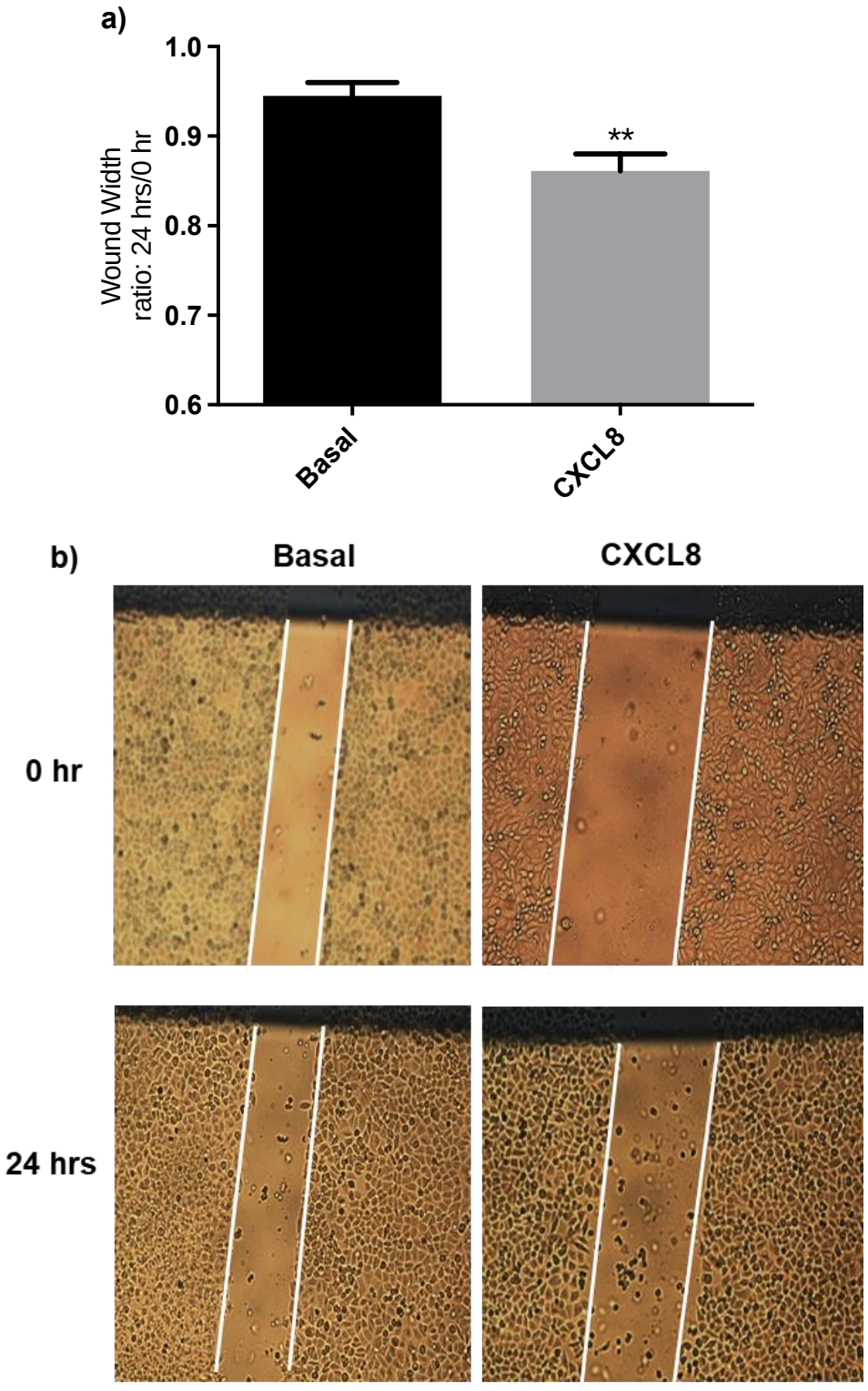

Figure 34. CXCL8-treated MCF-7 cells display an enhanced migration in a wound healing assay. a) CXCL8 (10 nM) promotes MCF-7 wound closure after 24 hrs. A value of 1 denotes no migration, whilst 0 denotes complete migration. **b)** Image representing CXCL8 (10 nM) wound closure in the cells after 24 hrs. MCF-7 cells treated with CXCL8 had a wound width ratio of 0.85 compared to 0.95 for the basal. Results represent the mean ± SEM of eight independent experiments. All images were taken at 10x objective using a Leica DMII inverted microscope and Leica imaging suite. (Unpaired t-test, ** = $p \leq 0.01$).

Furthermore, the wound healing assays were used to assess the inhibitory capacity of CXCR1 and CXCR2 small molecule antagonists; Reparixin (500 nM), SCH527123 (500 nM) and SB225002 (250 nM). CXCL8-activated cells migrated significantly more than the untreated basal cells ($p \leq 0.05$). Whilst Reparixin and SCH527123 did not significantly affect the migration of cells, SB225002 seemed to block the binding of CXCL8 to CXCR1 and CXCR2, therefore less migration was noted upon activation with CXCL8 (10 nM) (**Figure 35**).

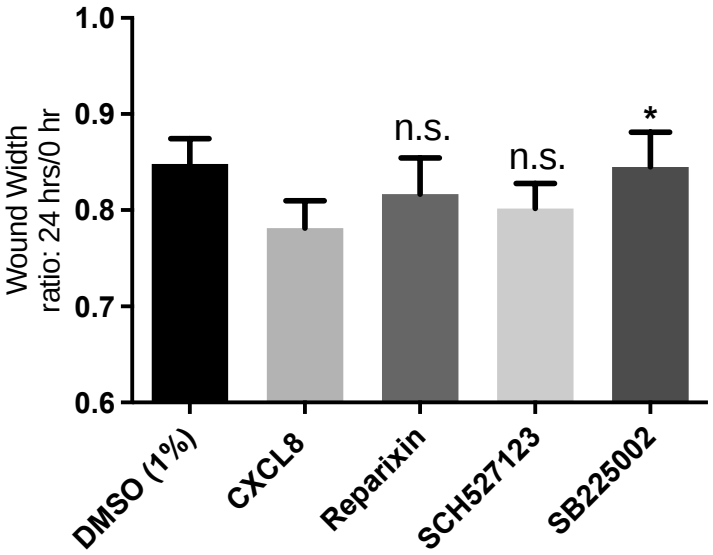

Figure 35. CXCR1 and CXCR2 antagonist SB225002 blocks the migration of MCF-7 cells in the presence of CXCL8. Pre-treatment of MCF-7 cells with SB225002 (250 nM) significantly reduced the migration of MCF-7 cells, while SCH527123 (500 nM) and Reparixin (500 nM) only slightly reduced the migration after activation with 10 nM CXCL8. A value of 1 denotes no migration, whilst 0 denotes complete migration. Comparison was made against CXCL8. 1% DMSO was added to the basal cells as a vehicle control. Results represent the mean ± SEM of three independent experiments (Two-way ANOVA, Tukey's multiple comparisons test, n.s.= no significance, $p > 0.05$, * = $p \leq 0.05$).

3.2.1.4.3 CXCL8 induces intracellular calcium release in a concentration-dependent manner in MCF-7 cells

The release of intracellular calcium was identified as an indicator of chemokines activating their cognate receptors [387]. Indeed, as for MCF-7 cells, CXCL8 could induce intracellular calcium release in a concentration-dependent manner (**Figure 36**).

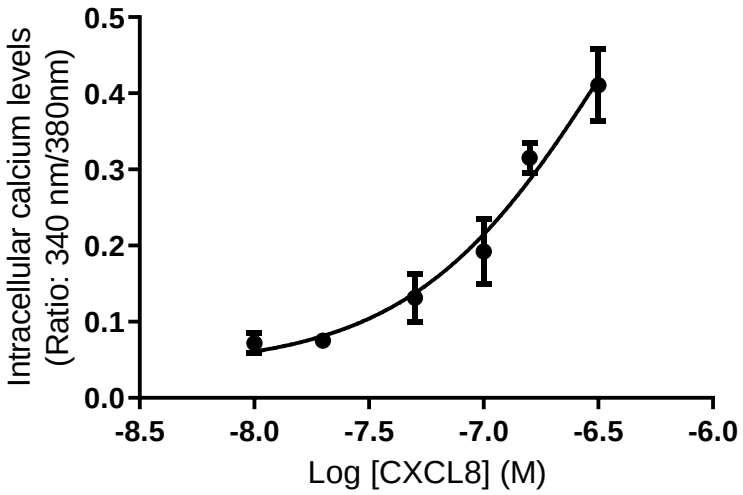

Figure 36. Intracellular calcium response of MCF-7 cells following treatment with varying concentrations of CXCL8. Data is expressed as changes in the fluorescence ratio (340nm/380nm) where the basal fluorescence, prior to the addition of CXCL8, is subtracted from peak fluorescence following addition of CXCL8. Data represents the mean ± SEM from three independent experiments. Non-linear regression dose-concentration response curve assuming a Hill coefficient of 1.

3.2.1.4.4 CXCR1 and CXCR2 antagonists inhibit intracellular calcium release in MCF-7 cells

Since CXCL8 induced release of intracellular calcium in MCF-7 cells, we blocked the receptors associated with CXCL8 signalling. Reparixin (500 nM), SCH527123 (500 nM), and SB225002 (250 nM) inhibited the release of intracellular calcium by CXCL8 (200nM; **Figure 37a**). Individual traces of calcium release were plotted to present the inhibitory effect of the antagonists used (**Figure 37b**).

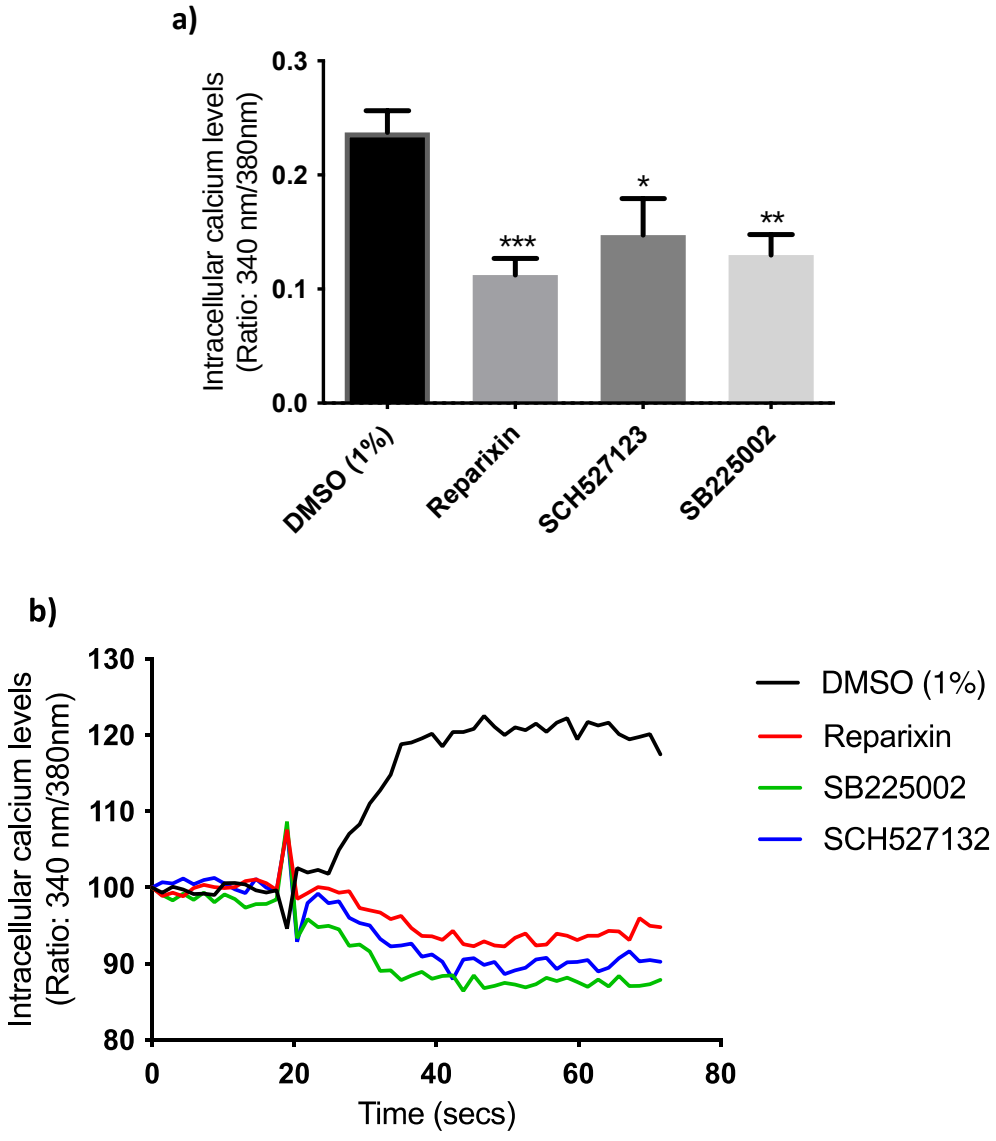

Figure 37. CXCR1 and CXCR2 antagonists reduce intracellular calcium release in CXCL8-activated MCF-7 cells. a) Reparixin (500 nM), SCH527123 (500 nM), and SB225002 (250 nM) significantly reduce the release of intracellular calcium of MCF-7 cells upon activation with 200 nM CXCL8. **b)** Calcium measurement traces (representative of one experiment) when activated with CXCL8 (200 nM). 1% DMSO was added to the basal cells as a vehicle control. Data represents the mean ± SEM of at least four independent experiments. (One-way ANOVA with a Dunnett's multiple comparisons test as post-test * = $p \leq 0.05$, ** = $p \leq 0.01$, *** = $p \leq 0.001$). Data are expressed as the relative ratio of fluorescence emitted at 510 nm after sequential stimulation at 340 and 380 nm.

3.2.1.4.5 Toxicity of CXCR1 and CXCR2 antagonists towards MCF-7 cells

To investigate whether the inhibitory effect of the antagonists on intracellular calcium release in MCF-7 cells was due to cytotoxicity, an MTS cytotoxicity assay was performed. Treatment of MCF-7 cells with increasing concentrations of Reparixin, SCH527123 and SB225002 for 24 hrs showed no cytotoxicity to the cells. Although there were high standard errors, possibly due to the experiment being repeated only twice, the concentrations tested by other groups [196], [448] were already higher than the concentrations used in our experiments. Therefore, we can be sure that there was no cytotoxic effect of the antagonists at the concentrations used in our experiments with MCF-7 cells (**Figure 38**).

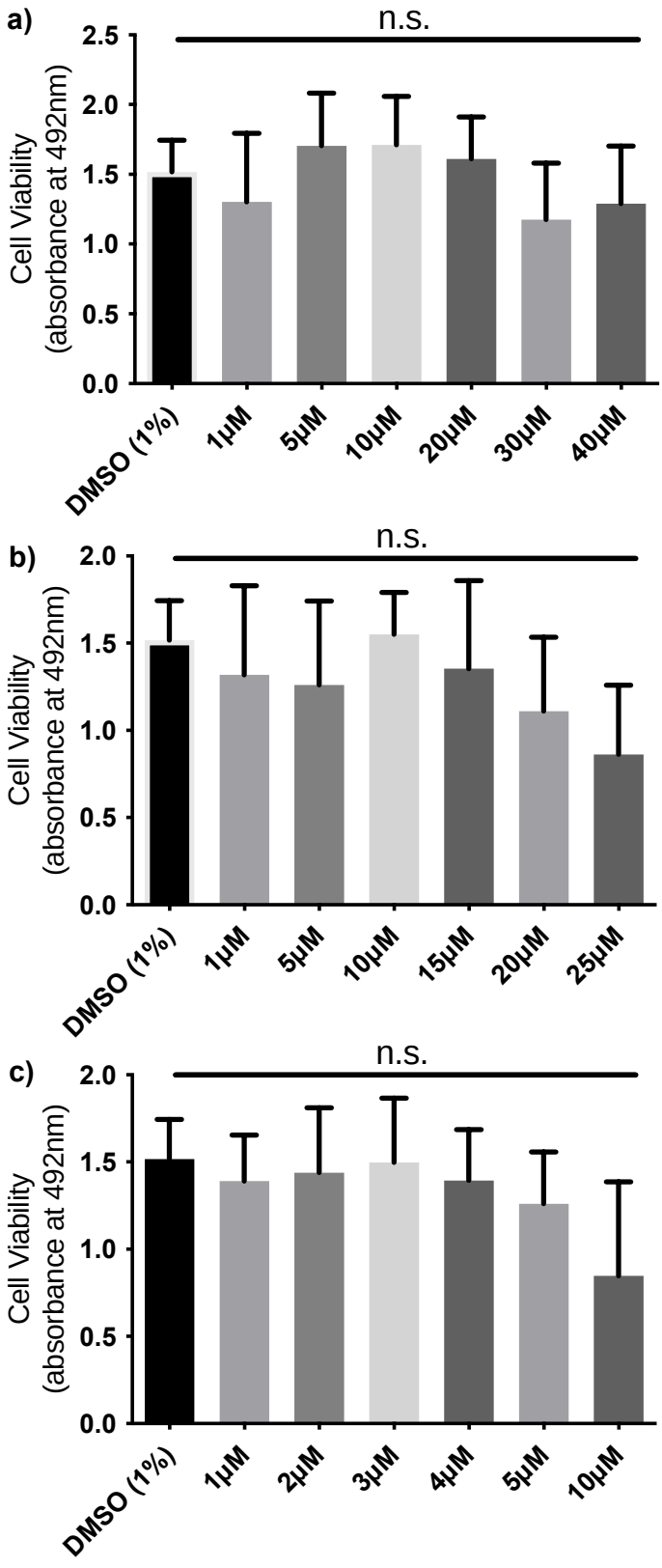

Figure 38. Toxicity of CXCR1 and CXCR2 antagonists towards MCF-7 cells. Toxicity of MCF-7 cells following treatment with **a)** Reparixin, **b)** SCH527123, and **c)** SB225002 for 24 hrs and MTS reagent for 2 hrs. 1% DMSO was added to the basal as a vehicle control. Data are representative of the mean ± SEM of two independent experiments.

3.2.1.5 The response of PC3 cells to CXCL8

3.2.1.5.1 Expression of CXCR1 and CXCR2 receptors on PC3 cells

PC3 cells have been used for many years and represent the aggressive form of prostate cancer [449]. CXCR1 and CXCR2 RNA transcripts were detected in PC3 cells using RT-PCR [450], [451]. We confirmed these findings via immunofluorescence and demonstrated that both CXCR1 and CXCR2 were expressed on PC3 cells (**Figure 39**).

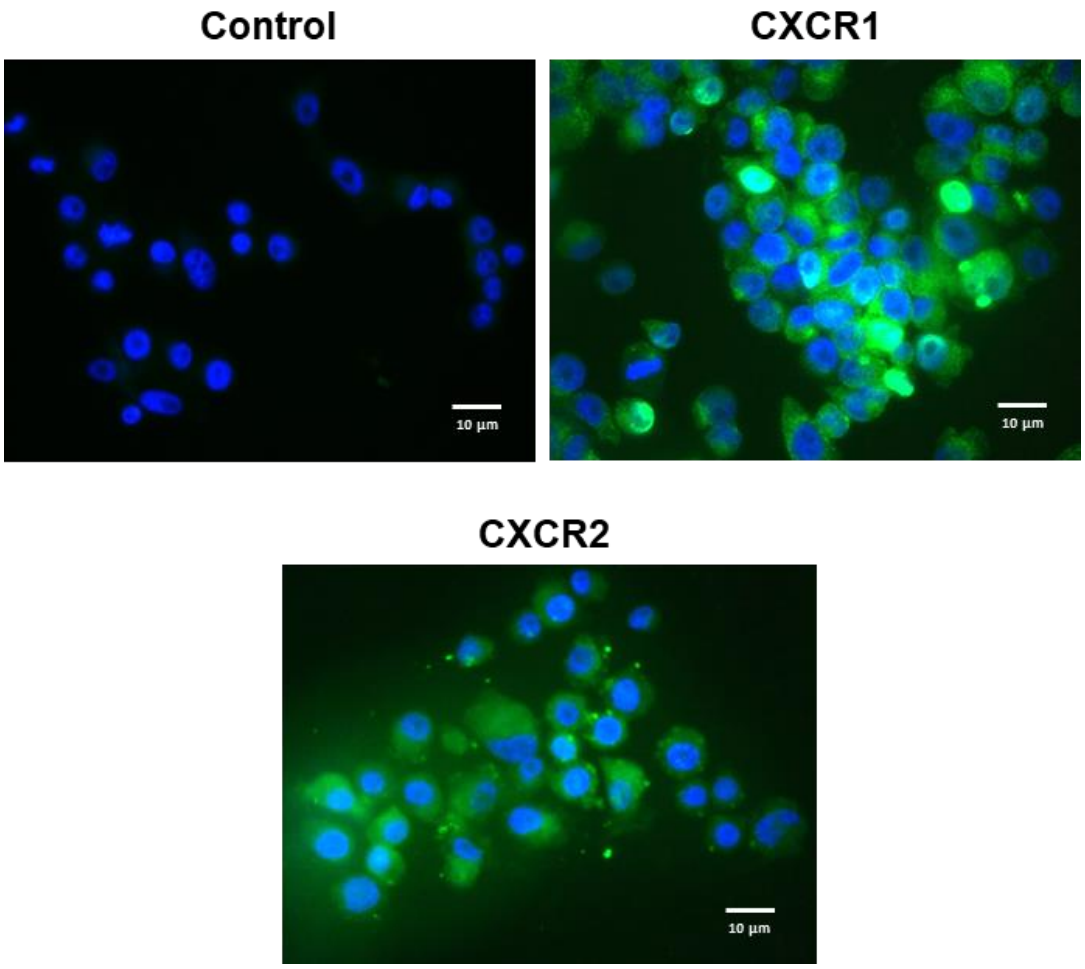

Figure 39. PC3 cells express CXCR1 and CXCR2. Immunofluorescence staining of PC3 cells using anti-CXCR1, anti-CXCR2 and their corresponding secondary Alexa-488 conjugated antibodies (green). Control was anti-mouse Alexa-488 alone. The nucleus was stained with DAPI (blue). Cells were fixed, and images are representative of the cell populations from one independent experiment out of a triplicate, acquired at 63x objective using a Leica DMII fluorescence microscope and Leica imaging suite.

3.2.1.5.2 CXCL8 induced the migration of PC3 cells in an Oris migration assay

To study the potential of PC3 cells to migrate towards CXCL8, an Oris migration assay was conducted. This assay is regarded to provide a more reproducible, accurate and precise results [412]. Cells were seeded in a well with a polymeric insert in the middle of the well to prevent cells penetrating the inner detection zone. Once cells attached and formed a monolayer, the chemokine was added overnight. A mask was also inserted into the bottom of the well to detect only the hole created by the gel insert. Following this, calcein (4 µM) was added to stain the cells and only cells that penetrated the middle detection zone were quantified. Significant numbers of cells migrated towards the analytical zone when stimulated with CXCL8, as detected via fluorescent endpoints on a microplate reader (**Figure 40**).

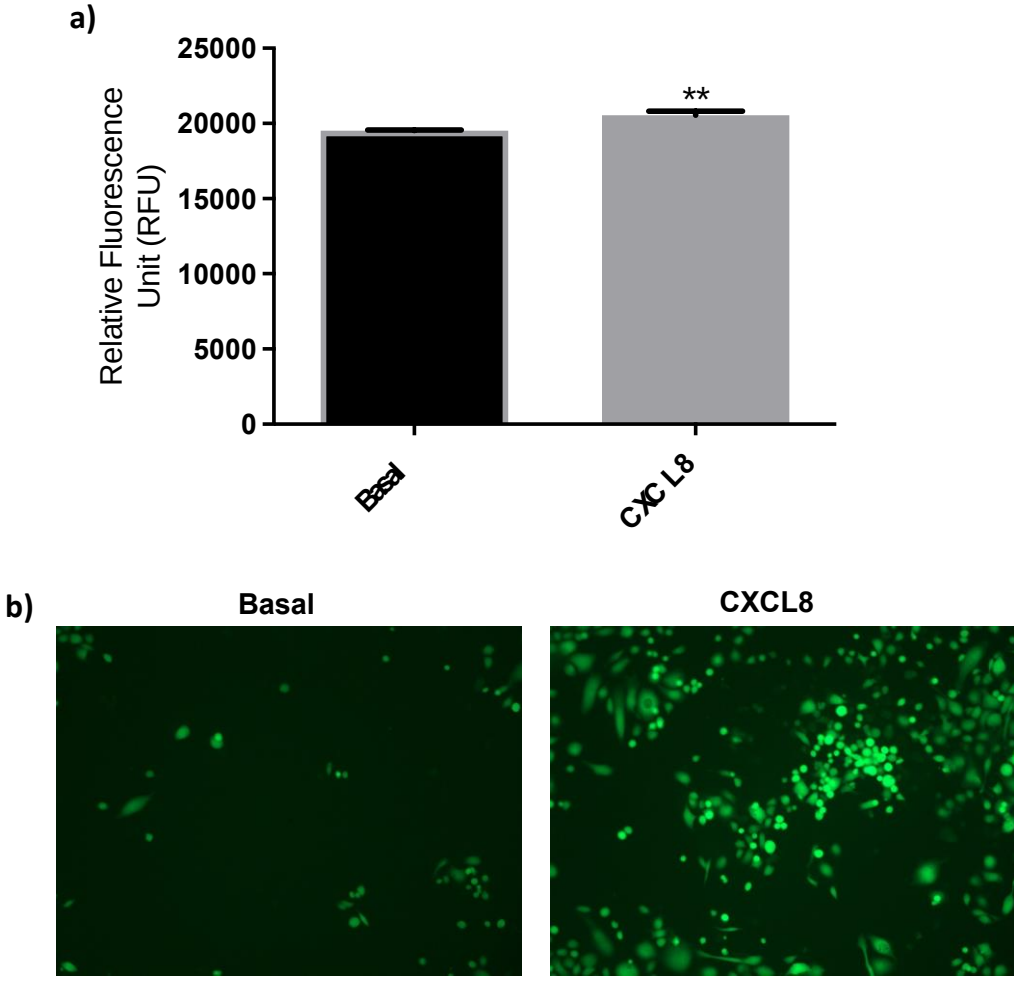

Figure 40. PC3 cells migrate more in the presence of CXCL8 in an Oris migration assay. a) Analysis of untreated (basal) and CXCL8 (10 nM) treated cells overnight. **b)** The detection area generated in the middle of the Oris well shows increased migration of cells in the CXCL8-treated sample relative to the basal. Data represent mean ± SEM from six independent experiments, (Unpaired t-test, ** = $p \leq 0.01$). Images are representative of the cell populations, acquired at 10x objective using a Leica DMII fluorescence microscope and Leica imaging suite.

3.2.1.5.3 The migration speed of PC3 cells increases when activated with CXCL8

To determine the speed that PC3 cells migrated in the presence of CXCL8, a time-lapse migration assay was performed. It was previously reported that the presence of CXCR2 on PC3 cells mediates cellular adhesion, migration on laminin, and direct invasion through a reconstructed basement membrane [450]. Upon treating the cells with CXCL8 (10 nM), a significant increase in the speed of cell migration was detected, with an average speed of 31.6 ± 3.5 µm/hr for the basal and 55.1 ± 4.4 µm/hr for CXCL8-treated cells (**Figure 41**).

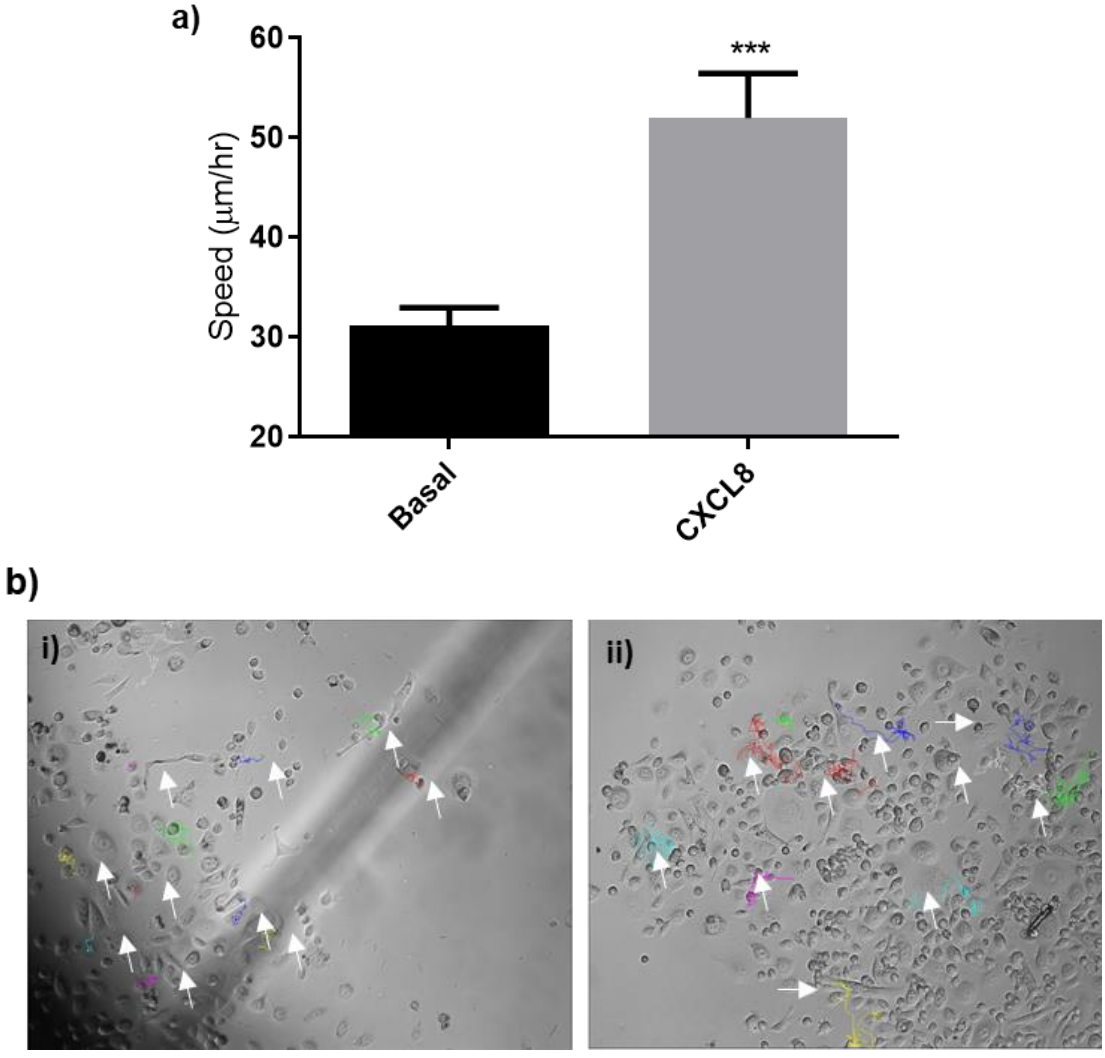

Figure 41. PC3 cells migrate faster in the presence of CXCL8. a) PC3 cells stimulated with CXCL8 (10 nM) displayed increased migratory speed upon analysing 10 cells per experiment. Data representative of the mean ± SEM of eight independent experiments (unpaired t-test, *** = p ≤ 0.001). **b)** Endpoint images from individual cell tracking using Fiji/ImageJ after 10 hrs, i) Basal, ii) CXCL8. Images are a representation of the cell population and were taken at 10x objective with a Zeiss Axiovert 200M microscope and processed using AxioVision Rel 4.8 software.

CXCR1 and CXCR2 antagonists, Reparixin (10 μM), SCH527123 (10 μM) and SB225002 (1 μM) were administered to block ligand-receptor binding. There was a significant difference between the untreated basal cell and CXCL8-activated cells ($p \leq 0.01$). The three compounds could significantly reduce the migration speed of PC3 cells in the presence of CXCL8. Average speeds of 30.1 ± 1.5 μm/hr, 22.1 ± 12.8 μm/hr, and 16.9 ± 4.1 μm/hr were reported following treatment with Reparixin, SCH527123, or SB225002, respectively (**Figure 42**).

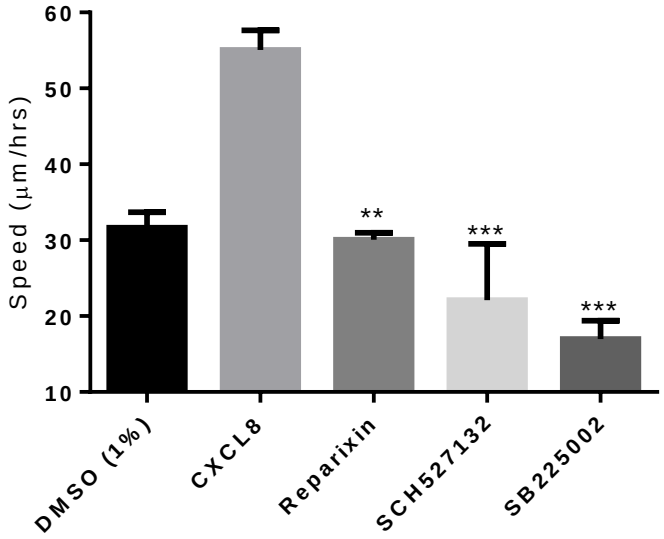

Figure 42. The migration speed of PC3 cells is reduced in the presence of CXCR1 and CXCR2 antagonists. Reparixin (10 μM), SCH527123 (10 μM), and SB225002 (1 μM) reduce the migration speed of PC3 cells activated with CXCL8 (10 nM). 1% DMSO was added to the basal cells as a vehicle control. Data are representative of three independent experiments (One-way ANOVA with a Dunnett's multiple comparisons test as post-test, ** = $p \leq 0.01$, *** = $p \leq 0.001$).

3.2.1.5.4 CXCL8 does increase the proliferation of PC3 cells, although not significantly

Seaton *et al.* [452] showed that the proliferation of PC3 cells rate were abrogated when CXCL8 expression was blocked. We utilised the same approach to measure proliferation as above (section **3.2.1.3.5**). We observed that there was no significant increase in the number of PC3 cells, however the standard error was high (p = 0.064), showing more cells proliferating in the presence of CXCL8 compared to the control (**Figure 43**).

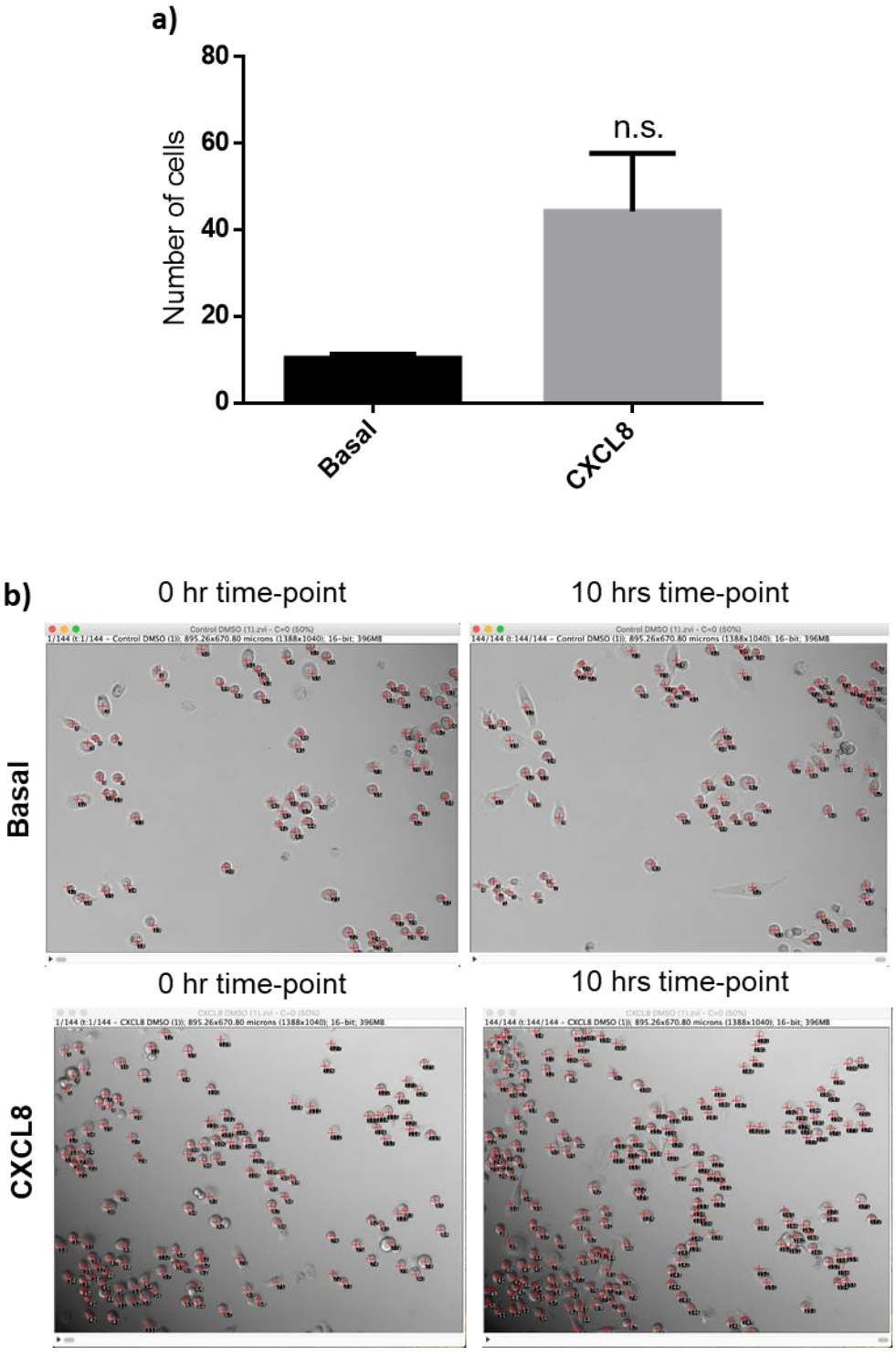

Figure 43. An increase in the proliferation rate of PC3 cells was observed in the presence of CXCL8. a) Almost double the number of cells were counted following CXCL8 (10 nM) stimulation. **b)** Images from 0 hr and 24 hrs-timepoints obtained from the time-lapse migration assay with the red crosses indicating the number of cells in each frame analysed using Fiji/ImageJ. Data are representative from three independent experiments (Unpaired t-test, n.s.= no significance p>0.05). Images are a representation of the cell population and were taken at 10x objective with a Zeiss Axiovert 200M microscope and processed using AxioVision Rel 4.8 software.

3.2.1.5.5 Toxicity of CXCR1 and CXCR2 antagonists towards PC3 cells

An MTS assay was performed to test the viability of PC3 cells towards the CXCR1 and CXCR2 antagonists. The concentrations chosen for the study were based on the IC_{50} of the compounds along with the concentrations used in published studies. Here, we observed that Reparixin, SCH527123, and SB225002 at 10 μM and 20 μM showed no toxicity (**Figure 44**).

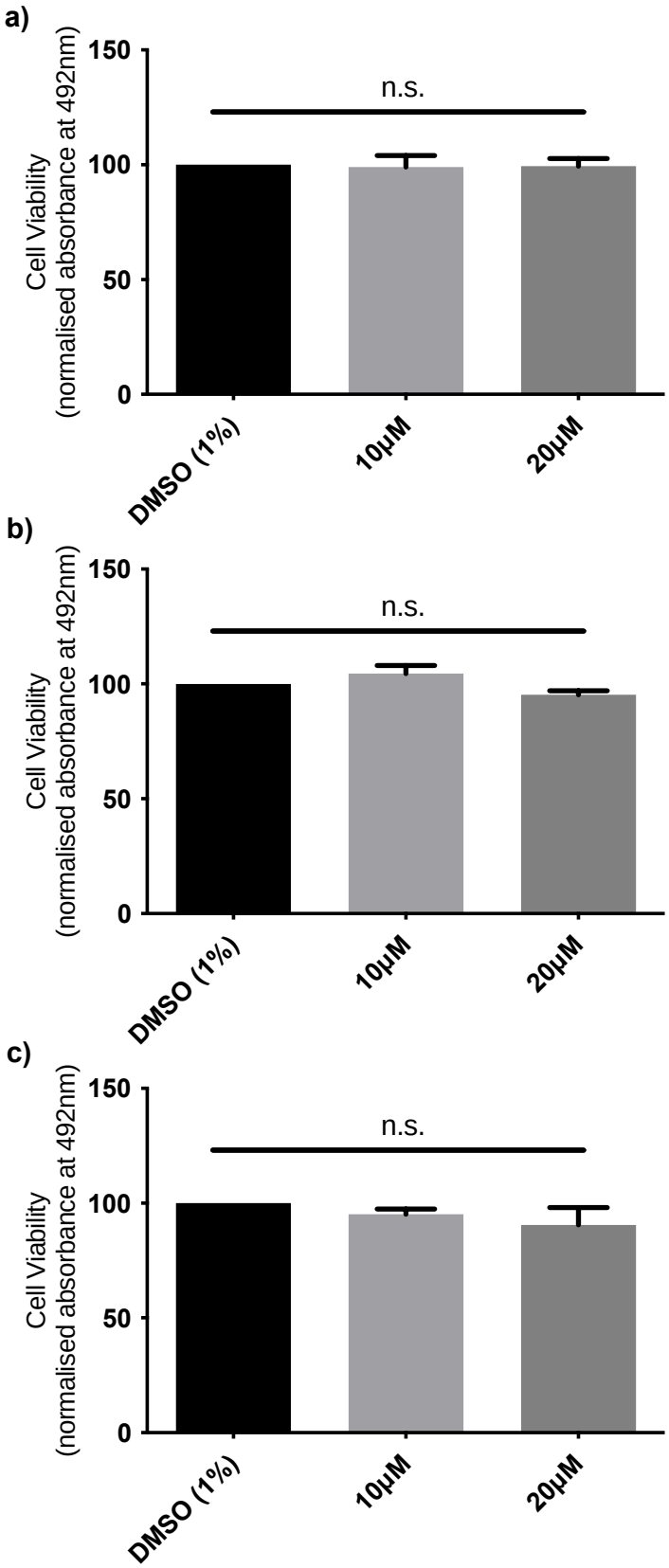

Figure 44. Toxicity of CXCR1 and CXCR2 antagonists towards PC3 cells. Toxicity of PC3 cells following incubation with **a)** Reparixin, **b)** SCH527123, and **c)** SB225002 for 24 hrs and treated with MTS reagent for 2 hrs. Data are representative of the mean ± SEM of three independent experiments (One-way ANOVA with a Dunnett's multiple comparisons test as post-test, n.s.=no significance $p > 0.05$).

3.2.2 Characterising the response of cancer cell to CXCL10

3.2.2.1 The response of THP-1 cells to CXCL10

3.2.2.1.1 Expression of CXCR3 receptors on THP-1 cells

Several studies showed that CXCL10 is a chemoattractant for circulating monocytes, leading to the accumulation of macrophages in the tissues [453], [454]. CXCL10 must bind to its receptor CXCR3 to elicit biological responses. Therefore, we first investigated the expression of CXCR3 on THP-1 cells via immunofluorescence. Indeed, cells stained positive for CXCR3, demonstrating receptor expression (**Figure 45**).

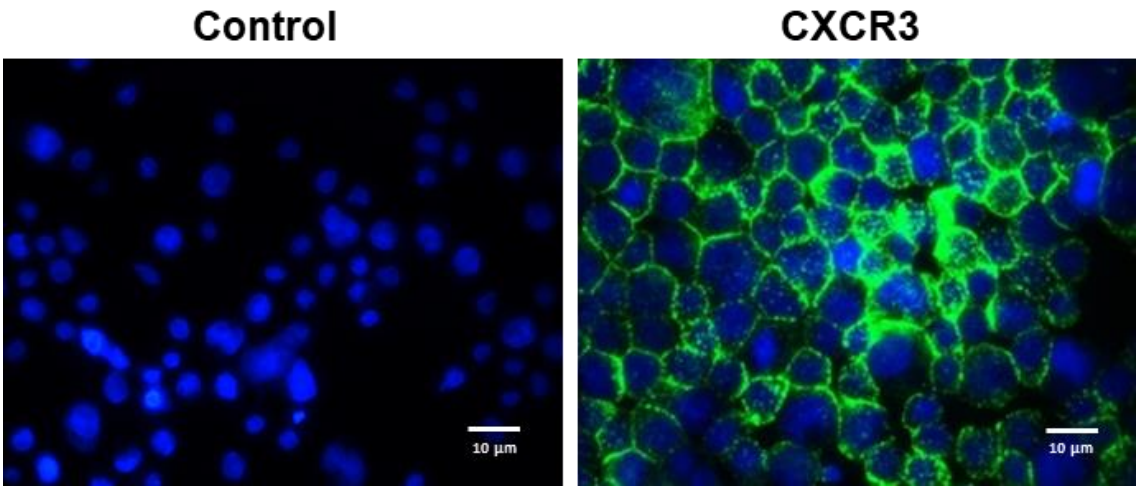

Figure 45. THP-1 cells express CXCR3. Immunofluorescence staining of the THP-1 cell line using anti-CXCR3, and its corresponding secondary Alexa-488 conjugated antibodies (green). Control was anti-mouse Alexa-488 alone. The nucleus was stained with DAPI (blue). Cells were fixed, and images are representative of the cell population of one experiment out of three independent repeats, acquired at 63x objective using a Leica DMII fluorescence microscope and Leica imaging suite.

3.2.2.1.2 THP-1 cells migrate towards CXCL10 using a chemotaxis assay

Following the results showing that CXCR3 is expressed by THP-1 monocytic cells, the response of cells to CXCL10 (1 nM) was measured using a chemotaxis assay (**Figure 46**). Petrovic-Djerovic and colleagues [455] already confirmed that recombinant human CXCL10 could stimulate chemotaxis in THP-1 cells. Our results supported their observations and CXCL10 could significantly enhance chemotaxis of THP-1 cells.

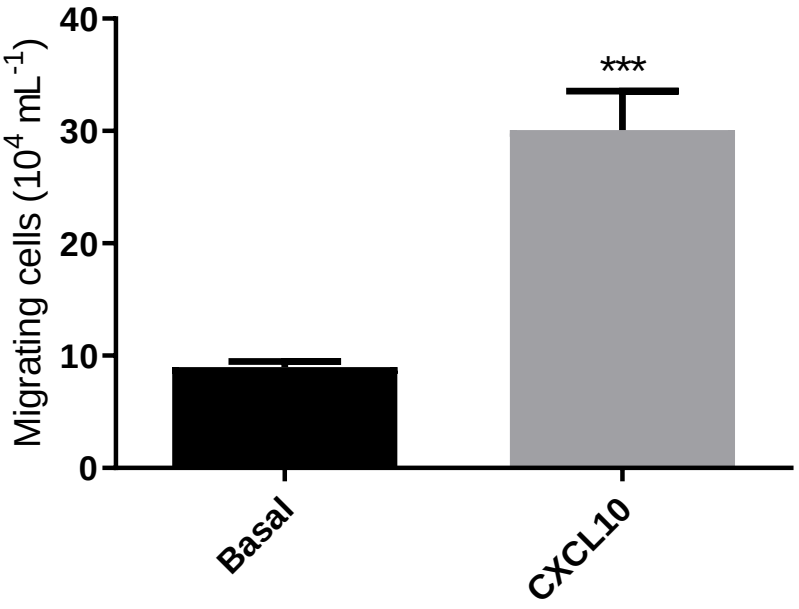

Figure 46. CXCL10 increases the migration of THP-1 cells in a chemotaxis assay. Cells were incubated with or without CXCL10 (1 nM) for 5 hrs. Data shown are the mean ± SEM of six independent experiments. (Unpaired t-test, *** = $p \leq 0.001$).

3.2.2.1.3 CXCL10 stimulates intracellular calcium response in THP-1 cells

To investigate receptor activation upon application of CXCL10, calcium flux assays were performed. CXCL10 was shown to induce intracellular calcium release in a concentration-dependent manner (**Figure 47**).

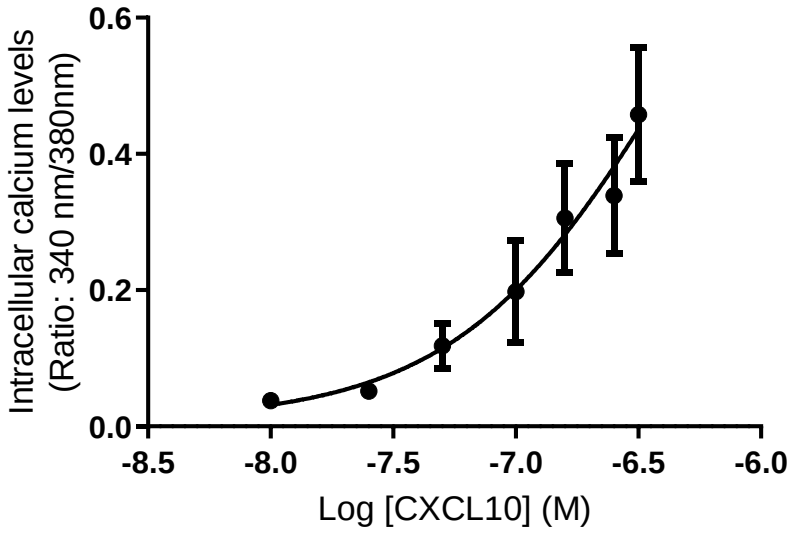

Figure 47. Intracellular calcium response of THP-1 cells following treatment with varying concentrations of CXCL10. Data is expressed as changes in fluorescence ratio (340 nm/380 nm) upon incubation with 4 µM Fura-2 for 30 min. The basal fluorescence, prior to the addition of CXCL10, is subtracted from peak fluorescence following injection of CXCL10. Data represent mean ± SEM from five independent experiments. (Non-linear regression dose-concentration response curve assuming a Hill coefficient of 1).

3.2.2.2 The response of MDA-MB231 cells to CXCL10

3.2.2.2.1 Expression of the CXCR3 receptor on MDA-MB231 cells

CXCR3 on MDA-MB231 cells was already highlighted to be highly expressed by flow cytometer [243]. Again, our immunofluorescence data confirms these previous observations (**Figure 48**).

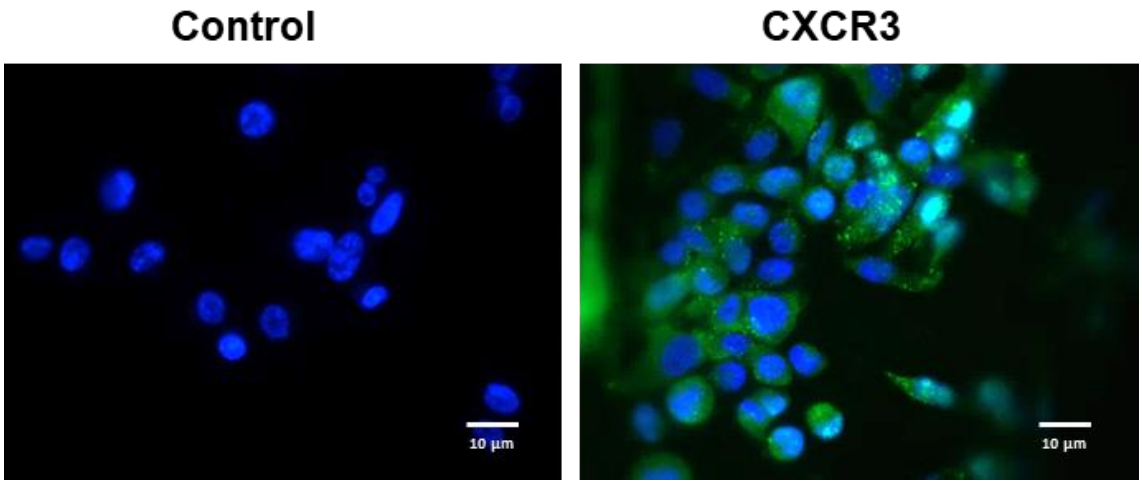

Figure 48. MDA-MB231 cells express CXCR3. Immunofluorescence staining of the MDA-MB231 cell line using anti-CXCR3, and its corresponding secondary Alexa-488 conjugated antibodies (green). Control was anti-mouse Alexa-488 alone. The nucleus was stained with DAPI (blue). Cells were fixed and images are representative of the cell population of one experiment out of three independent repeats, acquired at 63x objective using a Leica DMII fluorescence microscope and Leica imaging suite.

3.2.2.2.2 MDA-MB231 cells migrate faster with CXCL10 in a time-lapse migration assay

Cell migration is a process required for wound healing, immune system function and cancer invasion [456]. It is a complex process that starts with cell polarization and extension of protrusions in the direction of migration [25]. Conventional methods like the Boyden chamber are often used to study chemotaxis *in vitro*. However, this method takes into account the endpoint of an assay and does not allow individual cell monitoring in real time. Although we have already shown that MDA-MB231 cells migrate towards CXCL8 (10 nM) with Boyden chamber assay, this method was not reproducible with other treatments. Therefore, random migration by applying a stimulus (chemokinesis) to the wells of adhered cells was conducted and the speed of migrating cells was analysed. The migration speed of MDA-MB231 cells significantly increased upon the application of CXCL10 (18.9 ± 6.3 μm/hr and 31.2 ± 5.2 μm/hr for the basal and CXCL10-stimulated cells, respectively; **Figure 49**).

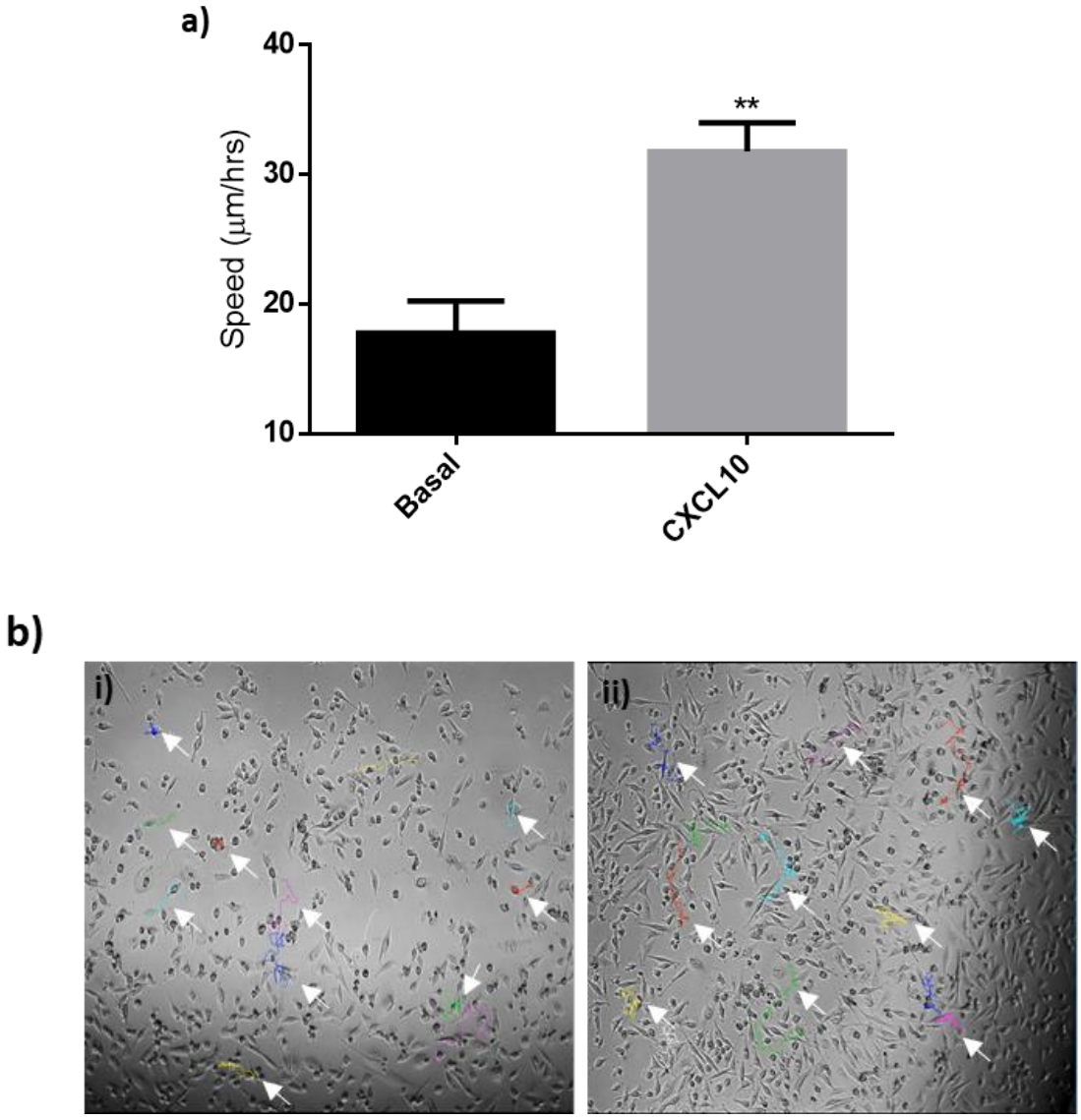

Figure 49. MDA-MB231 cells migrate faster in the presence of CXCL10. a) MDA-MB231 cells stimulated with CXCL10 (10 nM) show a significant increase in the speed of cell migration (average speed of 10 cells in each experiment). **b)** endpoint images from individual cell tracking using Fiji/ImageJ after 10 hrs, i) Basal, ii) CXCL10 (10 nM). Data shows representative cell tracks from individual cell tracks from three independent experiments (Unpaired t-test, ** = $p \leq 0.01$). Images are representative of the cell population and were taken at 10x objective with a Zeiss Axiovert 200M microscope and processed using AxioVision Rel 4.8 software.

3.2.2.2.3 The Oris migration assay is not reproducible with MDA-MB231 cells

The Oris migration assay could be considered as a robust alternative method to the wound healing assay. It allows the formation of an accurate cell free area for the free migration of cells without the presence of dead cells following the formation of a wound. Upon testing the wound healing assay with MDA-MB231 cells, no migration towards closing the wound was observed and results were too inconsistent to make conclusions. MDA-MB231 cells in the Oris migration assay showed similar patterns of cell migration. Cells seemed to be migrating to the edges, rather than moving towards the centre of the Oris detection area. Therefore, when staining the migrating cells, many of them migrated to the sides of the wells, and not towards the detection area as shown from the images taken with light and fluorescence microscopy (**Figure 50**). Subsequently, it was decided that this assay was not adequate for measuring MDA-MB231 cell migration.

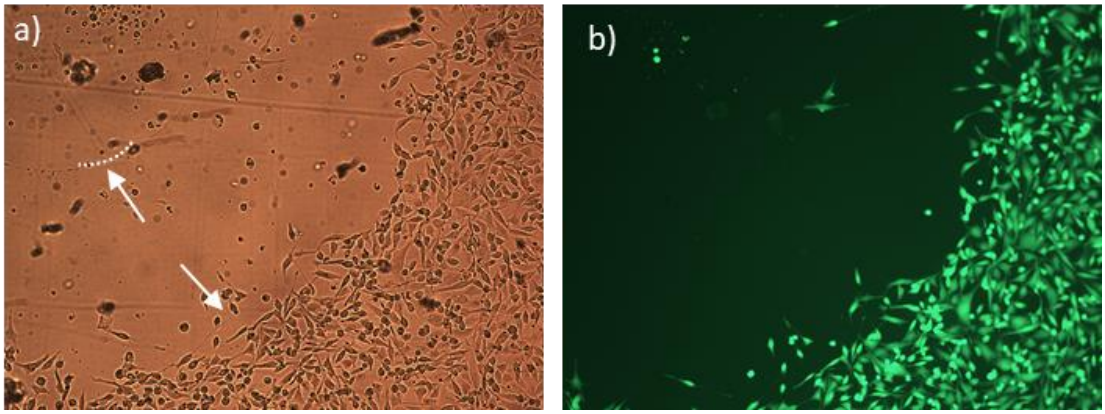

Figure 50. Oris migration assay is not a suitable system to study MDA-MB231 cell migration. MDA-MB231 cells appear to migrate to the edges rather than to the middle of the detection area. This made Oris migration assay an un-suitable system for quantifying migration. **a)** Shows a bright-field image of the well after stimulation with CXCL10 (10 nM) over 24 hrs; arrows indicate where the cells are residing away from the centre of the detection area demonstrated by the dash line. **b)** Calcein-stained image of the same location captured with fluorescence microscopy. Images were taken at 10x objective with a Leica DM16000 inverted microscope and using Leica imaging suite.

3.2.2.3 The response of PC3 cells to CXCL10

3.2.2.3.1 Expression of the CXCR3 receptor on PC3 cells

CXCR3 binding ligands has been acknowledged to block the migration of adherent cells such as fibroblasts and endothelial cells, despite being chemotactic for leukocytes [205], [457], [458]. CXCR3 mRNA was already reported by Wu *et al.,* [226] to be expressed in PC3 cells. Here, immunofluorescence staining confirmed that CXCR3 was expressed on PC3 cells (**Figure 51**).

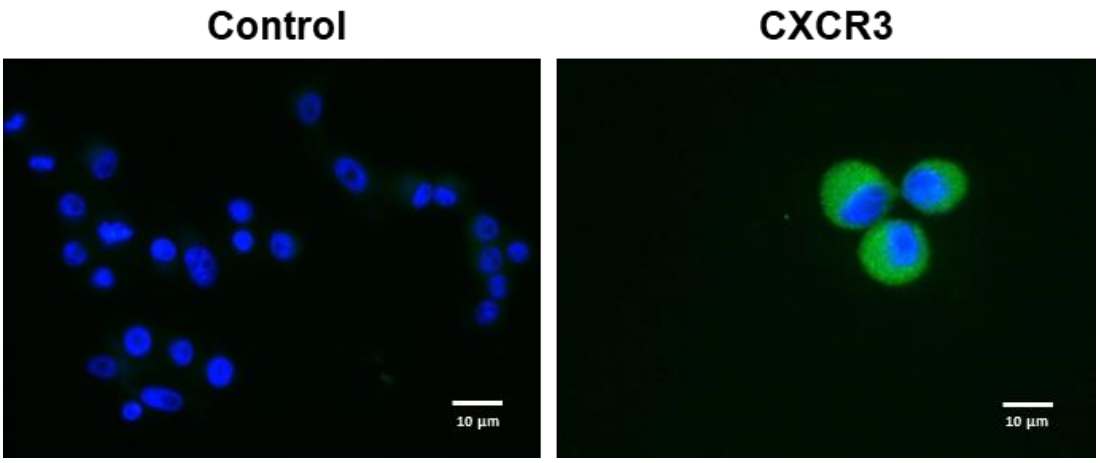

Figure 51. PC3 cells express CXCR3. Immunofluorescence staining of the PC3 cell line using anti-CXCR3, and its corresponding secondary Alexa-488 conjugated antibodies (green). Control was anti-mouse Alexa-488 alone. The nucleus was stained with DAPI (blue). Cells were fixed, and images are representative of the cell population from one experiment out of three independent repeats, acquired at 63x objective using a Leica DMII fluorescence microscope and Leica imaging suite.

3.2.2.3.2 PC3 cells migrate faster with CXCL10 in a time-lapse migration assay

Cells were incubated with CXCL10 (10 nM) and a time-lapse migration assay was performed to assess the effect of this chemokine on the speed of migration. The speed of untreated cells was 18.9 ± 2.7 μm/hr which increased to 50.4 ± 8.7 μm/hr following the addition of CXCL10 (**Figure 52**).

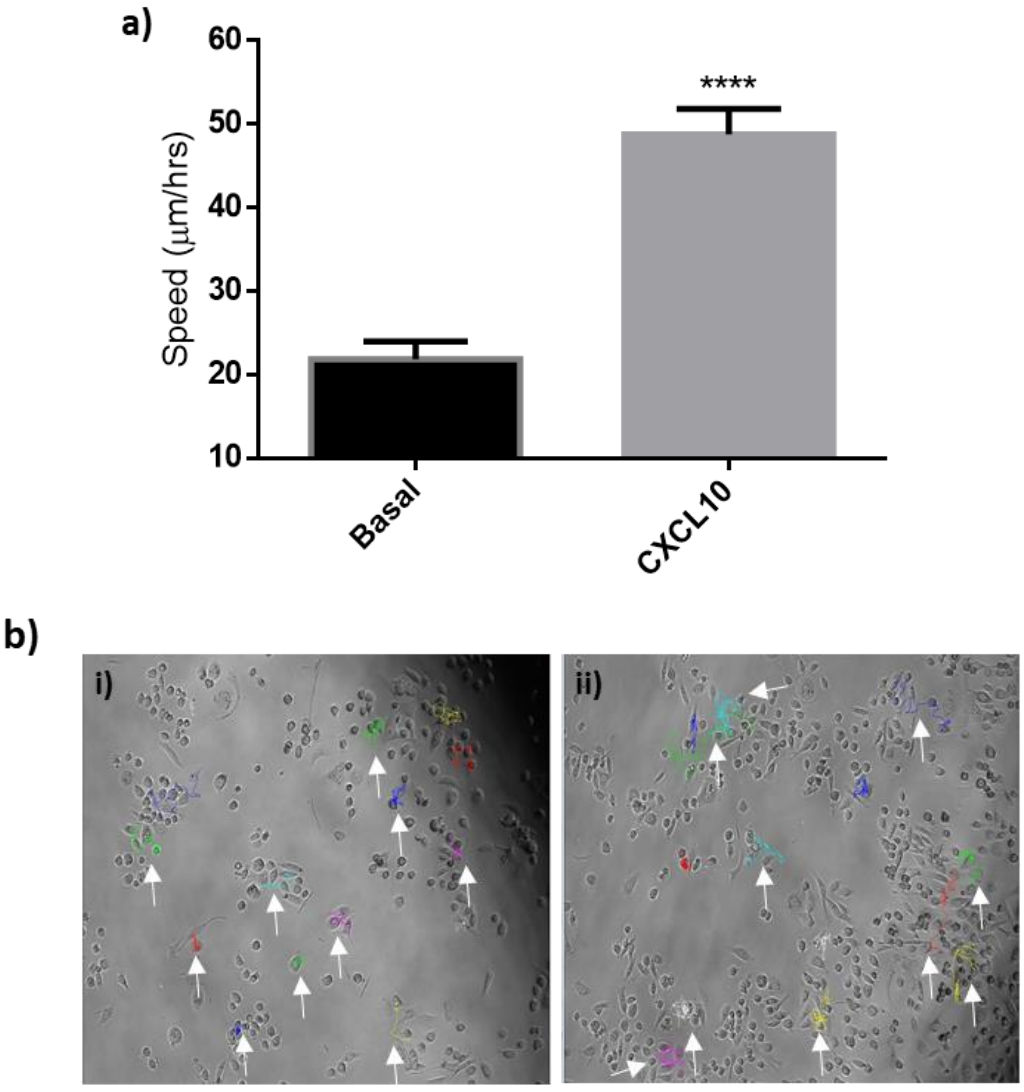

Figure 52. PC3 cells migrate faster in the presence of CXCL10. a) PC3 cells stimulated with CXCL10 (10 nM) displayed a significant increase in the speed of migration (average speed of 10 cells in each experiment). **b)** Endpoint images from individual cell tracking using Fiji/ImageJ after 10 hrs, i) Basal, ii) CXCL10 (10 nM). Data shows representative cell tracks from individual cell tracks from three independent experiments (Unpaired t-test, **** = p ≤ 0.0001). Images are representative of the cell population and were taken at 10x objective with a Zeiss Axiovert 200M microscope and using AxioVision Rel 4.8 software.

3.3 Discussion

Chemokines and chemokine receptors are acknowledged to provide navigational cues for leukocytes or cancer cells, induce migration and metastasis, promote entry into the circulation, and enhance invasion into specific tissues [78]. Various cancer cell types have been found to have elevated expression of both chemokines and their receptors, resulting in dysregulated chemokine signalling [78]. CXCL8 was first characterized as a leukocyte chemoattractant, however, further studies have shown its pleiotropic role in tumour progression. For example, CXCL8 has a demonstrable role in recruiting neutrophils to the tumour microenvironment, inducing angiogenesis, regulating the progression and aggressiveness of cancer cells, and protecting the cancer stem cell population from cancer therapy [459]. Aberrant expression of CXCL8 and its cognate receptors therefore contribute to the invasive phenotype observed in breast, ovarian, pancreatic, thyroid and other cancers (as reviewed by [131] and [459]).

CXCR1 and CXCR2 are GPCRs that share roughly 76% sequence homology [460], and are directly involved in the physiological and pathological signalling of CXCL8. CXCR1 has high affinity and specificity for CXCL8, and CXCR2 can bind to chemokines CXCL1-3 and CXCL5-8, with higher affinity to CXCL8 [461], [462]. The expression of CXCR1 and CXCR2 on different cancer cell types and the effect of CXCL8 binding on the migration speed and chemotaxis of these cell types was investigated in this chapter.

The transient intracellular calcium release upon chemokine binding was also investigated to assess receptor activation on these cells. When GPCRs are activated, the intracellular calcium in chemokine-stimulated cells can rise rapidly. The low basal intracellular calcium levels and the rapid rise of the cytosolic calcium allows the use of the fluorescent dye Fura-2 to measure transient changes in cytosolic calcium concentrations [463]. Receptor activation promotes PLC which cleaves PIP2 to IP3 and DAG. DAG is membrane bound, while IP3 is released into the cytosol where it opens IP3 channels present on intracellular calcium stores [464].

Several cancer cell types were used to screen the effects of CXCL8, including the human monocytic leukaemia THP-1, acute T-cell leukaemia Jurkat, breast MDA-MB231 and MCF-7, and prostate PC3 cancer cell lines (**Table 5**). Jurkat cells stimulated with CXCL8 showed no increases in migration (**Figure 23**), however, they migrated towards CXCL12. This effect of CXCL12 on Jurkat cells was previously confirmed by Mills *et al.* [388]. Intracellular calcium release was used as a tool to inspect CXCR1 and CXCR2 activation upon CXCL8 administration. Indeed, Jurkat cells responded poorly when stimulated with varying concentrations of CXCL8, with the EC_{50} being difficult to determine. To our knowledge, CXCL8 and its receptor axis had not been investigated previously in Jurkat cells. We assumed that Jurkat cells do not express CXCL8 receptors, as indicated by the chemotaxis and calcium flux experiments, or that CXCL8 is unable to induce chemotactic activity in this cell type. Indeed, GPCRs can mediate many other functions such as cell survival or apoptosis, cell proliferation, and gene transcription. However, these functions are dependent on the cell type, receptor, and stimulus [465], [466]. So, even if there was activation of the receptor in the cells, it is does not necessarily mean that induction of intracellular signalling would only lead to chemotaxis.

Table 5. Summary of the response of different cancer cell types to CXCL8 or CXCL10 along with chemokine receptor expression. N/A: not applicable

	Receptor expression	Calcium release	Migration
THP-1	↓CXCR1 ↑CXCR2 ↑CXCR3	**Dose response** ↑CXCL8 ↑CXCL10	**Chemotaxis** ↑CXCL8 ↑CXCL10
Jurkat	N/A	CXCL8: No response CXCL10: N/A	CXCL8: No migration CXCL10: N/A
MDA-MB231	↑CXCR1 ↑CXCR2 ↑CXCR3	N/A	**Boyden chamber** ↑CXCL8 **Time-lapse migration** ↑CXCL8 ↑CXCL10
MCF-7	↑CXCR1 ↑CXCR2 ↑CXCR3	**Dose response** ↑CXCL8	**Wound healing** ↑CXCL8
PC3	↑CXCR1 ↑CXCR2 ↑CXCR3	N/A	**Oris Migration** ↑CXCL8 **Time-lapse migration** ↑CXCL8 ↑CXCL10

THP-1 cells on the other hand, showed elevated expression level of CXCR2 which agrees with a previous study [421]. Since intracellular calcium changes and chemotaxis are mediated by CXCL8 receptors, these cellular responses can be utilized to assess receptor usage. Migrating cell numbers were significantly increased in the presence of exogenous CXCL8. Furthermore, blocking CXCR1 and/or CXCR2 with the antagonists SCH527123 or SB225002 reduced the number of migrating cells significantly. Reparixin also decreased the number of cells migrating, although not significantly, and this could be because it has a lower inhibitory effect towards CXCR2 than CXCR1 [467]; as THP-1s did not express CXCR1.

The metastatic potential of breast cancer cell lines is highly correlated with ectopic expression of CXCL8. Studies have found that CXCL8 production is elevated in metastatic breast cells compared to their less metastatic counterparts [167]. Miller *et al.* [468] found that CXCR1 and CXCR2 were expressed in all breast cancer cells while only 50% of the benign breast cells expressed either of the receptors. Using RT-PCR, Freund *et al.* [439] reported that CXCR1 expression level was very low. However, several other studies have shown the expression of CXCR1 is actually much higher than that first reported in MDA-MB231 cells [243], [424], [445]. Another study reported CXCR2 levels are low in MCF-7 but high in MDA-MB231 cells [446]. MCF-7 and MDA-MB231 cells were tested for receptor expression as well as their migratory behaviour. Although there is controversy around the expression of CXCL8 receptors on MCF-7 cells [439], [446], [447], our findings showed that both MCF-7 and MDA-MB231 expressed both CXCR1 and CXCR2 (**Figure 25** and **Figure 33**). This controversy could be due to the oestrogen receptor dependency of the cells [469]. The oestrogen receptor is a contributing factor to the invasiveness of the breast cancer cell lines, for example, MDA-MB231 cells are oestrogen receptor negative and constitutively express elevated levels of CXCL8 which is suggested to be associated with its invasive and metastatic features [439], [470]. Conversely, MCF-7 cells are oestrogen receptor positive and were reported not to express CXCL8 using RT-PCR, ELISA, and Northern blot, thus have a low invasion potential profile [470].

As there is not enough data from the current literature to conclude the effects of CXCL8 on the motility of breast cancer cells, we examined the migratory behaviour of both MCF-7 and MDA-MB231 cell lines in response to exogenous CXCL8. Using wound healing migration assays, MCF-7 cells migrated more in the presence of CXCL8, and the CXCR1 and CXCR2 antagonist, SB225002, significantly blocked this migration over 24 hrs (**Figure 35**). CXCL8 also induced calcium flux in MCF-7 cells in a concentration-dependent manner, giving an EC_{50} of 364 nM. Moreover, Reparixin and SB225002 significantly blocked the release of calcium. MDA-MB231 cells reacted similarly to

CXCL8, and increased migration was observed in a Boyden chamber migration assay. In addition, faster cell migration in response to CXCL8 was observed using a time-lapse migration assay. The migration speed was significantly reduced when CXCR1/2 was inhibited by SCH527123 or SB225002. Comparing the migratory response of both cell types, we found that the migration speed of MCF-7 cells was too low to be analysed via a time-lapse migration assay or in a Boyden chamber. In fact, Larco *et al.* [470] looked at the morphological changes of both cell types and reported that MDA-MB231 (oestrogen-independent) displayed a more mesenchymal cellular shape. Whereas MCF-7 (oestrogen-dependent), with lower CXCL8 production, exhibited an epithelioid shape, forming more cell-to-cell interactions associated with a non-migratory response. Therefore, we observed that both MCF-7 and MDA-MB231 cells respond to CXCL8, however, the response varied between the cell lines, presumably because of their invasiveness which is associated with their oestrogen-receptor dependency.

CXCL8 was also shown to significantly enhance proliferation of MDA-MB231 cells. However, the approach we used to analyse the results here was merely based on observation. Screenshots of MDA-MB231 cells in the time-lapse migration assay were taken before and after the addition of CXCL8. More cells appeared in the picture frame in the presence of CXCL8 in the three experiments undertaken. Xu *et al.* [446] have suggested that high expression of CXCR2 in MDA-MB231 cells promoted their proliferation and tumorigenesis activity. However, in another study that linked CXCL8 to the invasion properties of MDA-MB231 cells, they did not see the proliferation rate being affected [439]. Subsequently, our preliminary analysis showed more MDA-MB231 cells proliferating in response to CXCL8, nonetheless, the role of this chemokine on mitogenic activity appears to be more complex and requires further investigation.

Increased CXCL8 levels is a contributing factor for poorer overall survival in men with metastatic prostate cancer [471]. We observed CXCR1 and CXCR2 expression on PC3 cells and found that they express both receptors. This is in agreement with previous reports that detected CXCR1 and CXCR2 RNA transcripts in PC3 cells using RT-PCR [450] [451]. PC3 cells migrated significantly faster in the presence of CXCL8 in an Oris migration assay, and their migration speed was doubled using time-lapse migration assay. Reparixin, SCH527123, or SB225002 drastically reduced the speed of cells. To further elucidate the mechanism of how CXCL8 stimulates migration, it is worth investigating the specific CXCL8 receptor involved in this process. For example, Reiland *et al.* [450] found that CXCL8 mediated its adhesive and migration effects through CXCR2. While Murphy *et al.* [331] attributed the increased mitogenic activity to both CXCR1 and CXCR2. Another study by Araki and colleagues [472] reported that CXCL8 expression was androgen dependent, whereby CXCL8 is highly expressed in androgen-

independent cells like PC3 and poorly expressed in androgen-responsive cells like LNCaP. They also found that CXCL8-transfected LNCaP along with PC3 cells, have increased chemotactic motility and invasion rates in the presence of CXCL8. Furthermore, CXCL8 could be associated with an enhanced mitogenic activity in several cell types [473]. We observed an increased proliferation rate in PC3 cells in the presence of CXCL8 relative to the basal sample (**Figure 43**). In agreement with this observation it has been reported that CXCL8 can stimulate PC3 proliferation via ERK-MAPK signalling or AKT phosphorylation [474], [331]. Additionally, blocking CXCR2 with SB225002 could reduce the number of proliferating cells [331]. Furthermore, silencing CXCL8 signalling using CXCL8 siRNA reduced proliferation and inhibited invasiveness [475]. Altogether, our data along with others highlight CXCL8 as a crucial chemokine involved in enhancing the metastasis and proliferation of prostate cancer PC3 cells. Yet, further investigation of the specific CXCL8 receptors involved or the dependency on androgen could give a better vision for developing more targeted treatments.

CXCR1 and CXCR2 are proven targets for small molecular antagonists, and thus considered as useful anticancer therapies. Reparixin is a non-competitive allosteric inhibitor of CXCR1 and, to a lesser extent, of CXCR2 [162]. It was reported to reduce metastasis of breast cancer and cancer stem cells in human and xenografts in mice, alone or with chemotherapy [424]. A recent study showed that Reparixin appeared safe, and cancer stem cells could be reduced in several patients, implying a role for CXCR1 [476]. Reparixin functions by locking CXCL8 receptors in an inactive conformation, therefore blocking receptor signalling [477]. This antagonist was found to induce its inhibitory effects at different concentrations based on the cell type. Experiments were initiated with low doses of the antagonist Reparixin calculated on the basis of the IC_{50}. Starting with MCF-7 cells, we found a significant decrease in intracellular calcium release with 500 nM Reparixin. Bertini *et al.* [162] found that polymorphonuclear (PMN) cells responded to Reparixin with a significant reduction in cell migration and calcium release observed with concentrations of 1 nM to 1 µM in the presence of CXCL8 (3, 10 or 30 nM). They suggested that the IC_{50} for CXCR1 was 1 nM while CXCR2 had a higher IC_{50} of around 100 nM in PMN cells, making Reparixin a more potent antagonist to CXCR1 than CXCR2. However, our results showed that MDA-MB231 and PC3 cells required higher concentrations of the antagonists to generate an inhibitory effect. At a concentration of 10 µM, Reparixin reduced the speed of migrating MDA-MB231 cells. In a relevant study, Reparixin induced a concentration-dependent inhibitory effect (1 µM - 1 mM) on cell viability, mammosphere size, focal adhesion kinase, and β-catenin levels [445]. Another study used 40 or 60 µM of Reparixin or SCH527123 on MDA-MB231 cells and found that there was an inhibitory effect on cell viability and a modest decrease to

cell migration or colony formation [443]. Furthermore, THP-1 cells also required slightly higher concentrations of the receptor's antagonists, suggesting that the cellular context may influence the susceptibility to Reparixin. The variability in the inhibitory concentrations required to cause an effect is possibly due to the heterogeneity of cancer cell types and cell batches used in different laboratories.

SCH527123 is an allosteric antagonist that binds to CXCR1 and CXCR2; while it has moderate affinity for CXCR1, it is CXCR2-selective [163]. SCH527123 has shown potential therapeutic value in inflammatory diseases, as well as inhibited recombinant cells (CXCR1 and CXCR2) and neutrophil chemotaxis [163]. Another study found that SCH527123 blocked melanoma cancer proliferation and colorectal cancer liver metastasis by reducing the growth and angiogenesis, and promoting apoptosis of malignant cells [424], [478]. We found that THP-1 chemotaxis and calcium flux were significantly inhibited by SCH527123. Additionally, MCF-7 cells intracellular calcium release was drastically reduced. Moreover, MDA-MB231 and PC3 cell motility was slowed down in SCH527123-treated cells in the presence of CXCL8.

SB225002 is another potent, specific CXCR2 receptor antagonist. *In vivo* studies of the antagonist showed that it could inhibit proliferation of prostate cancer cells [429]. This is in agreement with the reduced migration speed of PC3 and MDA-MB231 cells we observed whilst using SB225002. Moreover, intracellular calcium flux and migration were also significantly reduced in THP-1 and MCF-7 cells following inhibition. Different articles reported that SB225002 induces cell death in ovarian cancer cells, as well as cell arrest in acute lymphoblastic leukemic cells [479], [480]. Our data showed no cytotoxicity with any of the antagonist concentrations used, therefore, the inhibitory response they induced on the cells was due to the interference with the ligand-receptor interaction and not cytotoxicity.

It is worth noting that the previous migration assays reported were applied to all cell lines, however, not all the cell lines reacted in the same way due to differences in the migration patterns. For example, the wound healing assay is widely used, and a cheap method to detect cell migration. Trying this method with MCF-7 cells did not produce reliable enough data to confirm the effects of CXCL8 and its receptors antagonists. MCF-7 are made of epithelial cell types that form cellular sheets. During tumour progression these epithelial cells can take on a mesenchymal morphology by displaying enhanced migratory capacity and less adhesion [481]. The wound healing assays were applicable for this cell type due to the cells being grown in sheets. However, this method was time consuming and gave varying results with different cell batches. This assay proved not to be reproducible with more invasive cell lines like PC3 and MDA-MB231 cells. Moreover, we were intrigued to try the agarose spot migration assay which

was already reported [442] as a method that forms a chemokine concentration gradient and therefore a potential determinant of the directionality of cell migration. Yet, this method was unreproducible, primarily due to the agarose spots sliding in the wells, even with changing the well types from plastic to glass (**Figure 27**). Time-lapse migration assays were an ideal technique for quantifying the migration speed of cells in real-time; sparse seeding of MDA-MB231 and PC3 cells allowed them to migrate freely, but MCF-7 moved too slow to analyse, even in the presence of a stimulus. Furthermore, Boyden transwell chambers are widely used [482] to measure the chemotactic behaviour to a specific stimulus. However, although some data was generated with MDA-MB231 cells responding to CXCL8, the reproducibility of this method declined giving variable and inconsistent results when attempted with different compounds. No data was generated with PC3 and MCF-7 cells using this method.

The results obtained with CXCL8 prompted us to investigate and compare the effects of CXCL10 in the previously used cell lines. CXCR3 can bind to CXCL9, CXCL10, and CXCL11 and has received much attention due to its role in regulating immune cell migration, differentiation, and activation. Many cells like natural killer and natural killer T cells, dendritic cells, $CD4^+$, $CD8^+$ T cells, and regulatory T cells express CXCR3 [483], [484]. It was reported that tumour cells can hijack the CXCR3/ligand signalling axis to migrate from the primary tumour and to metastasize to niches with elevated levels of CXCR3 ligands, such as the lymph node or lungs [240], [249], [250], [253]. Moreover, overexpression of CXCL9 and CXCL10 was found to induce higher numbers of tumour-infiltrating lymphocytes and enhanced survival rates in multiple cancer types like in breast, ovarian, colon, lung and other cancers (as reviewed by [485]). Other studies have reported that CXCR3 expression by cancer cells is correlated with poorer prognosis in these cancers by recruiting tumour-promoting regulatory T cells [486], therefore the overall effect of CXCR3 overexpression by tumour cells should be further investigated.

CXCR3 is a GPCR that is identified to have three different isoforms. CXCR3-A and CXCR3-B bind to CXCL9, CXCL10, CXCL11, CXCL4 and CXCL4L1, with varying affinity. CXCR3-A activates several signals involved in functions such as chemotaxis, invasion, proliferation, and cell survival [487]. Whereas, CXCR3-B does not induce chemotaxis, instead it is responsible for anti-angiogenic and anti-proliferative responses [205]. The third isoform is CXCR3-Alt, which was found to have affinity to CXCL11 but not CXCR9 or CXCL10, initiates moderate chemotaxis and calcium flux responses [227], [487].

The expression of CXCR3 in different cancer cell types along with the migratory behaviour in the presence of CXCL10 is discussed here. Immunofluorescence assays demonstrated the expression of CXCR3 by THP-1 cells. Chemotaxis assays showed

enhanced migration of THP-1 cells towards CXCL10. This agrees with a study reporting THP-1 chemotaxis was increased by CXCL10 but not CXCL11 [455]. CXCR3 activation in THP-1 cells was identified by calcium flux. Indeed, CXCL10 induced calcium release in a concentration-dependent manner giving an estimate EC_{50} of 416 nM. CXCL10 was already reported to induce calcium flux and chemotaxis [217]. Furthermore, immunofluorescence analysis also revealed CXCR3 receptor expression on breast MDA-MB231 cells. The high expression of CXCR3 by these cells was already reported by flow cytometer measurements [243]. Time-lapse migration assays demonstrated an increase of the speed of cell migration in the presence of CXCL10. This corresponds to a study showing an increased motility rate associated with CXCR3 [244]. Moreover, prostate cancer PC3 cells also showed expression of CXCR3. However, the robustness of the CXCL10/CXCR3 axis is challenged by the variant isoforms of CXCR3. As mentioned before, CXCR3-A and CXCR3-B appear to have contradictive downstream signalling effects. We could hypothesise that the previous cell lines have potentiated their migratory effect through CXCR3-A, which was already reported to have induced cell migration; and possess lower levels of CXCR3-B, having a lower inhibition effect on migration. Nonetheless, further experiments looking into the dominant expression levels of both receptors as well as ruling out the main receptor involved in the migration process could give us better insights into understanding the underlying effect of CXCL10.

3.4 Conclusion

This chapter explored the expression of CXCL8 and CXCL10-receptors on different cancer cell lines along with their roles in controlling migratory behaviour. This resulted in several conclusions:

1. MCF-7, MDA-MB231, and PC3 cells express CXCR1 and CXCR2. THP-1 cells do not express CXCR1 but express CXCR2.
2. CXCL8 induces intracellular calcium signalling in a concentration-dependent manner in THP-1 and MCF-7 cells.
3. THP-1, MCF-7, MDA-MB231, and PC3 cells migrate more in the presence of CXCL8 either directly or randomly based on the migration assay used.
4. MDA-MB231 cells have higher proliferation rate in the presence of CXCL8. PC3 cells too showed a similar trend but it was not significant.
5. Small molecular antagonists for CXCR1 and CXCR2 - Reparixin, SCH527123, and SB225002 reduce CXCL8 signalling by reducing calcium release, wound healing, and/or migration speed.
6. THP-1, MDA-MB231, and PC3 cells express CXCR3.
7. Significant number of THP-1 cells migrate towards CXCL10, as well as increasing intracellular calcium in a concentration-dependent manner was reported in the presence of CXCL10.
8. MDA-MB231 cells migrate faster in the presence of CXCL10 and PC3 cells with CXCL10 and CXCL11.
9. We tested several migration assays such as agarose spot assay, Oris migration assay, wound healing assay, Boyden chamber, time-lapse migration assay, and highlighted the most reproducible system for each cell line.

Chapter 4: Intracellular signalling pathways involved in the migration of CXCL8-activated cancer cells

4.1 Introduction

Protein phosphorylation regulates several aspects of cellular functions, including cell migration and actin reorganisation [262]. This process involves transferring phosphoryl groups onto target proteins to alter their activity. The reverse of this action is carried out by phosphatases, which remove phosphoryl groups from target proteins [323]. Once the target protein is phosphorylated, a series of signalling-transduction pathways are induced, allowing intracellular and extracellular signals to be transduced through the cell to the nucleus. The abnormal behaviour of kinases due to the loss of inhibitory regulators or mutations could lead to diseases that are associated with uncontrolled survival and/or proliferation of cells, such as in cancer [488], [489]. Several strategies have been established that are aimed at targeting protein kinases, such as the development of small molecule inhibitors and antibodies. These approaches work by a) targeting the ATP-binding site of the catalytic site of the kinase, b) recognising the inactive conformation of the kinase c) binding outside the ATP-binding site to an allosteric site, or d) irreversibly forming covalent bonds to the kinase active site [490].

Targeting signalling molecules involved in chemokines-driven cancer cell migration could lead to more precise cancer therapeutic advancements. Chemokines are involved in cell migration by activating intracellular signalling cascades that lead to cytoskeletal rearrangement and cell polarization [77]. The process of cell migration begins with cell polarization, characterised by the formation of lamellipodia, filipodia, and stress fibres. These three structures are vital to drive the several stages of actin-based endothelial cell motility [491]. Several signal transduction molecules are involved in the regulation of migration. The Rho GTP-binding family, Rho, Rac, and Cdc42 control the formation of focal adhesion, lamellipodia, and filipodia, respectively [25]. In addition, Ras, MAPK, FAK, Pi3K, and PLC and their effects on intracellular calcium have been implicated in the activation of cell migration [282]. Collectively, further investigation should be carried out to clarify how these signalling molecules convert the recognition of chemokines via their receptors into physical action.

Chapter aim:

Investigate the main signalling pathways involved in CXCL8-induced cell migration and cell morphology changes in MDA-MB231 and PC3 cells.

It is worth noting that the time-lapse migration assay conducted throughout this chapter involved all the set of inhibitors run together for each cell line at the same time. However, data was presented separately by categorizing inhibitors according to signalling pathways.

4.2 Results

4.2.1 Pi3K and AKT signalling pathway

4.2.1.1 Pi3K/AKT signalling is important for cells migration

In the previous chapter, we investigated the migratory behaviour of MDA-MB231 cells after being stimulated with 10 nM CXCL8. The migration speed of the cells almost doubled within the 10 hrs time-lapse imaging assay performed, relative to the basal untreated cells. Growing evidence has highlighted that Pi3K acts as the major downstream intracellular signalling molecule of CXCL8. Here, it is implicated in the regulation of a diverse array of cellular functions such as cell survival, actin reorganisation, and chemotaxis [336], [492]. LY294002, is a well-established potent pharmacological inhibitor of Pi3K and its use has advanced our knowledge on the importance of this signalling pathway [290]–[292]. A time-lapse migration experiment was conducted to compare the speed of cells treated with CXCL8 in the presence or absence of LY294002 (10 µM). We observed a significant decrease in the speed of cells with the inhibitor. Untreated basal cells had a speed of 21.07 ± 7.5 µm/hr and addition of 10 nM CXCL8 increased this speed to 48.3 ± 4.4 µm/hr ($p \leq 0.0001$). Furthermore, cells incubated with 10 µM LY294002 and activated with CXCL8 displayed a speed comparable to untreated cells of 26.1 ± 3.3 µm/hr (**Figure 53**).

AKT (or PKB) is a serine/threonine kinase and a critical downstream component of the receptor tyrosine kinase-Pi3K complex [493]. Interest in AKT has emerged because of its role in regulating cell survival, growth, angiogenesis, and migration [282], [283]. Migration of MDA-MB231 cells has been demonstrated to be dependent on AKT proteins [494]. Indeed, MDA-MB231 cells incubated with the AKT inhibitor (AKTi) at a concentration of 20 µM drastically slowed the motility of CXCL8-treated cells down to a speed of 18.9 ± 3.3 µm/hr (**Figure 53**). This data agrees with a study showing that both LY294002 and AKTi can slow the motility of EGF-treated MDA-MB231 cells [495]. This same study found no effect of Pi3K and AKT inhibitors on the migration of MDA-MB231 without stimulation.

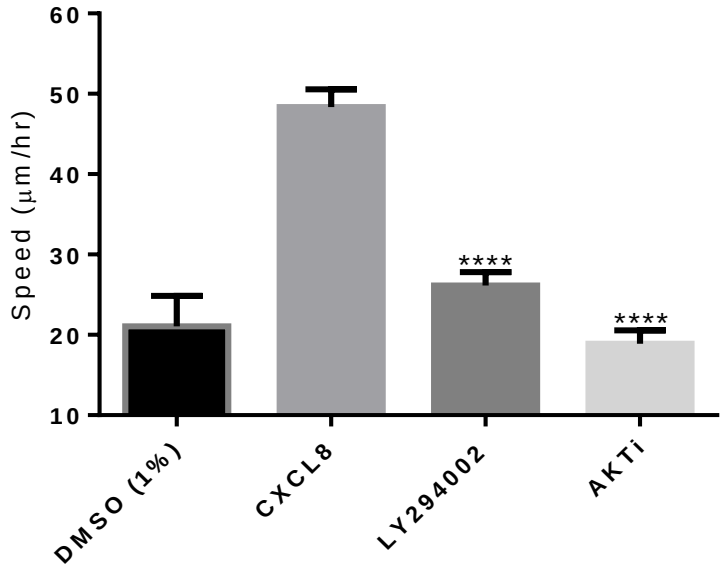

Figure 53. CXCL8-activated MDA-MB231 cells migrate slower in the presence of Pi3K or AKT inhibitors. Cells were incubated with the Pi3K inhibitor: LY294002 (10 µM) or AKT inhibitor: AKTi (20 µM) and activated with CXCL8 (10 nM). Significant reduction in the speed of migrating cells with both inhibitors was observed when compared to CXCL8. 1% DMSO was added to the basal cells as a vehicle control. Data are representative of the mean ± SEM of four independent experiments (One-way ANOVA with a Dunnett's multiple comparisons test as post-test, **** = $p \leq 0.0001$).

Prostate PC3 cells seem to be affected by Pi3K/AKT inhibition in a similar fashion to MDA-MB231 cells. Indeed, the basal speed of cells after 10 hrs was 25.7 ± 7.9 µm/hr, and the addition of CXCL8 (10 nM) increased this speed to 59.0 ± 21.4 µm/hr ($p \leq 0.0001$). LY294002 treatment could reduce this speed to 22.1 ± 11.1 µm/hr. While treatment with AKTi almost completely inhibited the migration of cells (speed of 3.4 ± 1.1 µm/hr; **Figure 54**). Notably, although cells treated with LY294002 alone without chemokine stimulation is not presented in this study, another group have demonstrated that this inhibitor did not affect the migration of unstimulated PC3 cells [496].

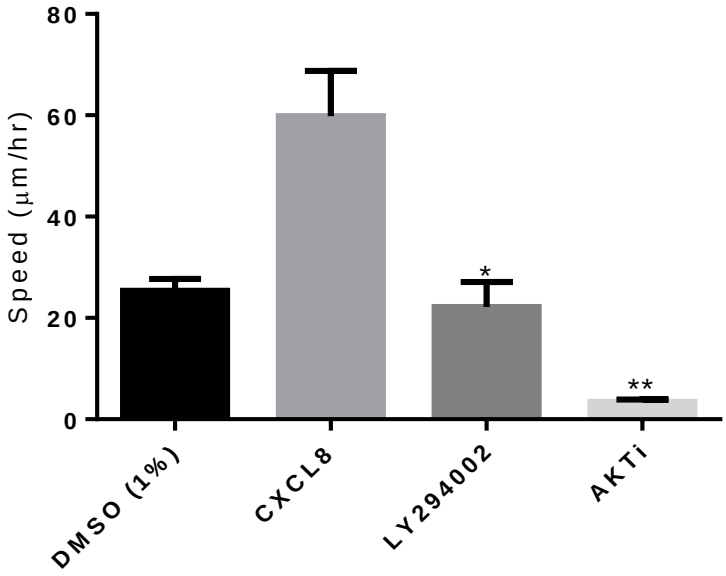

Figure 54. CXCL8-activated PC3 cells migrate slower in the presence of Pi3K or AKT inhibitors. Cells were incubated with the Pi3K inhibitor LY294002 (10 µM) or AKT inhibitor AKTi (20 µM) and activated with CXCL8 (10 nM). Both inhibitors reduced the speed of migrating cells when compared to CXCL8. Ten cells were analysed from each experiment using Fiji/ImageJ after 10 hrs. 1% DMSO was added to the basal cells as a vehicle control. Data are representative of the mean ± SEM of four independent experiments (One-way ANOVA with a Dunnett's multiple comparisons test as post-test, * = $p \leq 0.05$, ** = $p \leq 0.01$).

Furthermore, chemotaxis assays were performed on THP-1 cells to assess the importance of Pi3K on their migration. We found that LY294002 (10 µM) significantly decreased the number of migrating cells towards CXCL8 (**Figure 55**). A similar effect has been demonstrated by another group, showing that the migration of neutrophils stimulated with CXCL8 was abrogated with LY294002 [497]. Notably, our group have already confirmed that LY294002-treated THP-1 cells without chemokine activation show no migration, as well as no adverse effects towards actin filament structures as observed using an Alexa488-phalloidin actin stain [498].

However, injecting CXCL8 (200 nM) on to LY294002 pre-treated cells, did not inhibit the release of intracellular calcium (**Figure 56**).

Taken together, the data suggests that the Pi3K/AKT pathway is essential for the CXCL8-stimulated migration of MDA-MB231, THP-1, and PC3 cells, but not for THP-1 intracellular calcium release.

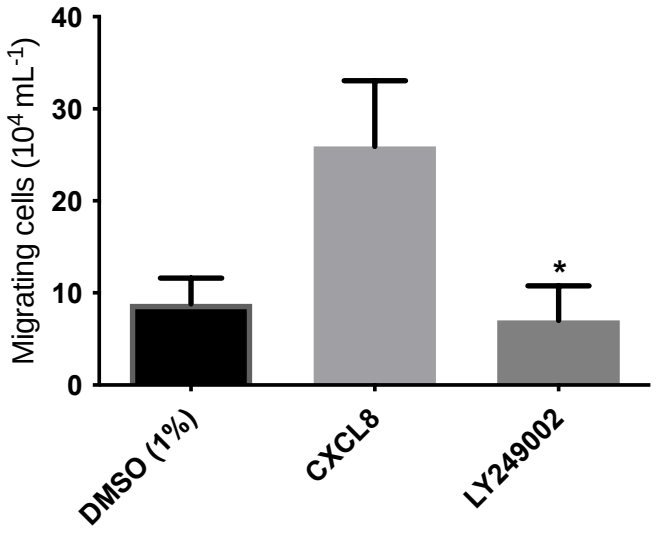

Figure 55. Pi3K inhibitor LY294002 decreases the migration of CXCL8-stimulated THP-1 cells in a chemotaxis assay. Significant reduction in the number of LY294002 (10 µM) treated cells towards CXCL8 (5 nM) compared to the migration of untreated cells after 5 hrs of incubation. 1% DMSO was added to the basal cells as a vehicle control. Data shown are the mean ± SEM of five independent experiments. (One-way ANOVA with a Dunnett's multiple comparisons test as post-test, *= p≤ 0.05).

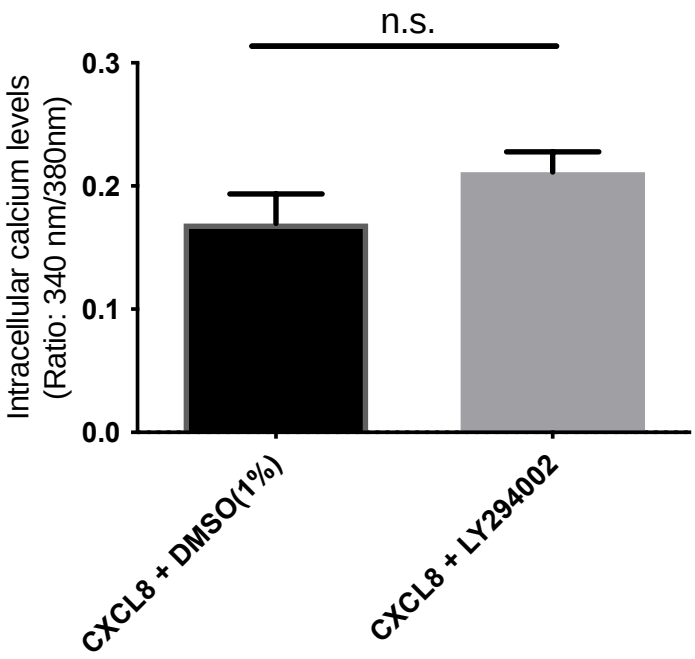

Figure 56. Pi3K inhibitor LY294002 does not inhibit intracellular calcium release in CXCL8-stimulated THP-1 cells. Basal, or LY294002 (10 µM) pre-treated cells shows no significant difference after stimulation with 200 nM CXCL8. 1% DMSO was added to the basal cells as a vehicle control. Data represents the mean ± SEM of five independent experiments. (Unpaired t-test, n.s. = no significance p > 0.05). Data are expressed as the relative ratio of fluorescence emitted at 510 nm after sequential stimulation at 340 and 380 nm.

4.2.1.2 Pi3K/AKT inhibitors induce changes to the cellular morphology

Pi3K has been identified as crucial for cell motility and establishment of cell polarity [499]. Clinical studies have demonstrated that cancer patients reporting elevated levels of AKT expression have more invasive and metastatic phenotypes which are correlated with poor prognosis [500]. These findings, along with our data, emphasize the role of AKT in cell migration in different tumour cells. In eukaryotic cells, the integrity and dynamic reorganisation of the cells actin cytoskeleton are vital for maintaining the cell morphology and generation of the forces required for migration [501]. LY294002, works like many other protein kinase inhibitors, by competing with ATP for binding to the Pi3K active site [290], [502]. Nonetheless, the molecular mechanisms associated with cell migration that are modulated by Pi3K/AKT are not fully known. We present here two sets of data: endpoint images of the time-lapse migration assay- the cells in these images were outlined to analyse the morphology. To do so, we looked at the aspect ratio; which is defined as the ratio of long axis (width) to short axis (length) [503], the circularity (where 0 denotes full circle and 1 denotes elongated polygon), and the cell area. We also show images of cells stained with Alexa488-phalloidin to observe any cytoskeletal changes after incubation with the inhibitors for 10 hrs.

The morphology of MDA-MB231 cells incubated with LY294002 or AKTi and stimulated with CXCL8 (10 nM) for 10 hrs were significantly compromised. Indeed, LY294002 (10 µM) treatment induced an elongation of the cells. This was possibly due to the inhibition of cytoskeletal fibre formation that is required for the development of protrusive endings necessary for cell migration. Also, inhibiting AKT resulted in the disruption of the cytoskeleton, noted visually and characterized by cells elongating excessively and forming sticky clusters in their bodies (indicated by red arrows in **Figure 57**). Moreover, light microscopy with 10x objective showed that cells adopted a distinct shape following treatment with LY294002 or AKTi and activation with CXCL8 (**Figure 58**). Upon identification of the cellular morphology, LY294002-treated cells showed a significant distribution in the aspect ratio. On the other hand, AKTi treatment caused a more disruptive phenotype with substantial changes to the aspect ratio, circularity, and area of the cells (**Figure 59**). Former studies have argued that AKT stimulation at the leading edge contributes to cell polarity, cytoskeletal reorganisation, and cellular body contraction, resulting in the cell moving in a certain direction [281]. Thus, we see a direct correlation between the hindered migration of cells and deformation of the cytoskeleton in MDA-MB231 cells.

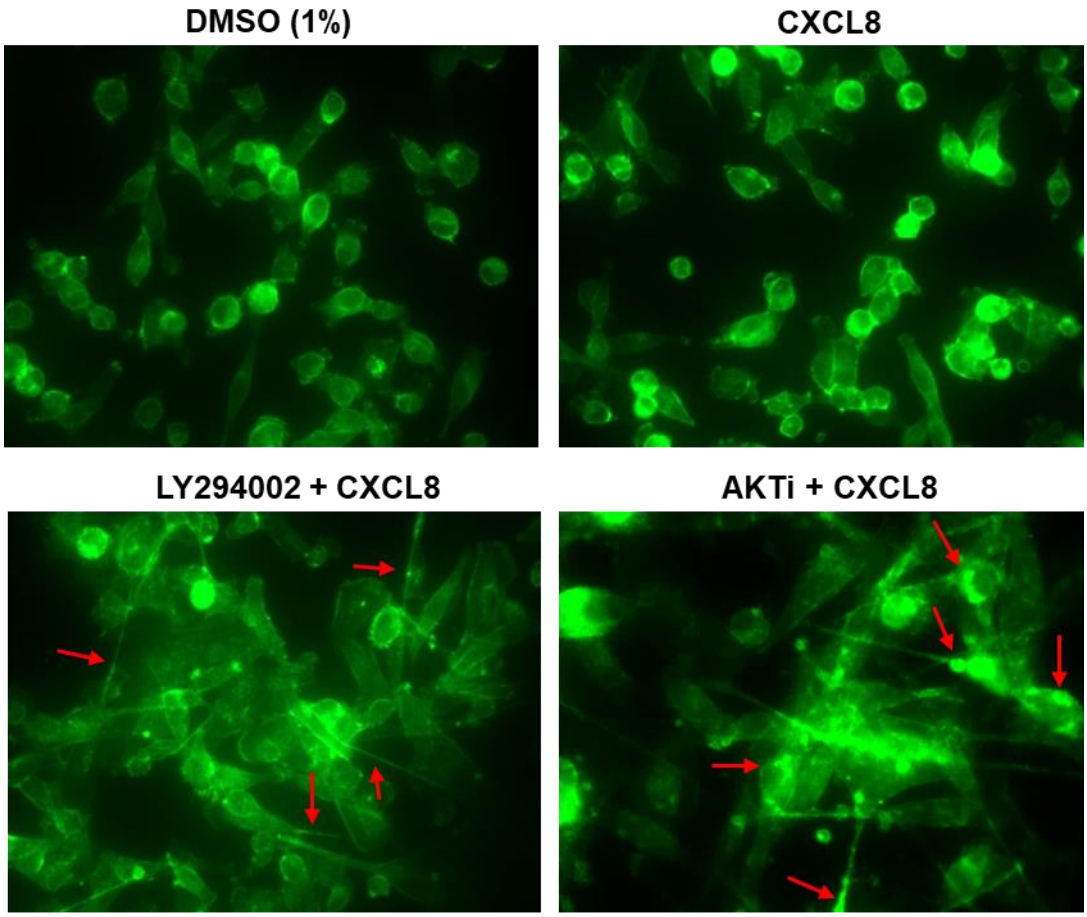

Figure 57. Phalloidin actin staining of CXCL8-stimulated MDA-MB231 cells in the presence of Pi3K or AKT inhibitors. Actin cytoskeleton changes in cells pre-treated with LY294002 (10 µM), or AKTi (20 µM) and activated with CXCL8 (10 nM). 1% DMSO was added to cells as a vehicle control. Few cells elongated in the presence of LY294002 as indicated by the red arrows, and elongation with aggregations appeared with AKTi-treated cells. Cells were fixed and stained with Alexa-488 phalloidin actin green stain. Cell images are representative of three independent repeats and were acquired at 63x magnification using a Leica DMII inverted microscope and Leica imaging suite.

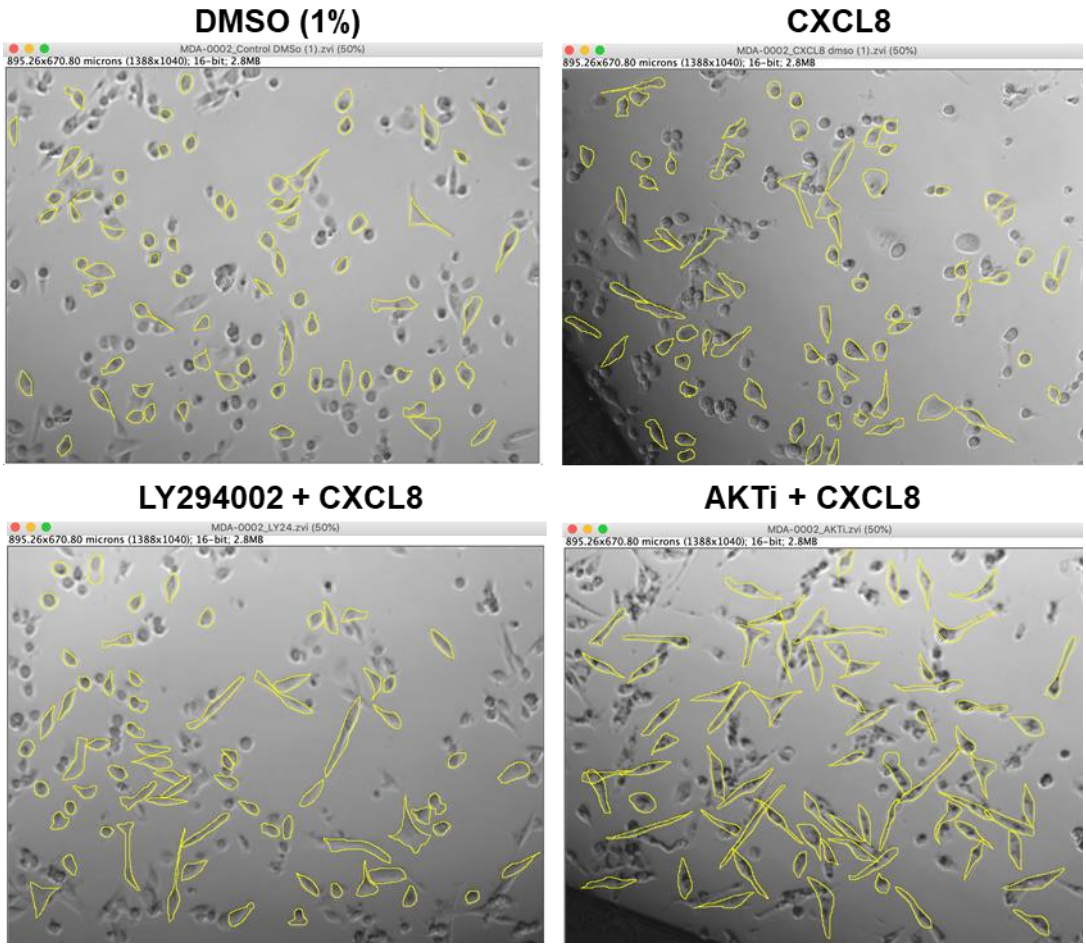

Figure 58. Illustrative images demonstrating morphological changes of MDA-MB231 cells stimulated with CXCL8 in the presence or absence of Pi3K or AKT inhibitor. Cells were activated with CXCL8 (10 nM) alone or activated following pre-treatment with LY294002 (10 µM), or AKTi (20 µM). 1% DMSO was added to the vehicle control. Cells were outlined using Fiji/ImageJ and measurements of 70 cells per image, per experiment were analysed. Experiments were repeated at least three times. Images are representative of the cell population and were taken at 10x objective with a Zeiss Axiovert 200M microscope and processed using AxioVision Rel 4.8 software.

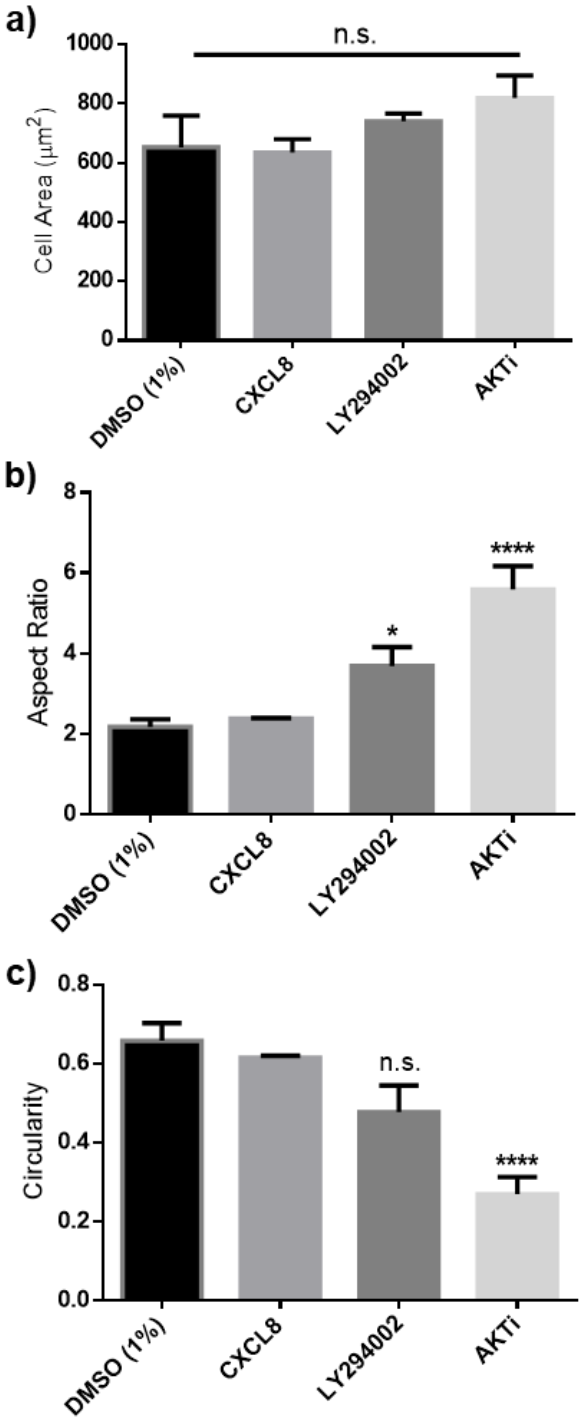

Figure 59. Analysis of the cellular morphology of MDA-MB231 cells stimulated with CXCL8 in the presence or absence of Pi3K or AKT inhibitors. Cells were incubated with LY294002 (10 µM) or AKTi (20 µM) prior to activation with CXCL8 (10 nM). Comparisons were made against the CXCL8 control. 1% DMSO was added to the basal cells as a vehicle control. Cells were outlined and measurements of **a)** area, **b)** aspect ratio, and **c)** circularity were analysed for an average of 70 cells per image per experiment. Experiments were repeated three times (One-way ANOVA with a Dunnett's multiple comparisons test as post-test, n.s.= no significance $p > 0.05$, * = $p \leq 0.05$, **** = $p \leq 0.0001$).

Furthermore, the morphology of PC3 cells were assessed under the same conditions but seemed to react slightly differently to MDA-MB231 cells. Phalloidin actin staining of PC3 cells identified small build-ups inside the cells in the presence of the AKT inhibitor (**Figure 60**) upon which the cells seemed lose their motility. Light microscopy analysis showed that CXCL8 activation of AKTi-treated cells induced the formation of small cluster inside the cells (**Figure 61**), although there was no significant effect on the area, aspect ratio, or circularity (**Figure 62**). On the other hand, CXCL8 activation of LY294002-treated cells appeared smaller with less assembly of stress fibres. Therefore, although cells reacted differently to Pi3K/AKT inhibitors, there was no doubt that this pathway was essential for maintaining the cytoskeleton and inducing cell migration.

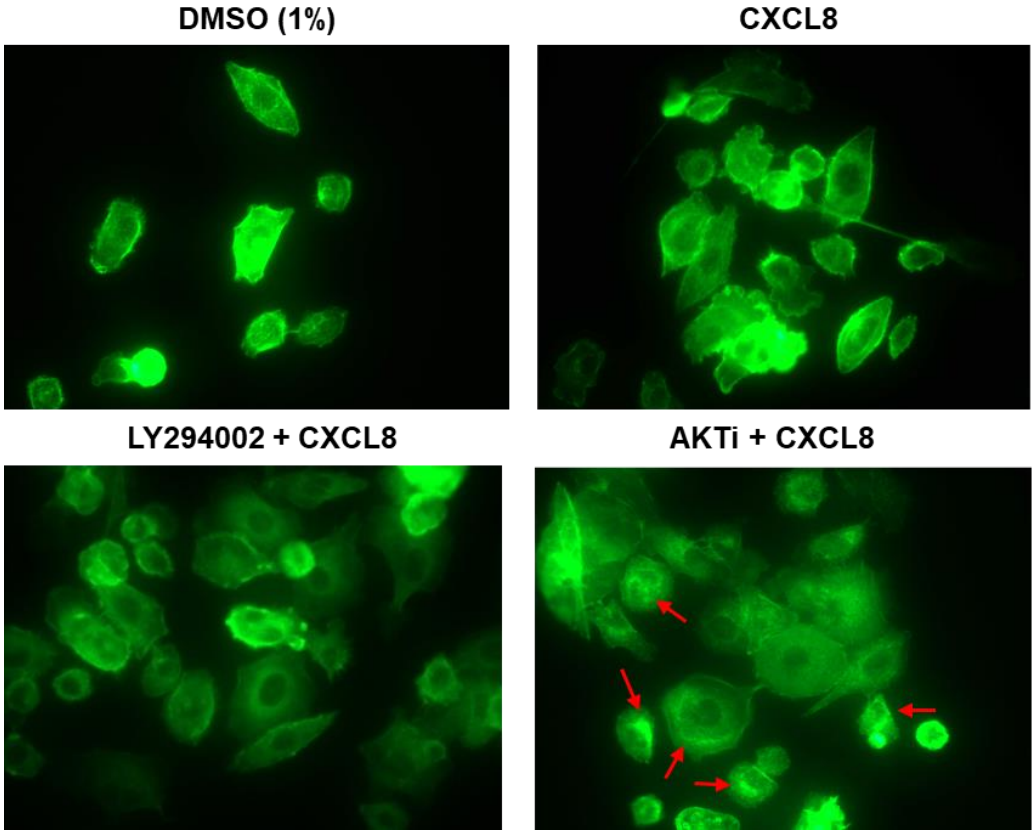

Figure 60. Phalloidin actin staining of CXCL8-stimulated PC3 cells in the presence or absence of Pi3K or AKT inhibitors. Actin cytoskeleton changes in cells pre-treated with LY294002 (10 µM), or AKTi (20 µM) and activated with CXCL8 (10 nM). The red arrows indicate the small cluster accumulations inside the cells. 1% DMSO was added to cells as the vehicle control. Cells were fixed and stained with Alexa-488 phalloidin actin green stain. Cells images are representative of the population of one experiment out of three repeats, acquired at 63X magnification using a Leica DMII inverted microscope and Leica imaging suite.

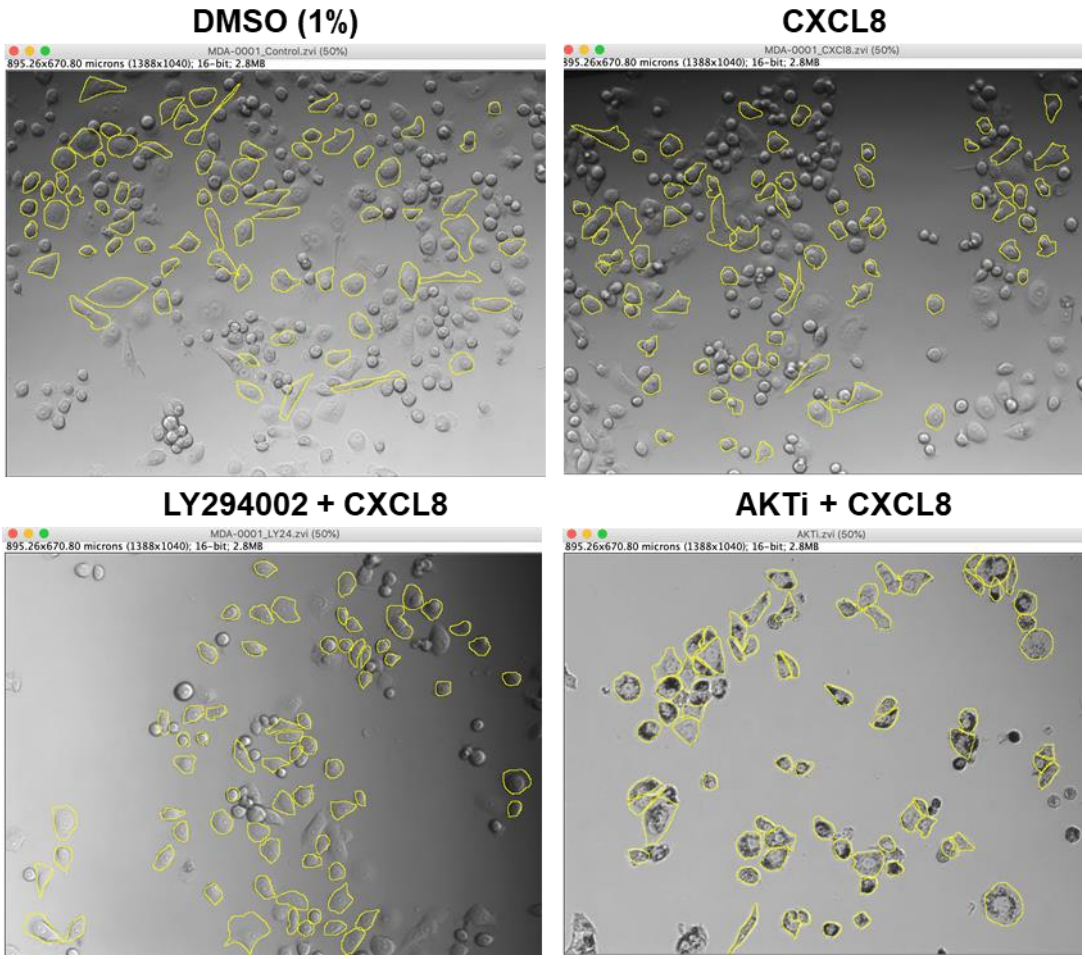

Figure 61. Illustrative images demonstrating morphological changes of PC3 cells stimulated with CXCL8 in the presence or absence of Pi3K or AKT inhibitor. Cells were activated with CXCL8 (10 nM) alone or following pre-treatment with LY294002 (10 µM), or AKTi (20 µM). 1% DMSO was added to the vehicle control. Cells were outlined using Fiji/ImageJ and measurements of 70 cells per image per experiment were analysed. Experiments were repeated at least three time. Images are a representation of the cell population and were taken at 10x objective with Zeiss Axiovert 200M microscope and processed using AxioVision Rel 4.8 software.

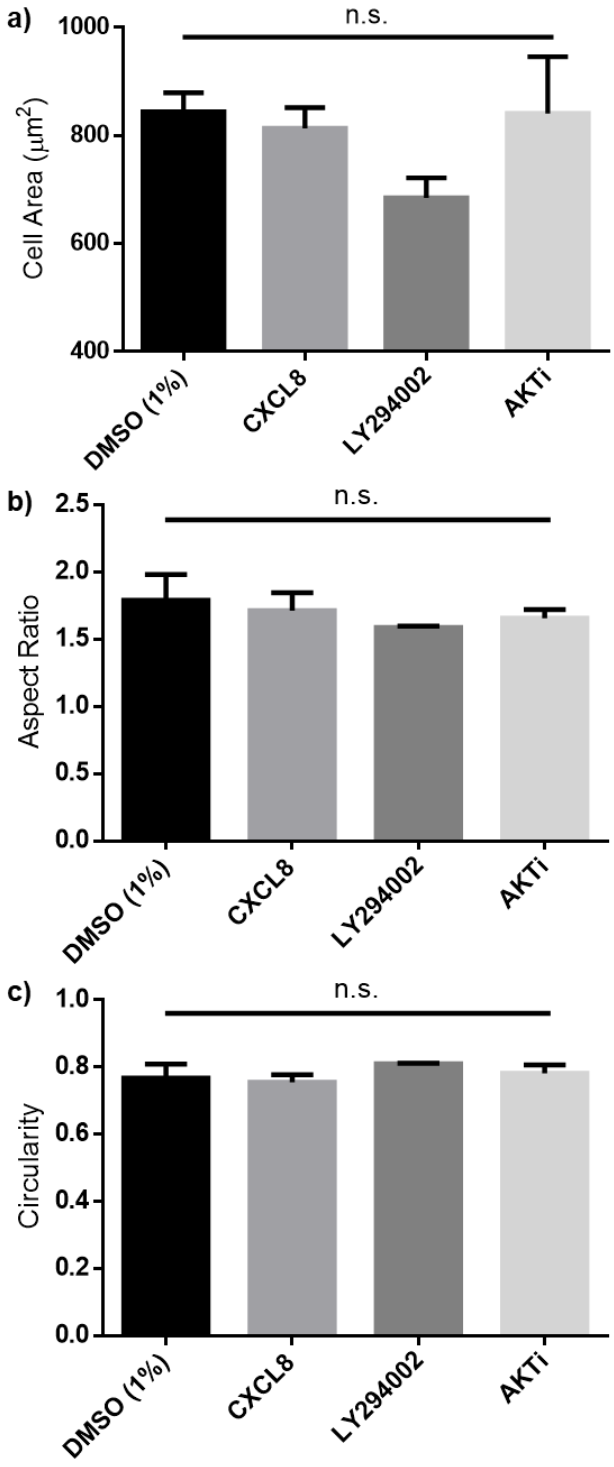

Figure 62. Analysis of cellular morphology of PC3 cells stimulated with CXCL8 in the presence or absence of Pi3K or AKT inhibitors. Cells were incubated with LY294002 (10 µM) or AKTi (20 µM) and activated with CXCL8 (10 nM). Comparisons were made against the CXCL8 control. 1% DMSO was added to the basal cells as a vehicle control. Cells were outlined and measurements of **a)** area, **b)** aspect ratio, and **c)** circularity were analysed for an average of 70 cells per image per experiment. Experiments were repeated three times (One-way ANOVA with a Dunnett's multiple comparisons test as post-test, n.s.= no significance $p > 0.05$).

4.2.1.3 MTS cytotoxic assay to quantify the cytotoxicity of Pi3K and AKT inhibitors

To identify the viability of MDA-MB231 and PC3 cells following 24 hrs incubation with LY294002 (10 µM) and AKTi (20 µM), an MTS assay was conducted. The absorbance was measured at 492 nm and cellular cytotoxicity was compared against basal cytotoxicity. The concentrations of the inhibitors used did not show any cytotoxicity towards MDA-MB231 or PC3 cells (**Figure 63**). The concentrations we used for the inhibitors had been used previously in other studies [294], [496].

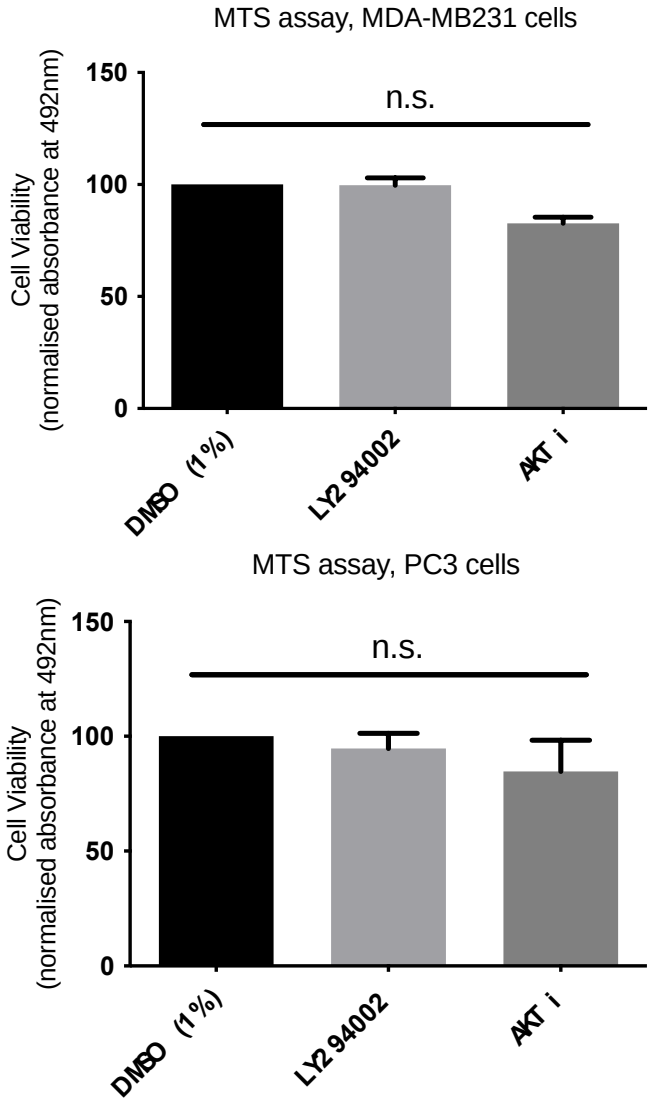

Figure 63. Toxicity of Pi3K and AKT inhibitors towards MDA-MB231 and PC3 cells. The absorbance following incubation with LY294002 (10 µM) or AKTi (20 µM) for 24 hrs, followed by treatment with MTS reagent for 2 hrs in **a)** MDA-MB231 cells, or **b)** PC3 cells. 1% DMSO was added to the basal cells as a vehicle control. Data are representative of the mean ± SEM of three independent experiments (Kruskal-Wallis test, Dunn's multiple comparisons test, n.s.= no significance $p > 0.05$).

4.2.2 The Ras/Raf/MEK/ERK, p38 MAPK, and β-catenin pathway

4.2.2.1 Ras/Raf/MEK/ERK, p38 MAPK are important for cells migration but not β-catenin

CXCL8 signalling modulates the activity of MAPK signalling pathways that comprise several serine/threonine kinases [143]. The best characterized pathway of these kinases is the Raf/Ras/MEK/ERK pathway. Pi3K has been identified as a mediator which couples CXCL8 to MAPK signalling in neutrophils [309]. CXCL8 induces rapid and transient phosphorylation of ERK1/2 and Pi3K in neutrophils [323]. The role of ERK1/2 in the migration of CXCL8-activated neutrophils is poorly understood [282], [309], [324]. Moreover, constitutive ERK1/2 stimulation by extracellular signals is suggested to have a dual effect on cancer cells; either enhancing or inhibiting cancer progression depending on the context and strength of stimulation [304]. Former studies suggested that ERK inhibition in lung cancer stimulates glycogen synthase kinase 3β, possibly leading to β-catenin degradation, which causes inhibition of cancer progression and migration [330]. Furthermore, p38 MAPK is part of the MAPK pathway that is identified as a regulator of inflammatory and stress responses [504]. Little is known about the role p38 MAPK plays in cell migration in response to CXCL8.

The involvement of Ras/Raf/MEK/ERK, p38 MAPK or β-catenin activation on the migration of MDA-MB231 cells was investigated by analysing the migratory speed of cells pre-treated with pathway inhibitors and stimulated with CXCL8. Basal cells had a speed of 21.07 ± 7.5 µm/hr, while addition of CXCL8 (10 nM) increased the speed to 48.3 ± 4.4 µm/hr over 10 hrs ($p \leq 0.0001$). Treating cells with the Raf inhibitor, L779450 (100 nM), after the addition of CXCL8 (10 nM) had a slight effect on the cells (38.3 ± 4.4 µm/hr). However, using another Raf inhibitor, ZM336372 (1 µM), the speed of cells significantly decreased to 25.5 ± 11.1 µm/hr. Moreover, MEK inhibitors SL327 (1 µM) and PD98059 (25 µM) both decreased the speed of cells to 32.9 ± 1.7 µm/hr, and 25.1 ± 2.6 µm/hr, respectively. The p38 MAPK inhibitor, SB203580 (1 µM), also reduced the speed of cells to 31.2 ± 9.9 µm/hr. Finally, the β-catenin inhibitor FH535 (1 µM) did not have any major effects on cell motility (40.2 ± 2.0 µm/hr; **Figure 64**).

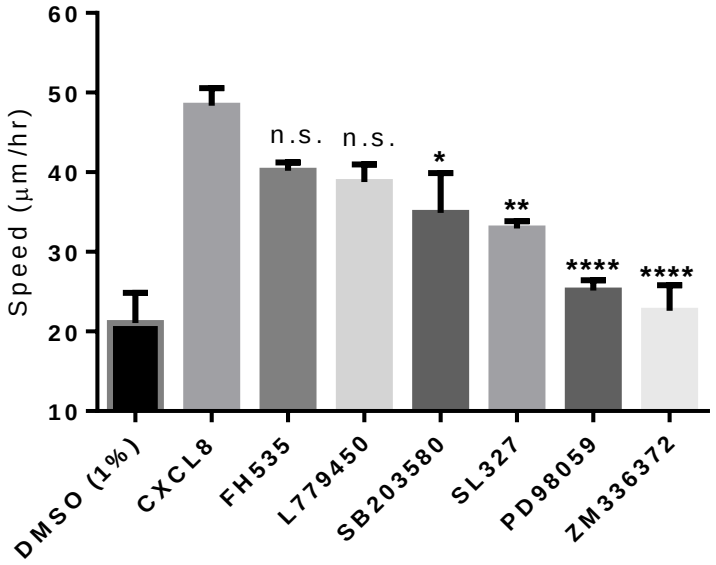

Figure 64. The effect of Raf/MEK/ERK, p38 MAPK, or β-catenin inhibition on the migration speed of CXCL8-activated MDA-MB231 cells. Cells were pre-treated with β-catenin inhibitor: FH535 (1 µM); Raf inhibitors: L779450 (100 nM), or ZM336372 (1 µM); MEK inhibitors: SL327 (1 µM), or PD98059 (25 µM); or p38 MAPK inhibitor: SB203580 (1 µM) and activated with CXCL8 (10 nM). Comparisons were made against CXCL8. 1% DMSO was added to the basal cells as a vehicle control. Data are representative of the mean ± SEM of four independent experiments (One-way ANOVA with a Dunnett's multiple comparisons test as post-test, n.s. = no significance $p>0.05$, * = $p \leq 0.05$, ** = $p \leq 0.01$, and **** = $p \leq 0.0001$).

PC3 cells were also affected by inhibition of Ras/Raf/MEK/ERK, p38 MAPK, and β-catenin signalling. Cells were treated with the compounds then activated with CXCL8. The speed of basal cells was 25.7 ± 7.9 µm/hr and addition of CXCL8 (10 nM) increased the speed to 59.0 ± 21.4 µm/hr ($p \leq 0.0001$). Unlike MDA-MB231 cells, L779450 (100 nM) significantly decreased the speed of PC3 cells to 37.2 ± 15.9 µm/hr. In addition, ZM336372 (1 µM), also reduced the speed to 27.2 ± 6.9 µm/hr. Likewise, both MEK inhibitors, SL327 (1 µM) and PD98059 (25 µM) attenuated the speed of cells significantly to 30.3 ± 2.8 µm/hr and 25.8 ± 5.0 µm/hr, respectively. p38 MAPK inhibitor SB203580 (1 µM) decreased the speed to 31.3 ± 5.8 µm/hr. Only β-catenin inhibitor, FH535 (1 µM) did not have a considerable effect on the speed (47.0 ± 5.3 µm/hr; **Figure 65**).

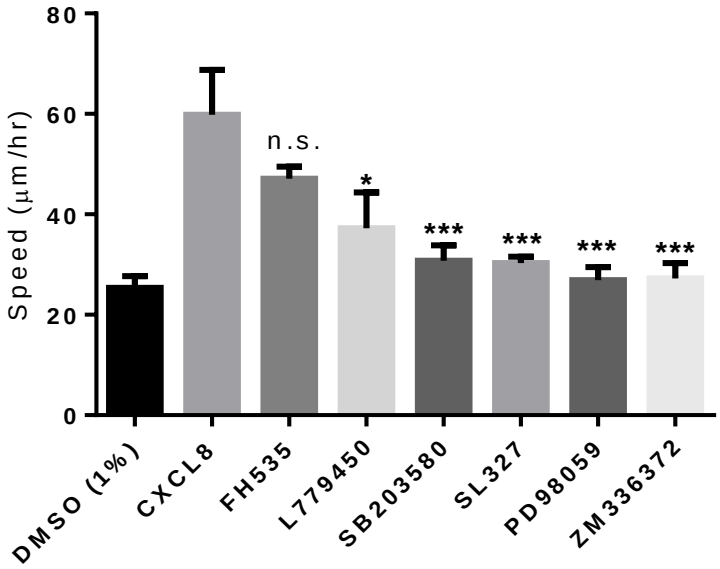

Figure 65. The effect of Raf/MEK/ERK, p38 MAPK, or β-catenin inhibition on the migration speed of CXCL8-activated PC3 cells. Cells were incubated with β-catenin inhibitor: FH535 (1 µM); Raf inhibitors: L779450 (100 nM), or ZM336372 (1 µM); MEK inhibitors: SL327 (1 µM), or PD98059 (25 µM); or p38 MAPK inhibitor: SB203580 (1 µM) and activated with CXCL8 (10 nM). Comparisons were made against CXCL8. 1% DMSO was added to the basal cells as a vehicle control. Data are representative of the mean ± SEM of four independent experiments (One-way ANOVA with a Dunnett's multiple comparisons test as post-test, n.s. = no significance $p>0.05$, * = $p \leq 0.05$, *** = $p \leq 0.001$).

4.2.2.2 Ras/Raf/MEK/ERK, p38 MAPK, or β-catenin inhibition did not induce a substantial morphological change in the cells

We aimed to observe and analyse the cytoskeletal rearrangements induced following Ras/Raf/MEK/ERK, p38 MAPK, and β-catenin inhibition and activation of cells with CXCL8, after 10 hrs incubation.

Visual assessment of phalloidin actin staining of MDA-MB231 cells with the different inhibitors: L779450, ZM336372, SL327, PD98059, SB203580, indicated that cells had increased in area compared to the controls, whereas FH535-treated cells looked slightly smaller (**Figure 66**). Cells treated with SB203580 seemed to have more microspikes formed at their edges. Additionally, few cells appeared elongated following ZM336372 treatment. However, when images were taken via light microscopy (**Figure 67**) and cells were outlined for morphology analysis, only PD98059-treated cells showed a minor increase to the aspect ratio, but overall no other significant differences appeared with any of the compounds used (**Figure 68**).

PC3 cells stained with phalloidin actin stain after being incubated with the previous set of inhibitors showed no substantial changes to the cellular morphology after 10 hrs (**Figure 69**). Notably, FH535-treated cells appeared slightly smaller compared to the control sample, this was similar to the observations noted with MDA-MB231 cells. Images taken via light microscopy (**Figure 70**) also did not show any crucial changes to the shape of the cells. This was confirmed following image analysis (**Figure 71**).

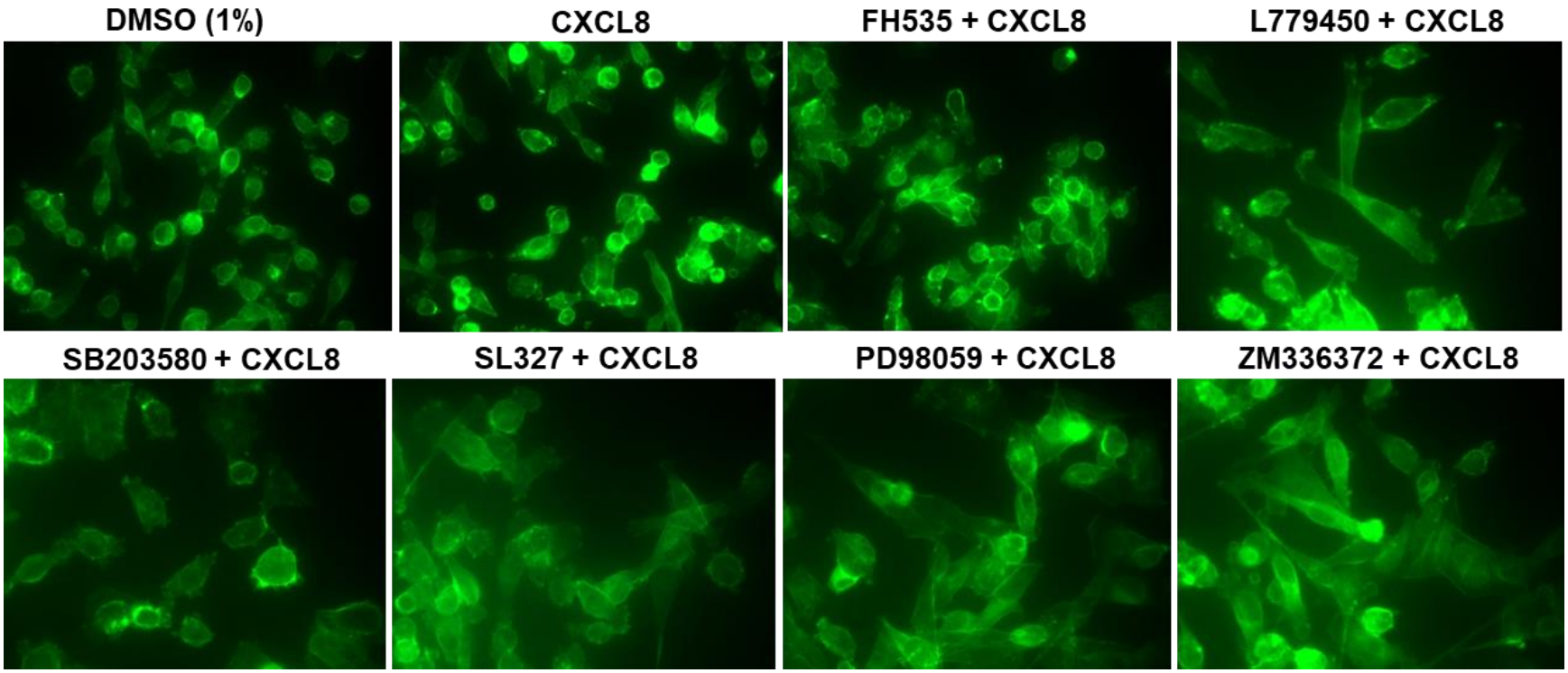

Figure 66. Phalloidin actin staining of CXCL8-stimulated MDA-MB231 cells in the presence or absence of Raf/MEK/ERK, p38 MAPK, and β-catenin inhibitors. Actin cytoskeleton changes to the cells pre-treated with β-catenin inhibitor: FH535 (1 μM); Raf inhibitors: L779450 (100 nM), or ZM336372 (1 μM), MEK inhibitors: SL327 (1 μM), or PD98059 (25 μM), or p38 MAPK inhibitor: SB203580 (1 μM) and activated with CXCL8. 1% DMSO was added as a vehicle control. Cells were fixed and stained with Alexa-488 phalloidin actin green stain. Cells images are representative of the population of cells from one experiment out of three repeats, acquired at 63X magnification using a Leica DMII inverted microscope and Leica imaging suite.

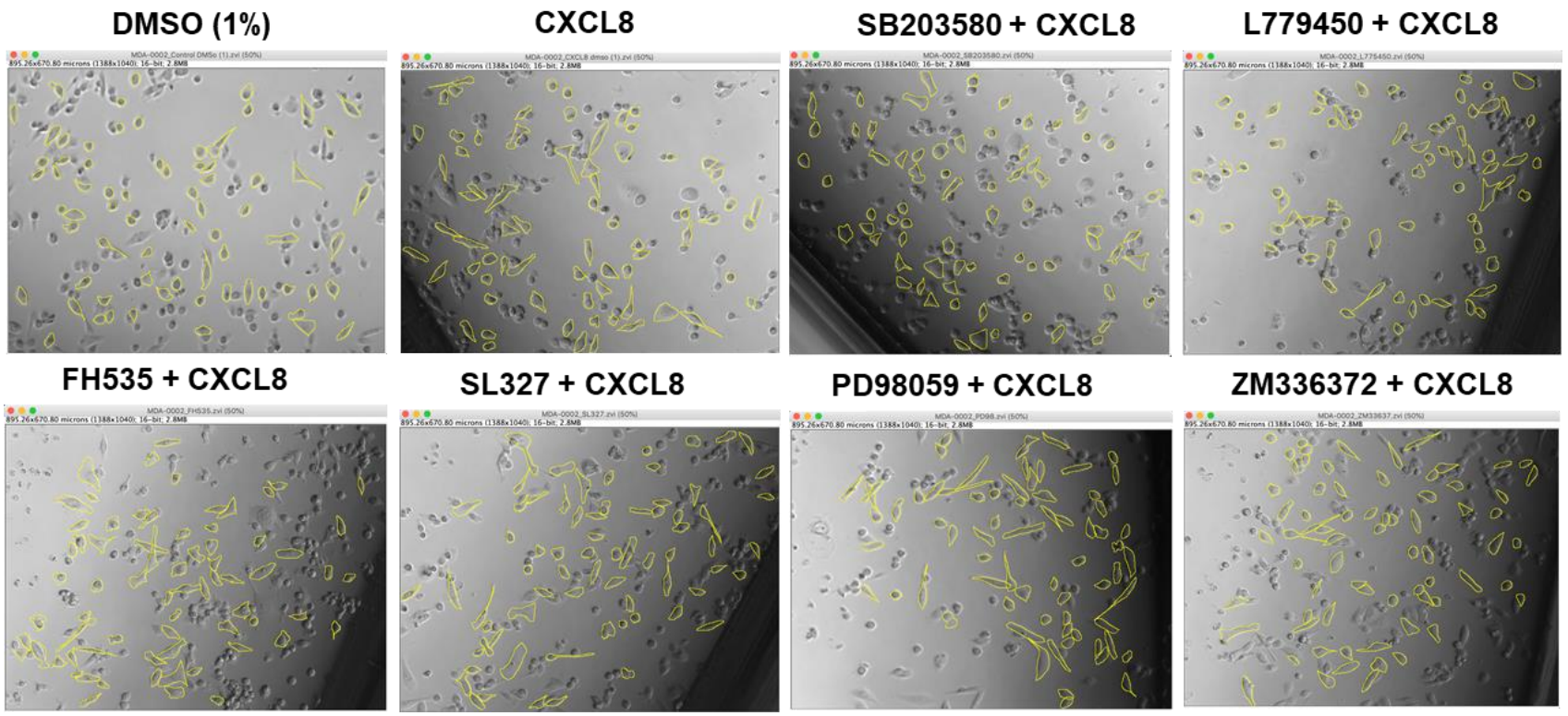

Figure 67. Illustrative images demonstrating morphological changes of MDA-MB231 cells treated with CXCL8 in the presence or absence of Raf/MEK/ERK, p38 MAPK, and β-catenin inhibitors. Cells were treated with the β-catenin inhibitor: FH535 (1 µM); Raf inhibitors: L779450 (100 nM), or ZM336372 (1 µM), MEK inhibitors: SL327 (1 µM), or PD98059 (25 µM); or p38 MAPK inhibitor: SB203580 (1 µM) and activated with CXCL8 (10 nM). 1% DMSO was added as a vehicle control. Cells were drawn around using Fiji/ImageJ and measurements of 70 cells per image per experiment were analysed. Experiments were repeated at least three times. Images are representative of the cell population and were taken at 10x objective with a Zeiss Axiovert 200M microscope and processed using AxioVision Rel 4.8 software.

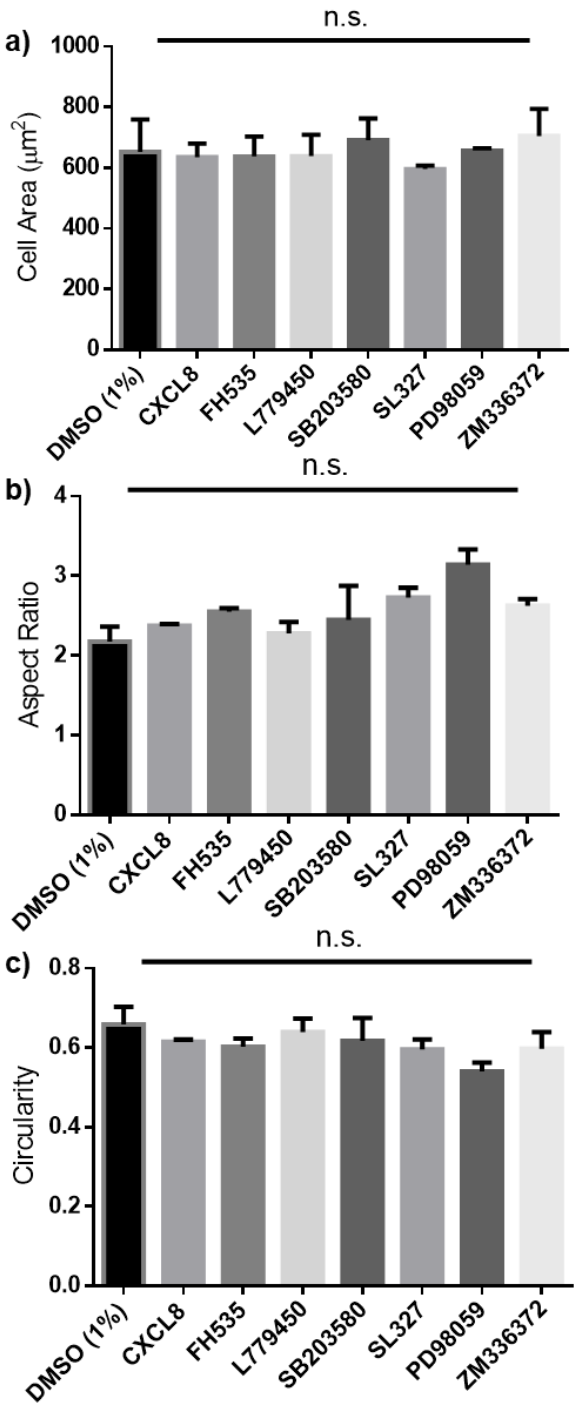

Figure 68. Analysis of the cellular morphology of MDA-MB231 cells following treatment with CXCL8 in the presence or absence of Raf/MEK/ERK, p38 MAPK, or β-catenin inhibitors. Cells were treated with β-catenin inhibitor: FH535 (1 µM); Raf inhibitors: L779450 (100 nM), or ZM336372 (1 µM), MEK inhibitors: SL327 (1 µM), or PD98059 (25 µM), or p38 MAPK inhibitor: SB203580 (1 µM) and activated with CXCL8 (10 nM). Comparisons were made against CXCL8. 1% DMSO was added to the basal cells as a vehicle control. Cells were outlined and measurements of **a)** area, **b)** aspect ratio, and **c)** circularity were analysed for an average of 70 cells per image per experiment. Experiments were repeated three times (One-way ANOVA with a Dunnett's multiple comparisons test as post-test, n.s.= no significance, $p > 0.05$).

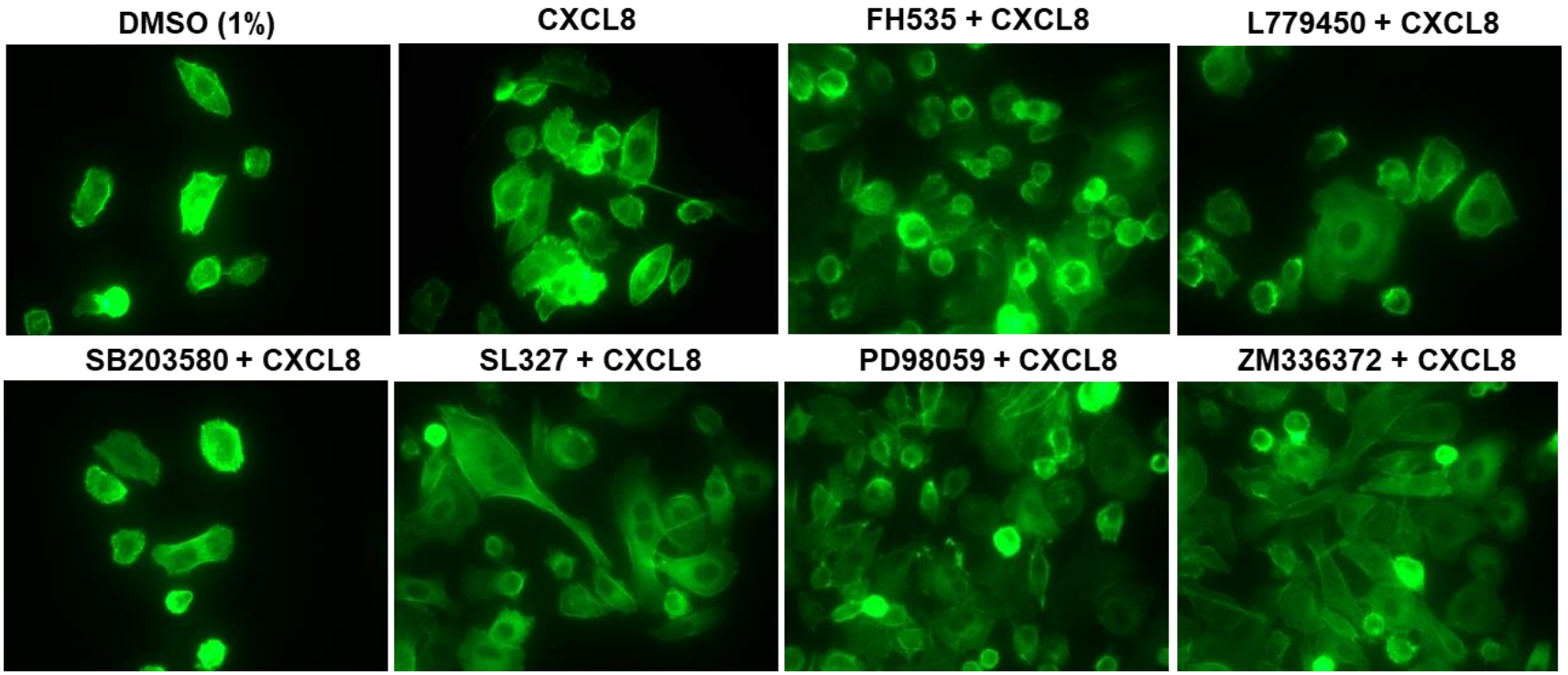

Figure 69. Phalloidin actin staining of CXCL8-stimulated PC3 cells with Raf/MEK/ERK, p38 MAPK, and β-catenin inhibitors. Actin cytoskeleton changes in cells pre-treated with β-catenin inhibitor: FH535 (1 µM); or Raf inhibitors: L779450 (100 nM), or ZM336372 (1 µM); or MEK inhibitors: SL327 (1 µM), or PD98059 (25 µM); or p38 MAPK inhibitor: SB203580 (1 µM) and activated with CXCL8 (10 nM). 1% DMSO was added to the cells as a vehicle control. Cells were fixed and stained with Alexa-488 Phalloidin actin green stain. Cells images are representative of the population of one experiment out of three repeats acquired at 63X magnification using a Leica DMII inverted microscope and Leica imaging suite.

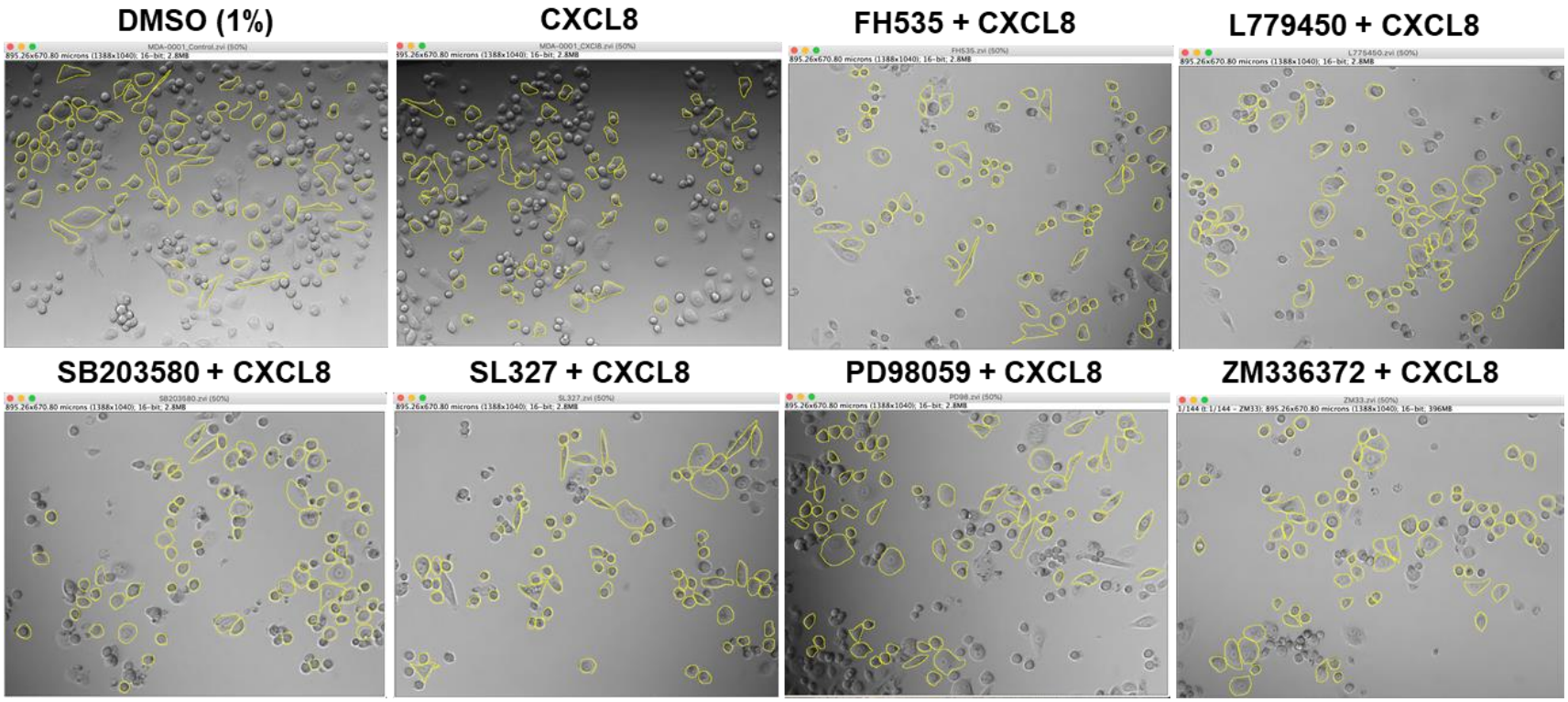

Figure 70. Illustrative images demonstrating morphological changes of PC3 cells treated with CXCL8 in the presence or absence of Raf/MEK/ERK, p38 MAPK and β-catenin inhibitors. Cells were treated with β-catenin inhibitor: FH535 (1 µM); Raf inhibitors: L779450 (100 nM), or ZM336372 (1 µM), MEK inhibitors: SL327 (1 µM), or PD98059 (25 µM), or p38 MAPK inhibitor: SB203580 (1 µM) and activated with CXCL8 (10 nM). 1% DMSO was added as a vehicle control. Cells were outlined using Fiji/ImageJ and measurements of 70 cells per image per experiment were analysed. 1% DMSO was added to the basal cells and CXCL8-treated cells. Experiments were repeated at least three times. Images are representative of the cell population and were taken at 10x objective with a Zeiss Axiovert 200M microscope and processed using AxioVision Rel 4.8 software.

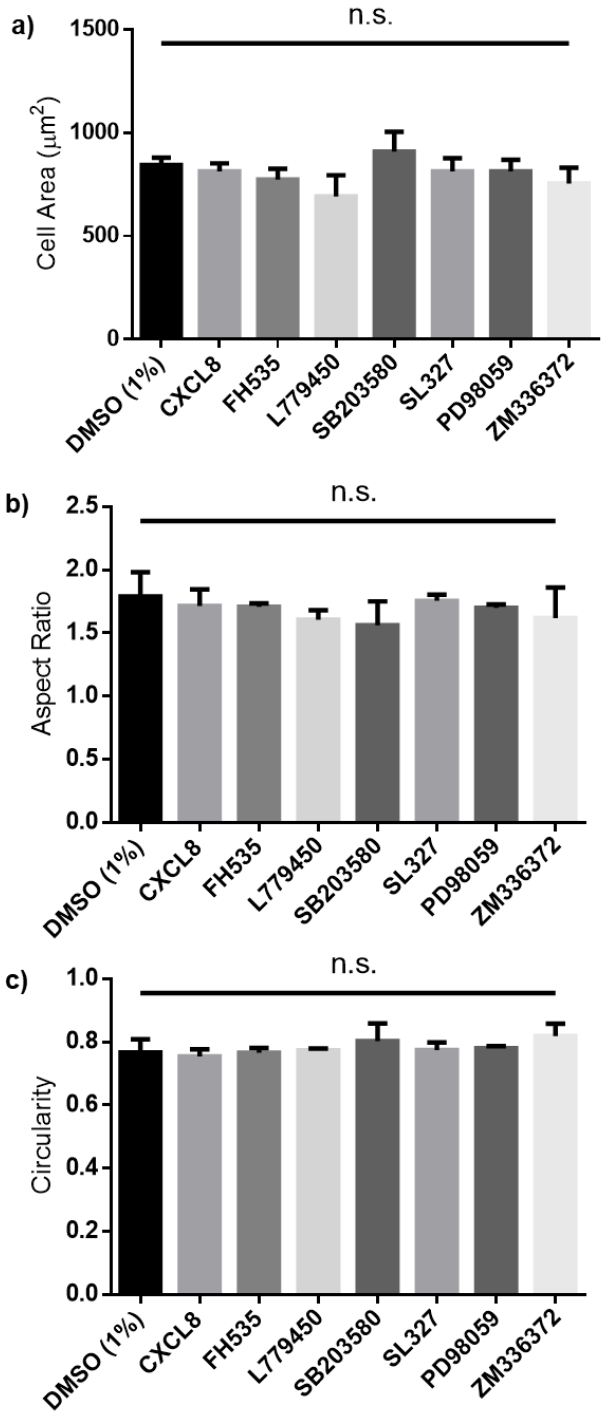

Figure 71. Cellular morphology analysis of PC3 cells treated with CXCL8 in the presence or absence of Raf/MEK/ERK, p38 MAPK, and β-catenin inhibitors. Cells were treated with β-catenin inhibitor: FH535 (1 μM); Raf inhibitors: L779450 (100 nM), or ZM336372 (1 μM); MEK inhibitors: SL327 (1 μM), or PD98059 (25 μM); or p38 MAPK inhibitor: SB203580 (1 μM) and activated with CXCL8 (10 nM). Comparisons were made against CXCL8. 1% DMSO was added to the basal cells as a vehicle control. Cells were outlined and measurements of **a)** area, **b)** aspect ratio, and **c)** circularity were analysed for an average of 70 cells per image per experiment. Experiments were repeated three times (One-way ANOVA with a Dunnett's multiple comparisons test as post-test, n.s.= no significance).

4.2.2.3 MTS cytotoxicity assay to quantify the cytotoxicity of Raf/MEK/ERK or β-catenin inhibitors

Treatment of MDA-MB231 and PC3 cells for 24 hrs with Raf inhibitors: L779450 (100 nM), or ZM336372 (1 µM), MEK inhibitors: SL327 (1 µM), or PD98059 (25 µM), p38 MAPK inhibitor: SB203580 (1 µM), or β-catenin inhibitor: FH535 (1 µM) showed no cytotoxicity (**Figure 72**). These concentrations were already tested in other studies [388], [505].

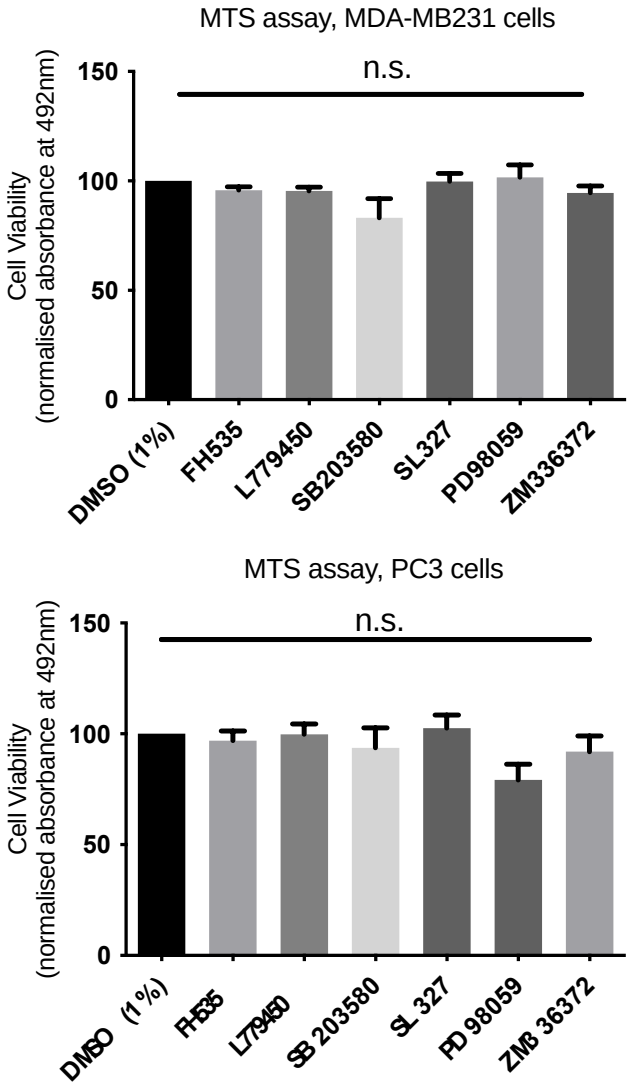

Figure 72. Toxicity of Raf/MEK/ERK, p38 MAPK, and β-catenin inhibitors towards MDA-MB231 and PC3 cells. The absorbance following incubation with β-catenin inhibitor: FH535 (1 µM); Raf inhibitors: L779450 (100 nM), or ZM336372 (1 µM); MEK inhibitors: SL327 (1 µM), or PD98059 (25 µM); or p38 MAPK inhibitor: SB203580 (1 µM) for 24 hrs and treatment with MTS reagent for 2 hrs in **a)** MDA-MB231 cells, or **b)** PC3 cells. 1% DMSO was added to the basal cells as a vehicle control. Data are representative of the mean ± SEM of three independent experiments (Kruskal-Wallis test, Dunn's multiple comparisons test, n.s.= no significance $p > 0.05$).

4.2.3 The Rho GTPases and DOCK1/2/5 signalling pathways

4.2.3.1 Rho GTPases and DOCK1/2/5 are important for cells migration

Amongst other signalling pathways which have been highlighted as being involved in CXCL8-stimulated migration are the Rho GTPases. This superfamily belongs to Ras and among its well-characterized molecules are Rho, Rac and Cdc42. Rho GTPases regulate cellular processes by working as a switch based on their GDP or GTP-bounding form. GTP hydrolytic activity is associated with Rho GTPases stimulation which is reported to be involved in the cytoskeleton rearrangement, migration, proliferation, transformation and differentiation [338]. For example, it was shown that the inhibition of RhoA and ROCK (Rho-activated kinase) inhibition block THP-1 cell migration towards CCL3 [506]. Here, we look at the correlation between CXCL8 activation and the migration speed of cells incubated with a range of small molecule inhibitors targeting Rho GTPases or DOCK1/2/5.

Time-lapse migration assay of MDA-MB231 cells showed an important role of the Rho GTPases in regulating the migration speed of the cells. The speed of basal cells is 21.07 ± 7.5 µm/hr, while addition of CXCL8 (10 nM) activated the cells to migrate faster with a speed of 48.3 ± 4.4 µm/hr after 10 hrs. Cells were further treated with different inhibitors and activated with CXCL8. Treating cells with the Rac1 inhibitor, NSC23766 (100 µM), did not affect the migration speed; 42.6 ± 6.1 µm/hr, however, the other Rac1 inhibitor used, EHT1864 (100 nM), significantly decreased the speed to 32.2 ± 3.6 µm/hr. In addition, inhibition of ROCK by Y27632 (20 µM) drastically reduced the speed of migrating cells to 26.9 ± 3.4 µm/hr. This is consistent with previous result showing around a 50% decrease in Y27632-treated MDA-MB231 cell migration [507]. CPYPP, a DOCK 1/2/5 inhibitor, had a similar effect giving a speed of 26.3 ± 10.0 µm/hr. CCG 1423 (1 µM) is a small-molecule inhibitor of RhoA, this inhibitor did not affect the speed of MDA-MB231 cells giving a speed of 41.4 ± 9.1 µm/hr. Finally, Cdc42 inhibitor, ZCL278 (20 µM) did not cause a significant reduction to the migration of the cells, however, the standard error bar associated with this observation was high19.6 ± 12.1 µm/hr (**Figure 73**), therefore requires further investigation. In summary, EHT1864, Y26732 and CPYPP inhibit the migration of MDA-MB231 cells, but NSC23766 and CCG 1423 did not.

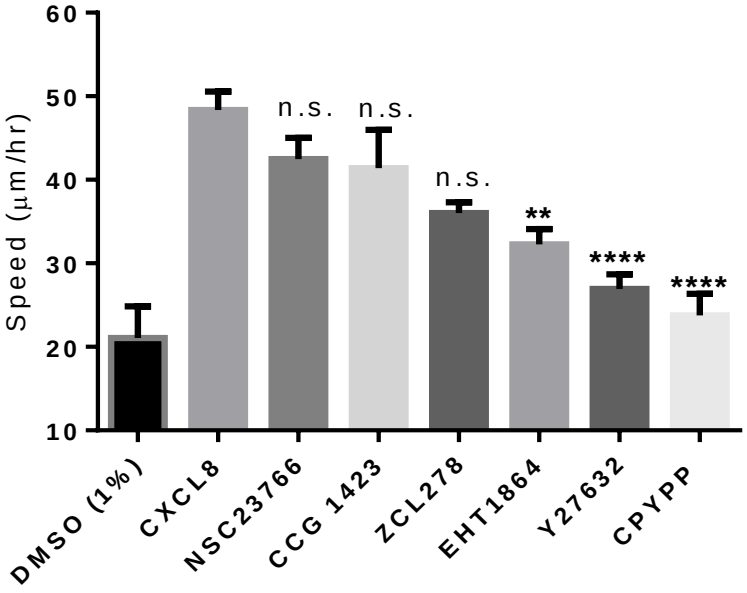

Figure 73. The effect of Rac/Rho/Cdc42 or DOCK1/2/5 inhibitors to the migration speed of CXCL8-activated MDA-MB231 cells. Cells were pre-treated with Rac1 inhibitors: NSC23766 (100 µM), or EHT1864 (100 nM), or Rho/ROCK inhibitors: CCG 1423 (1 µM), or Y27632 (20 µM), or Cdc42 inhibitor*:* ZCL278 (20 µM), or DOCK1/2/5 inhibitor: CPYPP (100 µM) and activated with CXCL8 (10 nM). Comparison was made against CXCL8. 1% DMSO was added to the basal cells as a vehicle control. Data are representative of the analysis of 10 cells in each experiment using Fiji/ImageJ, with the mean ± SEM of four independent experiments (One-way ANOVA with a Dunnett's multiple comparisons test as post-test, n.s. = no significance $p>0.05$, ** = $p \leq 0.01$, **** = $p \leq 0.0001$).

The same set of inhibitors and conditions were applied to PC3 cells and this cell line showed some similarities to MDA-MB231 cells with some variations. The speed of basal cells was 25.7 ± 7.9 µm/hr, activation with CXCL8 (10 nM) increased the speed to 59.0 ± 21.4 µm/hr. Cell were then treated with the inhibitors and then activated with CXCL8. Treatment with Rac1 inhibitor NSC23766 (100 µM) modestly reduced the speed to 40.4 ± 7.4 µm/hr, but not significantly. The other Rac1 inhibitor used, EHT1864 (100 nM), substantially reduced the speed to 24.5 ± 13.1 µm/hr. Unlike MDA-MB231 cells, the inhibitory effect of ROCK inhibitor, Y27632 (20 µM), on the migration speed of PC3 cells was not greatly affected; 39.9 ± 7.1 µm/hr. Additionally, CPYPP (100 µM), DOCK1/2/5 inhibitor, affected PC3 cells in a similar fashion as MDA-MB231, with the speed drastically decreasing to 21.8 ± 12.5 µm/hr. Moreover, the RhoA inhibitor, CCG 1423 (1 µM), did not affect the speed significantly; 41.9 ± 12.9 µm/hr. Eventually, although Cdc42 inhibitor, ZCL278 (20 µM), did not affect the speed of MDA-MB231 considerably, it had a significant inhibitory effect on PC3 cells giving a speed of 27.6 ± 13.7 µm/hr (**Figure 74**). In all, the migration speed of PC3 cells was mainly affected by EHT1864, ZCL278, and CPYPP but not with NSC23766, CCG 1423, or Y27632.

Taken together, the small molecule inhibitors of Rho GTPases or DOCK1/2/5 showed slightly variable effects on the migration speed between the two cell lines, although they both shared the attenuation of their speed with treatment with EHT1864 and CPYPP.

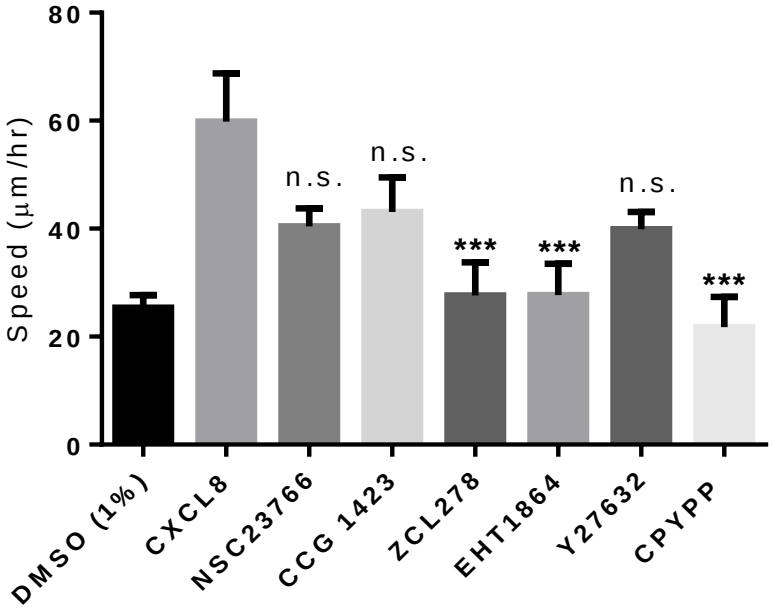

Figure 74. The effect of Rac/Rho/Cdc42 or DOCK1/2/5 inhibitors to the migration speed of CXCL8-activated PC3 cells. Cells were pre-treated with Rac1 inhibitors: NSC23766 (100 µM), or EHT1864 (100 nM), or Rho/ROCK inhibitors: CCG 1423 (1 µM), or Y27632 (20 µM), or Cdc42 inhibitor*:* ZCL278 (20 µM), or DOCK1/2/5 inhibitor: CPYPP (100 µM) and activated with CXCL8 (10 nM). Comparison was made against CXCL8. 1% DMSO was added to the basal cells as a vehicle control. Data are representative of the analysis of 10 cells in each experiment using Fiji/ImageJ, with the mean ± SEM of four independent experiments (One-way ANOVA with a Dunnett's multiple comparisons test as post-test, n.s. = no significance $p > 0.05$, *** = $p \leq 0.001$).

4.2.3.2 ROCK inhibition affects the cellular morphology

Re-arrangement of the cytoskeleton contribute significantly to cell migration and chemotaxis, and Rho GTPases (Rac, Rho and Cdc42) play a vital role in these processes [340]. Indeed, actin filament reorganisation is a process that involve actin polymerising and depolymerizing factors. Rho modulate stress fibres and focal adhesion formation via stimulating downstream signals mDia, ROCKI and ROCKII [508]; Rac is involved in the formation of lamellipodia; and Cdc42 is required for the cell polarity and filopodia formation, guiding the direction of migration [341]. The absence of Rho can cause an inhibition to the cell tail detachment through reduced actin-myosin contraction [347]. Activation of chemokine receptors involves actin stress fibres and membrane ruffling [509]–[511]. We saw before that some of the Rac/Rho/Cdc42 and DOCK1/2/5 signals were important for the migration of cells upon stimulation with CXCL8, therefore, we investigated if the inhibitory effect of blocking these signals was associated with changes to the cellular morphology.

For visual observation, images were obtained with phalloidin actin staining of MDA-MB231 cells upon their activation with CXCL8. NSC23766 is a Rac1 inhibitor that has been useful to address the role of Rac in cellular responses and to reverse tumour cell phenotypes correlated with Rac deregulation [512]. This inhibitor did not cause a significant difference to the speed of migration, but with the actin stain, cells seemed to have formed small clusters in the form of accumulation of punctate actin at their sides (**Figure 75**). Cells treated with ZCL278 (Cdc42 inhibitor) exhibited similar formation of small actin lumps. CCG 1432 (RhoA inhibitor) gave few cells some elongated appearance. Additionally, cells treated with Rac1 inhibitor, EHT1864, looked more compact with no obvious formation of lamellipodia or filopodia necessary for cell migration compared with the control samples. CPYPP (DOCK 1/2/5) showed no substantial changes to the cells. Moreover, Y27632 is an orthosteric ROCK inhibitor that compete with ATP binding on the catalytic domain of ROCK, leading to interference with actin stress fibre formation [509]. Cells treated with Y27632 demonstrated a tangled actin meshwork, complete abolishment to the cell junctions, and elongation of the leading/tail endings of the cells. These observations along with the reduced migration speed agrees with previous studies [507], [513].

Having taken images of the cells using light microscope at 10x objective, none of the Rho GTPases or DOCK1/2/5 inhibitors caused a substantial change to the morphology of the cells except for Y27632 (**Figure 76**). Although CCG 1432 and NSC23766 caused some elongation to the cells, analysis of the images did not detect these changes in the cell shape (**Figure 77**).

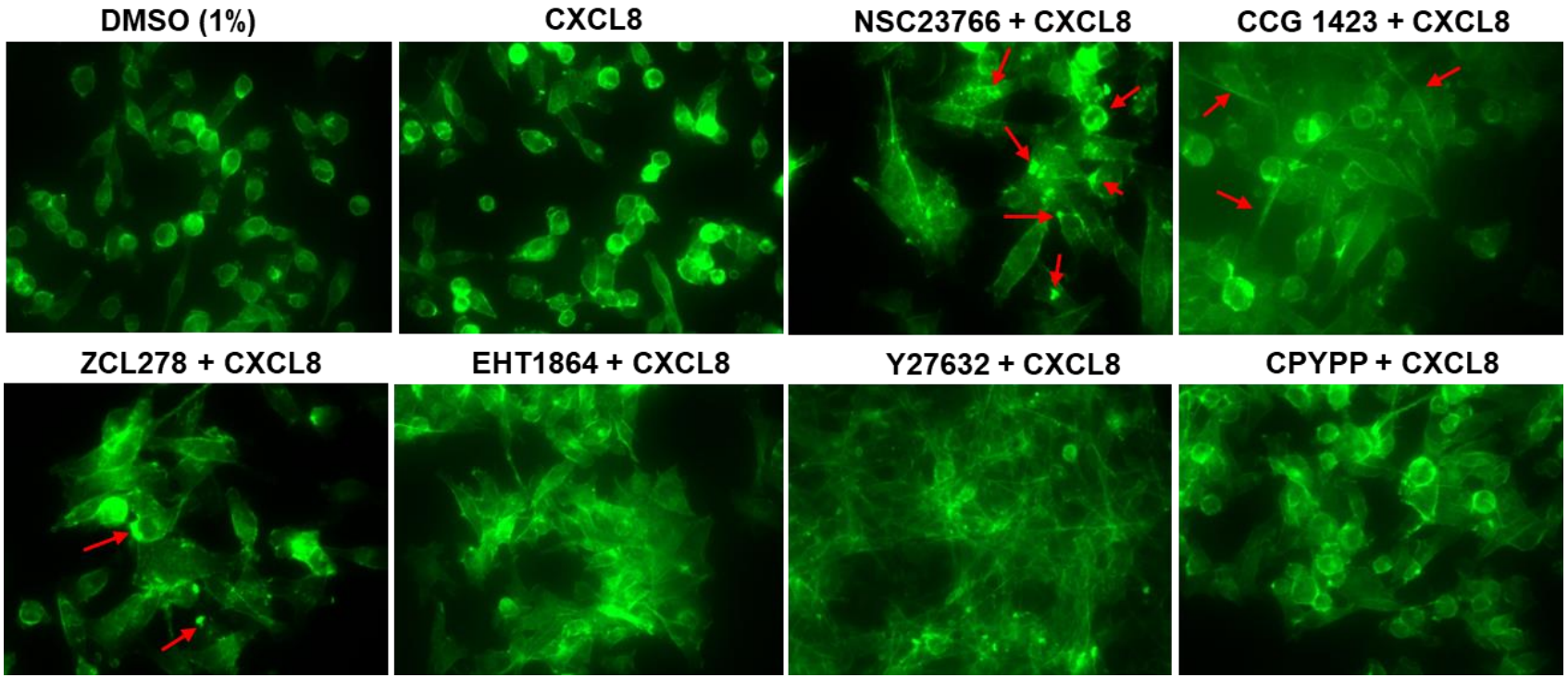

Figure 75. Phalloidin actin staining of CXCL8-activated MDA-MB231 cells in the presence or absence of Rac/Rho/Cdc42 and DOCK1/2/5 inhibitors. Actin cytoskeleton changes to the cells pre-treated with Rac1 inhibitors: NSC23766 (100 µM), EHT1864 (100 nM), Rho/ROCK inhibitors: CCG 1423 (1 µM), Y27632 (20 µM), or Cdc42 inhibitor: ZCL278 (20 µM), DOCK1/2/5 inhibitor: CPYPP (100 µM) and activated with CXCL8 (10 nM). The red arrows point out accumulation of punctate actin or cells elongation. 1% DMSO was added as a vehicle control. Cells were fixed and stained with Alexa-488 Phalloidin actin green stain. Cells images are representative of the population of cells from one experiment out of three repeats, acquired at 63x magnification using a Leica DMII inverted microscope and Leica imaging suite.

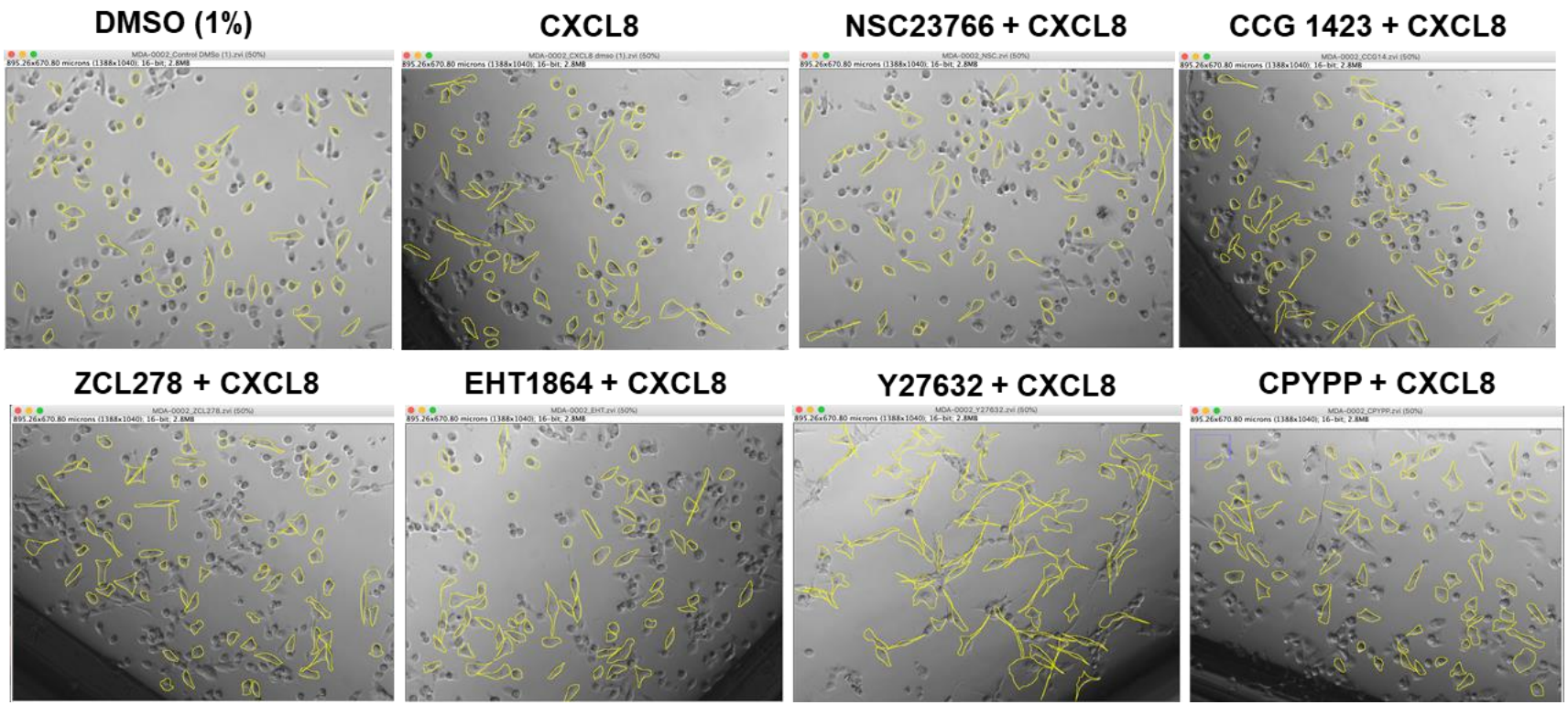

Figure 76. Illustrative images demonstrating morphological changes of MDA-MB231 cells treated with CXCL8 in the presence or absence of Rac/Rho/Cdc42 or DOCK1/2/5 inhibitors. Cells were treated with Rac1 inhibitors: NSC23766 (100 µM), or EHT1864 (100 nM), or Rho/ROCK inhibitors: CCG 1423 (1 µM), or Y27632 (20 µM), or Cdc42 inhibitor: ZCL278 (20 µM), or DOCK1/2/5 inhibitor: CPYPP (100 µM) and activated with CXCL8 (10 nM). 1% DMSO was added to the vehicle control. Cells were drawn around using Fiji/ImageJ and measurements of 70 cells per image per experiment were analysed. Experiments were repeated at least three times. Images are representative of the cell population and were taken at 10x objective with Zeiss Axiovert 200M microscope and processed using AxioVision Rel 4.8 software.

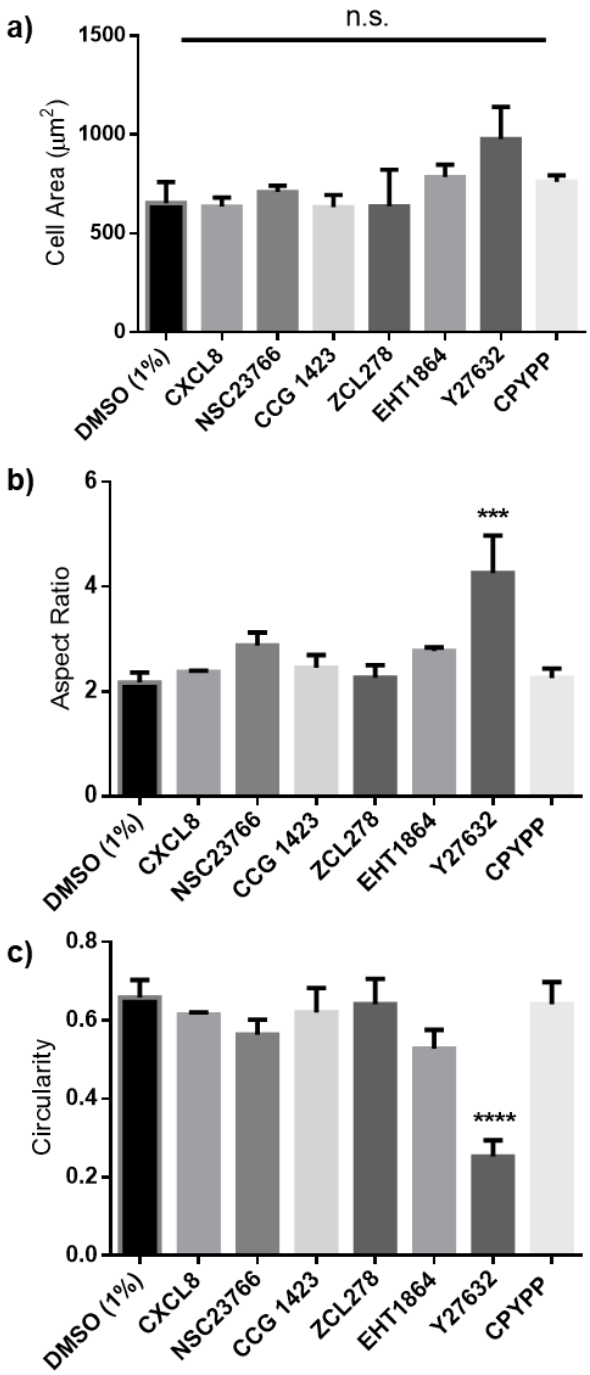

Figure 77. Analysis of the cellular morphology of MDA-MB231 cells following treatment with CXCL8 in the presence or absence of Rac/Rho/Cdc42 or DOCK1/2/5 inhibitors. Cells were treated with Rac1 inhibitors: NSC23766 (100 µM), EHT1864 (100 nM), Rho/ROCK inhibitors: CCG 1423 (1 µM), Y27632 (20 µM), Cdc42 inhibitor: ZCL278 (20 µM), or DOCK1/2/5 inhibitor: CPYPP (100 µM) and activated with CXCL8 (10 nM). 1% DMSO was added to the basal cells as a vehicle control. Comparisons were made against the positive control of cells incubated with CXCL8. Cells were drawn around and measurements of **a)** area, **b)** aspect ratio, and **c)** circularity were analysed for an average of 70 cells per image per experiment. Experiments were repeated three times (One-way ANOVA with a Dunnett's multiple comparisons test as post-test, n.s.= no significance $p>0.05$, *** = $p \leq 0.001$ **** = $p \leq 0.0001$).

The effect of Rho GTPases and DOCK 1/2/5 on the cellular morphology of PC3 cells is presented. Phalloidin actin stain with 10 nM CXCL8 stimulated membrane ruffling and lamellipodia formation as pointed out with the white arrows in **Figure 78**. When PC3 cells were treated with Rac1 inhibitor, NSC23766, even more bleb-like membrane ruffles were noticed (white arrows) as well as formation of microspikes (red arrows). Moreover, few cells with CCG 1423 (Rho inhibitor) treatment had a more pointed leading edge with actin reorganising at the leading edge and cells assuming a polarized morphology (pointed with red arrow heads). Cdc42 inhibitor, ZCL278, showed few membrane ruffling. More protrusive ends and membrane ruffling appeared with Rac1 inhibitor EHT1864. ROCK inhibitor, Y27632, impacted the morphology of the cells where they assumed an extensive thin elongation to their bodies, and cells were interlaced with no barriers. Indeed, Zhang *et al.* [514] found similar findings with Y27632, but with imaging at 400x magnification using confocal microscopy, they also noticed a considerable reduction in stress fibres formation identified by the decreased intensity of actin meshwork and compacted cellular morphology. ROCK has been demonstrated to phosphorylate the regulatory myosin light chain, which promotes its binding to F-actin [515]. Furthermore, DOCK 1/2/5 inhibitor, CPYPP gave the cells a widely spread with bigger cell area shape comparing with the control samples.

Images obtained with a light microscope using lower objective (10x) showed changes of the cells overall without specifically detecting actin reorganisation. Just like the previous observation, PC3 cells treated with Y27632 over 10 hrs demonstrated substantial elongation of the cells (**Figure 79**). The alternation of cell shape was analysed and resulted in a significant change to the cell area, aspect ratio and circularity (**Figure 80**). The other inhibitors tested showed no significance towards CXCL8-activated cells.

In summary, Rho/Rac/Cdc42 or DOCK1/2/5 inhibitors presented distinct effects on the speed of migration of MDA-MB231 and PC3 cells stimulated with CXCL8, while ROCK inhibitor, Y27632, significantly affected the morphology of both cell lines.

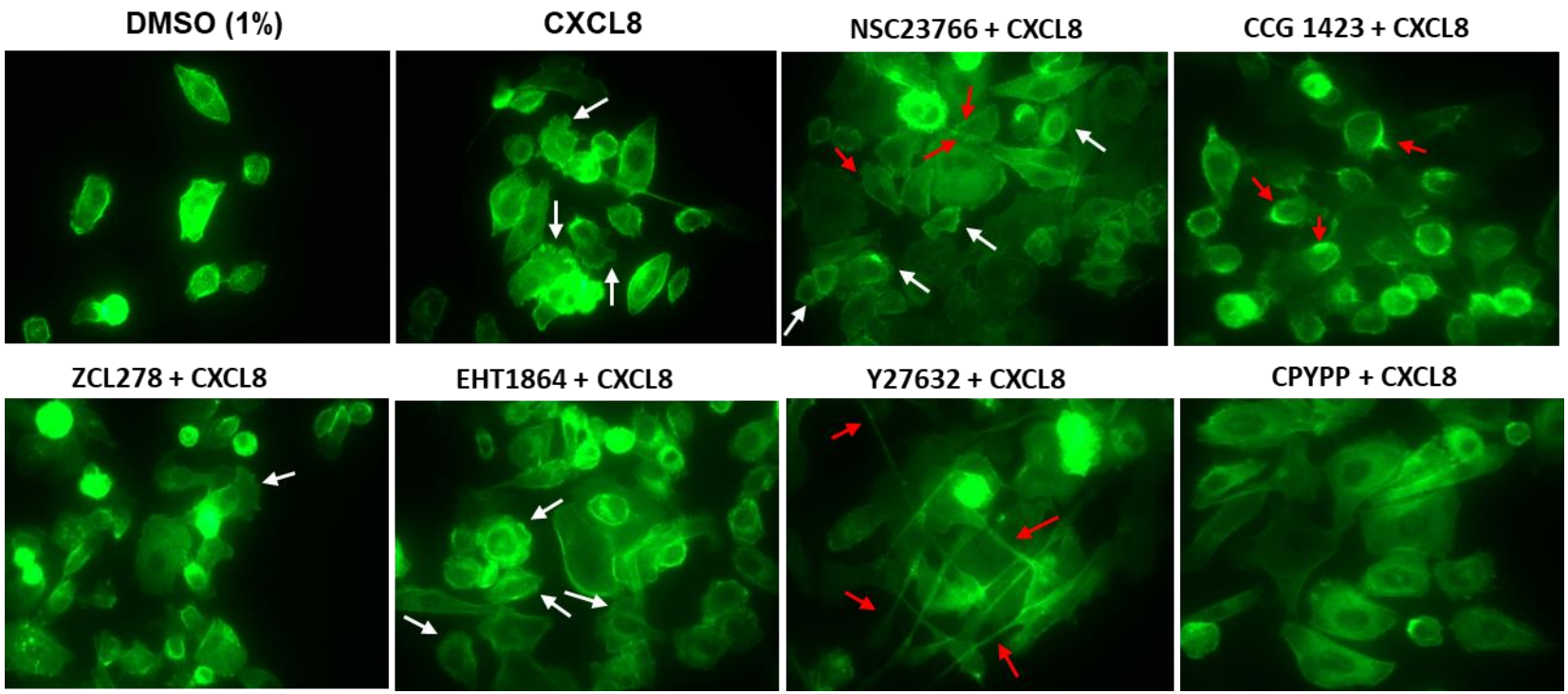

Figure 78. Phalloidin actin staining of CXCL8-activated PC3 cells in the presence or absence of Rac/Rho/Cdc42 or DOCK1/2/5 inhibitors. Actin cytoskeleton changes to pre-treated cells with Rac1 inhibitors: NSC23766 (100 µM), or EHT1864 (100 nM), or Rho/ROCK inhibitors: CCG 1423 (1 µM), or Y27632 (20 µM), or Cdc42 inhibitor: ZCL278 (20 µM), or DOCK1/2/5 inhibitor: CPYPP (100 µM) and activated with CXCL8 (10 nM). The red arrows indicate membrane microspikes formation or apical-basal polarity as well as elongating cells, while the white arrows show membrane ruffling. 1% DMSO was added to cells as the vehicle control. Cells were fixed and stained with Alexa-488 Phalloidin actin green stain. Cells images are representative of the population of one experiment out of three repeats, acquired at 63x magnification using a Leica DMII inverted microscope and Leica imaging suite.

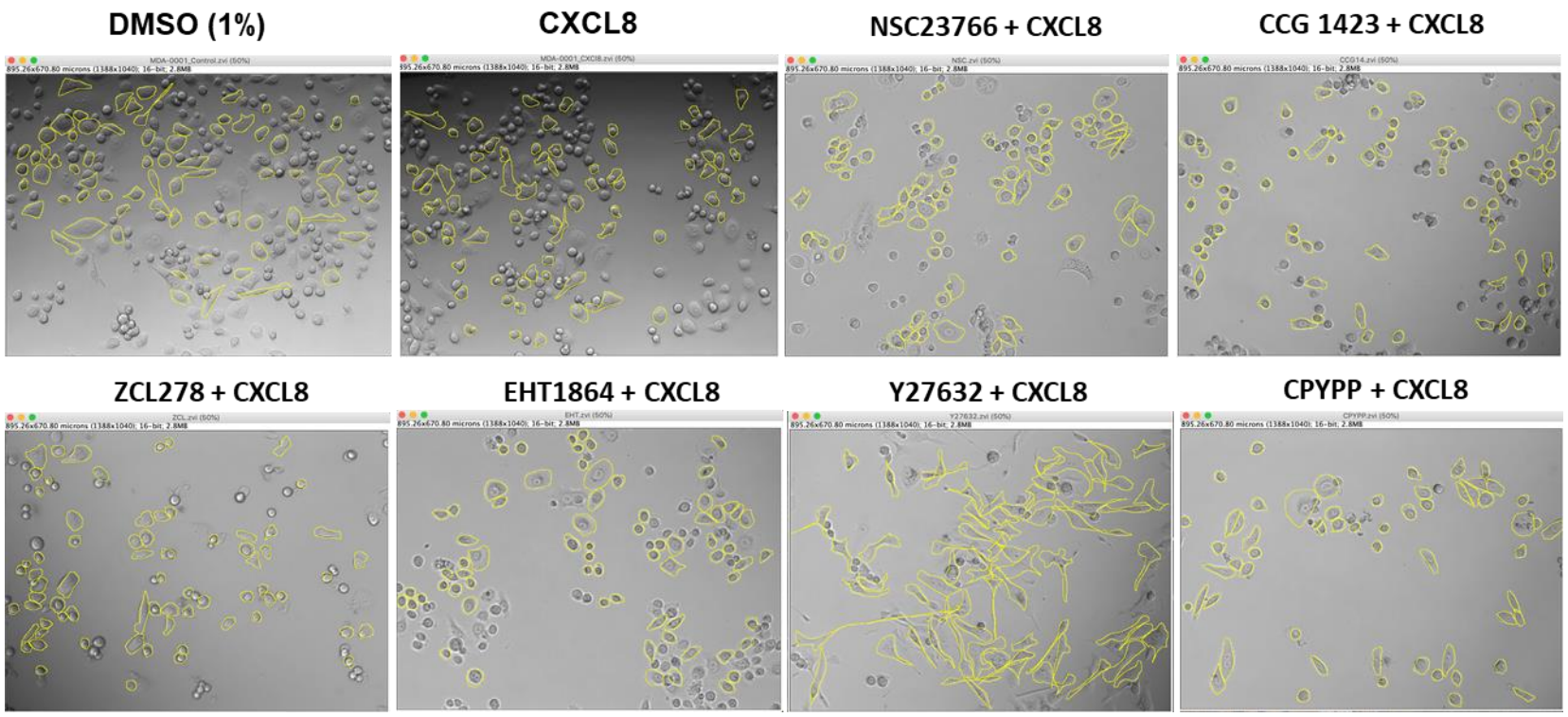

Figure 79. Illustrative images demonstrating morphological changes of CXCL8-stimulated PC3 cells in the presence or absence of Rac/Rho/Cdc42 or DOCK1/2/5 inhibitors. Cells were activated with CXCL8 (10 nM) alone or following pre-treatment with Rac1 inhibitors: NSC23766 (100 µM), or EHT1864 (100 nM), or Rho/ROCK inhibitors: CCG 1423 (1 µM), or Y27632 (20 µM), or Cdc42 inhibitor: ZCL278 (20 µM), or DOCK1/2/5 inhibitor: CPYPP (100 µM). 1% DMSO was added to the vehicle control. Cells were outlined using Fiji/ImageJ and measurements of 70 cells per image per experiment were analysed. Experiments were repeated at least three time. Images are a representation of the cell population and were taken at 10x objective with Zeiss Axiovert 200M microscope and processed using AxioVision Rel 4.8 software.

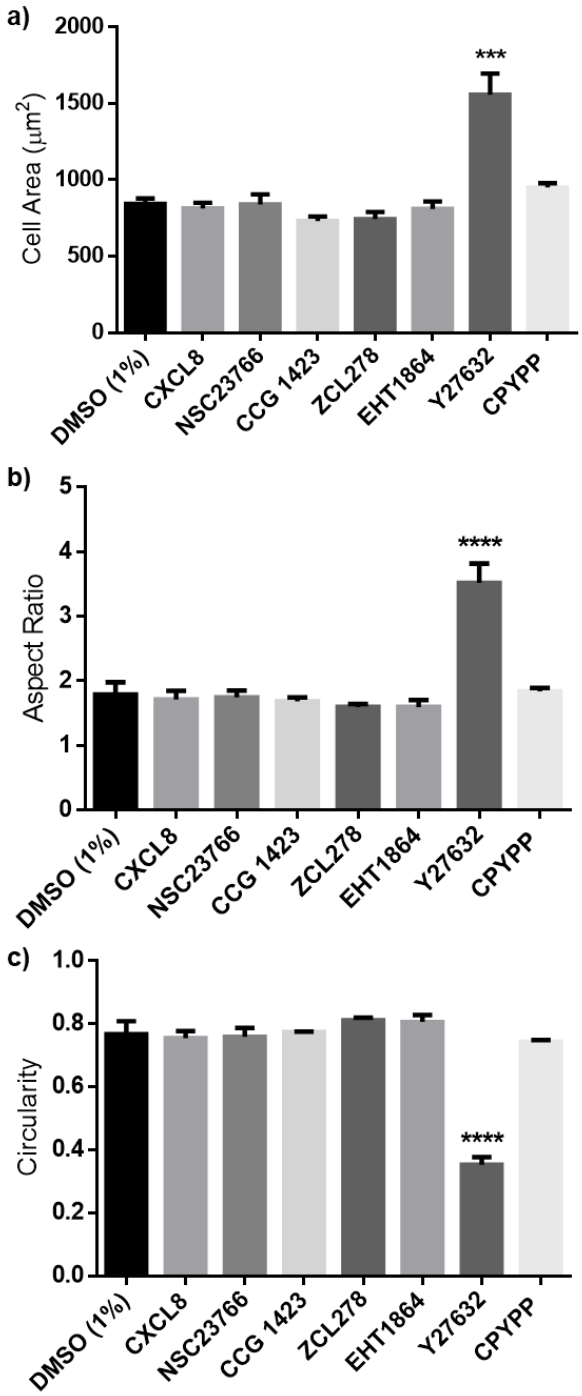

Figure 80. Analysis of cellular morphology of CXCL8-stimulated PC3 cells in the presence or absence of Rac/Rho/Cdc42 and DOCK1/2/5 inhibitors. Cells were treated with Rac1 inhibitors: NSC23766 (100 µM), or EHT1864 (100 nM), or Rho/ROCK inhibitors: CCG 1423 (1 µM), or Y27632 (20 µM), or Cdc42 inhibitor: ZCL278 (20 µM), or DOCK1/2/5 inhibitor: CPYPP (100 µM) and activated with CXCL8 (10 nM). Comparisons were made against CXCL8. 1% DMSO was added to the basal cells as a vehicle control. Cells outlined around and measurements of **a)** area, **b)** aspect ratio, and **c)** circularity were analysed of an average of 70 cells per image per experiment. Experiments were repeated three times (One-way ANOVA with a Dunnett's multiple comparisons test as post-test, n.s.=no significance $p>0.05$, *** = $p \leq 0.001$ **** = $p \leq 0.0001$).

4.2.3.3 MTS cytotoxic assay to quantify the cytotoxicity of Rac/Rho/Cdc42 and DOCK1/2/5

To identify the cells viability of MDA-MB231 and PC3 cells following 24 hrs incubation with Rho GTPases or DOCK1/2/5 inhibitors Rac1 inhibitors: NSC23766 (100 µM), or EHT1864 (100 nM), or Rho/ROCK inhibitors: CCG 1423 (1 µM), or Y27632 (20 µM), or Cdc42 inhibitor: ZCL278 (20 µM), or DOCK1/2/5 inhibitor: CPYPP (100 µM) an MTS assay was conducted. The concentrations used of the inhibitors did not show any cytotoxicity to MDA-MB231 cells (**Figure 81**). However, in PC3 cells Cdc42 inhibitor, ZCL278, showed a significant toxicity to the cells at 20 µM. Therefore, the reduced effect on the migration speed presented in **Figure 74** could possibly be due to the cytotoxicity of the inhibitor on the cells. Nonetheless, amid observation of cells migration in real-time using the time-lapse migration assay, we noticed that the cells slowed down but did not stop migrating or proliferating - no visible cytotoxicity demonstrated by floating or dying cells appeared. Indeed, Friesland *et al*. [362] used even a higher concentration reaching to 50 µM of ZCL278 on PC3 cells and found that the cell viability was not affected while cell motility was abolished. Another plausible explanation could be that the observation of the time-lapse migration assay was made over a period of 10 hrs, while for the MTS assay, the cells viability was detected after 24 hrs incubation period. Therefore, the inhibitor could have shown cytotoxicity over an extended period. It is worth performing another cell cytotoxicity assay for confirmation, such as Countess Automated Cell Counter (provided by Invitrogen) and combine it with a trypan blue dye staining assay, or LDH-cytotoxicity assay.

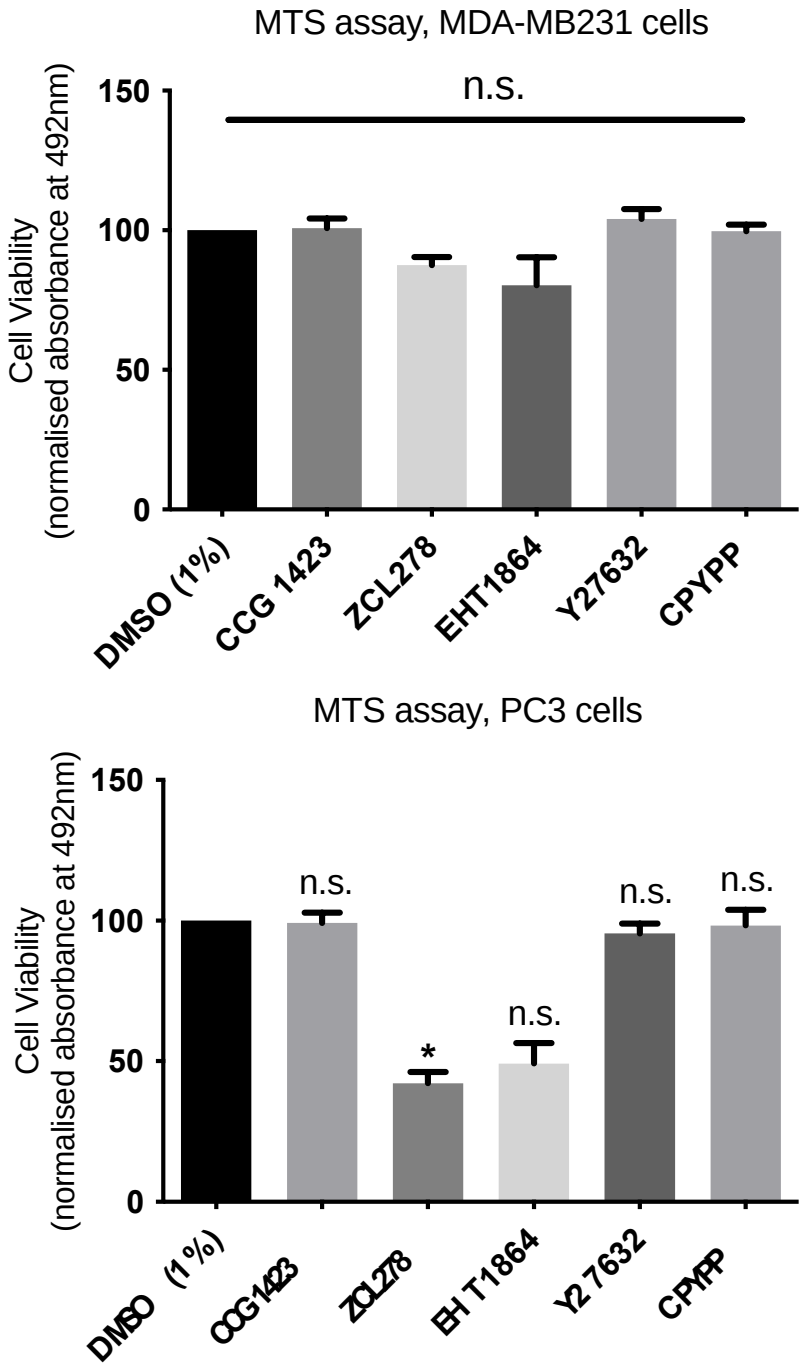

Figure 81. Toxicity of Rac/Rho/Cdc42 and DOCK1/2/5 inhibitors towards MDA-MB231 and PC3 cells. The absorbance following incubation with Rac1 inhibitors: NSC23766 (100 µM), or EHT1864 (100 nM), or Rho/ROCK inhibitors: CCG 1423 (1 µM), or Y27632 (20 µM), or Cdc42 inhibitor: ZCL278 (20 µM), or DOCK1/2/5 inhibitor: CPYPP (100 µM), for 24 hrs and treatment with MTS reagent for 2 hrs in **a)** MDA-MB231 cells, or **b)** PC3 cells. 1% DMSO was added to the basal cells as a vehicle control. Data are representative of the mean ± SEM of three independent experiments (Kruskal-Wallis test, Dunn's multiple comparisons test, n.s.= no significance $p>0.05$, * $p \leq 0.05$).

4.2.4 The FAK and Src signalling pathway

4.2.4.1 FAK and Src are important for cells migration

Activation of CXCR1 and CXCR2 in response to CXCL8 stimulates members of Rho GTPases family and thus, promotes stimulation of protein kinases such as Src and FAK [143]. Induction of these protein kinases was previously reported to elevate cells proliferation and migration [368]. Indeed, activation of RBL cells with CXCL8 promoted FAK phosphorylation and re-localization, which was correlated with increased cell spreading and migration [143], [375], [376].

FAK inhibitor: PF562271 (10 nM) and Src inhibitor: Bosutinib (1 µM) significantly reduced the speed of CXCL8-activated MDA-MB231 and PC3 cells. MDA-MB231 basal cells had a speed of 21.07 ± 7.5 µm/hr, while addition of CXCL8 (10 nM) increased the speed to 48.3 ± 4.4 µm/hr. Cells treated with PF562271 had a speed of 29.9 ± 13.6 µm/hr, and Bosutinib almost completely abolished the migration; 4.2 ± 2.1 µm/hr (**Figure 82**).

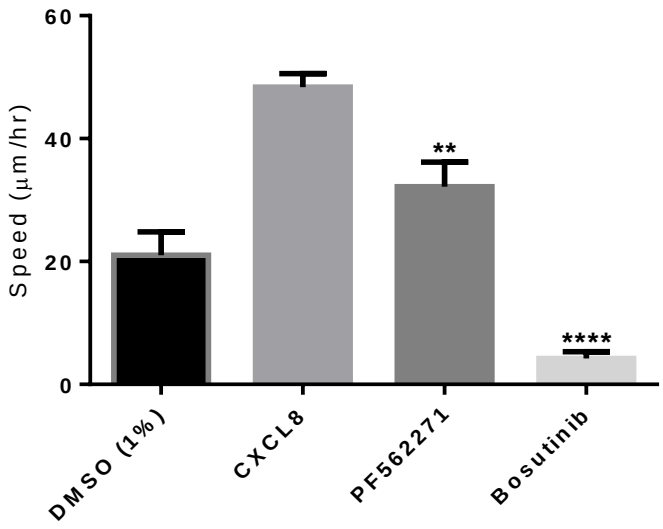

Figure 82. The effect of FAK and Src inhibitors on the migration speed of CXCL8-activated MDA-MB231 cells. Cells were pre-treated with FAK inhibitor: PF562271 (10 nM) or Src inhibitor: Bosutinib (1 µM) and activated with CXCL8 (10 nM). Comparisons were made against CXCL8. 1% DMSO was added to the basal cells as a vehicle control. Data are representative of the analysis of 10 cells in each experiment using Fiji/ImageJ, with the mean ± SEM of four independent experiments (One-way ANOVA with a Dunnett's multiple comparisons test as post-test, ** = p ≤0.01, **** = p ≤ 0.0001).

PC3 cells reacted in the same way; having a basal speed of 25.7 ± 7.9 µm/hr, addition of CXCL8 (10 nM) increased the speed to 59.0 ± 21.4 µm/hr, incubating with PF562271 had a speed of 34.8 ± 11.1 µm/hr, and incubating with Bosutinib drastically reduced the speed to 6.6 ± 1.4 µm/hr (**Figure 83**).

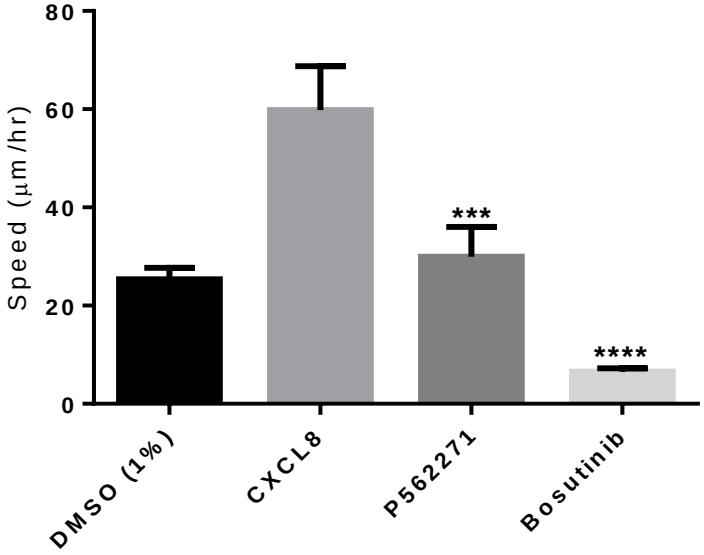

Figure 83. The effect of FAK and Src inhibitors on the migration speed of CXCL8-activated PC3 cells. Cells were pre-treated with FAK inhibitor: PF562271 (10 nM) or Src inhibitor: Bosutinib (1 µM) and activated with CXCL8 (10 nM). Comparisons were made against CXCL8. 1% DMSO was added to the basal cells as a vehicle control. Data are representative of the analysis of 10 cells in each experiment using Fiji/ImageJ, with the mean ± SEM of four independent experiments (One-way ANOVA with a Dunnett's multiple comparisons test as post-test, *** = p ≤0.001, **** = p ≤ 0.0001).

4.2.4.2 Src inhibition affects the cellular morphology

Cancer cells have the ability to grow in an anchorage-independent fashion and FAK is thought to be associated with this phenotype [516]. FAK localizes in focal adhesions plaques and function as a scaffolding and signalling protein for other adhesion molecules. The stimulation of Src-kinases and FAK are observed in cancer cells after induction with CXCL8 [367]. Indeed, CXCR1 and CXCR2 transfected HEK293 and RBL cells confirm that Src and FAK are upstream signalling cascades of CXCL8 [375], [376]. Therefore, their activation was reported to be associated with cell proliferation, spreading, migration and invasion [368], [397].

Since integrin signalling is mediated through FAK catalytic activity [517], we used PF562271 as a small molecule inhibitor of FAK which could lead to integrin signalling inhibition. Phalloidin actin stain of MDA-MB231 cells pre-treatment with PF562271 (10 nM) and activation with CXCL8 (10 nM) showed that cells have lost their intact structures and clustered around each other (red arrows **Figure 84**). It is thought that FAK stimulates actin and β-tubulin re-localization to promote spreading and migration that is directly associated with CXCL8-activated migratory response [376]. Indeed, Cohen-Hillel *et al*. [376] have suggested that induction with CXCL8 controls actin and microtubule rearrangements associated with regulating FAK. This could explain the cellular morphological changes upon FAK inhibition which corresponds to the abrogation of cellular speed (as shown above). However, having bright-field microscopy images obtained after 10 hrs incubation with the inhibitor did not show a substantial effect on the cell area, aspect ratio and circularity of the cells (**Figure 85**). This was indicated with the analysis of these images by randomly selecting cells and drawing around them (**Figure 86**).

On the other hand, Src inhibitor, Bosutinib (1 μM), showed a significant effect on the MDA-MB231 cellular morphology. Bosutinib is an FDA approved drug for chronic myeloid leukaemia [518]. With Bosutinib treatment, cells seemed to have lost their structure. They are stretched out with overlapping filaments of interlacing cells along with disorganised stress fibres appeared. Some cells showed accumulation of crosslinked networks of lamellipodia and filopodia at the leading/tailing edge (red arrows **Figure 84**). The changes in cell shape were also witnessed in the images obtained by light microscopy (**Figure 85**), along with a significant increase in the cell area presented from the images analysis (**Figure 86**).

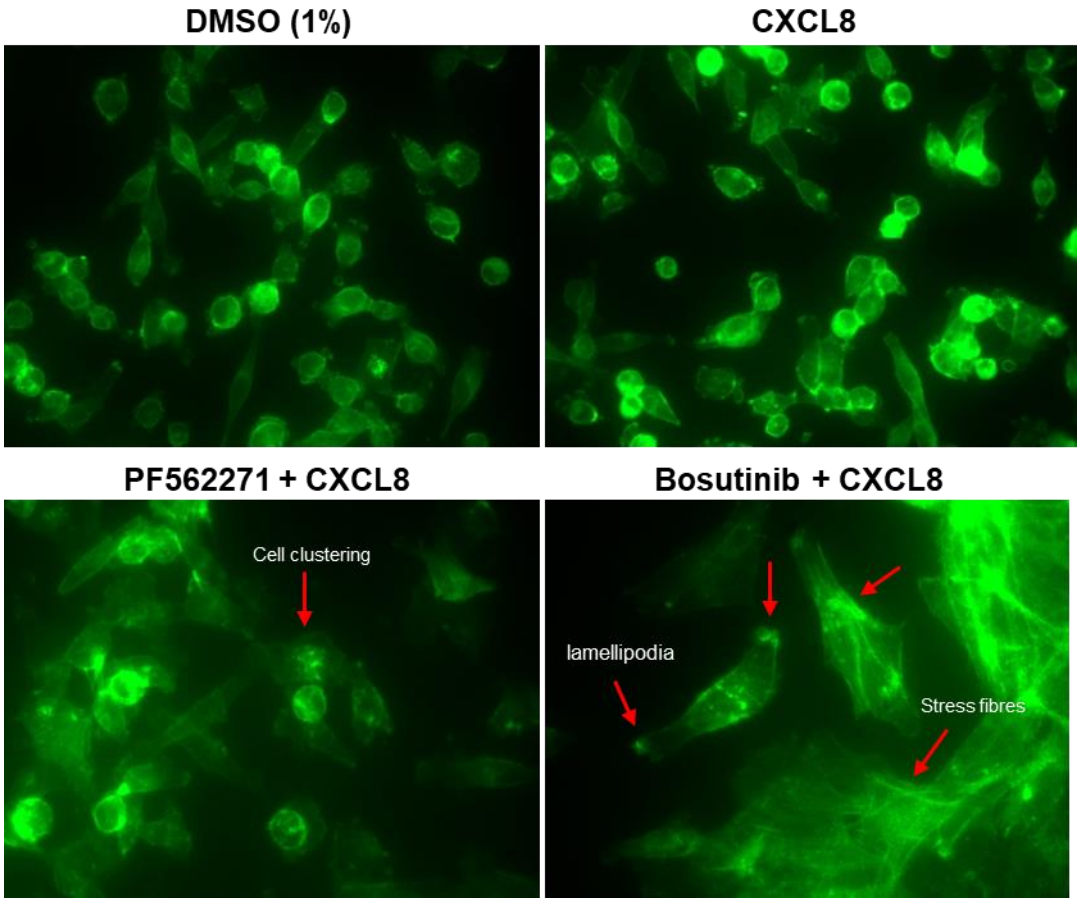

Figure 84. Phalloidin actin staining of CXCL8-activated MDA-MB231 cells in the presence or absence of FAK and Src inhibitors. Cells were treated with FAK inhibitor: PF562271 (10 nM) or Src inhibitor: Bosutinib (1 µM) and activated with CXCL8 (10 nM). 1% DMSO was added as a vehicle control. Cells were fixed and stained with Alexa-488 Phalloidin actin green stain. Cells images are representative of the population of cells from one experiment out of three repeats, acquired at 63x magnification using a Leica DMII inverted microscope and a Leica imaging suite.

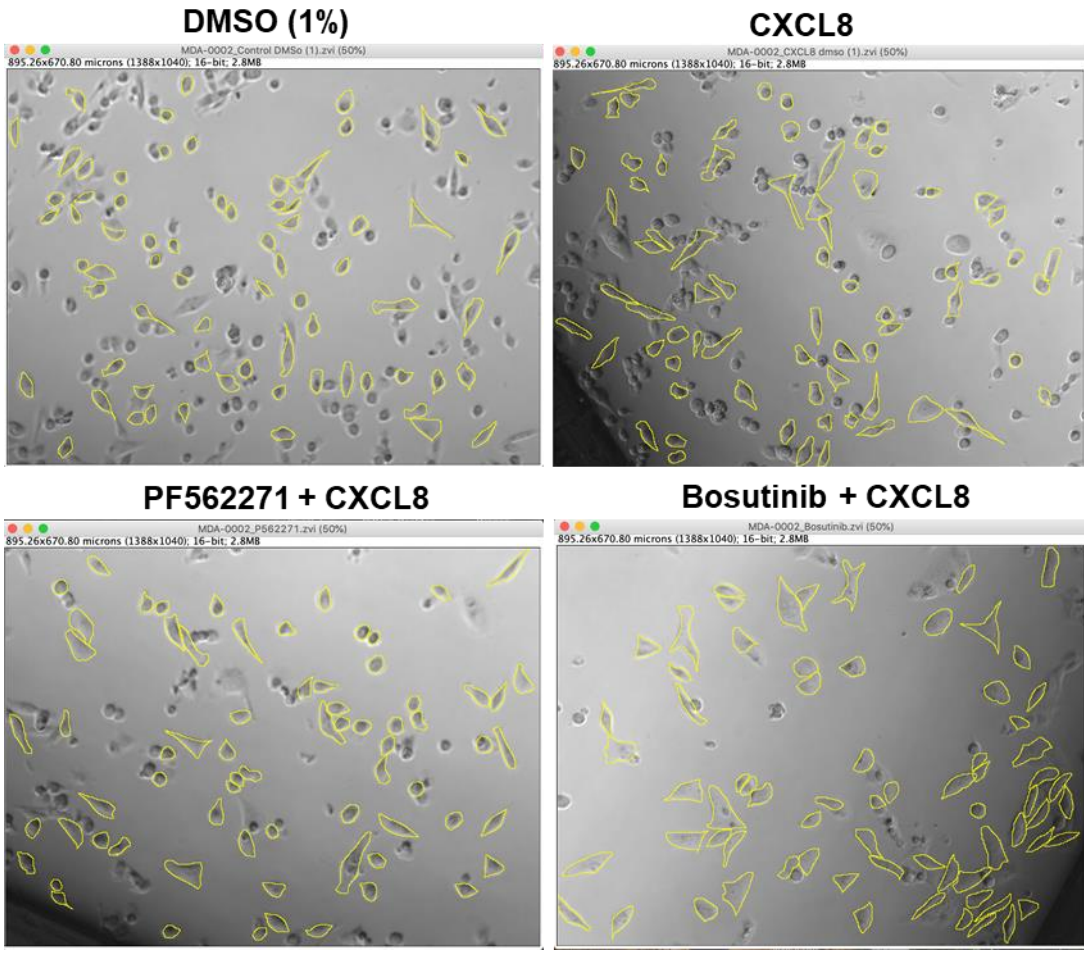

Figure 85. Illustrative images demonstrating morphological changes of CXCL8-stimulated MDA-MB231 cells in the presence or absence of FAK and Src inhibitors. Cells were pre-treated with the FAK inhibitor: PF562271 (10 nM) or Src inhibitor: Bosutinib (1 µM) and activated with CXCL8 (10 nM). 1% DMSO was added as a vehicle control. Cells were drawn around using Fiji/ImageJ and measurements of 70 cells per image per experiment were analysed. Experiments were repeated at least three times. Images are representative of the cell population and were taken at 10x objective with a Zeiss Axiovert 200M microscope and processed using AxioVision Rel 4.8 software.

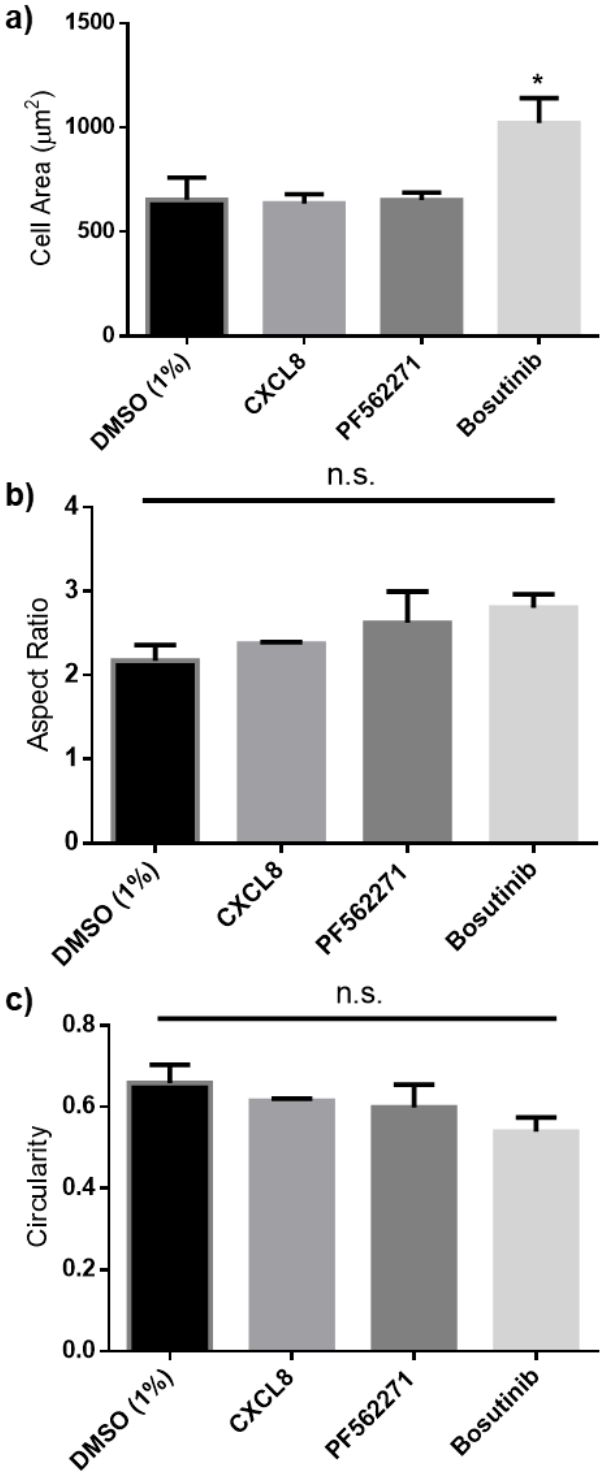

Figure 86. Analysis of the cellular morphology of CXCL8-stimulated MDA-MB231 cells in the presence or absence of FAK and Src inhibitors. Cells were treated with FAK inhibitor: PF562271 (10 nM) or Src inhibitor: Bosutinib (1 µM) and activated with CXCL8 (10 nM). Comparison was made against CXCL8. 1% DMSO was added to the basal cells as a vehicle control. Cells were drawn around and measurements of **a)** area, **b)** aspect ratio, and **c)** circularity were analysed for an average of 70 cells per image per experiment. Experiments were repeated three times (One-way ANOVA with a Dunnett's multiple comparisons test as post-test, n.s.= no significance $p>0.05$, * = $p \leq 0.05$).

Actin rearrangement was observed by staining PC3 cells with phalloidin showed no major effect with PF562271 (10 nM) treatment. However, Bosutinib has yet again induced changes to the cell morphology characterised by significant enlargement of the cells area going up to almost double the size comped to the control samples as shown in **Figure 87**. Furthermore, the effect of Bosutinib was obvious with images generated from light microscopy (**Figure 88**), where a significant impact on the cell area is presented in (**Figure 89**).

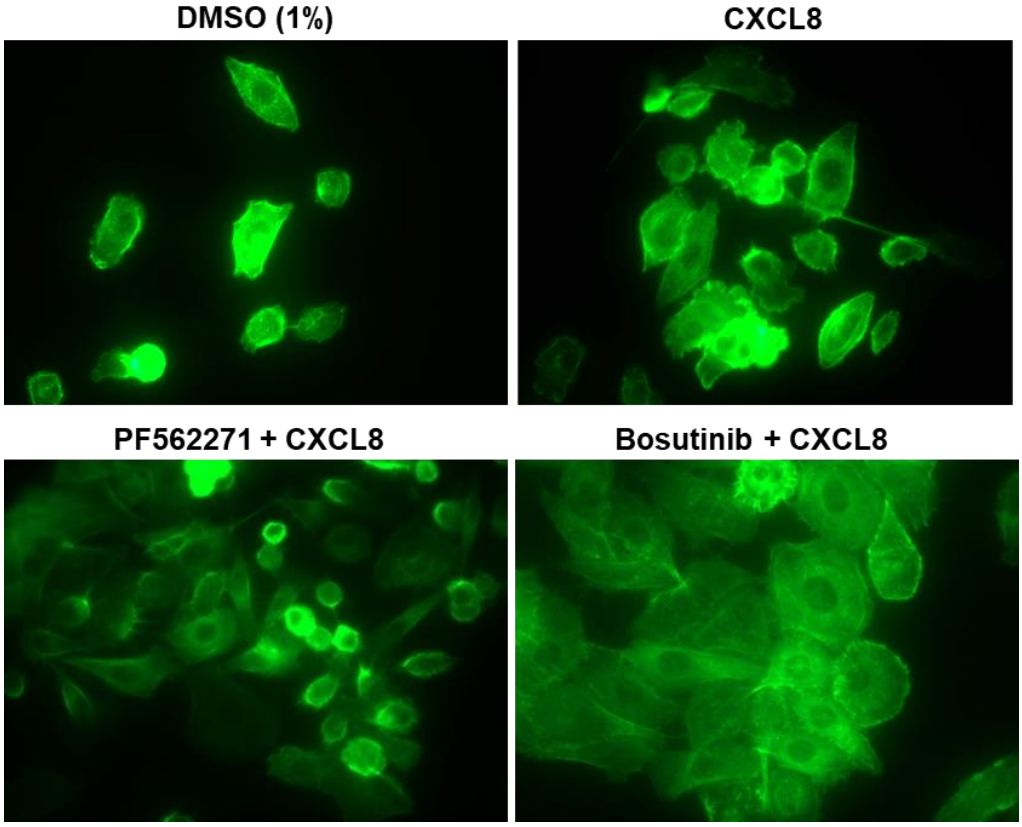

Figure 87. Phalloidin actin staining of CXCL8-activated PC3 cells in presence or absence of FAK and Src inhibitors. Cells were treated with FAK inhibitor: PF562271 (10 nM) or Src inhibitor: Bosutinib (1 µM) and activated with CXCL8 (10 nM). 1% DMSO was added to the cells as a vehicle control. Cells were fixed and stained with Alexa-488 Phalloidin actin green stain. Cells images are representative of the population of one experiment out of three repeats, acquired at 63x magnification using a Leica DMII inverted microscope and Leica imaging suite.

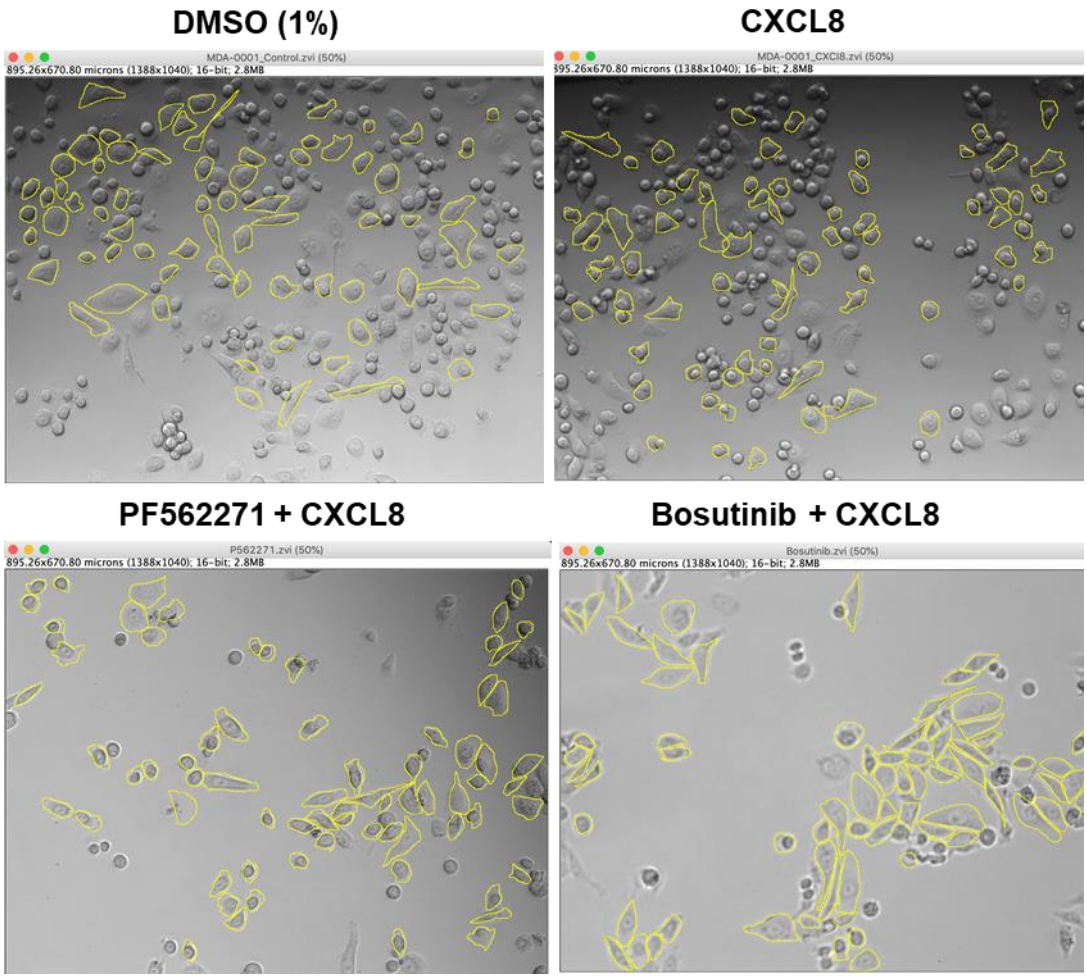

Figure 88. Illustrative images demonstrating morphological changes of PC3 cells in the presence or absence of FAK and Src inhibitors. Cells were treated with FAK inhibitor: PF562271 (10 nM) or Src inhibitor: Bosutinib (1 µM) and activated with CXCL8 (10 nM). 1% DMSO was added as a vehicle control. Cells were outlined using Fiji/ImageJ and measurements of 70 cells per image per experiment were analysed. Experiments were repeated at least three times. Images are representative of the cell population and were taken at 10x objective with a Zeiss Axiovert 200M microscope and processed using AxioVision Rel 4.8 software.

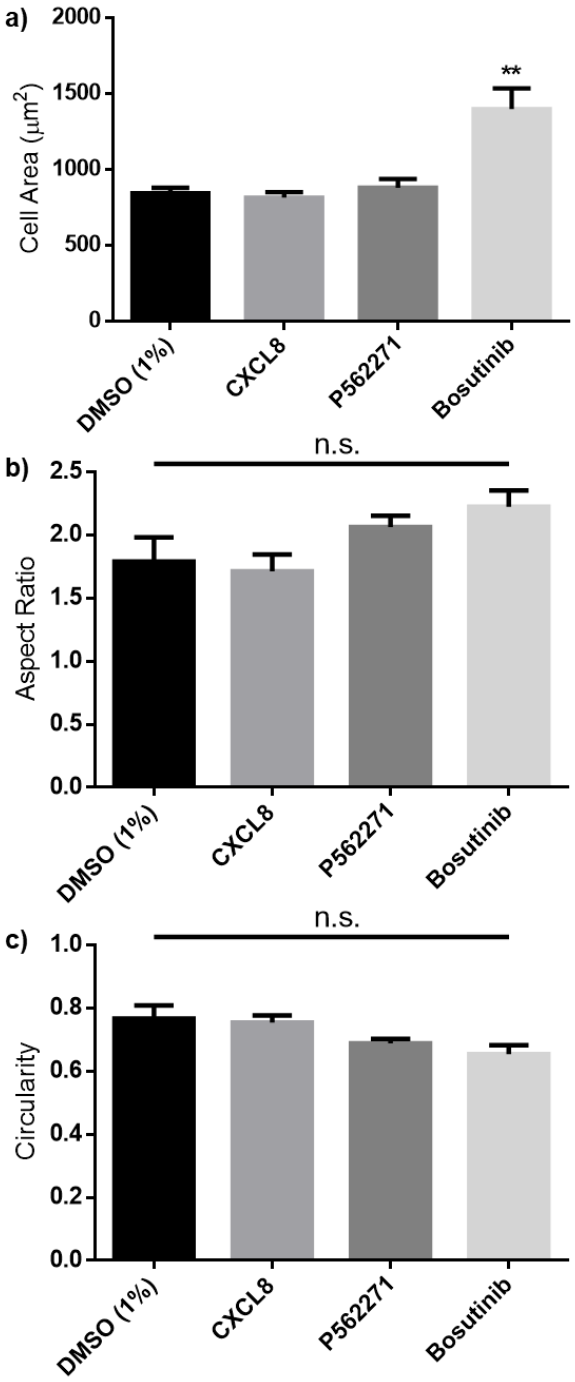

Figure 89. Cellular morphology analysis of CXCL8-stimulated PC3 cells in the presence of FAK and Src inhibitors. Cells were pre-treated with FAK inhibitor: PF562271 (10 nM) or Src inhibitor: Bosutinib (1 µM) and activated with CXCL8 (10 nM). Comparisons were made against CXCL8. 1% DMSO was added to the basal as a vehicle control. Cells were outlined and measurements of **a)** area, **b)** aspect ratio, and **c)** circularity were analysed for an average of 70 cells per image per experiment. None demonstrated any significance except for Bosutinib cell area. Experiments were repeated three times (One-way ANOVA with a Dunnett's multiple comparisons test as post-test, n.s.= no significance $p>0.05$, ** = $p \leq 0.01$).

4.2.4.3 MTS cytotoxic assay to quantify the cytotoxicity of FAK and Src inhibitors

Strong evidence has suggested the presence of activated FAK [368] and Src [369] in CXCL8-activated cancer cells [139]. Using FAK inhibitor, PF62271, at a concentration of 10 nM, and Src inhibitor, Bosutinib, at a concentration of 1 µM, over a period of 24 hrs has yielded in no cytotoxic effects on either MDA-MB231 or PC3 cells (**Figure 90**) using an MTS assay. Different studies have used a range of concentrations of Bosutinib starting from 25 nM to 250 nM [505] where no effect on the cell migration was reported, and 10 µM [388], [519] where this concentration inhibited cells migration. However, the latter concentration caused cell morphology changes associated with cytotoxicity on neuroblastoma cells and HeLa cells [520], [521]. Therefore, using 1 µM seemed ideal to have generated a response without being cytotoxic.

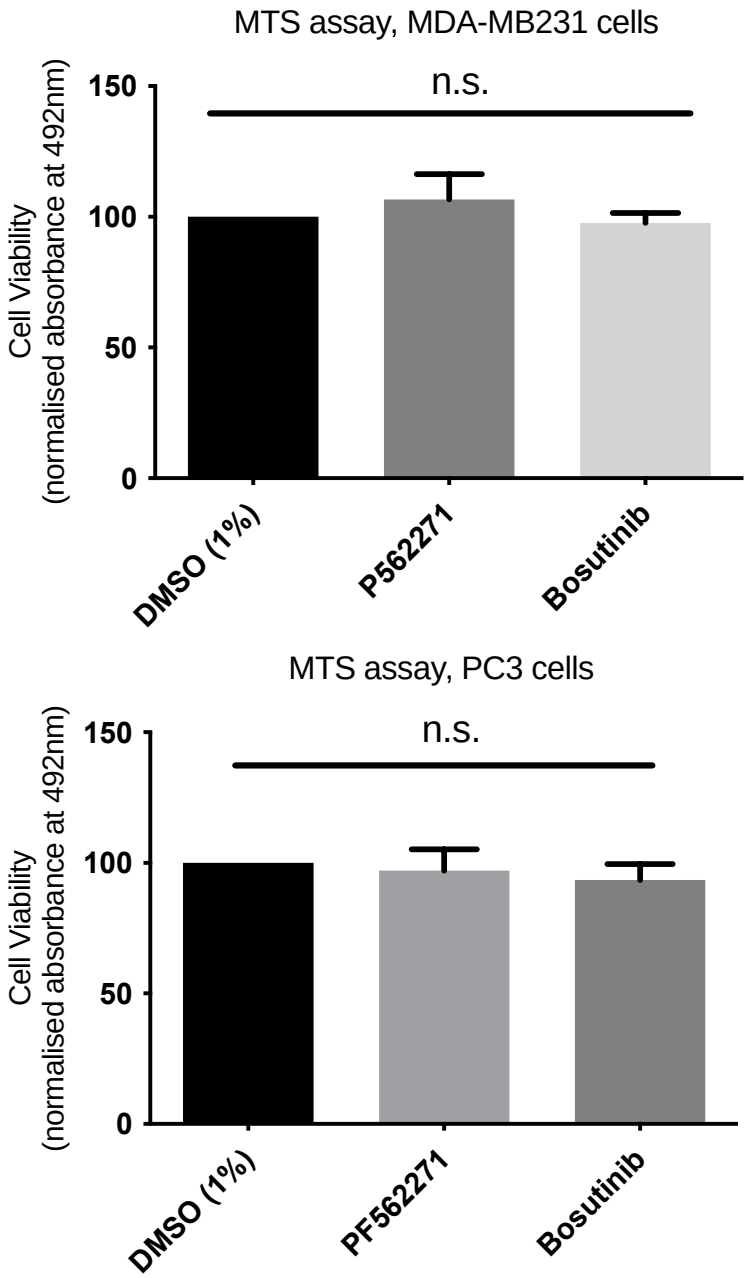

Figure 90. Toxicity of FAK and Src inhibitors towards MDA-MB231 and PC3 cells. The absorbance of FAK inhibitor: PF562271 (10 nM) or Src inhibitor: Bosutinib (1 µM), incubated for 24 hrs and treatment with MTS reagent for 2 hrs in **a)** MDA-MB231 cells, or **b)** PC3 cells. 1% DMSO was added to the basal cells as a vehicle control. Data are representative of the mean ± SEM of three independent experiments (Kruskal-Wallis test, Dunn's multiple comparisons test, n.s.= no significance $p > 0.05$).

4.2.5 The PKA, Arp2/3, and PKD signalling pathways

4.2.5.1 PKA, Arp2/3 or PKD have an important effect on cell migration

Protein phosphorylation regulated by protein kinases has a vital role in cellular signal transduction [522]. H89, is a potent PKA small molecule inhibitor that has a wide spectrum effect on other protein kinases depending on the concentration used. CXCL8 was reported to activate vasodilator-stimulated phosphorylation (VASP) through PKA and PKC signalling, which is crucial for the chemotaxis and polarization of HL-60 cells. A study by Lee *et al.* [523] found that the inhibition of the Arp2/3 complex abrogates PKA activity and tyrosine phosphorylation causing disturbance to actin polymerization. Additionally, protein kinase D (PKD) is identified as an upstream regulator of Arp2/3 and F-actin binding protein cortactin [524]. CID755673 is a PKD inhibitor that was identified for its tumour-enhancing role in prostate cancer cells [525].

Treatment of MDA-MB231 cells with H89 (10 µM) in the presence of CXCL8 (10 nM) was made over 10 hrs. Untreated MDA-MB231 basal cells had a speed of 21.07 ± 7.5 µm/hr, and the activation with CXCL8 (10 nM) increased the speed to 48.3 ± 4.4 µm/hr. Treatment with H89 (10 nM) generated a speed of 43.1 ± 4.0 µm/hr. However, Arp2/3 inhibitor CK666 (80 µM) significantly attenuated the speed to 19.5 ± 4.4 µm/hr. A total abrogation of cell migration was reported with CID755673 (11 µM) giving a speed of 3.8 ± 1.3 µm/hr (**Figure 91**).

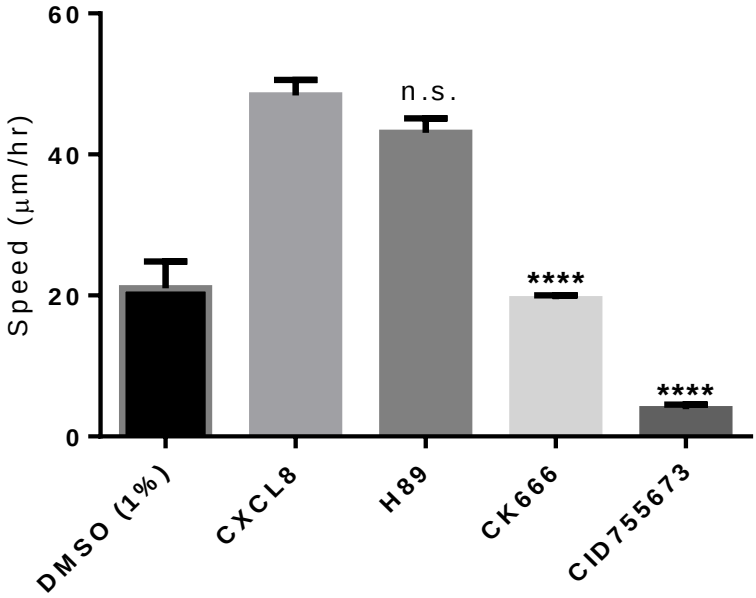

Figure 91. CXCL8-activated MDA-MB231 cells migration speed in the presence or absence of PKA, Arp2/3, or PKD inhibitors. Cells were pre-treated with PKA inhibitor: H89 (10 nM), or Arp2/3 complex inhibitor: CK666 (80 µM), or PKD inhibitor: CID755673 (11 µM) and activated with CXCL8 (10 nM). Comparisons were made against CXCL8. 1% DMSO was added to the basal cells as a vehicle control. Data are representative of the analysis of 10 cells in each experiment using Fiji/ImageJ, with the mean ± SEM of four independent experiments (One-way ANOVA with a Dunnett's multiple comparisons test as post-test, n.s.= no significance $p>0.05$, **** = $p \leq 0.0001$).

PC3 cells reacted differently to the PKA inhibitor H89 compared to MDA-MB231 cells. The speed of PC3 basal cells was 25.7 ± 7.9 µm/hr, addition of CXCL8 (10 nM) increased the speed to 59.0 ± 21.4 µm/hr. H89 treatment had reduced the speed to 30.6 ± 12.6 µm/hr. Additionally, Arp2/3 complex inhibitor CK666 (80 µM) had completely paralysed the cells; 4.4 ± 2.5 µm/hr. PKD inhibitor CID755673 (11 µM) had also reduced the speed of cells, although not as dramatically; 24.9 ± 18.7 µm/hr (**Figure 92**).

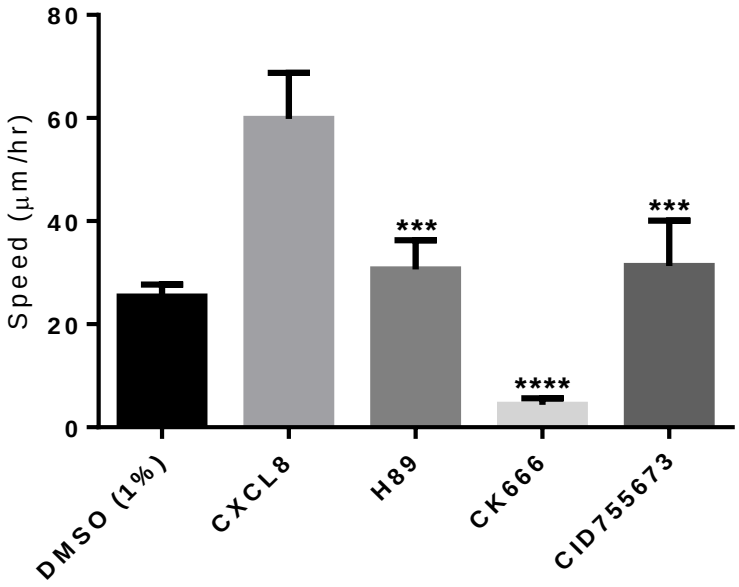

Figure 92. CXCL8-activated PC3 cells migration speed in the presence of PKA, Arp2/3, or PKD inhibitors. Cells were treated with the PKA inhibitor: H89 (10 nM), or Arp2/3 complex inhibitor: CK666 (80 µM), or PKD inhibitor: CID755673 (11 µM) and activated with CXCL8 (10 nM). Comparisons were made against CXCL8. 1% DMSO was added to the basal cells as a vehicle control. Data are representative of the analysis of 10 cells in each experiment using Fiji/ImageJ, with the mean ± SEM of four independent experiments (One-way ANOVA with a Dunnett's multiple comparisons test as post-test, *** = $p \leq 0.001$, **** = $p \leq 0.0001$).

4.2.5.2 PKD inhibition affects cellular morphology

Since the Arp2/3 complex and PKD proved to be vital for the migration of PC3 and MDA-MB231 cells, and H89 for PC3 cells, we further inspected the cellular changes of the cells. Mills. [498] found that H89 treatment of THP-1 cells have caused a significant reduction of the migration of the cells towards CXCL12 using a chemotaxis assay as well as disrupted the directional F-actin responses of CHO.CCR5 and MCF-7 cells to both CCL3 and CXCL12.

For CXCL8-activated MDA-MB231 cells, Arp2/3 complex inhibitor, CK666, slightly decreased the appearance of spiked protrusions of actin assembly density at the leading edge with few lamellipodia extensions to some cells (**Figure 93**). In fact, Yang *et el.* [43] described the effect of CK666 (80 µM) to have disrupted actin veils with actin retraction. Another study has also found that CK666 leads to the disappearance of lamellipodia [526]. Moreover, PKA inhibitor H89 (10 nM) had no significant effect, although cells looked modestly bigger than the controls with elongation to few cells. Additionally, having incubated CID755673 (11 µM) with the cells have radically changed their shape; appearance of very long stretched cells growing over each other and overlapping filaments indicating that cells have lost their ability to retract or move forward.

The effect of CID755673 was also evident using lower magnification (10x) with bright-field microscope, where the cells looked bigger in size with pointed leading edges (**Figure 94**). Quantification of the cellular morphology with the above inhibitors showed that CID755673 majorly affected the circularity and cell area while H89 and CK666 did not (**Figure 95**).

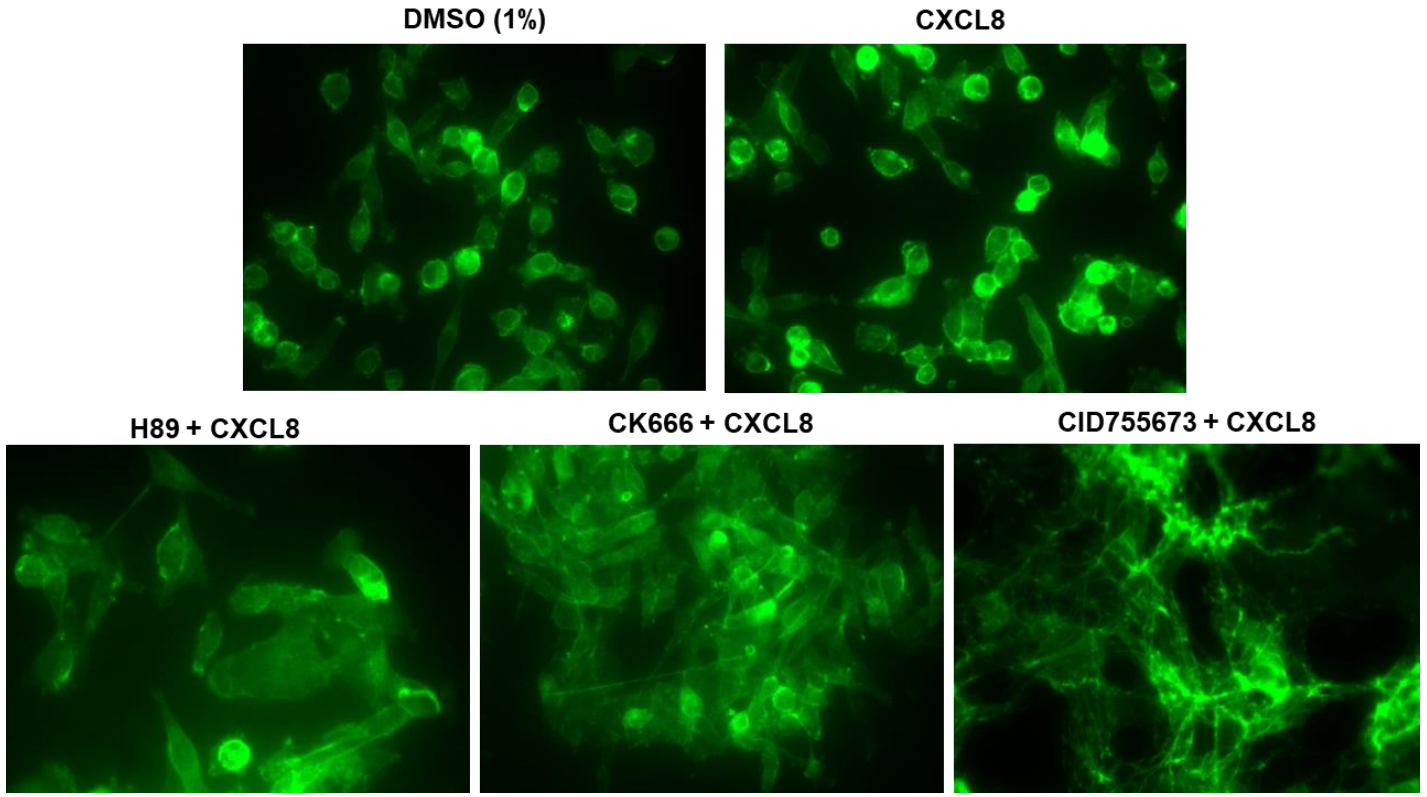

Figure 93. Phalloidin actin staining of CXCL8-activated MDA-MB231 cells in presence or absence of PKA, Arp2/3, or PKD inhibitors. Cells were treated with PKA inhibitor: H89 (10 nM), or Arp2/3 complex inhibitor: CK666 (80 µM), or PKD inhibitor: CID755673 (11 µM) and activated with CXCL8 (10 nM). 1% DMSO was added to the cells as a vehicle control. Cells were fixed and stained with Alexa-488 phalloidin actin green stain. Cells images are representative of three independent repeats and were acquired at 63x magnification using a Leica DMII inverted microscope and Leica imaging suite.

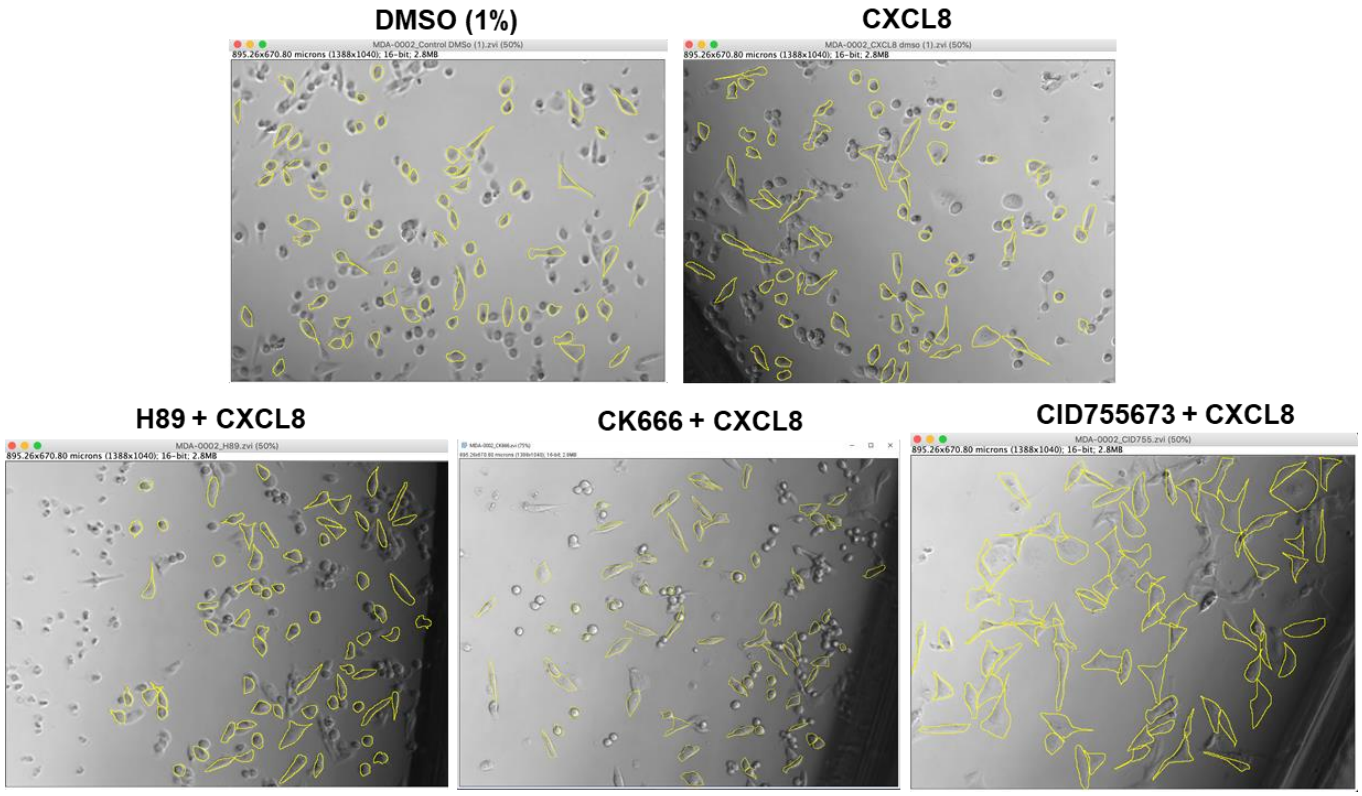

Figure 94. Illustrative images demonstrating morphological changes of CXCL8-stimulated MDA-MB231 cells in the presence of PKA, Arp2/3, or PKD inhibitors. Cells were treated with PKA inhibitor: H89 (10 nM), or Arp2/3 complex inhibitor: CK666 (80 μM), or PKD inhibitor: CID755673 (11 μM) and activated with CXCL8 (10 nM). 1% DMSO was added to the vehicle control. Cells were drawn around using Fiji/ImageJ and measurements of 70 cells per image per experiment were analysed. Experiments were repeated at least three time. Images are a representation of the cell population and were taken at 10x objective with Zeiss Axiovert 200M microscope and processed using AxioVision Rel 4.8 software.

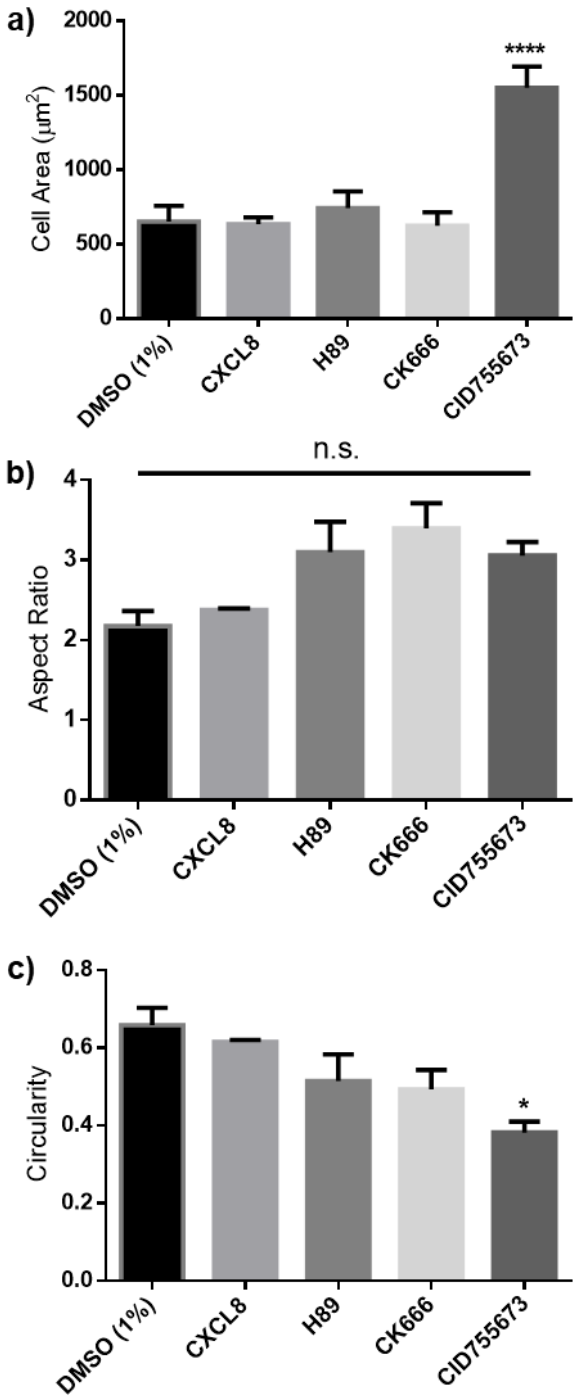

Figure 95. Analysis of the cellular morphology of CXCL8-stimulated MDA-MB231 cells in the presence or absence of PKA, Arp2/3, or PKD inhibitors. Cells were pre-treated with PKA inhibitor: H89 (10 nM), or Arp2/3 complex inhibitor: CK666 (80 µM), or PKD inhibitor: CID755673 (11 µM) and activated with CXCL8 (10 nM). Comparisons were made against CXCL8. 1% DMSO was added to the basal cells as a vehicle control. Cells were outlined and measurements of **a)** area, **b)** aspect ratio, and **c)** circularity were analysed for an average of 70 cells per image per experiment. Experiments were repeated three times (One-way ANOVA with a Dunnett's multiple comparisons test as post-test, n.s.= no significance $p>0.05$, * = $p \leq 0.05$, **** = $p \leq 0.0001$).

CXCL8-activated PC3 cells incubated with the same set of inhibitors demonstrated similar responses to MDA-MB231 cells. Although H89 (PKA inhibitor)-treated cells decreased the speed of migrating cells, using phalloidin actin stain to inspect actin rearrangement only showed a slight increase to the cells area with this inhibitor relative to the controls (**Figure 96**). CK666 (Arp2/3 inhibitor)-treated cells had more membrane ruffles (indicated by the white arrows), formed some microspikes tips (indicated with the red arrows) as well as caused actin clumping demonstrated by the little dots' accumulation inside the cells. Moreover, CID755673 (PKD inhibitor)-treated cells appeared bigger in size with extensive amount of visible microspikes of lamellipodia and filopodia forming antenna-like shapes almost surrounding all the cell with no particularly directed protrusions.

Further observations of the cellular morphology using bright-field microscope presented again that with CID755673 treatment, cells looked bigger, although microspikes formations did not show with these images (**Figure 97**). The cellular area, aspect ratio and circularity where significantly different as presented with statistical analysis (**Figure 98**). This change of the cellular morphology with CID755673 was associated with reduction of the migration speed of PC3 cell.

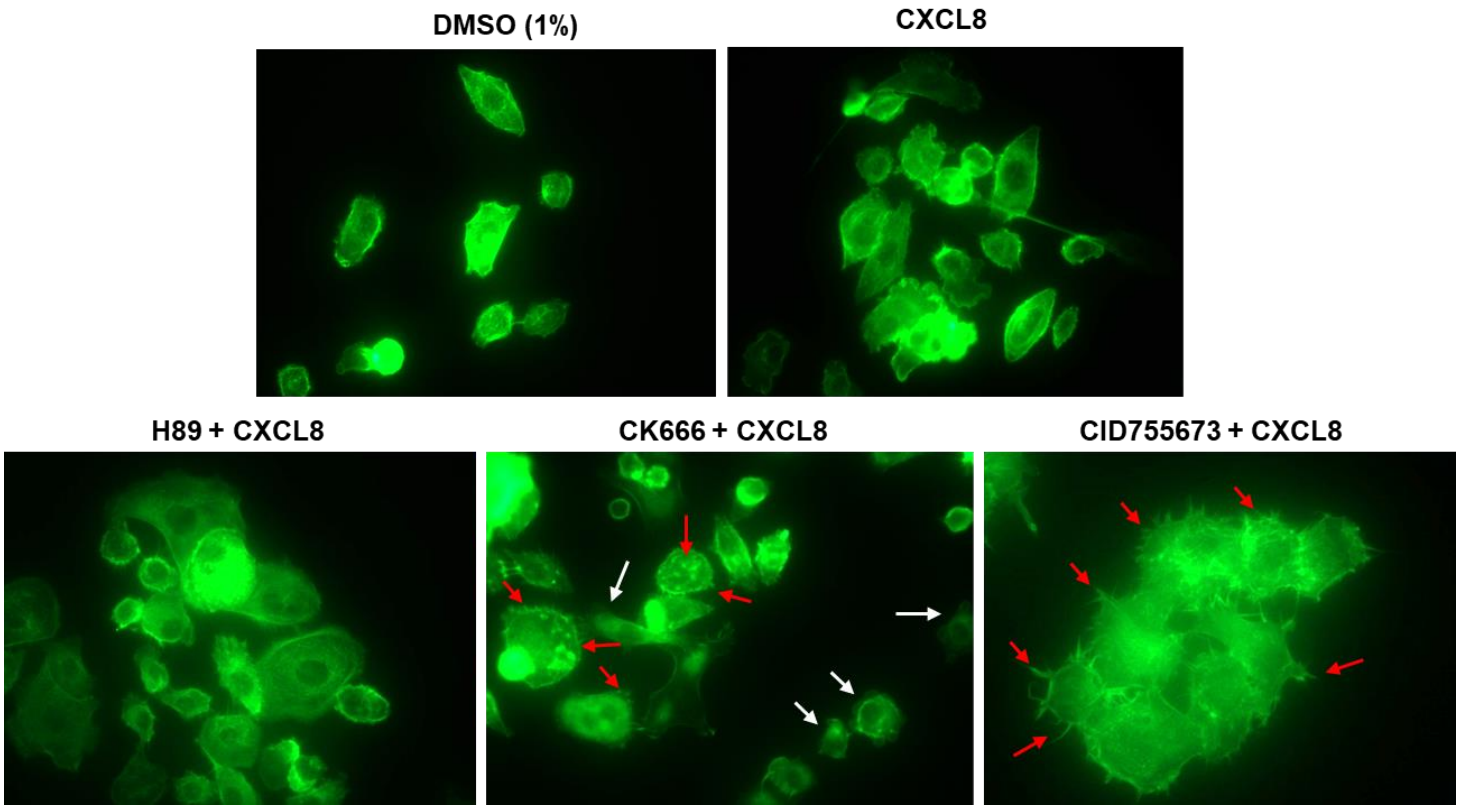

Figure 96. Phalloidin actin staining of CXCL8-activated PC3 cells in the presence or absence of PKA, Arp2/3, or PKD inhibitors. Cells were treated with PKA inhibitor: H89 (10 nM), or Arp2/3 complex inhibitor: CK666 (80 µM), or PKD inhibitor: CID755673 (11 µM) and activated with CXCL8 (10 nM). White arrows point out membrane ruffling, and red arrows show actin clumping and microspikes. 1% DMSO was added to cells as the vehicle control. Cells were fixed and stained with Alexa-488 Phalloidin actin green stain. Images are representative of a population of one experiment out of three repeats, acquired at 63x magnification using a Leica DMII inverted microscope and Leica imaging suite.

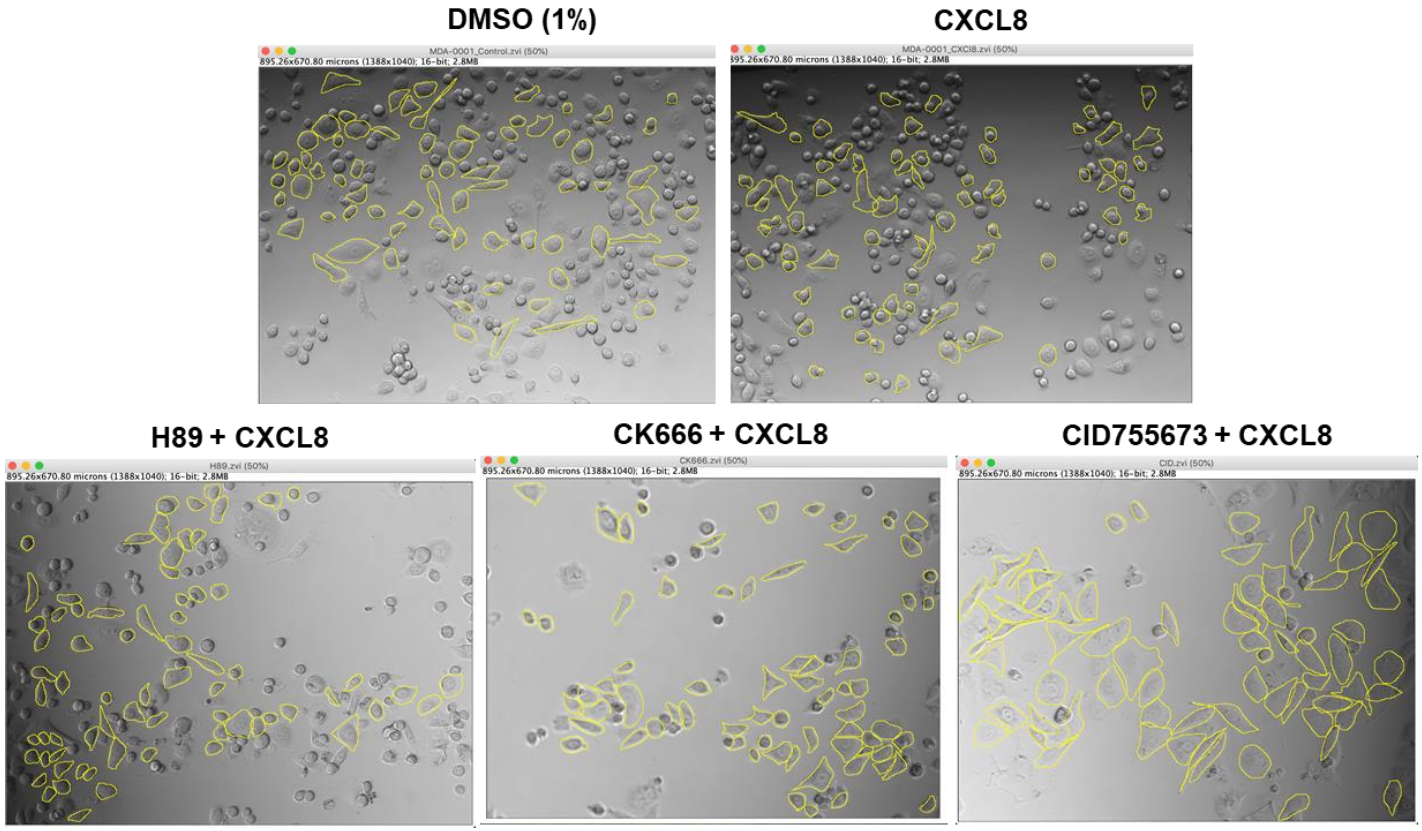

Figure 97. Illustrative images demonstrating morphological changes of CXCL8-stimulated PC3 cells in the presence or absence of PKA, Arp2/3, or PKD inhibitors. Cells were treated with PKA inhibitor: H89 (10 nM), or Arp2/3 complex inhibitor: CK666 (80 µM), or PKD inhibitor: CID755673 (11 µM) and activated with CXCL8 (10 nM). 1% DMSO was added to the vehicle control. Cells were outlined using Fiji/ImageJ and measurements of 70 cells per image per experiment were analysed. Experiments were repeated at least three time. Images are a representation of the cell population and were taken at 10x objective with Zeiss Axiovert 200M microscope and processed using AxioVision Rel 4.8 software.

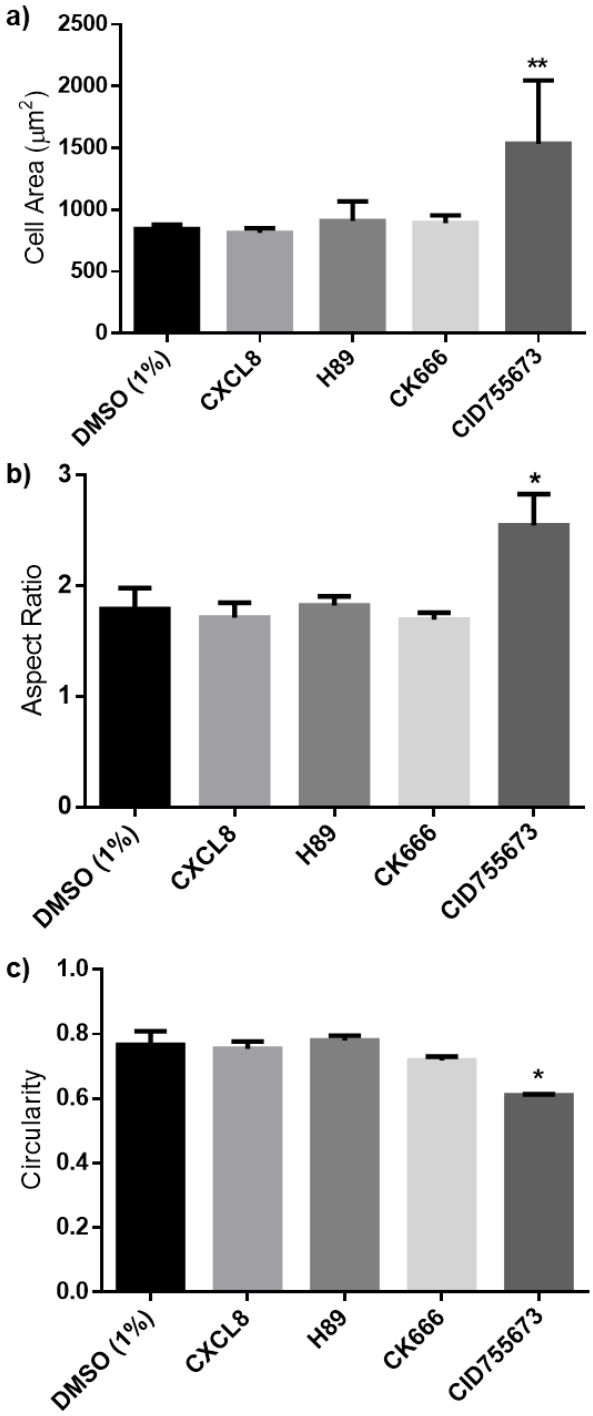

Figure 98. Analysis of cellular morphology analysis of CXCL8-stimulated PC3 cells in the presence or absence of PKA, Arp2/3, or PKD inhibitors. Cells were treated with PKA inhibitor: H89 (10 nM), or Arp2/3 complex inhibitor: CK666 (80 μM), or PKD inhibitor: CID755673 (11 μM) and activated with CXCL8 (10 nM). Comparisons were made against CXCL8. 1% DMSO was added to the basal as a vehicle control. Cells were outlined and measurements of **a)** area, **b)** aspect ratio, and **c)** circularity were analysed of an average for 70 cells per image per experiment. Experiments were repeated three times (One-way ANOVA with a Dunnett's multiple comparisons test as post-test, * = $p \leq 0.05$, ** = $p \leq 0.01$).

4.2.5.3 MTS cytotoxic assay to quantify the cytotoxicity of PKA, Arp2/3, and PKD inhibitors

Since the inhibition of Arp2/3 inhibitor and PKD inhibitor has greatly reduced the speed of MDA-MB231 and PC3 cells. We wanted to see if this inhibition was due to a cytotoxic effect. Indeed, CK666 at 80 µM in PC3 cells and CID755673 at 11 µM in MDA-MB231 cells have showed cytotoxicity of the inhibitors in the MTS assay (**Figure 99**). However, this assay was performed over 24 hrs, while the time-lapse migration assay was conducted over 10 hrs. From the observations of the treated cells in real time, we did not see any abnormal behaviour of the cells resembled by their death. Therefore, it is unlikely that the inhibitory response CK666 and CID755673 induce on the cells is due to toxicity. Nonetheless, it is preferable to test these inhibitors for the time period used in the migration assay and also confirm the results with another cytotoxicity assay.

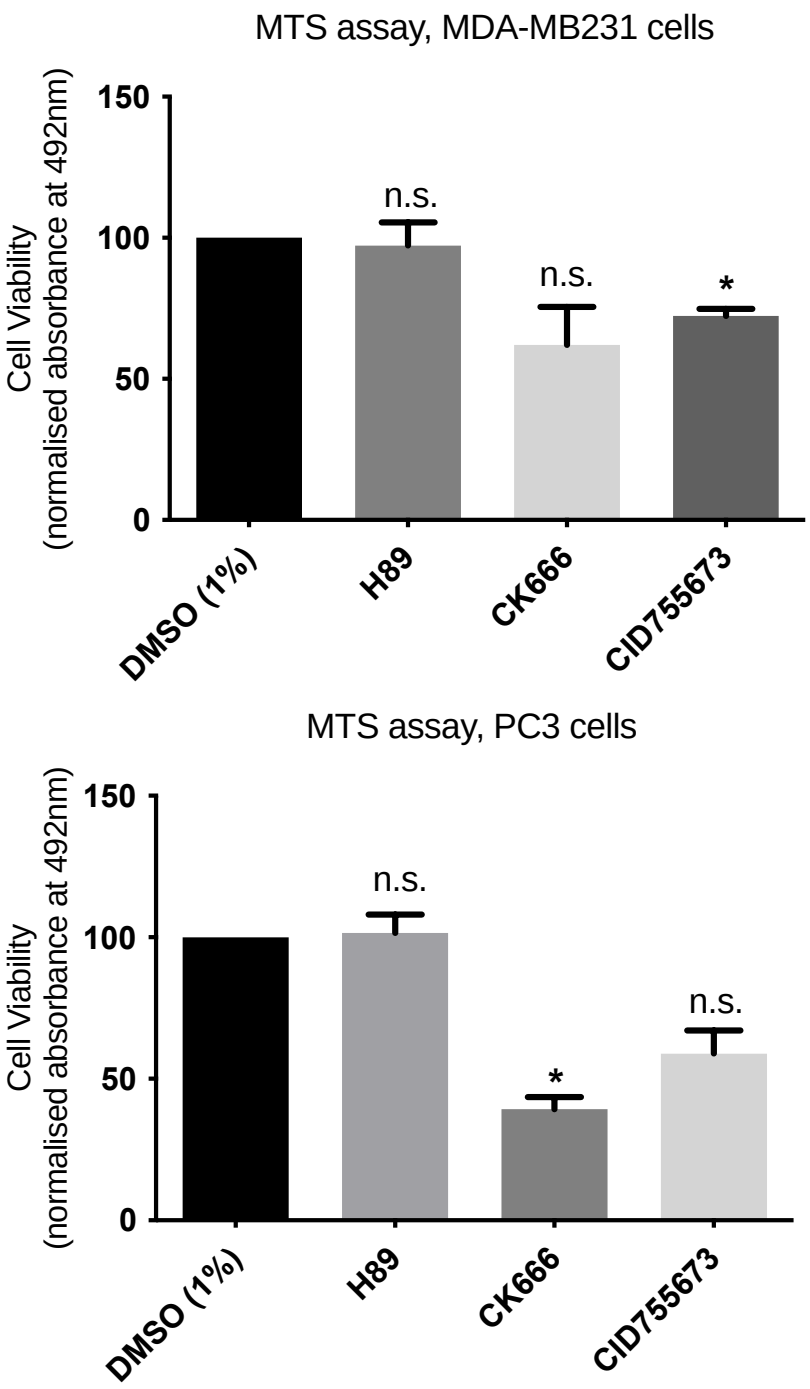

Figure 99. Toxicity of PKA, Arp2/3, or PKD inhibitors towards MDA-MB231 and PC3 cells. The absorbance of PKA inhibitor: H89 (10 nM), or Arp2/3 complex inhibitor: CK666 (80 µM), or PKD inhibitor: CID755673 (11 µM), incubated for 24 hrs and treatment with MTS reagent for 2 hrs in **a)** MDA-MB231 cells, or **b)** PC3 cells. 1% DMSO was added to the basal cells as a vehicle control. Data are representative of the mean ± SEM of three independent experiments (Kruskal-Wallis test, Dunn's multiple comparisons test, n.s.= no significance $p > 0.05$, * = $p \leq 0.05$).

4.3 Discussion

Binding of chemokines to their respective receptors leads to the stimulation of various intracellular signalling cascades associated with several cellular responses such as, cell adhesion, proliferation, and migration [77]. Signalling pathways involved in CXCL8 activation have attracted a lot of attention due to their involvement in cancer, angiogenesis, survival, proliferation, and tumorigenesis [280]. One of the most widely studied signalling pathways is the Pi3K-associated pathway. This pathway has been proven to contribute significantly to the ability of cells to sense a chemokine gradient and migrate in response to chemokine receptor activation in multiple cell types [281]. Several studies have reported that Pi3K is crucial for cell polarization and chemotaxis induced by chemoattractant activation in a number of cell types, although different cells respond distinctly to the effect of Pi3K inhibitors [527], [528]. For example, our group showed that Pi3K activation was crucial for the migration of leukemic Jurkat cells in response to CXCL12, although MCF-7 cells did not respond in the same manner and did not migrate [388].

AKT is believed to be a promising target for pharmacological intervention. CXCL8 has been reported to elevate the expression of AKT in androgen-independent prostate cancer cell lines [452]. AKT stimulation phosphorylates several substrates, including cytoskeleton-regulating proteins and EMT-stimulating proteins that have different roles in the cell, particularly in the regulation of cell migration [281]. Moreover, activation of chemokine receptors on neutrophils result in F-actin polymerization and cytoskeletal contraction from PIP3 signalling [529]. This means that the assembly of actin is necessary for pseudopod extension, leading to the migration of neutrophil towards a chemokine gradient, which is dependent on AKT activity [529]. Indeed, another study identified that increased filopodia formation in breast BT549 cancer cells was AKT-dependent. Inhibition of AKT in these breast cancer cells using a specific AKT inhibitor, AKT/protein kinase 2 signalling inhibitor-2 (API-2), resulted in the blockage of filopodia formation [493]. Furthermore, Pi3K/AKT inhibitors were tested on mesodermal cells and were found to inhibit membrane protrusive structures. These involved filopods and pseudopods, as well as disorganisation of the symmetric distribution of AKT at the leading edge, resulting in migration inhibition during vertebrate gastrulation [530]. Further evidence highlighted that Pi3K is involved in regulating the cytoskeletal changes during PDGF-induced lamellipodium formation [531]. The Pi3K inhibitor, wortmannin, was reported to inhibit membrane ruffling via the Rac-dependent pathway. This suggests that Pi3K might be

an upstream stimulator of Rac and Rho in CXCL8-activated cells, consequently affecting the cytoskeleton and cell migration [532].

Decreased cell migration could be a consequence of disruption of the dynamic remodelling of the cytoskeleton. This is characterised by defective actin polymerization and cell polarization in relation to inhibition of specific signals necessary for the cellular responses. We presented that Pi3K or AKT inhibition in MDA-MB231 cells disrupted the morphology of the cells and this coincided with a significant reduction in the speed of migrating cells. The disruption was characterised by excessively elongated cells, and in the case of AKT inhibition, the formation of aggregates in the cell body. The Pi3K inhibitor, LY294002, also resulted in stretched front and rear ends of MDA-MB231 cells. This was possibly due to the loss of the ability of the cell to form protrusive structures necessary for crawling and adhesion. This same effect on cell migration and morphology following Pi3K/AKT inhibition was noted in chicken embryo fibroblasts. The latter study inferred that the effects of Pi3K/AKT were transmitted through p70S6L1, which requires Rac and mediates actin filaments remodelling and cell migration [533]. A similar trend was observed in PC3 cells pre-treated with Pi3K or AKT inhibitors and stimulated with CXCL8. The speed of migrating cells slowed down dramatically with the inhibitors. While the changes in cellular morphology were not statistically significant, visual observations of actin staining in AKTi-treated PC3 cells activated with CXCL8 demonstrated small accumulations inside the cells. Moreover, cells were completely immobile. LY294002-treated PC3 cells looked slightly smaller in area, but this was not significant. These contradictory outcomes regarding the effects on cellular morphology were previously reported. Indeed, AKT mediated the remodelling of actin filaments and endothelial cell migration in response to VEGF [534], but not in PDGF-induced NIH3T3 cells [535]. We suggest that MDA-MB231 cells could utilize the Pi3K/AKT-Rho GTPase pathway to induce actin reorganization, leading to cellular migration. However, Pi3K/AKT signalling was found to be crucial for PC3 cell migration, but not actin reorganisation. This proposes that a Rho-GTPase-independent pathway was involved.

Furthermore, THP-1 cells incubated with LY294002 showed a significant reduction in migration towards CXCL8 in a chemotaxis assay; which, as mentioned before, could be due to the substantial role of Pi3K in regulating the cellular polarity associated with directed cell migration [527], [528]. On the other hand, THP-1 cells did not show any dependence on Pi3K activity for intracellular calcium signalling when activated with CXCL8. This implies that cell migration can occur independently of

calcium release [387]. Nonetheless, using LY294002 in CX3CL1-induced CHO cells could abrogate intracellular calcium signalling [536] suggesting that the role of Pi3K in the induction of calcium flux is chemokine and cell line specific. Taken together, the increased migratory effect of CXCL8 activation in MDA-MB231, PC3, and THP-1 cells was abolished with Pi3K or AKT inhibitors. This loss of migration was accompanied by disruption of the actin cytoskeleton with some variabilities between the two adherent cell lines, and no effect on intracellular calcium release in THP-1 cells.

The Ras/Raf/MEK/ERK signalling cascade has an important role in tumour proliferation, survival, migration, invasion, and angiogenesis [537], [538]. ERK signalling is historically associated with cell proliferation, however, further studies have correlated its deregulation to be associated with different tumour phenotypes [304]. ERK is stimulated upon phosphorylation of MEK which itself is stimulated by Raf phosphorylation. Stimulation of the receptor tyrosine kinase triggers GTP loading of Ras GTPase, which in turn recruits Raf kinase to the plasma membrane for activation. Indeed, there is strong evidence validating the involvement of Raf and MEK in tumour growth and progression [539], [540]. We found that inhibiting Raf with ZM336372, which is a C-Raf selective inhibitor, could significantly reduce the migration speed of both MDA-MB231 and PC3 cells. This is in agreement with a study that found the same inhibitory effect in mesenchymal stromal cells [541]. Conversely, the other Raf inhibitor used, L779450, which is selective to B-Raf, did not significantly inhibit the migration of MDA-MB231 cells, while the effect on migration speed in PC3 cells was substantial. This suggested that B-Raf was not important for CXCL8-induced migration of MDA-MB231 cells, but essential for migration of PC3 cells. C-Raf was important for both. The impact of these inhibitors on the migration speed was not associated with major changes to the cellular morphology of either cell lines.

It has been suggested that MEK could be a suitable target for therapeutic intervention in cancer [323]. Our group have previously reported that MEK inhibitors: SL327 and PD98059 block the migration of CXCL12-stimulated Jurkat cells [388]. Here, we see the same effect with CXCL8-stimulated MDA-MB231 and PC3 cells. Cells migrate considerably slower in the presence of SL327 or PD98059. However, there are many contradictive studies concerning the effect of MEK inhibition on cancer proliferation and migration. For example, the MEK inhibitor, PD98059, works by preventing MEK phosphorylation by upstream activators, therefore, preventing the stimulation of ERK1/2 in the downstream signalling pathway. This inhibitor was found to supress the proliferation of MCF-7, MDA-MB231, and HCC1937 cells [542]–[544].

Nonetheless, according to Zhao *et al.* [544], PD98059 enhanced the migration of MCF-7 and MDA-MB231 cells by promoting β-catenin nuclear translocation. Other studies have also shown that PD98059 had no effect on CXCL8-activated neutrophil chemotaxis [309], [497]. While Xythalis *et al*. [324] reported the opposite, whereby PD98059 supressed CXCL8-activated neutrophil chemotaxis. Moreover, Bian *et al.* [545] found that PD98059 did not affect cytokine expression mediated by the MAPK/ERK signalling pathway. PD98059 exerted no effect on cytoskeleton rearrangement leading to cytokine production. This study added that SB203580 promoted cytoskeletal reorganisation in LPS-stimulated macrophages, leading to cell migration. Our results agreed that PD98059 did not affect cytoskeletal reorganization; however, we also see that SB203580 did not alter the cellular morphology associated with the reduced cell migration. Additionally, unlike the study reporting reduced migration with FH535 in CXCL12-induced Jurkat cells [388], here we did not see any effect of this β-catenin inhibitor on either MDA-MB231 or PC3 cell lines. Altogether, these distinctive effects are possibly due to the differences in the cell type tested and the stimulus used. Overall, we found that perturbations in the Ras/Raf/MEK/ERK and p38 MAPK pathways, but not β-catenin pathways, had a profound impact on the migration of both MDA-MB231 and PC3 cells without causing substantial changes to the cellular morphology.

Cell migration relies on actin cytoskeleton rearrangement and cellular responses that are regulated by Rho family GTPases which cause the formation of lamellipodia and actin polymerisation [546]. The abnormal activity of Rho GTPases has been associated with cancer and other human pathologies [547], [548]. Participation of Rho GTPases and their downstream effectors in chemokine-elicited motility is poorly understood. In this chapter, we examined the role of different Rho GTPases: Rac, Rho, ROCK, Cdc42, and DOCK1/2/5 in cell migration speed and cellular morphology. Rac1 inhibitor: EHT1864, ROCK inhibitor: Y27632, as well as DOCK1/2/5 inhibitor: CPYPP were important for the migration of MDA-MB231 cells. Moreover, along with EHT1864 and CPYPP, the Cdc42 inhibitor: ZCL278 reduced the migration speed of PC3 cells. Indeed, our group have already published that Rac1 is important for the migration of CXCL12-stimulated MCF-7, THP-1, and Jurkat cells, while it is not necessary for CCL3 signalling [435]. This highlights the variability of cellular responses in each cell line to different chemokines.

Inhibition of Rho, Rac, and Cdc42 was reported previously to reduce the speed of cells as well as cause abnormal cellular morphological changes; characterised by elongation, rounding, loss of lamellipodia, and appearance of thick membrane extensions [549]. PC3 cells activated with CXCL8 presented some membrane ruffling, which is a character of a migratory cell forming a network of freshly formed polymerized actin filaments. This formation of membrane ruffles has been identified to be due to the activation of Rac [550]. When PC3 cells were treated with the Rac1 inhibitor NSC23766, there was an increase in bleb-like membrane ruffles, as well as formation of microspikes. MDA-MB231 cells on the other hand, showed a different response to NSC23766. These cells displayed less membrane ruffling, along with mild extension to both ends of the cells. This could be due to the loss of formation of sheet-like lamellipodia associated with Rac function. Gao *et al*. [551] have tested the effect of NSC23766 on PDGF-stimulated Swiss 3T3 fibroblast cells and found that this inhibitor reduced lamellipodia formation and membrane ruffling. While Hernández *et al*. [552] found that there was no crucial difference to the morphology of MDA-MB435 cells treated with NSC23766, although this inhibitor did cause a significant reduction in cell migration. Moreover, the other Rac1 inhibitor used, EHT1864, appeared to be more potent [553]. This inhibitor resulted in slowing the migration of both PC3 and MDA-MB231 cells, yet no significant differences to their cellular morphology was noted. In this study, EHT1864 treatment of CXCL8-activated MDA-MB231 cells resulted in the cells displaying a tangled actin meshwork, with elongation to both endings of the cells, as visualised with phalloidin staining. EHT1864 also caused a significant reduction in the speed of cell migration, while NSC23766 did not. No considerable changes to the cell shape in either cell line was noted, although, MDA-MB231 cells displayed interesting pattern changes in cellular morphology, which should be further investigated. In summary, the Rac1 inhibitor NSC23766 did not affect the migration speed of MDA-MB231 cells, whilst EHT1864 had a significant effect in reducing the speed.

Moreover, the ROCK inhibitor Y26732 completely degraded the integrity of MDA-MB231 cells. The cells presented extensive elongation to both ends, with frequently branching cell processes, and formation of tangled networks of interlaced actin filaments, also described as “deadhesion and retraction” [554], [456]. The formation of lamellipodia at the leading edge seemed to be driving the cells forward, however, the tail would stretch with the cytoplasm without moving ahead. Hence, the migration speed of MDA-MB231 cells was significantly reduced. A study confirmed the inhibitory effect of Y27632 on cell motility and deconstruction of the actin

cytoskeleton in MDA-MB231 and MCF-7 cells [507]. This effect was suggested to be due to ROCK regulating c-Myc, a transcription factor associated with breast cancer progression and metastasis [555]. PC3 cells treated with Y27632 also demonstrated considerable changes to their shape. Avril *et al.* [556] characterised Y27632-treated PC3 cells as having long extensions with stubborn detachment at the tailing end. However, the effect on cellular morphology was not as dramatic as what we see with MDA-MB231 cells, which could explain why Y27632 did not affect the migration speed of PC3 cells. Moreover, the Rho inhibitor CCG 1423, did not affect either the cellular morphology or the migration speed of either cell lines. In fact, little is known about the potency of this inhibitor. Evelyn *et al.* [557] associated the Rho inhibitory effect of CCG 1423 with functional blocking of transcription of the serum response factor (SRF). All in all, the cellular morphology of MDA-MB231 and PC3 cells was facilitated by ROCK, but the effect of this pathway on cell migration varied between the cell types; being crucial for MDA-MB231 cells but not PC3 cells.

DOCK2 binds to Rac and mediates the GTP-GDP exchange reaction. Inhibition of DOCK2 is thought to be an attractive target for inflammatory-related pathologies [356]. CPYPP interact with the DHR-2 domain of DOCK1/2/5, to inhibit the activity of guanine nucleotide exchange, leading to Rac stimulation [558]. DOCK1/2/5 was identified as a major regulator of Rac in neutrophils, therefore, blocking it could inhibit chemotactic migration of neutrophils [355]. Results from the Mueller group showed that CPYPP blocked CXCL12-stimulated Jurkat cell migration in a chemotaxis assay, but not migration of THP-1 cells [505]. Here, we presented that DOCK1/2/5 was essential for CXCL8-driven MDA-MB231 and PC3 cell migration. Although this effect was not associated with changes to the cellular morphology. Therefore, we proposed that DOCK1/2/5 was not directly involved in the rearrangement of the actin cytoskeleton.

FAK and Src activation are recognized to play a vital role in cell migration [367], [134], [559]. Evidence came from studies that showed that CXCL8 could stimulate the migration of LNCaP cells [367] and bone marrow endothelial cells [134] through the activation of FAK and Src. Prostate cancer biopsy tissue showed the expression of CXCL8 was associated with elevated levels of FAK and Src [134]. The FAK inhibitor, PF562271, was reported to inhibit proliferation and colony formation in osteosarcoma cell lines. This was associated with a drastic reduction in osteosarcoma tumour volume, weight, and angiogenesis *in vivo* [560]. Indeed, Cohen-Hillel *et al*. [376] argued that CXCL8-induced cytoskeletal reorganisation by FAK activation and cytoskeleton contraction is necessary for the force and polarity-

dependent process of cell motility. It was not surprising that our results supported the importance of FAK and Src in cell migration. PF562271 could inhibit the migration speed of both CXCL8-activated MDA-MB231 and PC3 cells. This agreed with data showing that PF562271 could block the migration of pancreatic ductal adenocarcinoma cells, cancer-associated fibroblasts, and macrophages [559]. Moreover, using an siRNA approach, Mills *et al.* [388] showed that Src knockdown could abolish CXCL12-stimulated Jurkat and MCF-7 migration. Indeed, our findings showed that the Src inhibitor, Bosutinib, abrogated the migration of CXCL8-stimulated MDA-MB231 and PC3 cells. Therefore, both FAK and Src play an important role in MDA-MB231 and PC3 cell migration following CXCL8 activation.

Src kinase regulates several cellular processes including maintenance of the actin cytoskeleton, cell morphology, and motility through its substrate cortactin [561]. Actin cytoskeleton rearrangement downstream of Src contributes to growth factor and integrin signalling, for instance, cellular Src facilitates EGF-activated cellular motility, morphology, and stress fibre reorganisation [377]. We presented that the Src inhibitor, Bosutinib, had a significant effect on the cell morphology. CXCL8-stimulated MDA-MB231 cells seemed to have lost their structure, appearing elongated, clustered, and with disorganised stress fibres. This was accompanied by visible accumulation of crosslinked networks of lamellipodia and filopodia and the leading/tailing edges. PC3 cells were also affected by Bosutinib and almost doubled in size. The FAK inhibitor, PF562271, had no substantial effect on either of the cell morphology. All in all, since FAK and Src-kinase are activated in CXCL8-stimulated cancer cells [139], we confirmed the crucial effects of both kinases on cell motility and Src-induced cytoskeletal regulation.

Protein Kinase A (PKA) is among the most widely studied kinases because of its association with a vast array of signal-transduction pathways; regulating proliferation, differentiation, cell cycle regulation, and/or metabolism [562]. H89, is a potent PKA small molecule inhibitor that was found to have a broad effect on other protein kinases, such as S6K1, MSK1, PKA, ROCKII, PKBα, and MAPKAP-K1b, depending on the concentration used [563]. H89 was reported to block ROCK activity significantly at 10 μM [564], [565]. Its inhibitory effect on the two substrates of ROCK, MYPT1 and MLC2, was similar to the inhibitory effect induced by Y27632 [566]. In fact, PKA on its own has been reported to block the actions of ROCK. Subsequently, PKA and H89 could have the same effect on ROCK, leading to misinterpreted conclusions [567], [568]. We also found that H89 blocked the migration of PC3 cells, but not MDA-MB231 cells. Additionally, H89 had no effect on the actin cytoskeleton

in both cell lines. Taken together, PC3 cells use the PKA signalling pathway for migration, but MDA-MB231 cells do not.

The Arp2/3 complex has been studied for its role in actin filament assembly. It emerged as a key regulator for nucleating actin filament forming networks at the leading edge of migrating cells [43], [569] (**Figure 2**). A study by Lee *et al.* [523] found that inhibition of the Arp2/3 complex abrogated PKA activity and tyrosine phosphorylation, causing disturbances to actin polymerization. We inhibited the Arp2/3 complex with a small molecule inhibitor, CK666, to investigate the effects on the migratory speed and morphology of cells after 10 hrs. At 80 µM, CK666 showed cytotoxicity to the cells after a 24 hrs incubation, but as explained earlier, observing time-lapse videos of cells treated with this inhibitor over the course of 10 hrs did not indicate that cells were dying. Indeed, CK666 was used by other groups at even higher concentrations of up to 200 µM and showed no cytotoxicity. This was evident by Ilatovskaya *et al.* [570] who reported that F-actin reorganization was associated with a reduction of cell migration in M-1 mouse kidney principle cells and no loss of cell viability following treatment with 200 µM CK666. Although, this study only tested the cytotoxicity of the inhibitor over 2 hrs. Another study reported that 100 µM CK666 caused glioma cells to lose their lamellipodia and polarity, along with a reduction in their migration [526], similar to our results. The concentration used by this study showed no cytotoxicity over a period of 30 mins. We concluded that although both CXCL8-stimulated motility in MDA-MB231 and PC3 cells were drastically slower in the presence of CK666, the toxicity of this inhibitor should be further investigated.

Protein Kinase D (PKD) is characterised as being an upstream regulator of Arp2/3 and the F-actin binding protein cortactin [524]. CID755673 is a PKD inhibitor that was described to have a tumour-enhancing role in prostate cancer cells [525]. A study confirmed that since PKD could act on PKC signalling, targeted inhibition with CID755673 could specifically block cellular responses without inducing any effects on upstream broad-spectrum PKCs [405]. CID755673 was reported to have an inhibitory effect on prostate cancer invasion, proliferation, and migration [389], [405], [525]. Our data agree with these studies where the migration speed of both MDA-MB231 and PC3 cells were attenuated with CID755673 after stimulation with CXCL8. Indeed, along with inhibition of migration, cellular morphology was considerably altered in both cell lines. Therefore, we could conclude that PKD was important for maintaining the cellular integrity and morphology of MDA-MB231 and PC3 cells stimulated with CXCL8, when migrating.

The previous discussion was based on the analysis that tried to find a correlation between morphological changes and migration. While we reported that some of the inhibitors have caused a significant reduction to the migration of cells with corresponding changes to the morphology, other inhibitors only affected the migration. The time-lapse experiments were designed in a way to fit in all the 19 inhibitors plus the control samples in a 24 well plate. Therefore, cells were stimulated with the chemokine, then exposed to the inhibitors. Whilst this way was beneficial in visualizing the effect of inhibitors on chemokine-stimulated cells at the same time, the lack of data representing the effect of inhibitors on unstimulated cells is an obstacle to achieve more certain conclusions. This opens the discussion to an alternative way of interpreting the data. We suggest that any drug that significantly alters cell morphology to be excluded from the analysis. The reason is that CXCL8 did not affect cell morphology and causes migration. For example, LY294002 affects cell migration but not morphology while AKTi affects both migration and morphology. This leads the conversation into investigating the effect of the inhibitors further before drawing conclusions associated with the effect on migration. Therefore, in retrospect, a different way to analyse the data is by considering the morphology effect as an exclusion criterion when the drug has caused a drastic change to the cells.

The discussion of this chapter extensively reviews the effect of the inhibitors in different settings. Consensus was not reached with many inhibitors in terms of their association with morphology and migration, and this could potentially be due to different factors like variations in cell types. Therefore, under ideal conditions, obtaining more information on the effect of these drugs on the cells without activation with the chemokine could give us a better understanding of their behaviour and thus more certain conclusions.

4.4 Conclusion

The main conclusions drawn from this chapter are presented in **Table 6.**

Table 6. Summary of the signal transduction molecules involved in MDA-MB231 and PC3 cell migration speed and cellular morphology.

		MDA-MB231		PC3	
Target	Inhibitor	Migration	Morphology	Migration	Morphology
Pi3K	LY294002	Yes	Yes	Yes	No
AKT	AKTi	Yes	Yes	Yes	No
B-RAF	L779450	No	No	Yes	No
C-RAF	ZM336372	Yes	No	Yes	No
MEK	SL327	Yes	No	Yes	No
MEK	PD98059	Yes	No	Yes	No
p38 MAPK	SB203580	Yes	No	Yes	No
β-catenin	FH535	No	No	No	No
Rac1	NSC23766	No	No	No	No
Rac1	EHT1864	Yes	No	Yes	No
RhoA	CCG 1423	No	No	No	No
ROCK	Y26732	Yes	Yes	No	Yes
Cdc42	ZCL278	No	No	Yes	No
DOCK1/2/5	CPYPP	Yes	No	Yes	No
FAK	PF562271	Yes	No	Yes	No
Src	Bosutinib	Yes	Yes	Yes	Yes
PKA	H89	No	No	Yes	No
Arp2/3	CK666	Yes	No	Yes	No
PKD	CID755673	Yes	Yes	Yes	Yes

Chapter 5: The role of PKC in CXCL8 and CXCL10 directed prostate, breast, and leukemic cancer cell migration

5.1 Introduction

The protein kinase C (PKC) family of serine/threonine kinases share structural homology yet demonstrate significant functional diversity. Activation of PKC is one of the earliest events involved in regulating cellular responses such as survival, proliferation, differentiation, apoptosis, and migration [571]. The different PKC isoforms are ubiquitously expressed in tissues, for example, PKCα, βI/II, δ, ε and ζ are found on most major tissues, while the expression of PKCγ is limited to the central nervous system and spinal cord, PKCη is expressed on the skin, lung, spleen and brain, and PKCθ in the skeletal muscle, lung, spleen, skin and brain [572], [573]. Genetic targeting of specific PKC isoforms has pointed out the redundancy in the function of PKCs while presenting the unique isoform-specific protein, which can alter particular cellular responses [574], [575]. Indeed, PKC isoforms can exhibit similar expression patterns in different types of cancer while demonstrating varying roles depending on the context and the cancer type [576]. Studies have shown that PKC isoforms are directly associated with cancer cells migration through chemokine receptors. For instance, PKCα is crucial for CXCL12-activated MCF-7 and Jurkat cells migration [388]. PKCζ inhibition blocked the migration of PC3 cells towards CXCL12 [389]. Furthermore, the important role of PKC in migration is highlighted by their ability to regulate the actin cytoskeleton by supressing stress fibres and forming membrane ruffles as part of the cells' mechanism to move [386]. The complexities and reversals in PKC pharmacology make it challenging to determine the role of each isoform in cellular responses [577]. Therefore, further investigations into the roles of these isoforms in CXCL8 and CXCL10 migration in different cellular subsets was the main objective of this chapter.

Chapter Aim:

To determine the role of PKC in CXCL8 or CXCL10-stimulated cancer cells using small molecule inhibitors. Specifically, looking at the effect PKC has on cytoskeletal rearrangement and migration and effects on intracellular calcium release.

5.2 Results

5.2.1 CXCL8 and CXCL10-activated chemotaxis in THP-1 cells is inhibited by PKCζi

THP-1 cells were confirmed to express CXCR2 and CXCR3 but not CXCR1 (**Figure 17**, **Figure 45**). The expression of CXCR2 but not CXCR1 in THP-1 cells was already confirmed in a study by Phillips *et al.* [421]. To determine the effect of PKC in CXCL8 (5 nM) and CXCL10 (1 nM) directed THP-1 cell migration we used three inhibitors: 5 μM GF109203X (inhibits cPKC (α and β1) and nPKC (δ and ε)), 10 nM staurosporine (inhibits cPKC (α and γ) and nPKC (η)), and 10 μM PKCζi were utilised in chemotaxis assays.

Initially, there was a significant difference in the migration of the untreated basal sample and the CXCL8-activated sample with $p \leq 0.05$, and with CXCL10 activation, $p \leq 0.05$ (**Figure 100**). Upon that, cells were treated with the PKC inhibitors then activated with CXCL8 (5 nM) or CXCL10 (1 nM). Treating cells with GF109203X or staurosporine did not cause any inhibitory effect on the THP-1 cells, however, PKCζi significantly reduced chemotaxis towards CXCL8 and CXCL10. An MTS assay determined that there was no cellular toxicity with these inhibitors (**Figure 122**).

Therefore, atypical PKCζ is important for the migration of THP-1 cells towards CXCL8 or CXCL10.

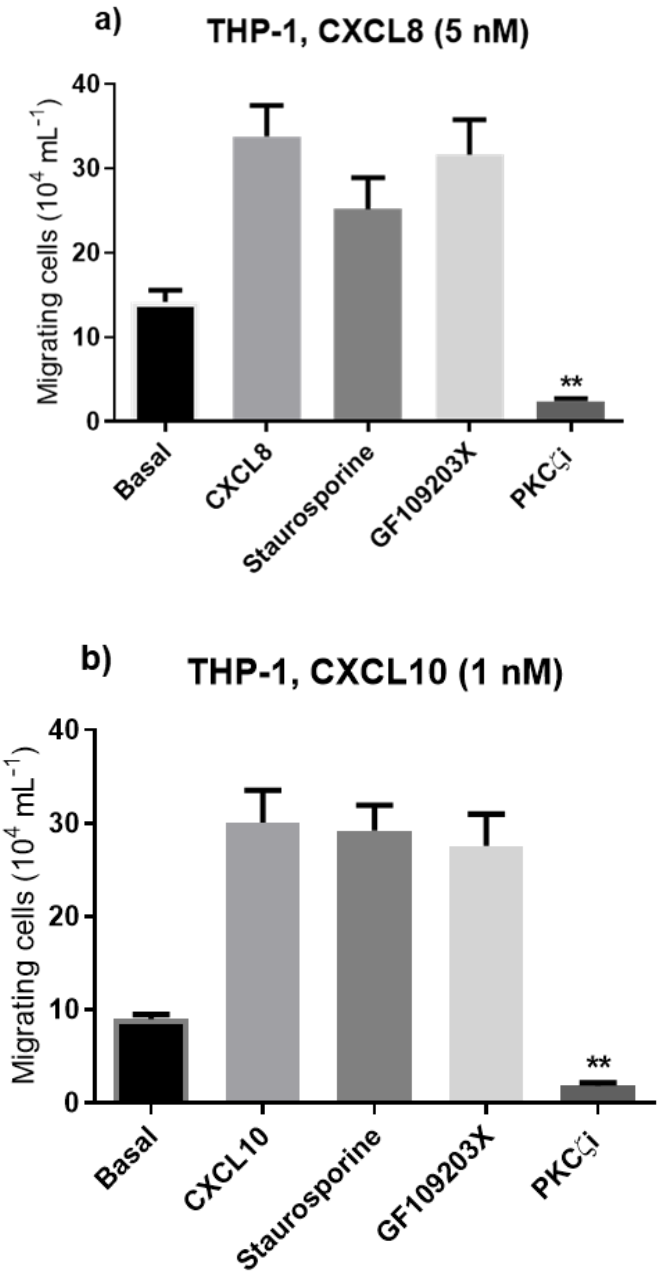

Figure 100. PKCζi blocks CXCL8 and CXCL10-stimulated THP-1 cells chemotaxis. Multiple comparison test with PKC inhibitors demonstrates that 10 µM PKCζi block the migration of THP-1 cells towards **a)** CXCL8 (5 nM), and **b)** CXCL10 (1 nM), while staurosporine (10 nM) and GF109203X (5 µM) in the presence of either chemokines do not affect the migration. The comparison of inhibitor-treated cells was made against the chemokine samples. 1% DMSO was added to basal cells as a vehicle control. Data shown are the mean ± SEM of at least three independent experiments. (One-way ANOVA with a Dunnett's multiple comparisons test as post-test, ** = $p \leq 0.01$).

5.2.2 PKC isoform activation is not important for CXCL8 induced migration in PC3 and MDA-MB231 cells

To study the importance of PKC signalling pathway on the migration speed of MDA-MB231 and PC3 cells activated by CXCL8, a time-lapse migration assay was conducted. Both cell lines express CXCR1 and CXCR2 receptors as determined previously by immunofluorescence assay (**Figure 25**, **Figure 39**).

MDA-MB231 and PC3 cells were incubated with three PKC inhibitors; 5 µM GF109203X, or 10 nM staurosporine, or 10 µM PKCζi then stimulated with 10 nM CXCL8. Ten individual cells were tracked per treatment and an average speed was calculated.

The basal speed of MDA-MB231 cells was 21.07 ± 7.1 µm/hr, whereas the addition of CXCL8 increased the speed to 42.6 ± 7.7 µm/hr ($p \leq 0.01$) (**Table 7**). There were no crucial changes to cell speeds with the treatment of staurosporine (44.0 ± 5.3 µm/hr), GF109203X (36.9 ± 4.8 µm/hr), or PKCζi (34.5 ± 7.6 µm/hr) (**Figure 101**).

Furthermore, the basal speed of PC3 cells was 23.7 ± 5.4 µm/hr, and the addition of CXCL8 increased the speed to 58.2 ± 16.8 µm/hr ($p \leq 0.001$). The treatment with staurosporine or GF109203X caused the average migratory speed to slightly drop, although not significantly, to 42.4 ± 12.1 µm/hr, and 43.4 ± 14.4 µm/hr, respectively. Finally, with the treatment with PKCζi, an average speed of 35.4 ± 10.4 µm/hr was calculated.

Therefore, out of the three inhibitors, PKCζi treatment led to a slight reduction in the migratory speeds of both CXCL8-activated MDA-MB231 and PC3 cells however, this reduction proved to not be significant. **Figure 102** and **Figure 103** demonstrate the tracks of the cells with each treatment. The images used where from the last frame (endpoint) image obtained from the time-lapse migration assay.

Table 7. The migration speed of PC3 and MDA-MB231 cells when activated with CXCL8 with or without PKC inhibitors. Data representative of the mean ± SD of four independent experiments.

	Basal (µm/hr)	**10 nM CXCL8 (µm/hr)**	**10 nM Staurosporine+ 10 nM CXCL8 (µm/hr)**	**5 µM GF109203X + 10 nM CXCL8 (µm/hr)**	**10 µM PKCζi + 10 nM CXCL8 (µm/hr)**
MDA-MB231	27.5 ± 7.1	42.6 ± 7.7	44.0 ± 5.3	36.9 ± 4.8	34.5 ± 7.6
PC3	23.7 ± 5.4	58.2 ± 16.8	42.4 ± 12.1	43.4 ± 14.4	35.4 ± 10.4

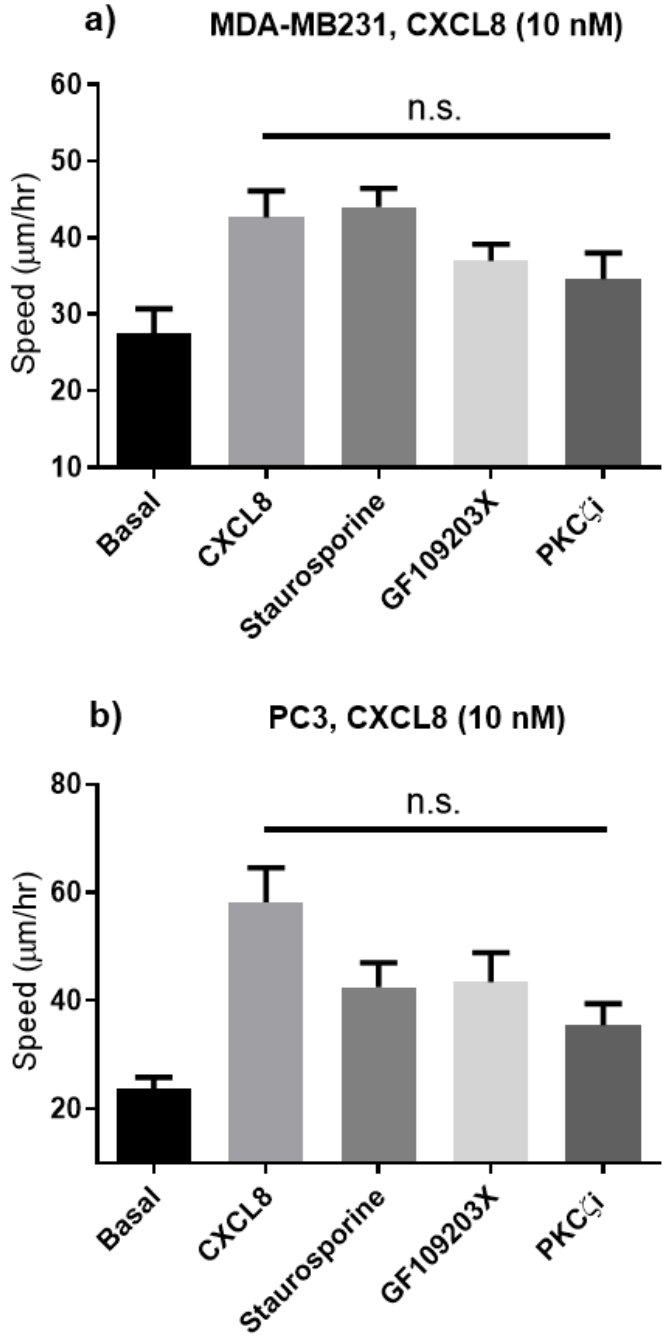

Figure 101. PKC inhibitors are not important for CXCL8-activated MDA-MB231 and PC3 cells migration. Pre-treatment with staurosporine (10 nM), GF109203X (5 µM), or PKCζi (10 µM) did not affect the migration speed within 10 hrs using a time-lapse migration assay after activation with CXCL8 (10 nM) in **a)** MDA-MB231 cells, and **b)** PC3 cells. Comparisons were made against CXCL8. 1% DMSO was added to the basal cells as a vehicle control. Data shown are the mean ± SEM of at least five independent experiments. (One-way ANOVA with a Dunnett's multiple comparisons test as post-test, n.s.= no significance, $p > 0.05$).

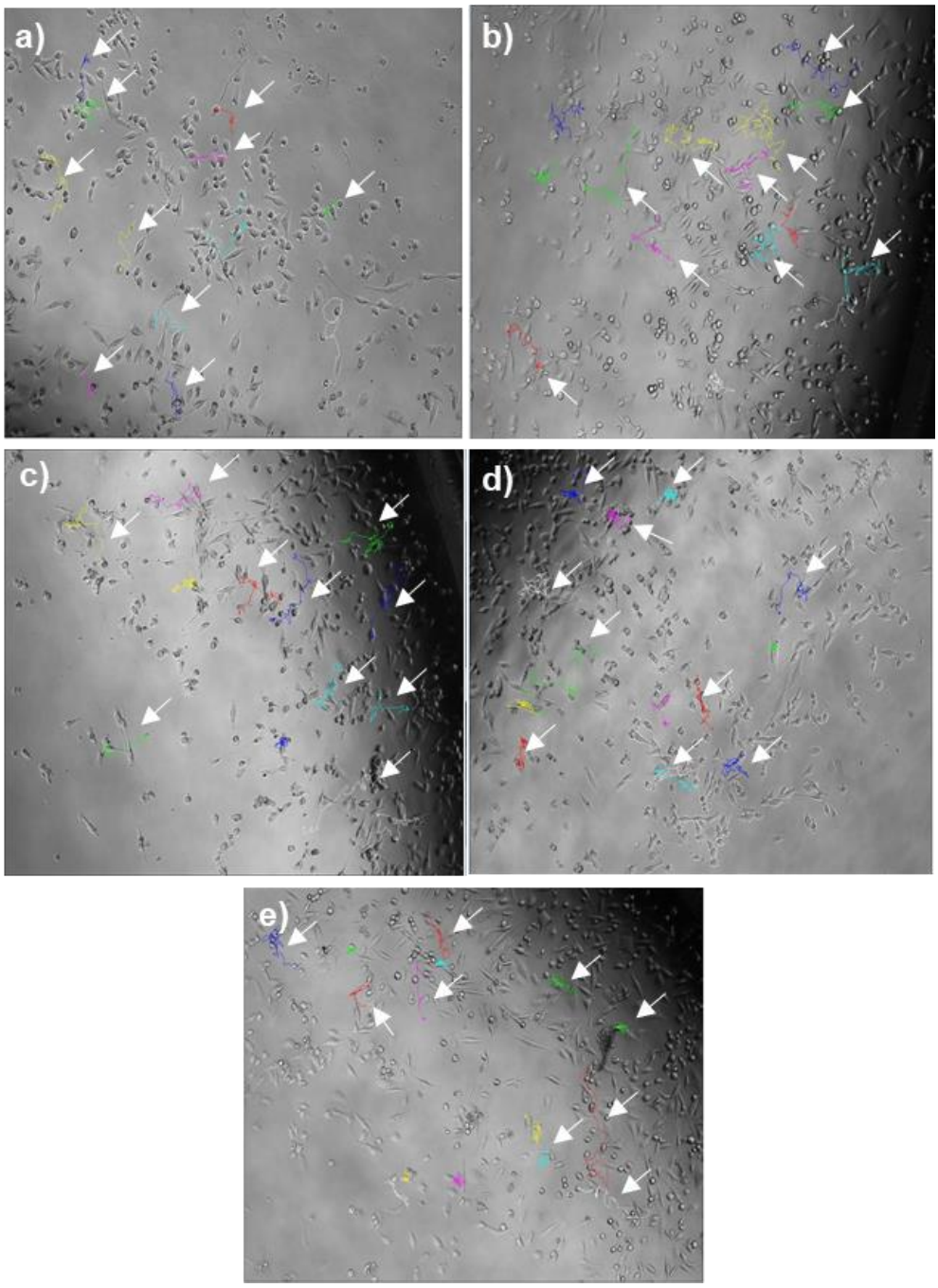

Figure 102. Endpoint images of time-lapse tracking of CXCL8-activated MDA-MB231 cells with PKC inhibitors. Manual individual cell tracking using Fiji/ImageJ of 10 cells per experiment. **a)** Basal, **b)** CXCL8 (10 nM), **c)** staurosporine (10 nM) and CXCL8 (10 nM), **d)** GF109203X (5 µM) and CXCL8 (10 nM), **e)** PKCζi (10 µM) and CXCL8 (10 nM). 1% DMSO was added to the basal cells as a vehicle control. Experiments were repeated five times. Images are representative of the cell population and were taken at 10x objective with a Zeiss Axiovert 200M microscope and processed using AxioVision Rel 4.8 software.

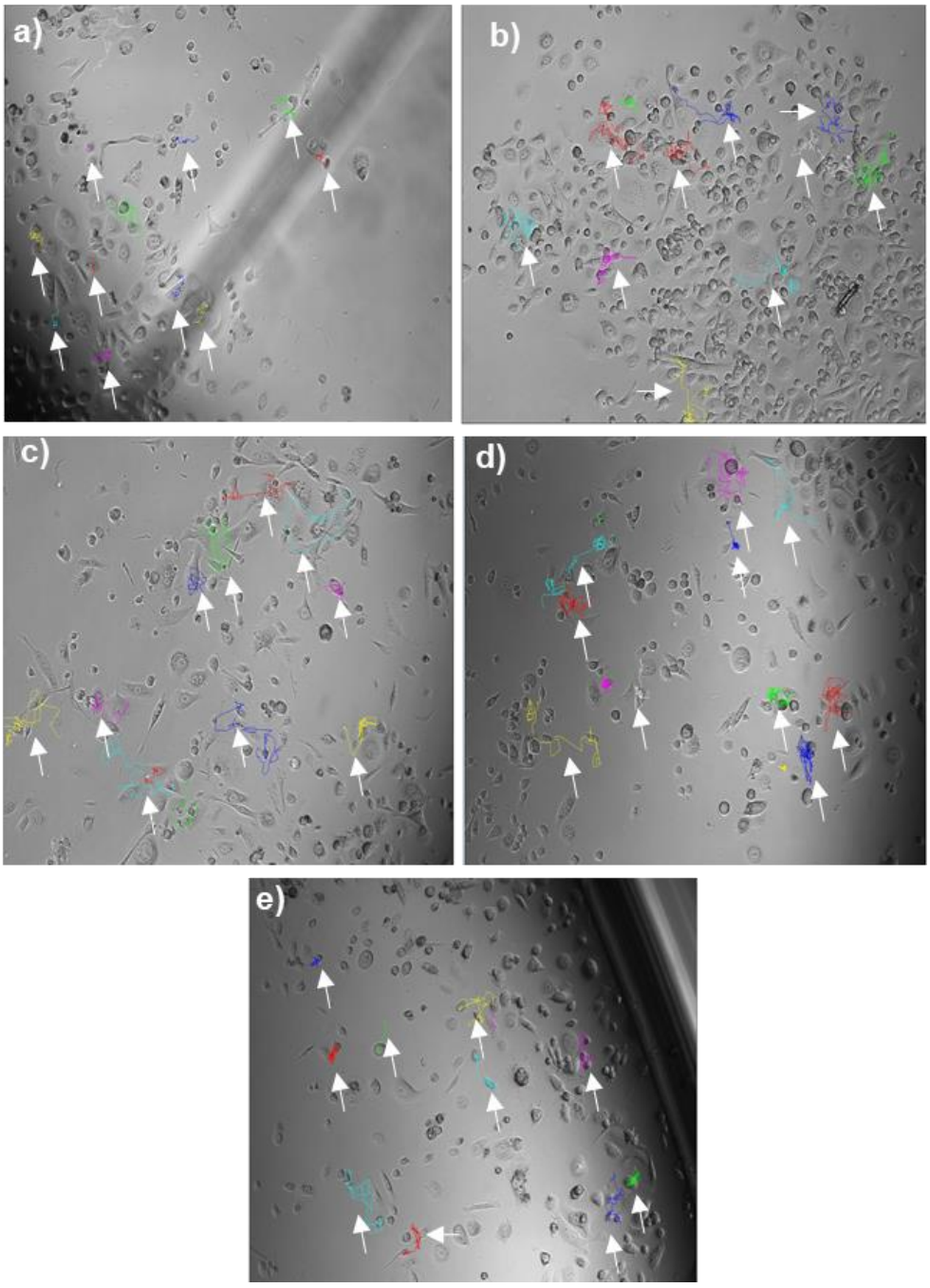

Figure 103. Endpoint images of time-lapse tracking of CXCL8-activated PC3 cells with PKC inhibitors. Manual individual cell tracking using Fiji/ImageJ of 10 cells per experiment. **a)** Basal, **b)** CXCL8 (10 nM), **c)** staurosporine (10 nM) and CXCL8 (10 nM), **d)** GF109203X (5 µM) and CXCL8 (10 nM), **e)** PKCζi (10 µM) and CXCL8 (10 nM). 1% DMSO was added to the basal cells as a vehicle control. Experiments were repeated five times. Images are representative of the cell population and were taken at 10x objective with a Zeiss Axiovert 200M microscope and processed using AxioVision Rel 4.8 software.

5.2.3 CXCL10 relies on PKC signalling for migration of PC3 and MDA-MB231 cells

Although PKC inhibitors do not significantly change the migratory speed of PC3 and MDA-MB231 cells upon activation with CXCL8, in the presence of CXCL10 (10 nM) there were significant changes. PC3 and MDA-MB231 cells both express CXCR3 receptor (**Figure 48**, **Figure 51**), which has also been confirmed by other reports [226], [578] respectively.

MDA-MB231 cells with no treatment had a speed of 18.9 ± 6.3 µm/hr, whereas the addition of CXCL10 (10 nM) increased the speed to 31.2 ± 5.2 µm/hr ($p \leq 0.05$) (**Table 8**). Cells were treated with PKC inhibitors and activated with CXCL10. PKCζi (10 µM) treatment caused a significant decrease in the migratory speed to 20.1 ± 3.2 µm/hr. GF109203X treatment caused a further reduction to 17.6 ± 2.6 µm/hr. Staurosporine, however, did not cause a difference to the migratory speed; 29.8 ± 5.6 µm/hr (**Figure 104**).

CXCL10-activated PC3 cells were also affected by the additions of the three PKC inhibitors. Basal untreated cells had a speed of 18.9 ± 2.7 µm/hr, whereas with CXCL10 (10 nM) activation, cells migrated faster at a speed of 50.4 ± 3.4 µm/hr ($p \leq 0.01$). The speed of migration was reduced significantly with the staurosporine, GF109203X and PKCζi, giving a speed of 32.3 ± 5.8 µm/hr, 26.9 ± 9 µm/hr, and 16.6 ± 3.4 µm/hr, respectively. The cells track in **Figure 105** and **Figure 106** shows the differences in the migrating distance with some treatments relative to the controls. Moreover, MTS assay showed no cytotoxicity when PC3 cells and MDA-MB231 cells were incubated with the equivalent concentrations of PKC inhibitors (**Figure 122**).

Thus, PKCs involvement in cell migration is cell-type and chemokine specific.

Table 8. The migration speed of PC3 and MDA-MB231 cells when activated with CXCL10 with and without PKC inhibitors. Data representative of the mean ± SD of four independent experiments.

	Basal (µm/hr)	**10 nM CXCL10 (µm/hr)**	**10 nM Staurosporine + 10 nM CXCL10 (µm/hr)**	**5 µM GF109203X + 10 nM CXCL10 (µm/hr)**	**10 µM PKCζ i+ 10 nM CXCL10 (µm/hr)**
MDA-MB231	18.9 ± 6.3	31.2 ± 5.2	29.8 ± 5.6	17.6 ± 2.6	20.1 ± 3.2
PC3	18.9 ± 2.7	50.4 ± 8.7	32.3 ± 5.8	26.9 ± 8.0	16.6 ± 3.4

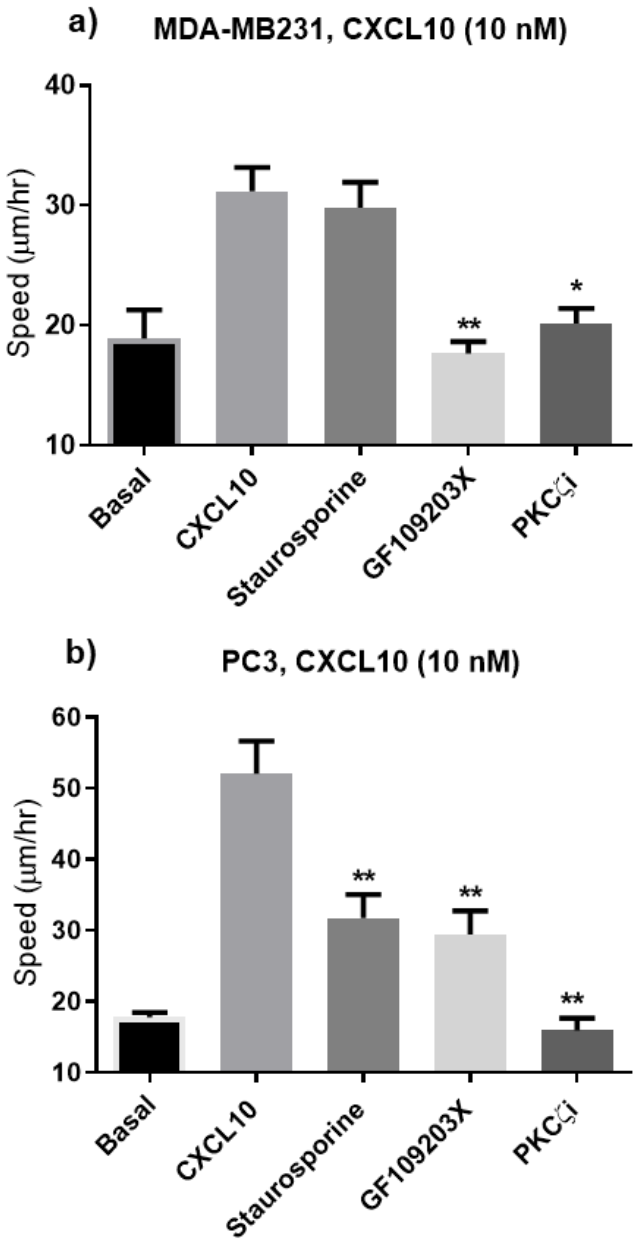

Figure 104. PKC inhibitors affect CXCL10-induced MDA-MB231 and PC3 cells migration speed. Pre-treatment with staurosporine (10 nM), GF109203X (5 µM), or PKCζi (10 µM) followed by activation with CXCL10 (10 nM) affected the migration of **a)** MDA-MB231 cells, and **b)** PC3 cells. Comparisons were made against CXCL10. 1% DMSO was added to the basal cells as a vehicle control. Data are representative of the mean ± SEM of at least four independent experiments. (One-way ANOVA with a Dunnett's multiple comparisons test as post-test, * = $p \leq 0.05$, ** = $p \leq 0.01$).

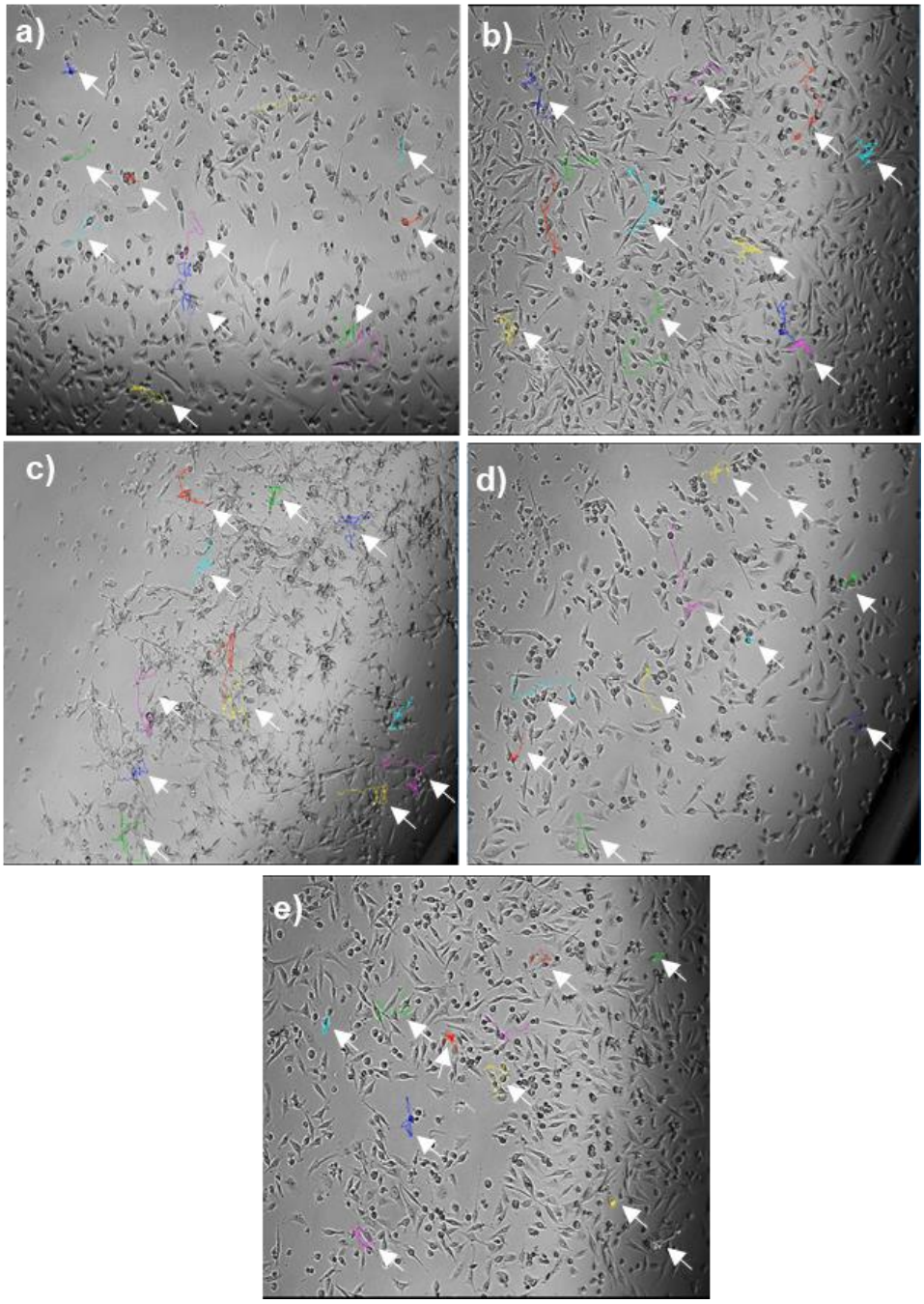

Figure 105. Endpoint images of time-lapse tracking of CXCL10-activated MDA-MB231 cells with PKC inhibitors. Manual individual cell tracking using Fiji/ImageJ of 10 cells per experiment. **a)** Basal, **b)** CXCL10 (10 nM), **c)** staurosporine (10 nM) and CXCL10 (10 nM), **d)** GF109203X (5 µM) and CXCL10 (10 nM), **e)** PKCζi (10 µM) and CXCL10 (10 nM). 1% DMSO was added to the basal cells as a vehicle control. Experiments were repeated four times. Images are representative of the cell population and were taken at 10x objective with a Zeiss Axiovert 200M microscope and processed using AxioVision Rel 4.8 software.

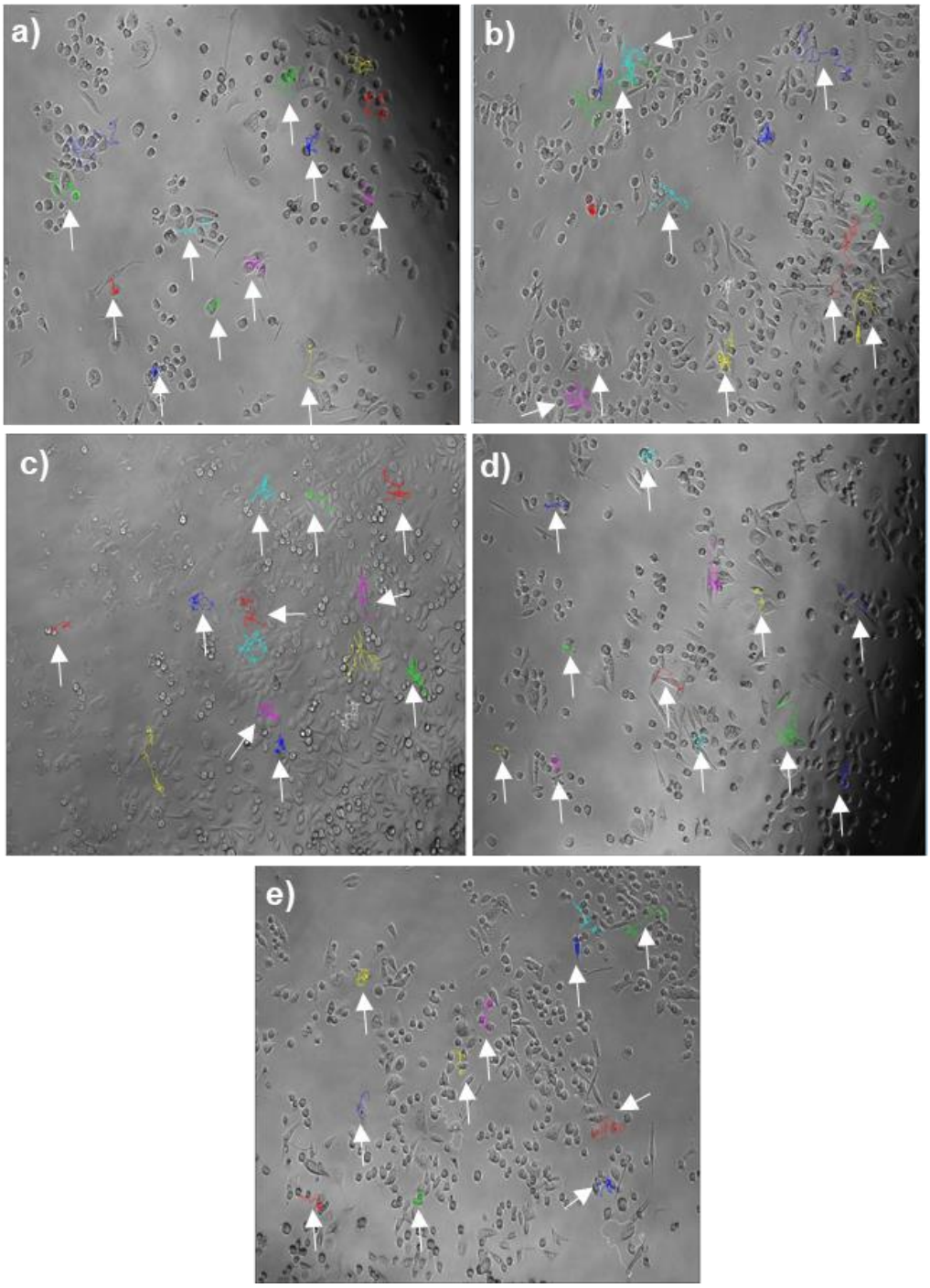

Figure 106. Endpoint images of time-lapse tracking of CXCL10-activated PC3 cells with PKC inhibitors. Manual individual cell tracking using Fiji/ImageJ of 10 cells per experiment. **a)** Basal, **b)** CXCL10 (10 nM), **c)** staurosporine (10 nM) and CXCL10 (10 nM), **d)** GF109203X (5 µM) and CXCL10 (10 nM), **e)** PKCζi (10 µM) and CXCL10 (10 nM). 1% DMSO was added to the basal cells as a vehicle control. Experiments were repeated four times. Images are representative of the cell population and were taken at 10x objective with a Zeiss Axiovert 200M microscope and processed using AxioVision Rel 4.8 software.

5.2.4 PKC inhibitors reduce the migration of CXCL10-activated PC3 cells, but not of CXCL8 activated cells

An Oris migration assay was performed to confirm the role of PKC isoforms in PC3 cells. Briefly, cells were left to adhere around a gel stopper followed by the removal of the gel stopper where the cells would respond to the stimulus by migrating towards the detection zone.

PC3 cells were treated with the three PKC inhibitors; 10 nM staurosporine, or 5 µM GF109203X, or 10 µM PKCζi then stimulated with 10 nM CXCL8 or 10 nM CXCL10. Upon staining the cells with calcein (4 µM), the fluorescence of the cells which migrated towards the detection zone was measured.

Untreated PC3 cells did not show a significant difference to cells activated with either CXCL8 or CXCL10. However, an increase is still noticed with the activation with both chemokines (**Figure 107**). We carried on treating the cells with PKC inhibitors. Upon activation with CXCL8 there was a modest reduction of migration with staurosporine, or GF109203X, or PKCζi, however, the reduction was not significant.

Furthermore, treating the cells with the same set of inhibitors but instead, activating with CXCL10 showed that both staurosporine and PKCζi reduced the migration to almost the level of the basal sample (**Figure 107b**). On the other hand, GF109203X significantly decreased the migration to even lower levels relative to the untreated basal sample.

These results agree with the previous time-lapse migration assay data showing that PKC inhibitors did not cause a substantial change to the migration speed of CXCL8-activated PC3 cells but caused a noticeable reduction in CXCL10-activated cells. This data, however, is not conclusive mainly because there was a lack of significance between the untreated and chemokine-activated samples. This lack of significance is likely related to cells behaviour observed during these experiments where PC3 cells tend to cluster around the sides of the wells instead of migrating towards the detection zone in the middle of the well, hence the large error bars present.

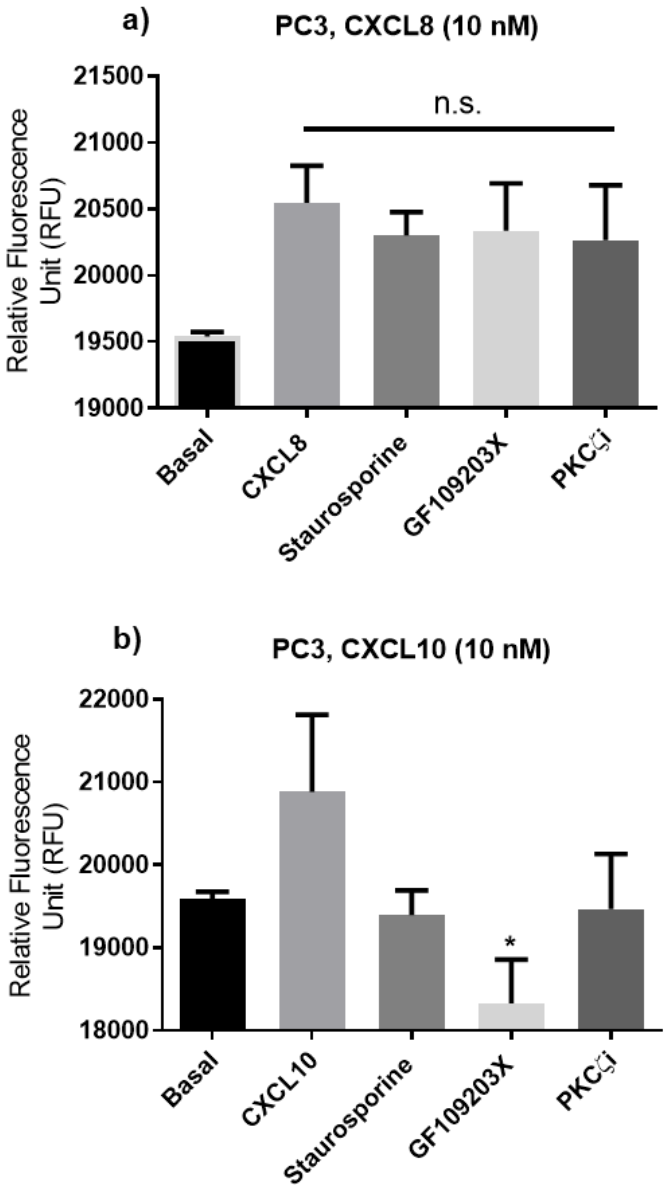

Figure 107. The effect of PKC inhibitors on PC3 cells migration with CXCL8 or CXCL10 using an Oris migration assay. Pre-treatment of PC3 cells with staurosporine (10 nM), GF109203X (5 μM), or PKCζi (10 μM) then stimulated with **a)** CXCL8 (10 nM), or **b)** CXCL10 (10 nM). The comparisons of the inhibitor-treated cells were made against the chemokine samples. 1% DMSO was added to the basal cells as a vehicle control. Data representative of the mean ± SEM of at least three independent experiments. (One-way ANOVA with a Dunnett's multiple comparisons test as post-test, n.s.=no significance $p > 0.05$, *= $p \leq 0.05$).

5.2.5 The PKC inhibitor staurosporine influences the cellular morphology of PC3 and MDA-MB231 cells

To determine the change of cellular morphology after 10 hrs incubation with PKC inhibitors with or without CXCL8 (10 nM) or CXCL10 (10 nM), manual drawing around the cells was conducted and analysed. The characterisation of the cellular morphology changes was resembled by the alternation to the cell area, the circularity, and aspect ratio.

The results below are laid out to show the changes in cell shape, followed by the analysis plotted in a graph. The images were obtained from the previous time-lapse migration assay where the last frame indicating the end point of 10 hrs images was obtained and analysed. MDA-MB231 cells were treated with the three PKC inhibitors; 10 nM staurosporine, or 5 µM GF109203X, or 10 µM PKCζi then stimulated with 10 nM CXCL8. Visual observation of the cells with different treatments showed that staurosporine-treated cells demonstrated the most distinct shape change relative to the control and inhibitor samples (**Figure 108**). Cells were extensively elongated and thinned out. Some cells stretched out with GF109203X and PKCζi but not as dramatic. Notably, in the CXCL8-activated cells sample, there were slightly more elongated cells compared to the inactivated basal cells. The analysis in **Figure 109** confirm that staurosporine out of the other inhibitors or control samples was the one to induce a significant decrease in the circularity (where the y-axis reflects that moving closer to 0 generates a prolonged shape while 1 denotes full circle). There was also an increase in the aspect ratio (indication of the ratio of long axis (width) to the short axis (length)). There were not any remarkable changes with the other treatments.

Furthermore, PC3 cells were treated in the same conditions and same set of inhibitors. Again, staurosporine has generated a notable effect on the cells. This effect was characterized by cells looking almost 1.5 times bigger than the other treatment (**Figure 110**). The data analysis showed that staurosporine affected the area, circularity, and aspect ratio significantly, whereas GF109203X and PKCζi did not (**Figure 111**).

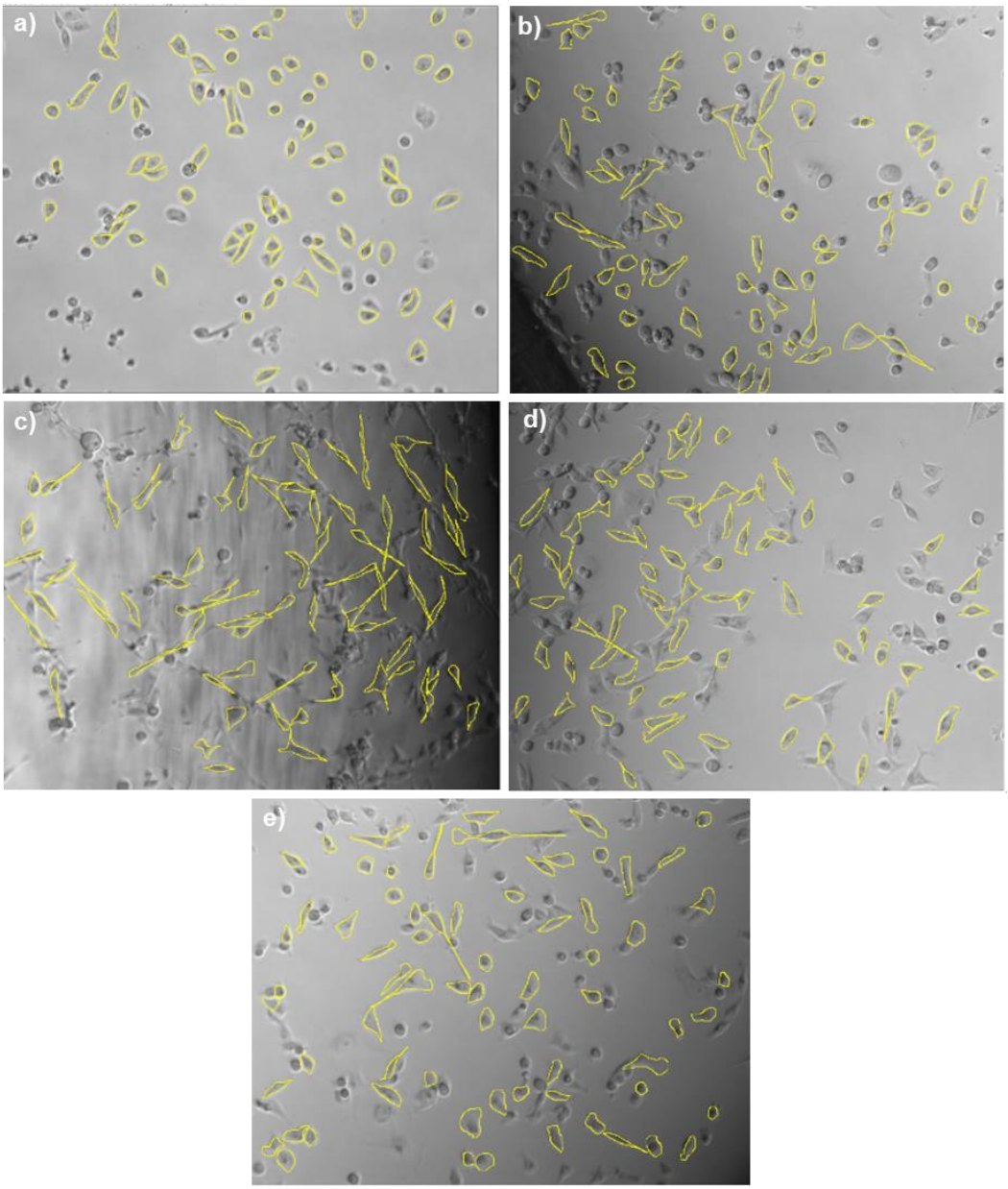

Figure 108. Illustrative images demonstrating morphological changes of CXCL8-activated MDA-MB231 cells with or without PKC inhibitors. a) Basal, **b)** CXCL8 (10 nM), **c)** staurosporine (10 nM) and CXCL8 (10 nM), **d)** GF109203X (5 μM) and CXCL8 (10 nM), **e)** PKCζi (10 μM) and CXCL8 (10 nM). 1% DMSO was added to the basal cells as a vehicle control. Cells were outlined using Fiji/ImageJ and measurements of 70 cells per image per experiment were analysed and repeated three independent times. Images are representative of the cell population and were taken at 10x objective with a Zeiss Axiovert 200M microscope and processed using AxioVision Rel 4.8 software.

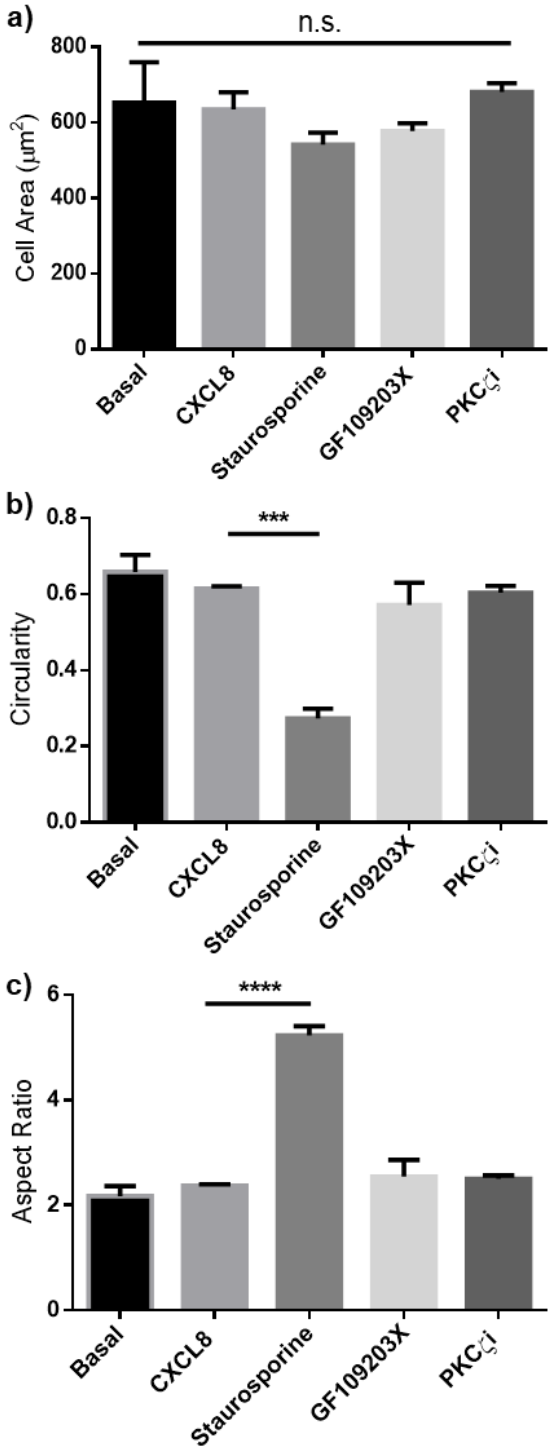

Figure 109. Cellular morphology analysis of MDA-MB231 cells treated with CXCL8 in the presence or absence of PKC inhibitors. Upon cells activation with CXCL8 (10 nM), pre-treatment with staurosporine (10 nM) yielded a significant effect on cells circularity and aspect ratio, whereas the treatment with GF109203X (5 μM), or PKCζi (10 μM) did not have any crucial effects. The comparisons were made against the CXCL8 sample. 1% DMSO was added to the basal cells as a vehicle control. Cells were outlined and measurements of **a)** area, **b)** circularity, and **c)** aspect ratio were an analysed for an average of 70 cells per image per experiment and repeated three independent times. (One-way ANOVA with a Dunnett's multiple comparisons test as post-test, n.s.= no significance, *** = $p \leq 0.001$, **** = $p \leq 0.0001$).

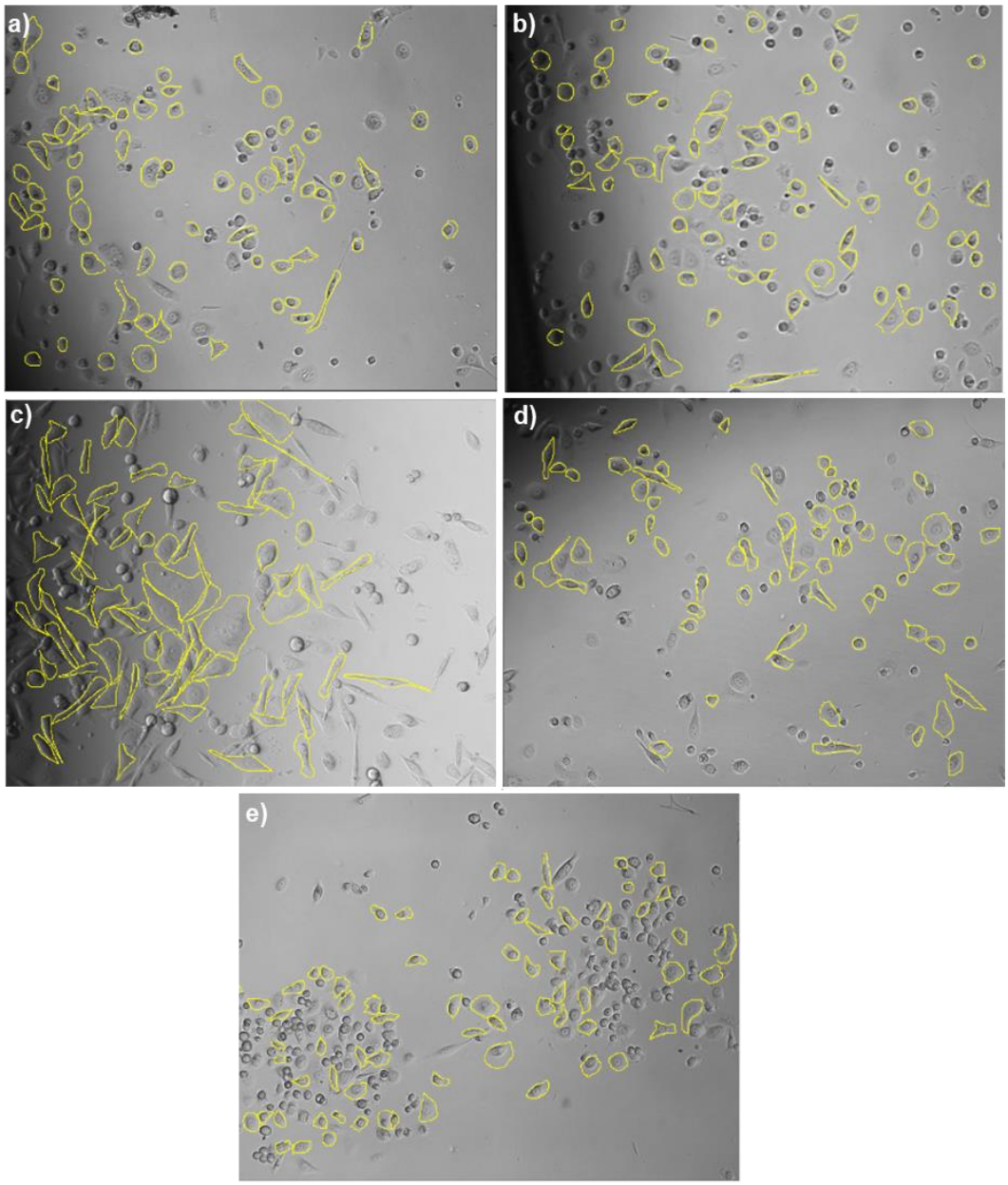

Figure 110. Illustrative images demonstrating morphological changes of CXCL8-activated PC3 cells with or without PKC inhibitors. a) Basal, **b)** CXCL8 (10 nM), **c)** staurosporine (10 nM) and CXCL8 (10 nM), **d)** GF109203X (5 µM) and CXCL8 (10 nM), **e)** PKCζi (10 µM) and CXCL8 (10 nM). 1% DMSO was added to the basal cells as a vehicle control. Cells were outlined using Fiji/ImageJ and measurements of 70 cells per image per experiment were analysed and repeated three independent times. Images are representative of the cell population and were taken at 10x objective with a Zeiss Axiovert 200M microscope and processed using AxioVision Rel 4.8 software.

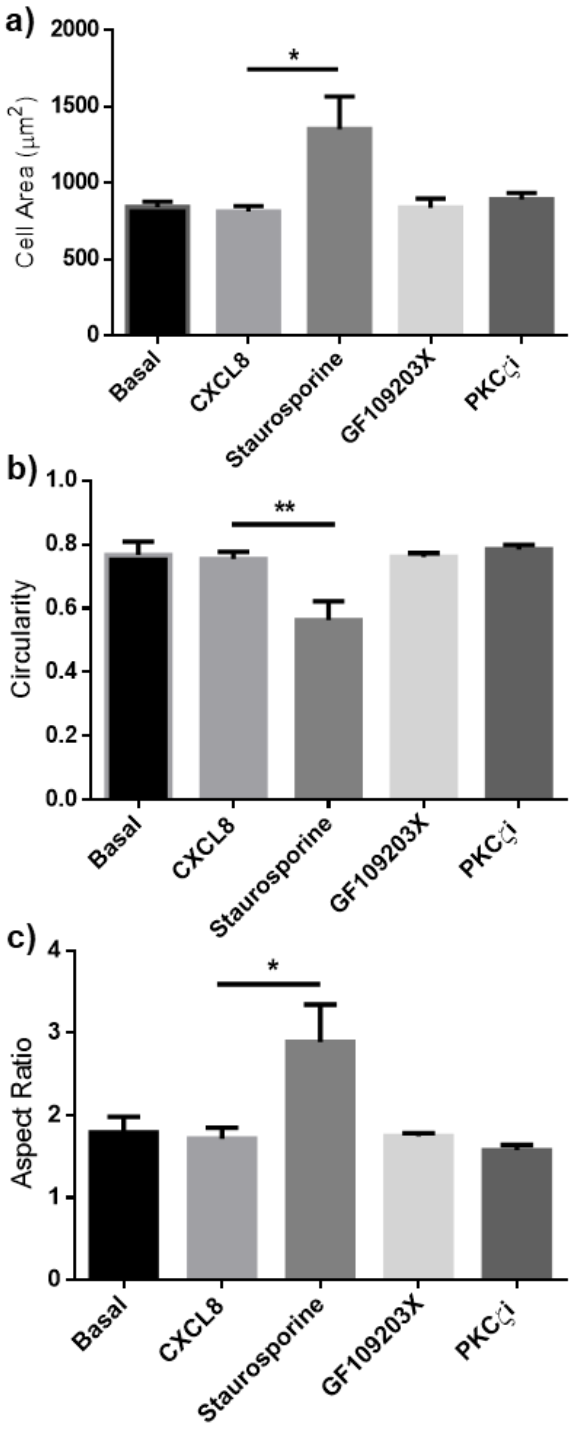

Figure 111. Cellular morphology analysis of PC3 cells treated with CXCL8 in the presence or absence of PKC inhibitors. Upon cells activation with CXCL8 (10 nM), pre-treatment with staurosporine (10 nM) yielded a significant effect on cells area, circularity, and aspect ratio, whereas the treatment with GF109203X (5 µM), or PKCζi (10 µM) did not have any crucial effects. 1% DMSO was added to the basal cells as a vehicle control. Cells were outlined and measurements of **a)** area, **b)** circularity, and **c)** aspect ratio were analysed for an average of 70 cells per image per experiment and repeated three independent times. Comparisons were made against CXCL8. (One-way ANOVA with a Dunnett's multiple comparisons test as post-test, * = $p \leq 0.05$, ** = $p \leq 0.01$).

The cellular morphology changes upon treating MDA-MB231 with PKC inhibitors followed by activation with CXCL10 (10 nM) is reported. Visual assessment of the cells shows again that 10 nM staurosporine treatment allowed the cells to assume a long shape, although the size of the cells did not seem to be different. GF109203X (5 μM) and PKCζi (10 μM) looked relatively similar to the control samples (**Figure 112)**. Statistical analysis was generated by zooming into the images to ease the process of manually drawing around the cells considering the small size of the cells. These analyses verify the significant effect generated on the cellular circularity and aspect ratio with staurosporine treatment with no notable effect by the other two inhibitors (**Figure 113**).

Moreover, treatment of PC3 cells with the previous PKC inhibitors followed by the activation with CXCL10 (10 nM) revealed slightly different outcomes. Here, GF109203X (5 μM) and staurosporine (10 μM) images show that cells look slightly smaller in size, and more circular (**Figure 114**). Data analysis reveal that the aspect ratio is significantly different with both GF109203X and staurosporine treatment, with no effect generated by PKCζi (10 μM) (**Figure 115**).

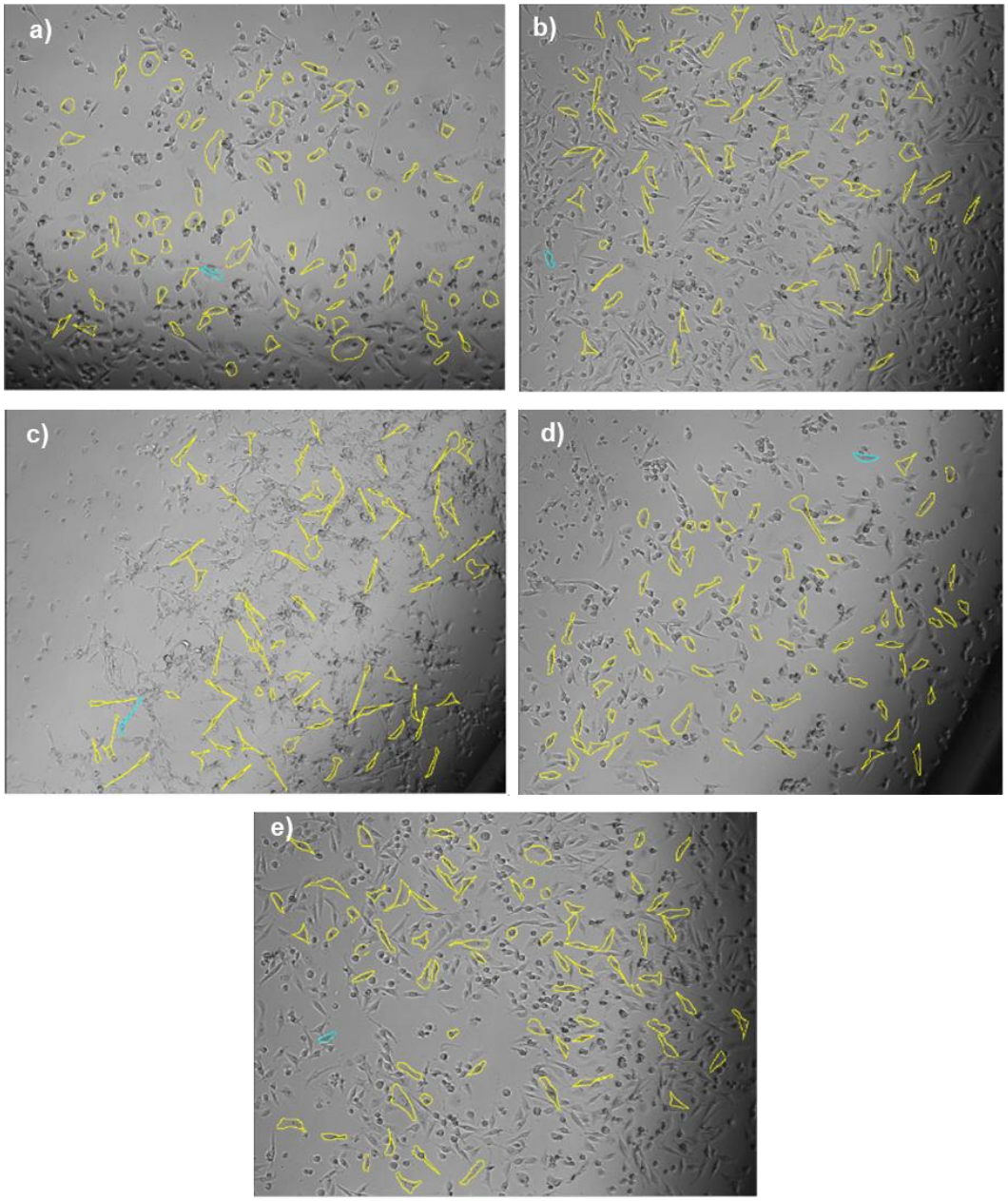

Figure 112. Illustrative images demonstrating morphological changes of CXCL10-activated MDA-MB231 cells with or without PKC inhibitors. a) Basal, **b)** CXCL10 (10 nM), **c)** staurosporine (10 nM) and CXCL10 (10 nM), **d)** GF109203X (5 µM) and CXCL10 (10 nM), **e)** PKCζi (10 µM) and CXCL10 (10 nM). 1% DMSO was added to the basal cells as a vehicle control. Cells were outlined using Fiji/ImageJ and measurements of 70 cells per image per experiment were analysed and repeated three independent times. Images are representative of the cell population and were taken at 10x objective with a Zeiss Axiovert 200M microscope and processed using AxioVision Rel 4.8 software.

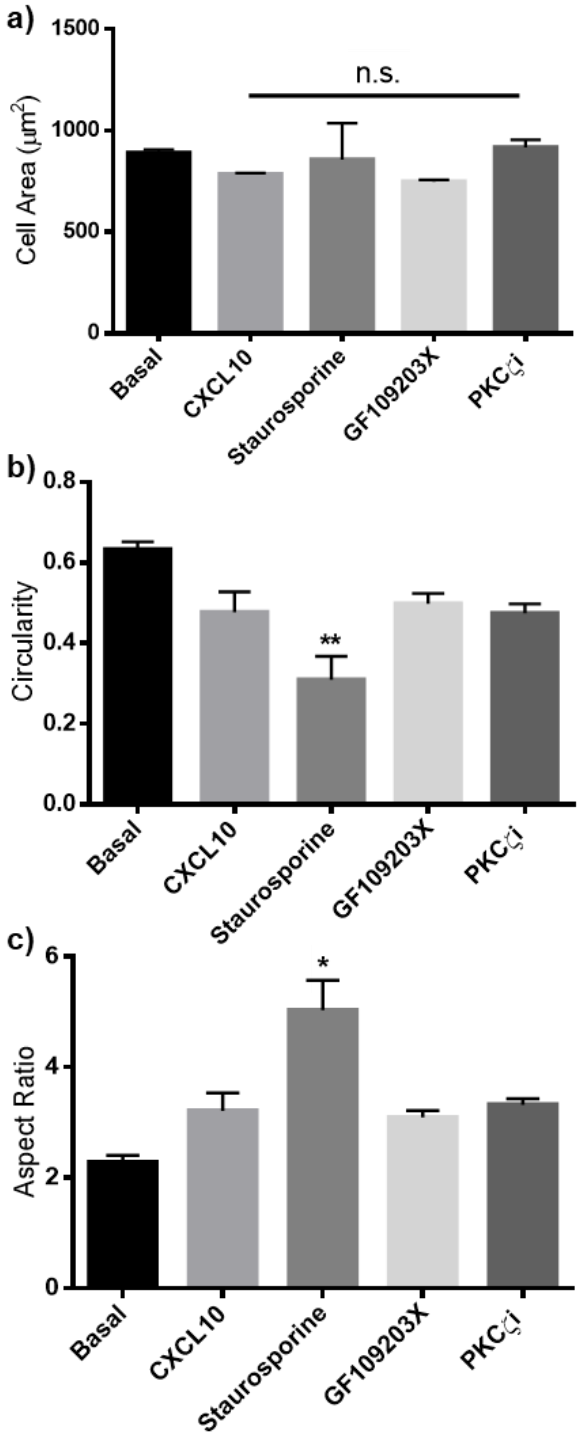

Figure 113. Cellular morphology analysis of MDA-MB231 cells treated with CXCL10 in the presence or absence of PKC inhibitors. Upon cells activation with CXCL10 (10 nM), pre-treatment with staurosporine (10 nM) yielded a significant change of the cells' circularity and aspect ratio, whereas the treatment with GF109203X (5 µM), or PKCζi (10 µM) did not have any crucial effects. 1% DMSO was added to the basal cells as a vehicle control. Cells were outlined and measurements of **a)** area, **b)** circularity, and **c)** aspect ratio were analysed of an average of 70 cells per image per experiment and repeated three independent times. Comparisons were made against CXCL10. (One-way ANOVA with a Dunnett's multiple comparisons test as post-test, * = $p \leq 0.05$, ** = $p \leq 0.01$).

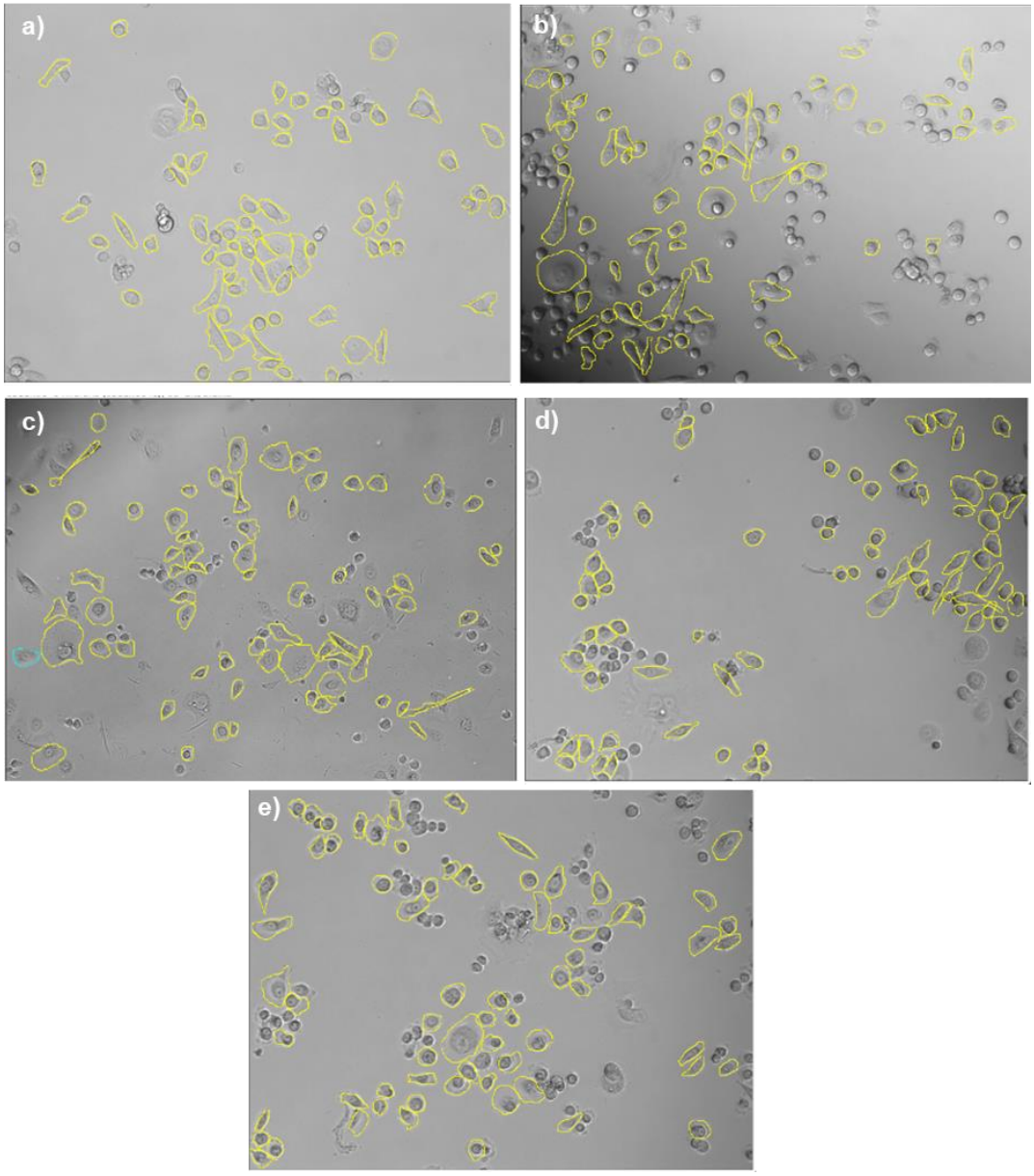

Figure 114. Illustrative images demonstrating morphological changes of CXCL10-activated PC3 cells in the presence or absence of PKC inhibitors. a) Basal, **b)** CXCL10 (10 nM), **c)** staurosporine (10 nM) and CXCL10 (10 nM), **d)** GF109203X (5 µM) and CXCL10 (10 nM), **e)** PKCζi (10 µM) and CXCL10 (10 nM). Cells were outlined using Fiji/ImageJ. 1% DMSO was added to the basal cells as a vehicle control. Cells were outlined using Fiji/ImageJ and measurements of 70 cells per image per experiment were analysed and repeated three independent times. Images are representative of the cell population and were taken at 10x objective with a Zeiss Axiovert 200M microscope and processed using AxioVision Rel 4.8 software.

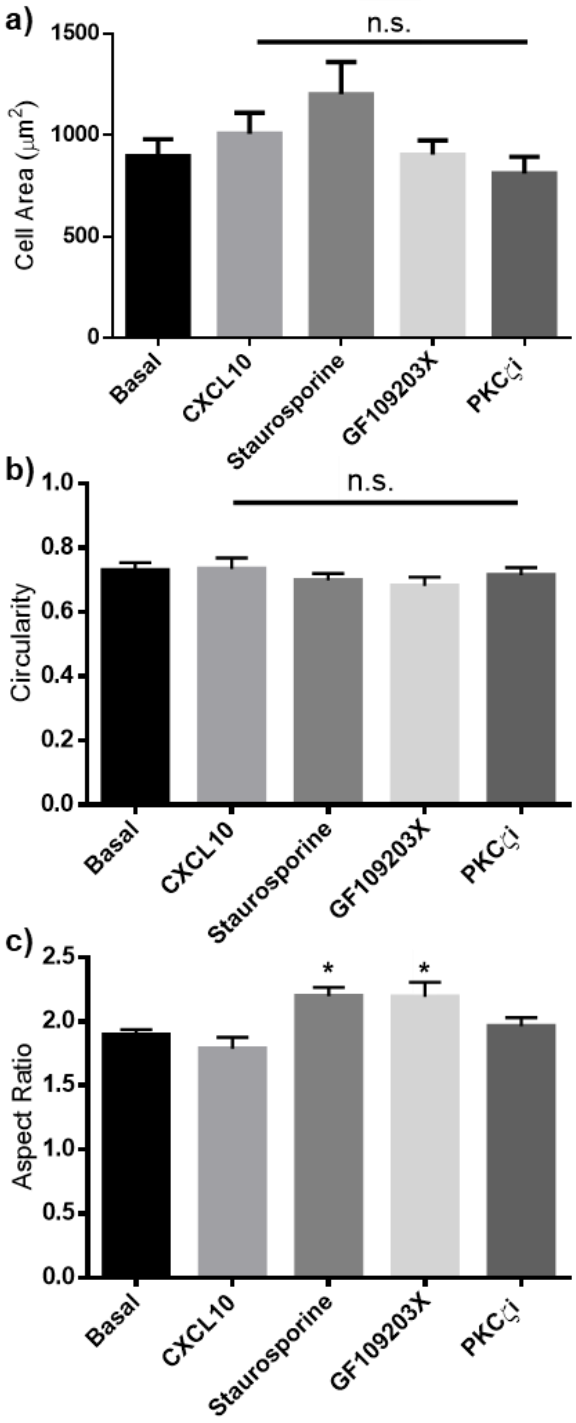

Figure 115. Cellular morphology analysis of PC3 cells treated with CXCL10 in the presence or absence of PKC inhibitors. Upon cells activation with CXCL10 (10 nM), pre-treatment with staurosporine (10 nM) and GF109203X (5 μM) yielded a significant effect on cells aspect ratio, whereas the treatment PKCζi (10 μM) did not have any crucial effects. 1% DMSO was added to the cells as a vehicle control. Cells were outlined and measurements of **a)** area, **b)** circularity, and **c)** aspect ratio were analysed of an average of 70 cells per image per experiment and were repeated at least three times. Comparisons were made against CXCL10. (One-way ANOVA with a Dunnett's multiple comparisons test as post-test, n.s.= no significance $p > 0.05$, * = $p \leq 0.05$).

5.2.6 Staurosporine effects actin rearrangement of PC3 and MDA-MB231 cells

PKCs reside in the cytosol in an inactive state. When activated they relocate to the plasma membrane or to subcellular sites (e.g. Golgi apparatus, or ER) to engage in various cellular functions, such as the rearrangement of the cytoskeleton and migration [571], [386]. Cancer cell migration is crucially dependent on the changes of the cell's morphology endorsed by dynamic modifications of actin polymerization causing rearrangement of the cytoskeleton [579].

Due to the low objective (10x) used in the previous experiment as well as limitations hindering our ability to decide the sort of changes happening inside the cells, we went on to stain the actin and visually assess the changes happening with a higher objective (63x). Phalloidin-iFlour 488 is a series of phalloidin conjugates that bind to actin filaments, also known as F-actin. Fixed monolayer of cells stained with phalloidin conjugates were visible with fluorescence microscopy at an excitation/emission= 493/517 nm.

Results showed that cells treated with the three PKC inhibitors; 10 nM staurosporine, or 5 μM GF109203X, or 10 μM PKCζi without the stimulation with the chemokine did not have a substantial effect on the actin cytoskeleton rearrangement in both PC3 and MDA-MB231 cells (**Figure 116**). Even though staurosporine shows inhibitory activity against a wide spectrum of kinases, including PKC, no elongation to the cells was observed in the absence of the stimulus.

Activation of cells with CXCL8 (10 nM) with and without PKC inhibitors, and its effect on inducing changes in the patterns of actin filaments rearrangement is reported. Comparison between the basal and CXCL8-activated cells did not show any substantial changes to the actin filaments. Pre-treatment of cells with GF109203X and PKCζi followed by stimulation with CXCL8 also did not show great changes to the rearrangement of the actin cytoskeleton. However, staurosporine treatment with CXCL8 activation immensely disrupted the cell structure. The disruption is characterised by thin elongated microfilament bundles along with a tangled network of cells overlapping with sticky endings of accumulating crosslinked actin filaments.

Moreover, when MDA-MB231 cells were activated with CXCL10 (10 nM), nothing major to the morphology of the cells was noted. However, in the presence of CXCL10, staurosporine-treated cells formed visible actin stress fibres with peripheral microspikes or filopodia pointed with the red arrows (**Figure 116**). GF109203X-treated cells appeared somehow more elongated too, while with PKCζi-treated did not look any different.

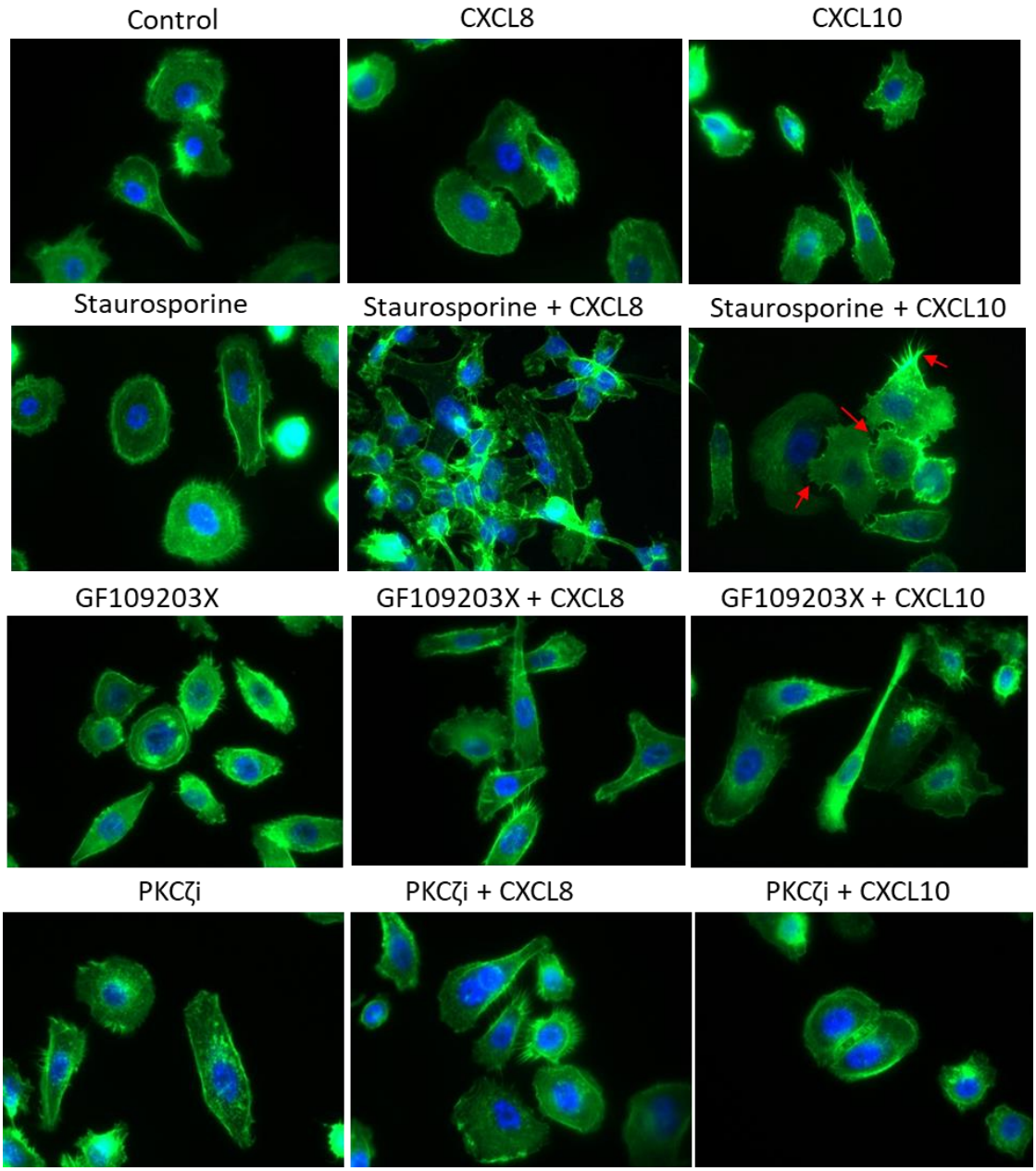

Figure 116. Fluorescence microscopy of actin polymerization in MDA-MB231 cells. Cells treated with CXCL8 (10 nM) or CXCL10 (10 nM) with or without PKC inhibitors-staurosporine (10 nM), GF109203X (5 μM), PKCζi (10 μM). Rapid elongation of cells forming sticky ending in a form of network appeared in CXCL8 and staurosporine treated cells. CXCL10 and staurosporine addition formed visible microspikes of filopodia, indicated by the red arrows. Cells were fixed and stained with Alexa-488 Phalloidin actin stain (green), and nucleus stain with DAPI (blue). Images are representative of the cell population of one experiment out of three independent repeats, acquired at 63x objective using a Leica DMII fluorescence microscope and Leica imaging suite.

In PC3 cells, the control and CXCL8 (10 nM) activated cells appeared to be similar in the cell morphology (**Figure 117**). Like before, cells were treated with PKC inhibitors and stimulated with CXCL8. Cells treated with staurosporine (10 nM) appeared to have accumulated protrusive endings forming sticky clusters at their leading edges, along with extensive stretching to the cell bodies with actin clumps spread throughout the cell margins. With GF109203X (5 µM) treatment, presence of dotty build-ups inside the cells was noticed. Moreover, in both GF109203X and PKCζi (10 µM) treatment, cells appeared to have developed more membrane ruffles.

Furthermore, comparing the control sample with CXCL10-stimulated cells showed that the latter exhibited modest appearance of membrane ruffles (**Figure 117**). These membrane ruffles are characterized by the formation of actin rich membrane protrusions [580]. Staurosporine treatment showed a remarkable amount of actin-enriched branched lamellipodia and membrane ruffles and again cells were elongated and interlaced over each other. Finally, GF109203X and PKCζi did not induce notable changes to the actin cytoskeleton.

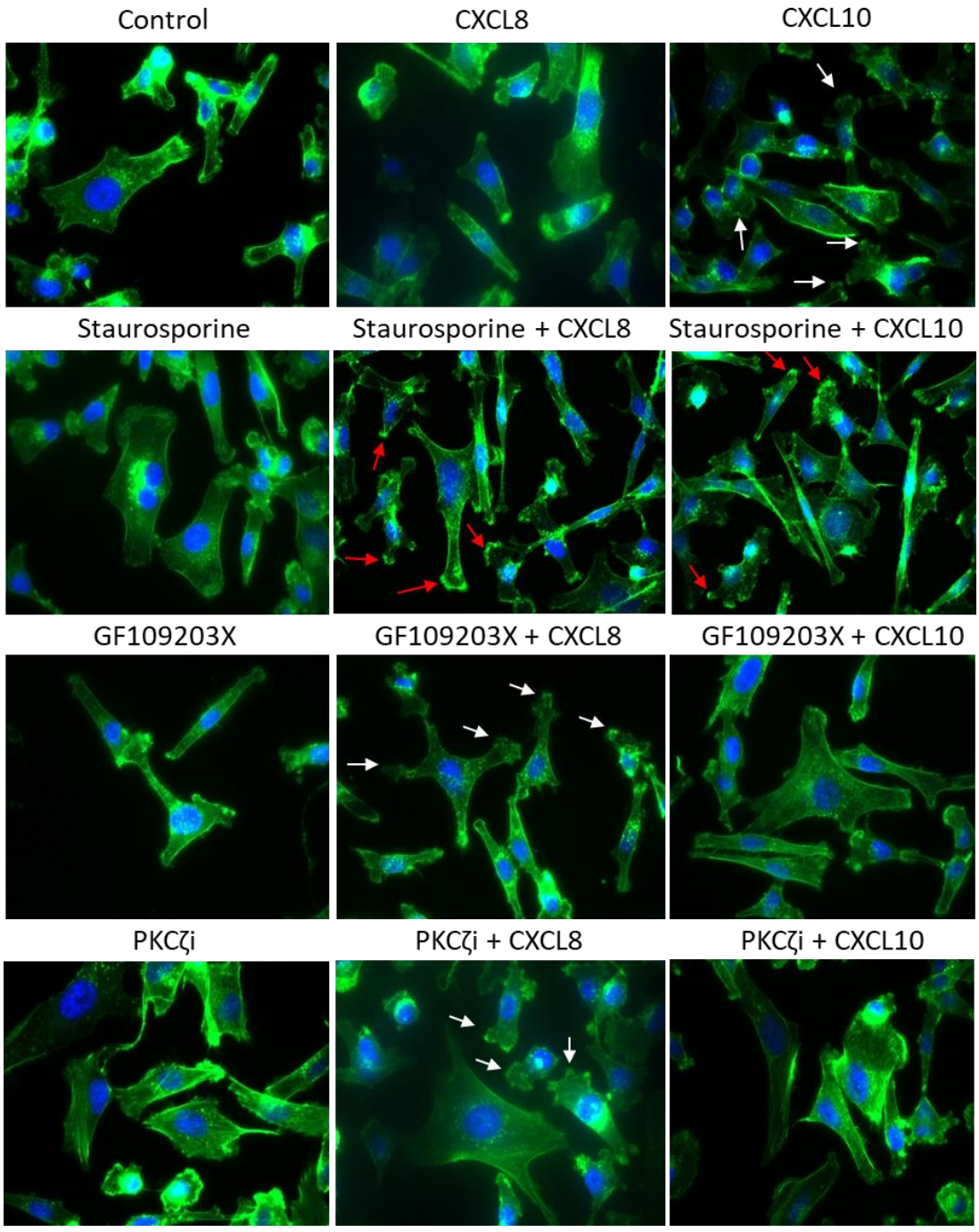

Figure 117. Fluorescence microscopy of actin polymerization in PC3 cells. Cells treated with CXCL8 (10 nM) or CXCL10 (10 nM) with or without PKC inhibitors-staurosporine (10 nM), GF109203X (5 μM), PKCζi (10 μM). Actin-enriched lamellipodia and membrane ruffles appeared at the endings of staurosporine treated cells in the presence of CXCL8 or CXCL10, pointed out with the red arrows. Cells were fixed and stained with Alexa-488 Phalloidin actin stain (green), and nucleus stain with DAPI (blue). Images representative of the cell population of one experiment out of three independent repeats, acquired at 63x objective using a Leica DMII fluorescence microscope and Leica imaging suite.

5.2.7 PKC inhibitors affect the release of intracellular calcium in THP-1, MDA-MB231, PC3 and MCF-7 cells

We have seen in chapter 3 that the stimulation of CXCR1-CXCR2 or CXCR3 induces a rapid rise in the intracellular calcium. PKCs inhibitors were used to elucidate the importance of PKC in the release of intracellular calcium upon activation with CXCL8 or CXCL10. Cells incubated with PKC inhibitors for 30 mins and activated with 200 nM CXCL8 or 100 nM CXCL10 gave varying intracellular calcium release responses.

MDA-MB231 cells activated with 200 nM CXCL8 showed no effect on intracellular calcium release with staurosporine (10 nM) or PKCζi (10 μM) pre-treatment, but a slight reduction appeared with GF109203X (5 μM). Moreover, cells incubated with staurosporine (10 nM) or GF109203X (5 μM) followed by activation with 100 nM CXCL10 slightly reduced the release of calcium but not PKCζi (10 μM) (**Figure 118**).

THP-1 cells treated with 10 nM staurosporine or 5 μM GF109203X significantly reduced the release of calcium upon activation with 200 nM CXCL8. There was also a similar trend with 100 nM CXCL10-activated cells, although not significant. PKCζi treatment reduced calcium release slightly but not as much as the two other inhibitors with both chemokines (**Figure 119**).

MCF-7 cells treatment with 5 μM GF109203X and activation with CXCL8 caused a significant reduction to the release of calcium. However, 10 nM staurosporine and PKCζi (10 μM) with CXCL8 (200 nM) or CXCL10 (100 nM) activation did not cause substantial changes to calcium release (**Figure 120**).

PC3 cells were treated with 10 nm staurosporine, 5 μM GF109203X and 10 μm PKCζi followed by activation with 200 nM CXCL8. From these experiments it was observed that there was significantly reduced intracellular calcium release when cells were incubated with staurosporine or GF109203X but no significance with PKCζi (**Figure 121**). Studies have noted that CXCL10 binding to its receptor CXCR3B is not associated with calcium flux, however, binding to CXCR3A was found to induce calcium mobilization [205], [230], [581]. In PC3 cells, the level of expression of either CXCR3A or CXCRB is not well determined. Therefore, we could not conclude the final outcome of calcium release upon induction with CXCL10.

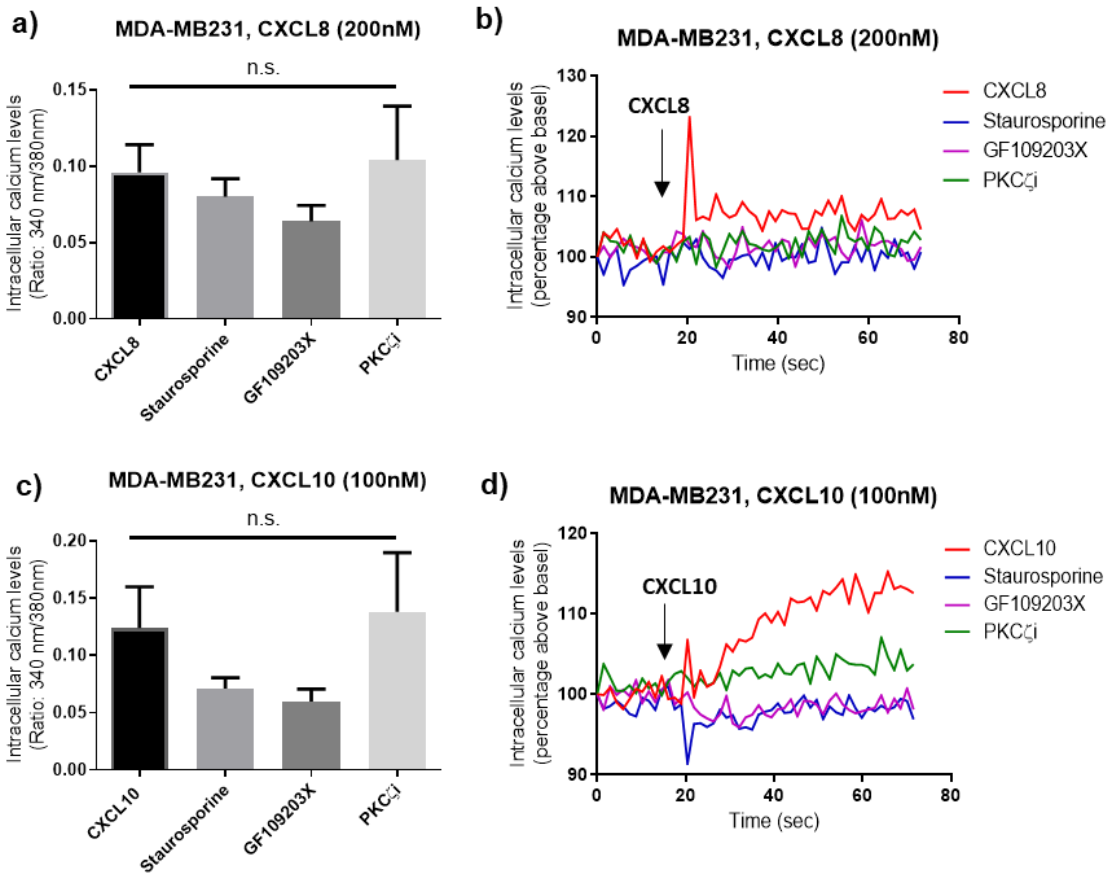

Figure 118. Effect of PKC inhibitors on the intracellular calcium release of CXCL8 or CXCL10 activated MDA-MB231 cells. a) None of the inhibitors: staurosporine (10 nM), GF109203X (5 µM), or PKCζi (10 µM) caused a significant effect on calcium release upon activation with 200 nM CXCL8, although there was a slight reduction with GF109203X treatment. **b)** intracellular calcium measurement traces were taken from a representative experiment. **c)** although GF109203X and staurosporine slightly reduced the release of calcium in 100 nM CXCL10-activated MDA-MB231 cells but not PKCζi, no significant difference was noted. **d)** intracellular calcium measurement traces were taken from a representative experiment. 1% DMSO was added to the cells as a vehicle control. Data represents the mean ± SEM of at least three independent experiments. (One-way ANOVA with a Dunnett's multiple comparisons test as post-test, n.s. = no significance $p > 0.05$). Data are expressed as the relative ratio of fluorescence emitted at 510 nm after sequential stimulation at 340 and 380 nm.

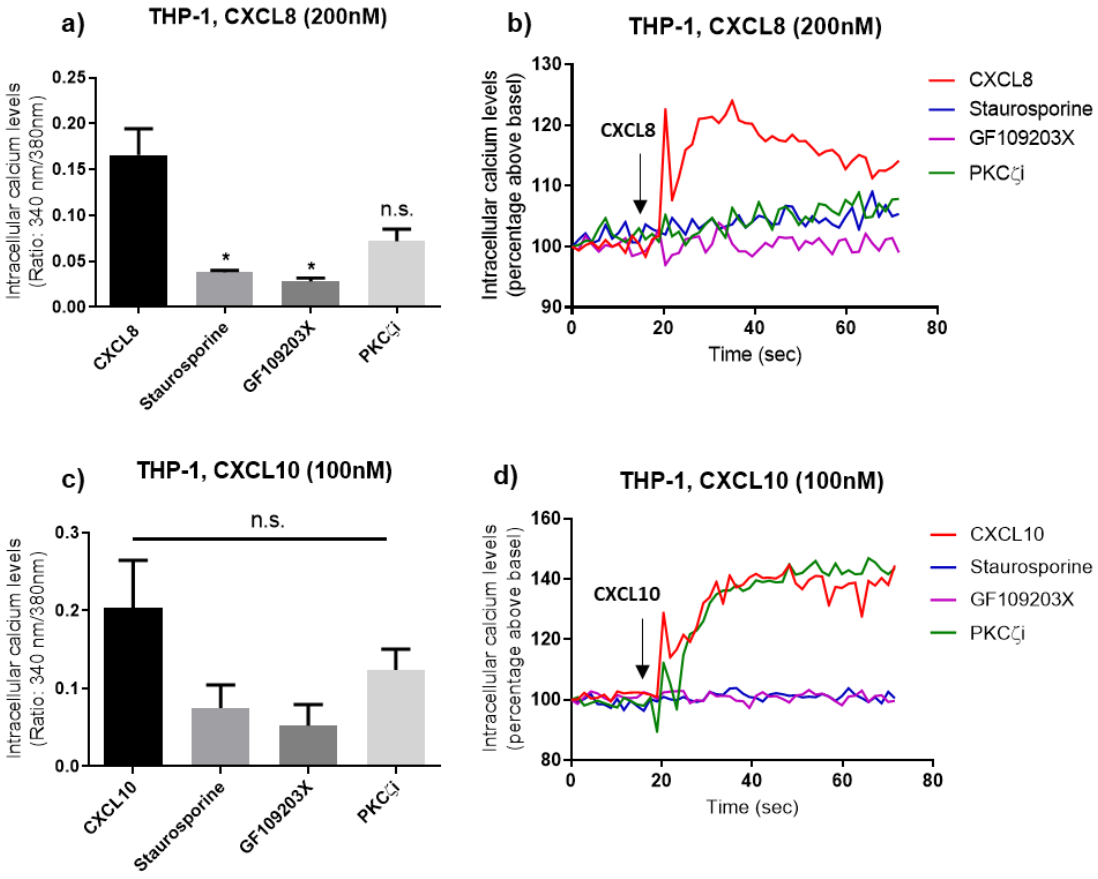

Figure 119. Effect of PKC inhibitors on the intracellular calcium release of CXCL8 or CXCL10 activated THP-1 cells. a) staurosporine (10 nM) and GF109203X (5 µM) significantly reduced calcium release, and PKCζi (10 µM) had a slight reduction effect on 200 nM CXCL8-activated cells. **b)** intracellular calcium measurement traces were taken from a representative experiment. **c)** 100 nM CXCL10-activated THP-1 cells showed a similar decrease of calcium release, although not significant. **d)** intracellular calcium measurement traces are taken from a representative experiment. 1% DMSO was added to the cells as a vehicle control. Data represents the mean ± SEM of at least three independent experiments. (One-way ANOVA with a Dunnett's multiple comparisons test as post-test, n.s. = no significance $p > 0.05$, * = $p \leq 0.05$). Data are expressed as the relative ratio of fluorescence emitted at 510 nm after sequential stimulation at 340 and 380 nm.

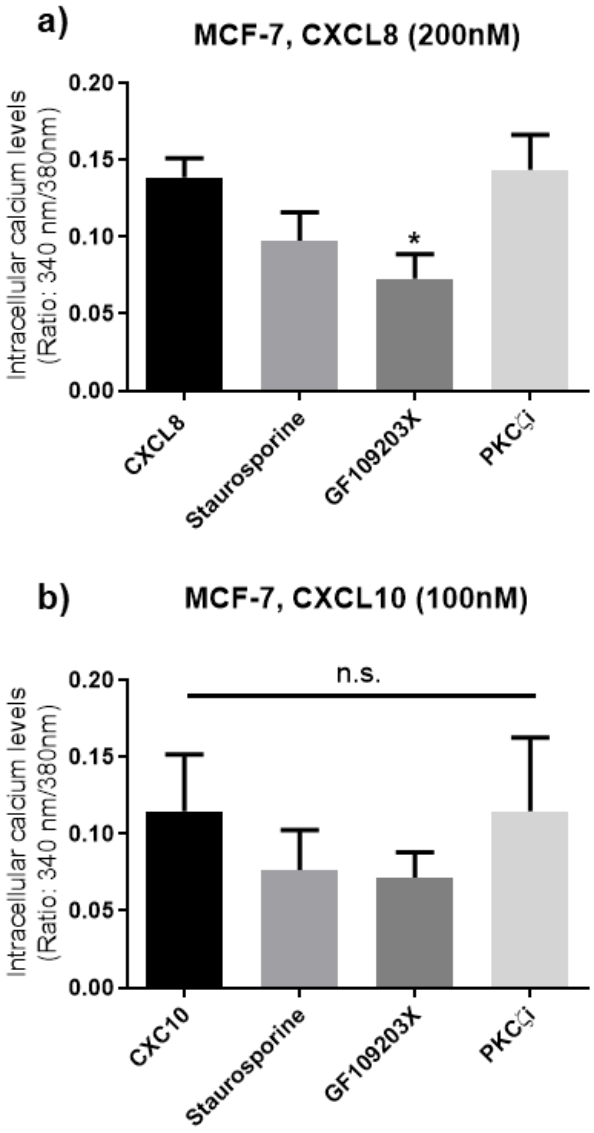

Figure 120. Effect of PKC inhibitors on the intracellular calcium release of CXCL8 or CXCL10 activated MCF-7 cells. a) GF109203X (5 µM) had significantly reduced the release of calcium in 200 nM CXCL8-activated MCF-7 cells, and staurosporine had a small effect on reducing calcium release but PKCζi did not have an effect. **b)** 100 nM CXCL10-activated MCF-7 calcium release was slightly reduced by staurosporine and GF109203X but not PKCζi, with no significant difference with any of the inhibitors. 1% DMSO was added to the cells as a vehicle control. Data represents the mean ± SEM of at least three independent experiments (One-way ANOVA with a Dunnett's multiple comparisons test as post-test, n.s. = no significance $p > 0.05$, * = $p \leq 0.05$). Data are expressed as the relative ratio of fluorescence emitted at 510 nm after sequential stimulation at 340 and 380 nm.

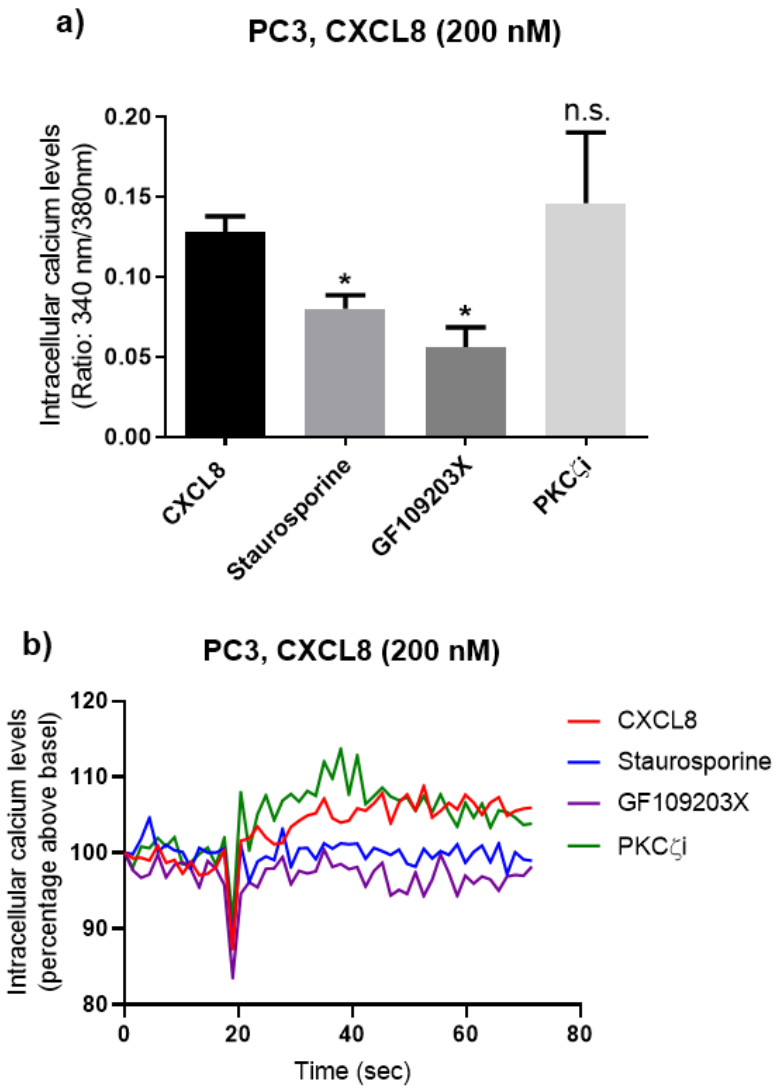

Figure 121. Effect of PKC inhibitors on the intracellular calcium release of CXCL8 activated PC3 cells. a) staurosporine (10 nM) and GF109203X (5 µM) significantly reduced calcium flux of 200 nM CXCL8-activated PC3 cells, but PKCζi (10 µM) had no effect. **b)** intracellular calcium measurement traces are taken from a representative experiment. 1% DMSO was added to the cells a vehicle control. Data represents the mean ± SEM of at least three independent experiments. (One-way ANOVA with a Dunnett's multiple comparisons test as post-test, n.s. = no significance $p > 0.05$, * = $p \leq 0.05$). Data are expressed as the relative ratio of fluorescence emitted at 510 nm after sequential stimulation at 340 and 380 nm.

5.2.8 MTS cytotoxic assay to quantify the cytotoxicity of PKC inhibitors

No cytotoxicity was reported when PKC inhibitors: 10 nM staurosporine, 5 µM GF109203X, and 10 µM PKCζi were incubated for 24 hrs with MDA-MB231, PC3 and THP-1 cells, as indicated in **Figure 122**.

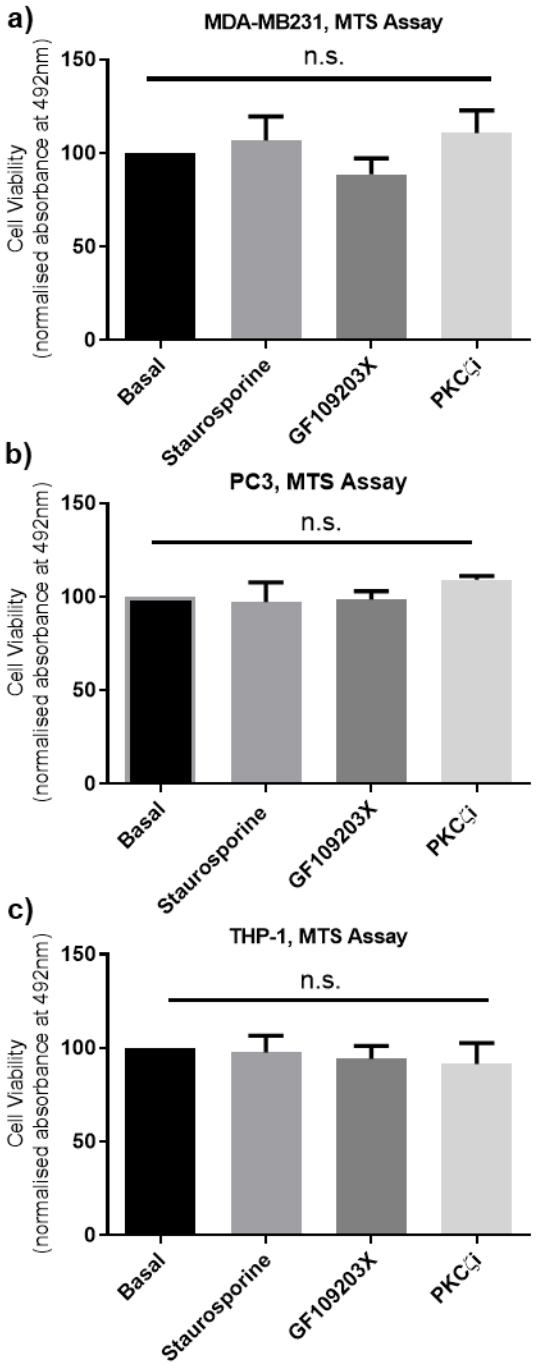

Figure 122. Toxicity of PKC inhibitors. The absorbance following incubation with staurosporine (10 nM), GF109203X (5 µM), or PKCζi (10 µM) incubated with **a)** THP-1, **b)** PC3, and **c)** MDA-MB231 cells for 24 hrs and MTS reagent for 2 hrs. 1% DMSO was added to the basal cells as a vehicle control. Data representative of the mean ± SEM of three independent experiments. (Kruskal-Wallis test, Dunn's multiple comparisons test, n.s.= no significance $p > 0.05$).

5.3 Discussion

Overexpression of chemokine receptors is thought to be a contributing factor in providing navigational cues for cancer cells to metastasize [582]. Therefore, investigating the mechanisms of migration can give a better understanding on how to block cancer cells metastasizing. CXCL8 acting on its receptors, CXCR1 and CXCR2, within the tumour microenvironment was found to be associated with cancer migration and proliferation [131]. Also, CXCR3 is found to be expressed in lymphatic leukaemia, splenic marginal zone lymphoma and breast cancer cells [578], suggesting its correlation to tumour progression and metastasis [583]. Although many studies have been trying to address the main signalling pathways involved in cell migration, there is still a knowledge gap with regards to whether PKC signalling is a positive or negative factor in cancer metastasis. Our approach was to investigate the role PKC plays in the migration and morphology change of different cancer cells which have been activated by either CXCL8 or CXCL10.

We studied the role of PKC family members in chemokine mediated migration by using small molecule inhibitors acting on different subtypes. We have already reported that PKC inhibition had no effect upon CCL3 migration in THP-1 cells [387]. However, Hamshaw *et al*. [389] found that PKC and PKD were important for the migration of CXCL12-activated PC3 cells. In addition, the migration of CXCL12-stimulated MCF-7 cells was reported to be blocked by PKC inhibitors but not Jurkat cells [388]. Here, we observed that both CXCL8 and CXCL10 promote cells to migrate faster comparing with the untreated control, yet when we added PKC inhibitors, cells reacted differently based on the chemokine and PKC inhibitor used.

Conventional (PKC α, β, γ), novel (PKC η, δ, ε), or atypical PKCζ isozymes are not important for CXCL8-induced MDA-MB231 and PC3 cells migration, but atypical PKCζ is crucial for THP-1 cells migration. The PKC inhibitor GF109203X- a less specific inhibitor of PKCα, β1, δ, and ε, staurosporine- inhibitor of PKCα, γ and η, as well as PKCζi did not affect the speed of migration of PC3 and MDA-MB231 cells when activated with CXCL8. This was confirmed using Oris migration assays, where CXCL8-activated PC3 cells incubated with staurosporine, GF109203X, and PKCζi did not cause an effect on migration. Moreover, using these inhibitors in THP-1 cell chemotaxis, we found that only PKCζi significantly reduced the number of cells migrating toward CXCL8. Guo *et al.* [584] reported that PKCζi blocked CSF-1 induced THP-1 chemotaxis and confirmed this with knocking down PKCζ with siRNA technique. Lie *et al.* [585] also found that PKCζ inhibition has reduced the chemotactic abilities of EGF-induced NSCLC cells. On the other hand, GF109203X had lowered

renal cancer cell migration using chemotaxis assay [586] and blocked CCL5-mediated migration [587]. Additionally, in former studies we reported that knocking down PKCα in MCF-7 and Jurkat cells abrogated cells migration towards CXCL12, while PKCζ did not have an effect [388]. Taking it together, we conclude that atypical PKCζi block the migration of CXCL8 activated THP-1 cells, while PKCζi, GF109203X and staurosporine did not have an effect on the CXCL8-induced migration of PC3 and MDA-MB231 cells.

In contrast, using the same set of inhibitors, we found that staurosporine (acts on PKC: α, γ, η), GF109203X (acts on PKC α, β, δ, ε) and PKCζi reduced the migration of CXCL10-activated PC3 cells. The migration speed of CXCL10-activated MDA-MB231 cells was also inhibited by GF109203X and PKCζi but not staurosporine. PKCζi was crucial for THP-1 cells chemotaxis, but GF109203X and staurosporine were not. Performing Oris migration assay on PC3 cells showed a lower migration rate of cells induced with CXCL10 and the PKC inhibitors. Although there was a trend that confirms the time-lapse migration assay results, yet they were fluctuating results demonstrated by high standard error (**Figure 107b**). This could be due to the migration pattern of PC3 cells, migrating to the sides of the Oris wells instead of the detection centre area where they would be detected.

Mills *et al.* [388] speculated that due to the different behaviours of PKC inhibitors on MCF-7 and Jurkat cells migration, MCF-7 could be using the catalytic region of PKC because knocking down PKCα and PKCζ have totally abrogated the migration of the cells, while Jurkat cells could be using another PKC domain because of the varying actions it causes on migration. It could also be due to certain isoform levels being elevated in these cell lines, and therefore they would be more prone to be targeted to inhibition. For example, MDA-MB231 cells were found to have increased levels of PKCε and were suggested to be used as a biomarker for aggressive breast cancer [588]. Additionally, inhibition of PKCε was associated with the inhibition of breast cancer cells migration as well as a mediator of EMT [589]. Therefore, the role of PKCε could further be investigated by testing selective inhibitors targeting this isoform, which should allow for improved and precise therapeutic intervention.

Cell migration is characterized by a series of morphological changes, endorsed by dynamic modifications of actin polymerization causing rearrangement of the cytoskeleton [491]. Accumulating evidence confirmed that PKC substrates phosphorylate many cytoskeletal proteins triggering dynamic alternations that lead cell adhesion and migration [386], [590], [591]. During the process of migration, actin filaments arrange in three-dimensional assemblies preparing for the next move [40].

The leading edge of the cell will contain protrusive structures called lamellipodia and filopodia. Lamellipodia are cellular sheets branched of actin network serving as the mechanical force to move the cell forward. Filopodia are formed of tight parallel bundles of F-actin that shape like spikes to detect changes in the microenvironment. When activated, an elongation of the protrusion of the leading edge (containing the filopodia and lamellipodia) will lead cell movement. On the other hand, the contraction of the cells which also mediates the preparation of the cell to move is generated by stress fibres acting as contractile structures. They are formed of actin and myosin bundles, also known as actomyosin structures, generating contractile forces for cell migration and morphogenesis [456].

Incubating cells with PKC inhibitors have presented some contradictory results dependent upon the chemokine used (**Figure 123**). Although staurosporine, GF109203X, and PKCζi did not cause any significant difference in the migration of CXCL8-activated PC3 and MDA-MB231 cells, staurosporine made a substantial change in the area, circularity or aspect ratio of both cell lines imaged using brightfield microscope. This was confirmed with observations of phalloidin-stained actin microfilaments with fluorescence microscopy generating a major actin disruption to the cells. Actin-enriched lamellipodia and membrane ruffles appeared at the tips of CXCL8-activated PC3 cells treated with staurosporine (**Figure 117**). MDA-MB231 cells treated with staurosporine and activated with CXCL8 showed a tangled network of cells overlapping over each other, as well as stretching their cytoskeleton. Both in brightfield and fluorescence microscope, cells displayed long spindled shapes with thinning to the cells' bodies exhibiting sticky endings with slender protrusions. Cell migration involving polymerization and depolymerisation of actin filaments in lamellipodia or membrane ruffles [456] were not affected by the changes staurosporine cause on both cell lines suggesting a different independent mechanism of action taking place.

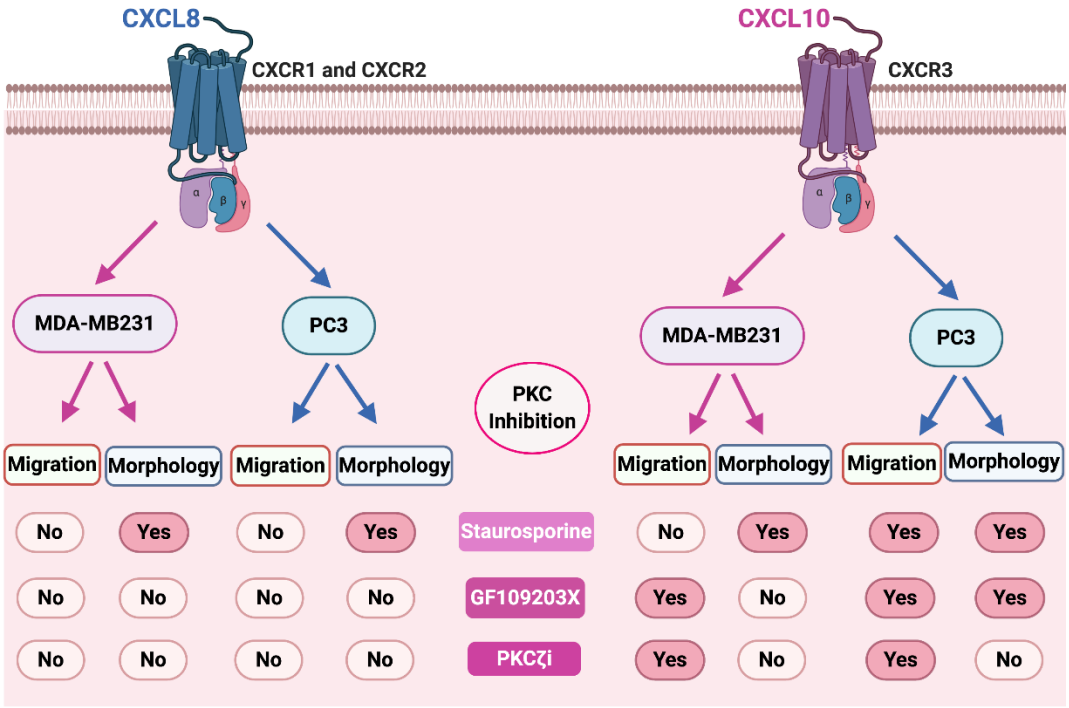

Figure 123. Illustration of the effect of PKC inhibitors on CXCL8 or CXCL10-activated MDA-MB231 or PC3 cells. Staurosporine inhibits PKCα, γ, and η, GF109203X inhibits PKC α, β, δ, and ε, and PKCζi inhibits PKCζ. 'No' denotes no effect, and 'Yes' denotes a significant effect on the cell migration speed or cellular morphology.

CXCL10-activated cells were also not affected by PKCζi, but staurosporine and GF109203X caused some morphological changes to PC3 or MDA-MB231 cells. GF109203X significantly changed the aspect ratio of CXCL10-activated PC3 cells. Hamshaw *et al.* [389] found that GF109203X reduced the size of CXCL12-activated PC3 cells with an increase to the number of cellular protrusions. Another study found that overexpression of PKCε (one of the PKC isoforms inhibited by GF109203X) displayed a polarized shape change to fibroblasts resulting in the formation of long cellular membrane protrusions [592]. PKCε was found to be associated with Rac1 activation [403] which is known for its role in migration and formation of lamellipodia [435], [546]. Indeed, PKCε expression was already confirmed in prostate cancer cells [403]. Another possibility for the morphology change assumed by GF109203X treatment is that RhoA could act downstream of PKC which leads to actin reorganisation. This was evident by Brandt *et al.* [593] who found that GF109203X blocked RhoA signalling in the vascular smooth muscle A7r5 cells. In addition, it was proposed that PKCε could induce EMT via downstream signals RhoC and STAT3, which mediate EMT regulation [588], [589], [594]. Moreover, the circularity of CXCL10-activated MDA-MB231 cells and aspect ratio of PC3 cells were challenged by staurosporine treatment where a rapid and dramatic disruption of actin stress fibres

with peripheral microspikes or filopodia formation in MDA-MB231 cells was observed. Ruffles accumulating at the membrane of CXCL10-activated PC3 cells treated with staurosporine were also observed. Collectively, although the morphological changes GF109203X and staurosporine induce on CXCL10-activated PC3 were associated with a reduction of the migration speed of the cells, this was not the case with CXCL8-activated PC3 or MDA-MB231 cells.

Staurosporine and GF109203X reduced the release of intracellular calcium in THP-1, MCF-7, MDA-MB231, and PC3 cells upon CXCL8 or CXCL10 induction either with a reduced trend or significantly, however, PKCζi did not have an effect on calcium release. This agrees with a study showing that staurosporine inhibit calcium influx from the external medium in antigen-induced RBL-2H3 cells [595]. Another study found that GF109203X inhibited the intracellular release of calcium in histamine-induced DD_1 MF-2 muscle cells [596]. However, Hamshaw *et al.* [389] and Goh. [434] showed that there was no reduction in calcium release upon incubation with PKC inhibitors and stimulation with CXCL12 in PC3 and MCF-7 cells. Therefore, the involvement of PKC isoforms in specific intracellular signalling pathways is dependent on the external stimulus activating them.

Staurosporine is a competitive PKC inhibitor with a high binding affinity and low specificity. It targets PKCα which has emerged as a general stimulus of cell spreading and migration by regulating actin-associated protein [597]. The level of PKCα is elevated in PC3 [598] and breast cancer cells [599], therefore, blocking it with staurosporine might be the reason for the morphological changes observed earlier, although its effects cannot be explained merely by PKCα inhibition. Several studies have used staurosporine to induce cell apoptosis demonstrated by the change of cell morphology it causes and induction of JNK pathway. Olguín-Albuerne *et al.* [600] found that treating astrocyte cells with staurosporine causes morphological changes to the actin and tubulin and related astrocytes death dependent on NOX family members. Indeed, staurosporine is thought to promote apoptosis because of its inhibitory effect on the cell cycle [601] and it is related to the shape change of the cells. Staurosporine was also found to supress the proliferation of vascular endothelial cells but did not affect the migration of the cells [602]. However, in our study, we used staurosporine at a nanomolar concentration (10 nM) which was not found to cause cell toxicity using MTS assay (**Figure 122**). Hedberg *et al.* [603] have reported that using staurosporine at a nanomolar concentration induces rapid change in the actin cytoskeleton of different cell types in PKC-deficient cells arguing that staurosporine might not be PKC dependent. Yet, our data show that staurosporine did not promote a change in the cells morphology unless they were stimulated with the chemokine,

suggesting the role of PKC as a downstream signalling pathway involved in the specified cellular response. Thus, the chemokine, cell type and dose of staurosporine defines its effect on cell mortality, mobility and/or morphology, this is mostly due to its non-selectivity.

In all, many questions remain to be answered; further investigation of PKC isoforms expression levels on the cells, as well as specific targeting of these isoforms could be an appropriate approach to establish a unifying understanding of how PKCs work in different cell types of cancer.

5.4 Chapter Conclusion

In summary, the PKC family is a large one that could exhibit extensive range of effects on the cells [386] with each PKC isoform phosphorylating a spectrum of intracellular signalling proteins in distinct subcellular locations [604]. We conclude that

1. Atypical PKCζ is important for the migration of CXCL8 or CXCL10-activated THP-1 cells and PC3 cells, whereas it is not important for CXCL8-stimulated PC3 or MDA-MB231 cells.
2. Staurosporine and GF109203X decreased intracellular calcium release in CXCL8-activated THP-1, PC3 and MCF-7 cells.
3. Staurosporine drastically changed the morphology of the cells, regardless of its impact on the cell migration, suggesting different mechanisms or signalling molecules involved in the process.

Although these results reveal some of the roles of PKCs, but they also add to the complexity of this system, therefore requires further investigation on a larger number of cell types and more specific inhibitors.

Chapter 6: Final discussion and future work

Migration of tumour cells is a fundamental process for the formation and progression of metastasis in malignant diseases. Chemokines binding to their cognate receptors could induce the migration of cancer cells. The expression of these chemokines and their effect could be cell-type specific [409], thus, it is challenging to be conclusive with the outcomes they generate on cancer cells. Also, the molecular signalling pathways involved in chemokine-driven cell migration remain to be fully characterised. The aim of this thesis was to investigate the role CXCL8 and CXCL10 play in different cancer cell lines, as well as the main signalling pathways involved in the induction of migration. The approach taken was to test for chemokine receptor expression using immunofluorescence assay. Moreover, intracellular calcium release upon administration of exogenous chemokine was measured for receptor activation. Whether it was an adherent or non-adherent cell line, migration assays were chosen based on their reproducibility with the specified cell line. Therefore, we aimed to expand our vision in the importance of the chemokine system upon which we could utilize as a novel therapeutic target for chemokine-driven cancer progression.

6.1 Chapter 3

To identify the involvement of CXCL8 and CXCL10 signalling in cancer metastasis, cognate receptors expression, intracellular calcium release, and the migratory behaviour were assessed in different cancer cell lines. Breast MCF-7 and MDA-MB231, prostate PC3, and leukemic THP-1 cancer cells responded to exogenous CXCL8 application, while leukemic Jurkat cells did not. Emerging evidence within the past two decades acknowledged the success of preclinical trials in targeting CXCL8-CXCR1/CXCR2 signalling axis [131]. Reparixin, a small molecule inhibitor of CXCR1 and CXCR2 has made it to clinical trials for being safe and well-tolerated as a cancer stem cells targeting agent in patients with metastatic triple-negative breast cancer (NCT02370238) [476], [605], [606]. Reparixin appeared to be a good candidate for breast cancer patient having an acceptable toxicity profile identified in Phase I and II clinical trials. This adds to its already addressed effect in blocking cancer cell migration in *in vitro* studies demonstrated by others [162], [443], [445] and confirmed with our results in this thesis. Furthermore, SCH527123 (also known as Navarixin), was tested in Phase II clinical trials for chronic obstructive pulmonary disease

(NCT01006616) by blocking the migration of neutrophils to the diseased lungs. In combination with Pembrolizumab, Phase II trials (NCT03473925) are currently being held for patients with metastatic solid tumours (such as NSCLC). We found that Reparixin, SCH527123 as well as SB225002 are able to block the migration of THP-1, MCF-7, MDA-MB231, and PC3 cells, highlighting the importance of the CXCL8-CXCR1/2 signalling axis in cancer cell migration. Nevertheless, it was challenging to generate data using the Boyden chamber transwell assay or agarose spot assay, which could have been beneficial to identify the directionality towards the chemokine of cancer cells treated with the above antagonists. It is also crucial to take in to account the different patterns of cell migration within the 2D environments used. For example, MCF-7 cells migrate very slowly in comparison to MDA-MB231 and PC3 cells when imaged using the time-lapse migration assay. In the Oris migration assay, PC3 cells migrated towards the edges rather than the centre, and this was the case with MDA-MB231 cells. Thus, there is still a need for robust and sensitive methods to identify chemokine-driven migration based on the cell line.

The migration ability of different cancer cells was also tested with CXCL10. Initially, CXCL10 receptor CXCR3 was found to be expressed in THP-1, MDA-MB231 and PC3 cells. These cell lines showed higher migration rates in the presence of exogenous CXCL10. However, the robustness of the CXCL10/CXCR3 axis is challenged by the variant isoforms of CXCR3. CXCR3-A and CXCR3-B appear to have contradictive downstream signalling effects. We hypothesized that the previous cell lines have potentiated their migratory effect through CXCR3-A, which is acknowledged in the literature for being responsible for the induced cell migration [487]; and possess lower levels of CXCR3-B, having a lower inhibition effect on migration. Yet, further experiments looking into the dominant expression levels of both receptors, and the main receptor involved in the migration process could give us better insights into understanding the underlying effects of CXCL10.

6.2 Chapter 4

Chemokines binding to their cognate receptors induce the migration of cancer cells, however, the molecular signalling pathways involved in this process are not fully understood. The signalling pathways that are mediated by chemokines and their receptors are complex and require further investigation. We primarily used MDA-MB231 and PC3 cells as a model to identify the pathways involved in CXCL8-CXCR1/CXCR2 driven migration. There appeared to be few distinctions in the pathways that these cells use to migrate when activated with CXCL8 (shown in **Table 6**). It is indeed evident that some chemokines may stimulate signalling pathways that others do not [388]. For example, while Pi3K did not seem to be important for T cells chemotaxis towards CXCL10 or CXCL11 [607], this signalling pathways was required for the chemotaxis of CXCL12-activated T-cells [388], [608]. The data generated in this study have highlighted the signalling pathways that are crucial for CXCL8-mediated cell migration in MDA-MB231 and PC3 cells. We found that upon CXCL8 activation, Pi3K/AKT, Rho GTPases, DOCK1/2/5, Ras/Raf/MEK/ERK, FAK, Src, PKA, Arp2/3, PKC and PKD were important for MDA-MB231 and PC3 migration with slight distinctions (**Figure 124**).

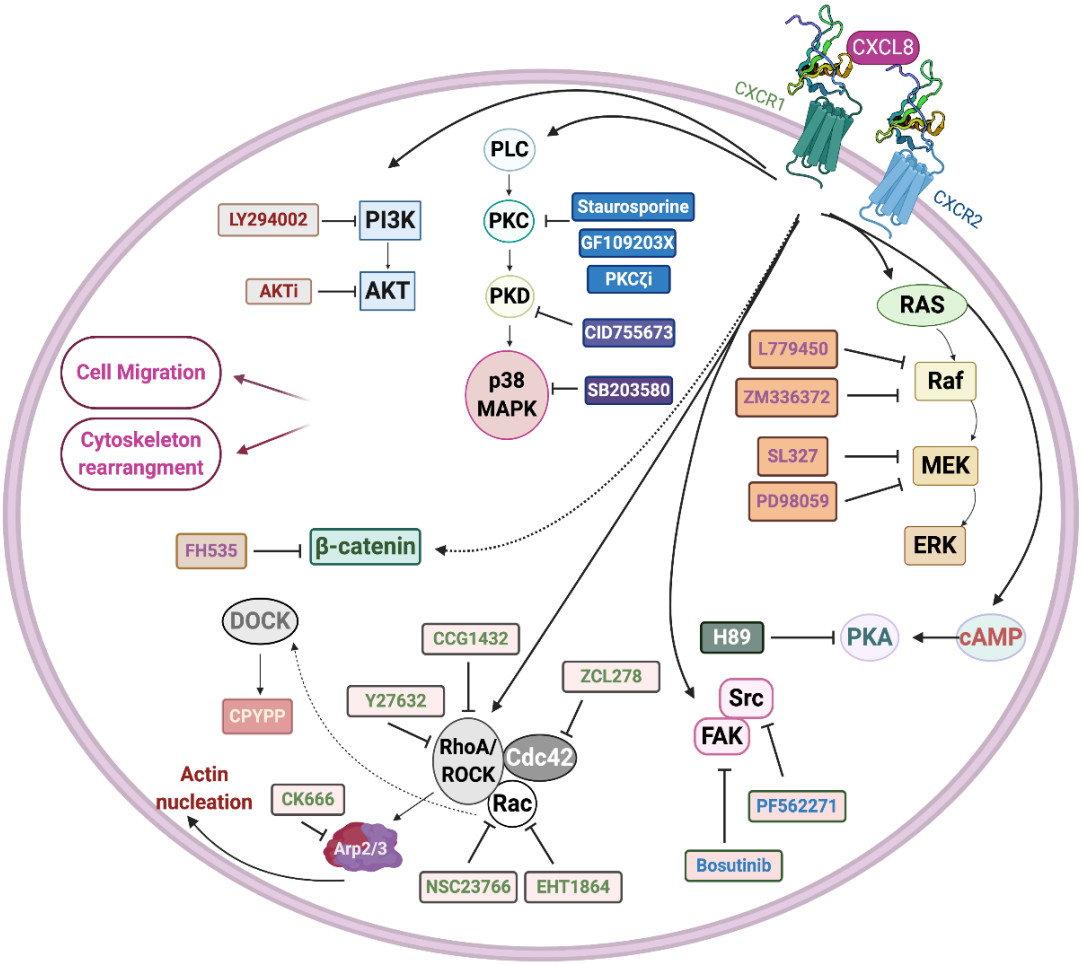

Figure 124. Schematic representation of the signalling pathways thought to be involved in CXCL8 cancer cell migration. Various inhibitors were used to block the effect of these signalling molecules in order to establish an understanding of the crucial pathways associated with MDA-MB231 and PC3 cell migration upon activation with CXCL8.

Moreover, one of the impressive effects of chemokines on MDA-MB231 and PC3 cells are the morphological changes identified by rearrangement of the cytoskeleton, formation of integrin-mediated focal adhesions, extension and retraction of cells leading edges to execute the directional migration. The mechanism underlying the regulation or reorganisation of the cytoskeleton in cells polarization and migration involve a complex system of signal transduction molecules. Using a range of small molecule inhibitors, the characterisation of the cellular morphology changes was resembled by the alternation to the cell area, the circularity, and aspect ratio. We also visually assessed phalloidin-actin stained cells at higher microscope objective for changes in actin rearrangement. Although some of the inhibitors for the signal transduction molecules were able to inhibit cells migration, they may or may not have induced a substantial change in the cell morphology.

6.3 Chapter 5

PKC has been shown to regulate cell migration, adhesion and proliferation [609]. In order to identify a connection between PKC and tumour progression in breast, prostate and leukaemia cells, the effect of PKC on CXCL8 or CXCL10 mediated cell migration and morphology was analysed. We tested the speed of the migrating cells, morphology, and chemotaxis in the presences of different PKC isoforms inhibitors-GF109203X, staurosporine and PKCζi. We found that the migration of CXCL8-activated PC3 and MDA-MB231 cells in the presence of conventional, novel, or atypical PKCs was not affected, but atypical PKCζ is crucial for THP-1 cells chemotaxis. The speed of CXCL10 induced PC3 and MDA-MB231 cells was significantly reduced in the presence of conventional, novel and PKCζ. THP-1 cells chemotaxis was again affected by PKCζ pseudosubstrate inhibitor. On the other hand, the cell area, circularity or aspect ratio were affected by staurosporine in CXCL8 or CXCL10 induced cells, demonstrating the role of PKCα in the rearrangement of the cytoskeleton regardless of the effect on the migration. Consequently, this allows the speculation that different PKC isoforms induce different outcomes in cells migration and actin cytoskeleton rearrangement based on the chemokine receptor and/or the cell type.

PKCζ is a member of the atypical PKC subfamily and has been vastly implicated in the regulation of cellular functions. Accumulating evidence using *in vitro* and *in vivo* systems highlight the critical role PKCζ plays in regulating intracellular signalling pathways. PKCζ is a well-known polarity protein, involving partition-defective 6 (PAR6) and PAR3, regulating cell polarity, cell motility, and invasion [610]. For example, PKCζ controls the polarity of migrating astrocytes with formation of protrusions in the direction of the chemotactic gradient [611]. PKCζ knockout or knockdown in PC3 cells decrease lymphatic metastasis of prostate cancer by impairing the activation of AKT, ERK, and NF-κB signalling [612]. Indeed, PKCζ induce the aggressive phenotype of prostate cancer cells [613] as it is important for the cells migration and invasion where it forms the PAR6-PKCζ complex in the leading edge of membrane ruffles that aids in cell directional migration [610]. Inhibition of PKCζ has been associated with CXCL12 and EGF-induced chemotactic migration in breast cancer cells [614] and EGF-induced macrophages chemotaxis [584]. Another study suggested a role of stimulated PKCζ and CXCR4 expression in elevating the *in vitro* migration and invasion of hepatocyte growth factor-induced MDA-MB436 cells [615]. The migration of CXCL8-induced mesenchymal stromal cells was abrogated with PKCζ pseudosubstrate inhibitor [616]. In our group, we found that PKCζ was

important for the migration of CCL3-activated MCF-7 cells [498], CXCL12-activated MCF-7, Jurkat [388] and PC3 cells [389]. Moreover, in this thesis, we found that CXCL10-activated MDA-MB231 and PC3 cells as well as CXCL8 and CXCL10-activated THP-1 cells utilize PKCζ for their migration. With such strong evidence demonstrating that PKCζ is crucial for the migration of multiple cancer cell types upon activation with different stimulus, it is tempting to conclude that the inhibition of PKCζ could decrease cancer spreading and metastasis. Further investigation of its role *in vivo* could potentially lead such pile of preclinical evidence to clinical trials.

Other PKC isoforms that were targeted using non-selective PKC inhibitors were staurosporine (acts on PKC: α, γ, η), GF109203X (acts on PKC α, β, δ, ε). Staurosporine induced actin remodelling dependent upon CXCL8 or CXCL10 stimulation as well as blocked the migration of CXCL10-activated MDA-MB231 and PC3 cells. GF109203X also induced cytoskeleton changes in CXCL10-stimulated PC3 cells and blocked the migration of CXCL10-activated MDA-MB231 and PC3 cells. These inhibitors could be targeting the elevated expression levels of PKCα in prostate [598] and breast cancer cells [599]. Additionally, PKCε expression was already confirmed in prostate cancer cells [403], hence the effect of GF109203X on PC3 cellular morphology and migration. However, due to these inhibitors not being selective, it is not conclusive which PKC isoform is the targeted one. Therefore, further work should be able to confirm which PKC isoforms are important for the migration of chemokine-activated cancer cells to help open a window for more precise therapeutic intervention. This could be accomplished by assessing the expression levels of PKC isoforms on a wide range of cell types and targeting the elevated levels of PKC associated with tumour progression with selective PKC inhibitors.

6.4 Future Directions

- Find alternative chemotaxis assays to determine the directed migration of adherent cells since Boyden chamber transwell assay and agarose spot assay were not proven to be reproducible for MDA-MB231, MCF-7 and PC3 cells throughout this thesis.
- We showed the expression levels of CXCR1 and CXCR2 using immunofluorescent assay. Flow cytometry analysis to determine cell surface expression of the receptors would be beneficial for deciding the antagonists required to block a specific effect associated with the overexpressed receptor.
- The role of CXCL8 in cancer cell proliferation remains controversial. Some studies have found that CXCL8 does not promote cell proliferation *in vitro* [439], [617] and suppress cancer proliferation by promoting neutrophil recruitment [618]. While other studies found that CXCL8 was involved in upregulating cyclin D1 expression and Pi3K/AKT/mTOR stimulation in prostate PC3 and DU145 cells, where blocking CXCL8 expression abolished cells proliferation [294]. Based on the preliminary data generated in this thesis supporting a role of CXCL8 in promoting proliferating, it is worth investigating the signalling pathways involved in this process. Cell proliferation could be measured using MTT/MTS assays.
- The distinct responses of carcinoma cells to CXCL10 may be due to either the cellular milieu or variations of CXCR3 isoforms (CXCR-A, CXCR-B, and CXCR-Alt), where the latter is thought to play a reciprocal role in cell migration [226]. There is a call for CXCR3 antagonists selective for each splice variant to grasp a better understanding of the role of CXCL10 in cell migration.
- The role of PKC in the migration of different cancer cell lines was analysed using migration assays. Using an siRNA approach to knockdown the different PKC isoforms is required to confirm the conclusions.
- The thesis looked at 21 different signal transduction molecules for their role in chemokine-driven cancer cell migration using small molecule inhibitors. Pi3K/AKT, Raf/MEK/ERK, p38 MAPK, Rho/Cdc42/Rac, DOCK1/2/5, Arp2/3, PKA/PKC/PKD, and Src/FAK, appeared to be important for the migration of PC3 and MDA-MB231 cells upon the activation with CXCL8. Confirmation of the exact roles of these signalling pathways could be achieved using chemically synthesized siRNA to specifically assess the importance of the different kinases.

References

[1] E. Alassaf and A. Mueller, “The role of PKC in CXCL8 and CXCL10 directed prostate , breast and leukemic cancer cell migration,” *Eur. J. Pharmacol.*, vol. 886, no. November, p. 173453, 2020, doi: 10.1016/j.ejphar.2020.173453.

[2] H. Yamaguchi, J. Wyckoff, and J. Condeelis, “Cell migration in tumors,” *Curr. Opin. Cell Biol.*, vol. 17, no. 5 SPEC. ISS., pp. 559–564, 2005, doi: 10.1016/j.ceb.2005.08.002.

[3] T. N. Seyfried and L. C. Huysentruyt., “On the origin of cancer metastsis,” *Crit. Rev. Oncog.*, vol. 18, no. 1–2, pp. 43–73, 2013, doi: 10.1002/1097-0142(195205)5:3<581::AID-CNCR2820050319>3.0.CO;2-Q.

[4] A. Giese, M. A. Loo, N. Tran, D. Haskett, S. W. Coons, and M. E. Berens, “Dichotomy of astrocytoma migration and proliferation,” *Int. J. Cancer*, vol. 67, no. 2, pp. 275–282, 1996, doi: 10.1002/(SICI)1097-0215(19960717)67:2<275::AID-IJC20>3.0.CO;2-9.

[5] A. Corcoran, R. F. Del Maestro, M. S. Berger, P. D. Canoll, and J. N. Bruce, “Testing the ‘Go or Grow’ hypothesis in human medulloblastoma cell lines in two and three dimension,” *Neurosurgery*, vol. 53, no. 1, pp. 174–185, 2003, doi: 10.1227/01.NEU.0000072442.26349.14.

[6] J. A. Gallaher, J. S. Brown, and A. R. A. Anderson, “The impact of proliferation-migration tradeoffs on phenotypic evolution in cancer,” *Sci. Rep.*, vol. 9, no. 1, pp. 1–10, 2019, doi: 10.1038/s41598-019-39636-x.

[7] E. Tzamali, G. Grekas, K. Marias, and V. Sakkalis, “Exploring the competition between proliferative and invasive cancer phenotypes in a continuous spatial model,” *PLoS One*, vol. 9, no. 8, 2014, doi: 10.1371/journal.pone.0103191.

[8] W. Yan, J. Chen, Z. Chen, and H. Chen, “Deregulated miR-296/S100A4 axis promotes tumor invasion by inducing epithelial-mesenchymal transition in human ovarian cancer,” *Am. J. Cancer Res.*, vol. 6, no. 2, pp. 260–269, 2016.

[9] Q. Guo *et al.*, “Endogenous Nodal promotes melanoma undergoing epithelial-mesenchymal transition via Snail and Slug in vitro and in vivo,” *Am. J. Cancer Res.*, vol. 5, no. 6, pp. 2098–2112, 2015.

[10] L. Huang, R.-L. Wu, and A.-M. Xu, “Epithelial-mesenchymal transition in gastric cancer,” *Am. J. Transl. Res.*, vol. 7, no. 11, pp. 2141–2158, 2015, doi: 10.1007/978-981-287-706-2_25.

[11] J. P. Thiery, “Epithelial–mesenchymal transitions in tumour progression,” *Nat. Rev. Cancer*, vol. 2, no. 6, pp. 442–454, 2002.

[12] K. Paňková, D. Rösel, M. Novotný, and J. Brábek, “The molecular mechanisms of transition between mesenchymal and amoeboid invasiveness in tumor cells,” *Cell. Mol. Life Sci.*, vol. 67, no. 1, pp. 63–71, 2010, doi: 10.1007/s00018-009-0132-1.

[13] P. Friedl and K. Wolf, “Plasticity of cell migration: A multiscale tuning model,” *J. Cell Biol.*, vol. 188, no. 1, pp. 11–19, 2010, doi: 10.1083/jcb.200909003.

[14] Y. Yang, H. Zheng, Y. Zhan, and S. Fan, “An emerging tumor invasion

mechanism about the collective cell migration," *Am. J. Transl. Res.*, vol. 11, no. 9, pp. 5301–5312, 2019.

[15] M. Lintz, A. Muñoz, and C. A. Reinhart-King, "The Mechanics of Single Cell and Collective Migration of Tumor Cells," *J. Biomech. Eng.*, vol. 139, no. 2, pp. 1–9, 2017, doi: 10.1115/1.4035121.

[16] A. Huttenlocher and A. R. Horwitz, "Integrins in cell migration," *Cold Spring Harb. Perspect. Biol.*, vol. 3, no. 9, pp. 1–16, 2011.

[17] P. Friedl, "Prespecification and plasticity: Shifting mechanisms of cell migration," *Curr. Opin. Cell Biol.*, vol. 16, no. 1, pp. 14–23, 2004, doi: 10.1016/j.ceb.2003.11.001.

[18] K. Wolf, R. Müller, S. Borgmann, E. B. Bröcker, and P. Friedl, "Amoeboid shape change and contact guidance: T-lymphocyte crawling through fibrillar collagen is independent of matrix remodeling by MMPs and other proteases," *Blood*, vol. 102, no. 9, pp. 3262–3269, 2003, doi: 10.1182/blood-2002-12-3791.

[19] C. D. Madsen and E. Sahai, "Cancer Dissemination-Lessons from Leukocytes," *Dev. Cell*, vol. 19, no. 1, pp. 13–26, 2010, doi: 10.1016/j.devcel.2010.06.013.

[20] P. Friedl and S. Alexander, "Cancer invasion and the microenvironment: Plasticity and reciprocity," *Cell*, vol. 147, no. 5, pp. 992–1009, 2011, doi: 10.1016/j.cell.2011.11.016.

[21] P. Friedl and K. Wolf, "Proteolytic interstitial cell migration: A five-step process," *Cancer Metastasis Rev.*, vol. 28, no. 1–2, pp. 129–135, 2009, doi: 10.1007/s10555-008-9174-3.

[22] I. Hecht *et al.*, "Tumor invasion optimization by mesenchymal-amoeboid heterogeneity," *Sci. Rep.*, vol. 5, pp. 1–11, 2015, doi: 10.1038/srep10622.

[23] N. Aceto *et al.*, "Circulating tumor cell clusters are oligoclonal precursors of breast cancer metastasis," *Cell*, vol. 158, no. 5, pp. 1110–1122, 2014, doi: 10.1016/j.cell.2014.07.013.

[24] M. L. Taddei *et al.*, "Mesenchymal to amoeboid transition is associated with stem-like features of melanoma cells," *Cell Commun. Signal.*, vol. 12, no. 1, pp. 1–12, 2014, doi: 10.1186/1478-811X-12-24.

[25] A. J. Ridley *et al.*, "Cell Migration: Integrating Signals from Front to Back," *merican Assoc. Adv. Sci.*, vol. 302, no. 5651, pp. 1704–1709, 2016.

[26] B. Ladoux, R.-M. Mège, and X. Trepat, "Front–Rear Polarization by Mechanical Cues: From Single Cells to Tissues Front–Rear Polarity in Single Cells and Cell Ensembles," *Trends Cell Biol.*, vol. 26, no. 6, pp. 420–433, 2016, doi: 10.1016/j.tcb.2016.02.002.

[27] N. Ann Mack and M. Georgiou, "The interdependence of the Rho GTPases and apicobasal cell polarity," *Small GTPases*, vol. 5, no. 2, pp. 37–41, 2014, doi: 10.4161/21541248.2014.973768.

[28] L. Blanchoin, R. Boujemaa-Paterski, C. Sykes, and J. Plastino, "Actin dynamics, architecture, and mechanics in cell motility," *Physiol. Rev.*, vol. 94, no. 1, pp. 235–263, 2014, doi: 10.1152/physrev.00018.2013.

[29] A. M. Weaver, M. E. Young, W. L. Lee, and J. A. Cooper, "Integration of

signals to the Arp2/3 complex," *Curr. Opin. Cell Biol.*, vol. 15, no. 1, pp. 23–30, 2003, doi: 10.1016/S0955-0674(02)00015-7.

[30] H. N. Higgs and T. D. Pollard, "Regulation of Actin Filament Network Formation Through ARP2/3 Complex: Activation by a Diverse Array of Proteins," *Annu. Rev. Biochem.*, vol. 70, no. 1, pp. 649–676, 2001, doi: 10.1146/annurev.biochem.70.1.649.

[31] H. Miki, S. Suetsugu, and T. Takenawa, "WAVE, a novel WASP-family protein involved in actin reorganization induced by Rac," *EMBO J.*, vol. 17, no. 23, pp. 6932–6941, 1998, doi: 10.1093/emboj/17.23.6932.

[32] B. Knight, C. Laukaitis, N. Akhtar, N. A. Hotchin, M. Edlund, and A. R. Horwitz, "Visualizing muscle cell migration in situ," *Curr. Biol.*, vol. 10, no. 10, pp. 576–585, 2000, doi: 10.1016/S0960-9822(00)00486-3.

[33] I. Royal, N. Lamarche-Vane, L. Lamorte, K. Kaibuchi, and M. Park, "Activation of Cdc42, Rac, PAK, and Rho-kinase in response to hepatocyte growth factor differentially regulates epithelial cell colony spreading and dissociation," *Mol. Biol. Cell*, vol. 11, no. 5, pp. 1709–1725, 2000, doi: 10.1091/mbc.11.5.1709.

[34] R. J. Cain and A. J. Ridley, "Phosphoinositide 3-kinases in cell migration," *Biol. Cell*, vol. 101, no. 1, pp. 13–29, 2009, doi: 10.1042/BC20080079.

[35] C. De Pascalis and S. Etienne-Manneville, "Single and collective cell migration: The mechanics of adhesions," *Mol. Biol. Cell*, vol. 28, no. 14, pp. 1833–1846, 2017, doi: 10.1091/mbc.E17-03-0134.

[36] P. C. Brooks *et al.*, "Localization of matrix metalloproteinase MMP-2 to the cell surface by interaction with integral αvβ3," *Cell*, vol. 10, no. 6, pp. 683–693, 1996.

[37] S. P. Palecek, J. C. Loftus, M. H. Ginsberg, D. A. Lauffenburger, and A. F. Horwitz, "Integrin-ligand binding properties govern cell migration speed through cell-substratum adhesiveness [published erratum appears in Nature 1997 Jul 10;388(6638):210]," *Nature*, vol. 385, no. 6616, pp. 537–540, 1997, [Online]. Available: https://www.nature.com/articles/385537a0.pdf.

[38] T. B. Deramaudt *et al.*, "FAK phosphorylation at Tyr-925 regulates cross-talk between focal adhesion turnover and cell protrusion," *Mol. Biol. Cell*, vol. 22, no. 7, pp. 964–975, 2011, doi: 10.1091/mbc.E10-08-0725.

[39] S. Ishibe, D. Joly, Z. X. Liu, and L. G. Cantley, "Paxillin serves as an ERK-regulated scaffold for coordinating FAK and Rac activation in epithelial morphogenesis," *Mol. Cell*, vol. 16, no. 2, pp. 257–267, 2004, doi: 10.1016/j.molcel.2004.10.006.

[40] P. K. Mattila and P. Lappalainen, "Filopodia: Molecular architecture and cellular functions," *Nat. Rev. Mol. Cell Biol.*, vol. 9, no. 6, pp. 446–454, 2008, doi: 10.1038/nrm2406.

[41] A. Akhmanova and M. O. Steinmetz, "Control of microtubule organization and dynamics: Two ends in the limelight," *Nat. Rev. Mol. Cell Biol.*, vol. 16, no. 12, pp. 711–726, 2015, doi: 10.1038/nrm4084.

[42] Hohmann and Dehghani, "The Cytoskeleton—A Complex Interacting Meshwork," *Cells*, vol. 8, no. 4, p. 362, 2019, doi: 10.3390/cells8040362.

[43] Q. Yang, X. F. Zhang, T. D. Pollard, and P. Forscher, "Arp2/3 complex-

dependent actin networks constrain myosin II function in driving retrograde actin flow," *J. Cell Biol.*, vol. 197, no. 7, pp. 939–956, 2012, doi: 10.1083/jcb.201111052.

[44] M. Larsen, M. L. Tremblay, and K. M. Yamada, "Phosphatases in cell-matrix adhesion and migration," *Nat. Rev. Mol. Cell Biol.*, vol. 4, no. 9, pp. 700–711, 2003, doi: 10.1038/nrm1199.

[45] V. Mollica Poeta, M. Massara, A. Capucetti, and R. Bonecchi, "Chemokines and Chemokine Receptors: New Targets for Cancer Immunotherapy," *Front. Immunol.*, vol. 10, no. March, pp. 1–10, 2019, doi: 10.3389/fimmu.2019.00379.

[46] M. Baggiolini, "Chemokines and leukocyte traffic.," *Nature*, vol. 392, pp. 565–568, 1998, doi: 10.1038/ni.f.214.

[47] G. E. White, A. J. Iqbal, and D. R. Greaves, "CC chemokine receptors and chronic inflammation-therapeutic opportunities and pharmacological challenges," *Pharmacol. Rev.*, vol. 65, no. 1, pp. 47–89, 2013, doi: 10.1124/pr.111.005074.

[48] B. Moser and K. Willimann, "Chemokines: role in inflammation and immune surveillance.," *Ann. Rheum. Dis.*, vol. 63 Suppl 2, no. suppl_2, pp. ii84–ii89, 2004, doi: 10.1136/ard.2004.028316.

[49] S. J. Allen, S. E. Crown, and T. M. Handel, "Chemokine:Receptor Structure, Interactions, and Antagonism," *Annu. Rev. Immunol.*, vol. 25, no. 1, pp. 787–820, 2007, doi: 10.1146/annurev.immunol.24.021605.090529.

[50] J. W. Griffith, C. L. Sokol, and A. D. Luster, "Chemokines and Chemokine Receptors: Positioning Cells for Host Defense and Immunity," *Annu. Rev. Immunol.*, vol. 32, no. 1, pp. 659–702, 2014, doi: 10.1146/annurev-immunol-032713-120145.

[51] C. A. Heberts, R. V Vitangcols, and J. B. Baker, "Scanning Mutagenesis of Interleukin-8 Identifies a Cluster of Residues Required for Receptor Binding," *J. Biol. Chem.*, vol. 266, no. 28, pp. 18989–18994, 1991.

[52] L. Rajagopalan and K. Rajarathnam, "Structural basis of chemokine receptor function - A model for binding affinity and ligand selectivity," *Biosci. Rep.*, vol. 26, no. 5, pp. 325–339, 2006, doi: 10.1007/s10540-006-9025-9.

[53] J. Y. Springael, E. Urizar, and M. Parmentier, "Dimerization of chemokine receptors and its functional consequences," *Cytokine Growth Factor Rev.*, vol. 16, no. 6, pp. 611–623, 2005, doi: 10.1016/j.cytogfr.2005.05.005.

[54] G. M. Clore, A. M. Gronenborn, E. Appella, M. Yamada, and K. Matsushima, "Three-Dimensional Structure of Interleukin 8 in Solution," *Biochemistry*, vol. 29, no. 7, pp. 1689–1696, 1990, doi: 10.1021/bi00459a004.

[55] P. J. Lodi *et al.*, "High-resolution solution structure of the β chemokine hMIP-1β by multidimensional NMR," *Science (80-.).*, vol. 263, no. 5154, pp. 1762–1767, 1994, doi: 10.1126/science.8134838.

[56] K. Rajarathnam *et al.*, "Neutrophil Activation by Monomeric Interleukin-8 Thomas Geiser , Marco Baggiolini and Ian Clark-Lewis Published by : American Association for the Advancement of Science Stable URL : http://www.jstor.org/stable/2883829 Neutrophil Activation by Monomeric In," vol. 264, no. 5155, pp. 90–92, 2016.

[57] X. Wang, J. S. Sharp, T. M. Handel, and J. H. Prestegard, *Chemokine oligomerization in cell signaling and migration*, 1st ed., vol. 117. Copyright © 2013, Elsevier Inc. All Rights Reserved., 2013.

[58] H. B. Lowman *et al.*, “Monomeric variants of IL-8: Effects of side chain substitutions and solution conditions upon dimer formation,” *Protein Sci.*, vol. 6, no. 3, pp. 598–608, 2008, doi: 10.1002/pro.5560060309.

[59] K. Rajarathnam *et al.*, “Neutrophil activation by monomeric interleukin-8.,” *Science (80-.).*, vol. 264, no. 5155, pp. 90–92, 1994.

[60] C. D. Paavola *et al.*, “Monomeric monocyte chemoattractant protein-1 (MCP-1) binds and activates the MCP-1 receptor CCR2B,” *J. Biol. Chem.*, vol. 273, no. 50, pp. 33157–33165, 1998, doi: 10.1074/jbc.273.50.33157.

[61] A. E. I. Proudfoot *et al.*, “Glycosaminoglycan binding and oligomerization are essential for the in vivo activity of certain chemokines,” *Natl. Acad. Sci.*, vol. 100, no. 4, pp. 1885–1890, 2016.

[62] I. Kufareva, C. L. Salanga, T. M. Handel, S. Diego, and L. Jolla, “Chemokine and chemokine receptor structure and interactions,” *Immunol. Cell Biol.*, vol. 93, no. 4, pp. 372–383, 2015, doi: 10.1038/icb.2015.15.Chemokine.

[63] A. E. I. Proudfoot *et al.*, “Glycosaminoglycan binding and oligomerization are essential for the in vivo activity of certain chemokines,” *Proc. Natl. Acad. Sci. U. S. A.*, vol. 100, no. 4, pp. 1885–1890, 2003, doi: 10.1073/pnas.0334864100.

[64] A. J. Hoogewerf *et al.*, “Glycosaminoglycans mediate cell surface oligomerization of chemokines,” *Biochemistry*, vol. 36, no. 44, pp. 13570–13578, 1997, doi: 10.1021/bi971125s.

[65] M. Metzemaekers, J. Van Damme, A. Mortier, and P. Proost, “Regulation of chemokine activity - A focus on the role of dipeptidyl peptidase IV/CD26,” *Front. Immunol.*, vol. 7, no. NOV, pp. 1–23, 2016, doi: 10.3389/fimmu.2016.00483.

[66] A. Mortier, J. Van Damme, and P. Proost, “Overview of the mechanisms regulating chemokine activity and availability,” *Immunol. Lett.*, vol. 145, no. 1–2, pp. 2–9, 2012, doi: 10.1016/j.imlet.2012.04.015.

[67] M. Metzemaekers *et al.*, “Glycosaminoglycans regulate CXCR3 ligands at distinct levels: Protection against processing by dipeptidyl peptidase IV/CD26 and interference with receptor signaling,” *Int. J. Mol. Sci.*, vol. 18, no. 7, 2017, doi: 10.3390/ijms18071513.

[68] K. H. Mayo and M. J. Chen, “Human Platelet Factor 4 Monomer–Dimer–Tetramer Equilibria Investigated by 1HNMR Spectroscopy,” *Biochemistry*, vol. 28, no. 24, pp. 9469–9478, 1989, doi: 10.1021/bi00450a034.

[69] I. V. Nesmelova, Y. Sham, J. Gao, and K. H. Mayo, “CXC and CC chemokines form mixed heterodimers: Association free energies from molecular dynamics simulations and experimental correlations,” *J. Biol. Chem.*, vol. 283, no. 35, pp. 24155–24166, 2008, doi: 10.1074/jbc.M803308200.

[70] F. Verkaar *et al.*, “Chemokine Cooperativity Is Caused by Competitive Glycosaminoglycan Binding,” *J. Immunol.*, vol. 192, no. 8, pp. 3908–3914, 2014, doi: 10.4049/jimmunol.1302159.

[71] A. Z. Dudek, I. Nesmelova, K. Mayo, C. M. Verfaillie, S. Pitchford, and A. Slungaard, “Platelet factor 4 promotes adhesion of hematopoietic progenitor cells and binds IL-8: Novel mechanisms for modulation of hematopoiesis,” *Blood*, vol. 101, no. 12, pp. 4687–4694, 2003, doi: 10.1182/blood-2002-08-2363.

[72] I. V. Nesmelova *et al.*, “Platelet factor 4 and interleukin-8 CXC chemokine heterodimer formation modulates function at the quaternary structural level,” *J. Biol. Chem.*, vol. 280, no. 6, pp. 4948–4958, 2005, doi: 10.1074/jbc.M405364200.

[73] M. D. Turner, B. Nedjai, T. Hurst, and D. J. Pennington, “Cytokines and chemokines: At the crossroads of cell signalling and inflammatory disease,” *Biochim. Biophys. Acta - Mol. Cell Res.*, vol. 1843, no. 11, pp. 2563–2582, 2014, doi: 10.1016/j.bbamcr.2014.05.014.

[74] B. Moser, M. Wolf, A. Walz, and P. Loetscher, “Chemokines: Multiple levels of leukocyte migration control,” *Trends Immunol.*, vol. 25, no. 2, pp. 75–84, 2004, doi: 10.1016/j.it.2003.12.005.

[75] G. Constantin *et al.*, “Chemokines trigger immediate β2 integrin affinity and mobility changes: Differential regulation and roles in lymphocyte arrest under flow,” *Immunity*, vol. 13, no. 6, pp. 759–769, 2000, doi: 10.1016/S1074-7613(00)00074-1.

[76] A. Zlotnik, A. M. Burkhardt, and B. Homey, “Homeostatic chemokine receptors and organ-specific metastasis,” *Nat. Rev. Immunol.*, vol. 11, no. 9, pp. 597–606, 2011, doi: 10.1038/nri3049.

[77] M. O’Hayre, C. L. Salanga, T. M. Handel, and S. J. Allen, “Chemokines and cancer: Migration, intracellular signalling and intercellular communication in the microenvironment,” *Biochem. J.*, vol. 409, no. 3, pp. 635–649, 2008, doi: 10.1042/BJ20071493.

[78] D. Raman, T. Sobolik-Delmaire, and A. Richmond, “Chemokines in health and disease,” *Exp. Cell Res.*, vol. 317, no. 5, pp. 575–589, 2011, doi: 10.1016/j.yexcr.2011.01.005.

[79] F. Bachelerie *et al.*, “International Union of Basic and Clinical Pharmacology. [corrected]. LXXXIX. Update on the extended family of chemokine receptors and introducing a new nomenclature for atypical chemokine receptors.,” *Pharmacol. Rev.*, vol. 66, pp. 1–79, 2014, doi: 10.1124/pr.113.007724.

[80] J. M. Baldwin, “Structure and function of receptors coupled to G proteins,” *Curr. Opin. Cell Biol.*, vol. 6, pp. 180–190, 1994.

[81] M. Szpakowska, V. Fievez, K. Arumugan, N. Van Nuland, J. C. Schmit, and A. Chevigné, “Function, diversity and therapeutic potential of the N-terminal domain of human chemokine receptors,” *Biochem. Pharmacol.*, vol. 84, no. 10, pp. 1366–1380, 2012, doi: 10.1016/j.bcp.2012.08.008.

[82] X. F. Shi *et al.*, “Structural analysis of human CCR2b and primate CCR2b by molecular modeling and molecular dynamics simulation,” *J. Mol. Model.*, vol. 8, no. 7, pp. 217–222, 2002, doi: 10.1007/s00894-002-0089-6.

[83] D. J. Scholten *et al.*, “Pharmacological modulation of chemokine receptor function,” *Br. J. Pharmacol.*, vol. 165, no. 6, pp. 1617–1643, 2012, doi: 10.1111/j.1476-5381.2011.01551.x.

[84] D. P. Dyer *et al.*, “Chemokine Receptor Redundancy and Specificity Are Context Dependent,” *Immunity*, vol. 50, no. 2, pp. 378-389.e5, 2019, doi: 10.1016/j.immuni.2019.01.009.

[85] E. Marcuzzi, R. Angioni, B. Molon, and B. Calì, “Chemokines and chemokine receptors: Orchestrating tumor metastasization,” *Int. J. Mol. Sci.*, vol. 20, no. 1, 2019, doi: 10.3390/ijms20010096.

[86] T. W. Schwartz, T. M. Frimurer, B. Holst, M. M. Rosenkilde, and C. E. Elling, “Molecular Mechanism of 7Tm Receptor Activation—a Global Toggle Switch Model,” *Annu. Rev. Pharmacol. Toxicol.*, vol. 46, no. 1, pp. 481–519, 2006, doi: 10.1146/annurev.pharmtox.46.120604.141218.

[87] H. Nomiyama and O. Yoshie, “Functional roles of evolutionary conserved motifs and residues in vertebrate chemokine receptors,” *J. Leukoc. Biol.*, vol. 97, no. 1, pp. 39–47, 2015, doi: 10.1189/jlb.2ru0614-290r.

[88] I. Clark-Lewis, I. Mattioli, J. H. Gong, and P. Loetscher, “Structure-function relationship between the human chemokine receptor CXCR3 and its ligands,” *J. Biol. Chem.*, vol. 278, no. 1, pp. 289–295, 2003, doi: 10.1074/jbc.M209470200.

[89] H. Nomiyama, N. Osada, and O. Yoshie, “The evolution of mammalian chemokine genes,” *Cytokine Growth Factor Rev.*, vol. 21, no. 4, pp. 253–262, 2010, doi: 10.1016/j.cytogfr.2010.03.004.

[90] G. Milligan and E. Kostenis, “Heterotrimeric G-proteins: A short history,” *Br. J. Pharmacol.*, vol. 147, no. SUPPL. 1, 2006, doi: 10.1038/sj.bjp.0706405.

[91] B. R. L. Sham, P. D. Phatak, T. P. Ihne, C. N. Abboud, and C. H. Packman, “Signal Pathway Regulation,” *Blood*, vol. 82, no. 8, pp. 2546–2551, 2013.

[92] J. Lee, R. Horuk, G. C. Rice, G. L. Bennett, T. Camerato, and W. I. Wood, “Characterization of two high affinity human interleukin-8 receptors,” *J. Biol. Chem.*, vol. 267, no. 23, pp. 16283–16287, 1992.

[93] V. Brinkmann *et al.*, “Neutrophil Extracellular Traps Kill Bacteria,” *Science (80-.).*, vol. 303, no. 5663, pp. 1532–1535, 2004, doi: 10.1126/science.1092385.

[94] N. Shao *et al.*, “Interleukin-8 upregulates integrin β3 expression and promotes estrogen receptor-negative breast cancer cell invasion by activating the PI3K/Akt/NF-κB pathway,” *Cancer Lett.*, vol. 364, no. 2, pp. 165–172, 2015, doi: 10.1016/j.canlet.2015.05.009.

[95] L. Rajagopalan and K. Rajarathnam, “Ligand selectivity and affinity of chemokine receptor CXCR1: Role of N-terminal domain,” *J. Biol. Chem.*, vol. 279, no. 29, pp. 30000–30008, 2004, doi: 10.1074/jbc.M313883200.

[96] M. J. Stone, J. A. Hayward, C. Huang, Z. E. Huma, and J. Sanchez, *Mechanisms of regulation of the chemokine-receptor network*, vol. 18, no. 2. 2017.

[97] E. M. Borroni, A. Mantovani, M. Locati, and R. Bonecchi, “Chemokine receptors intracellular trafficking,” *Pharmacol. Ther.*, vol. 127, no. 1, pp. 1–8, 2010, doi: 10.1016/j.pharmthera.2010.04.006.

[98] R. Feniger-Barish, M. Ran, A. Zaslaver, and A. Ben-Baruch, “Differential modes of regulation of CXC chemokine-induced internalization and recycling of human CXCR1 and CXCR2,” *Cytokine*, vol. 11, no. 12, pp. 996–1009,

1999, doi: 10.1006/cyto.1999.0510.

[99] J. J. Rose, J. F. Foley, P. M. Murphy, and S. Venkatesan, “On the mechanism and significance of ligand-induced internalization of human neutrophil chemokine receptors CXCR1 and CXCR2,” *J. Biol. Chem.*, vol. 279, no. 23, pp. 24372–24386, 2004, doi: 10.1074/jbc.M401364200.

[100] Y. Xu *et al.*, “Endocytosis and membrane receptor internalization: Implication of F-BAR protein Carom,” *Front. Biosci. - Landmark*, vol. 22, no. 9, pp. 1439–1457, 2017, doi: 10.2741/4552.

[101] B. L. Lei and Q. D. Han, “Effect of receptor kinases and arrestins in g protein-coupled receptor regulation,” *Chinese Pharmacol. Bull.*, vol. 15, no. 4, pp. 293–296, 1999.

[102] L. M. Luttrell and R. J. Lefkowitz, “The role of β-arrestins in the termination and transduction of G-protein-coupled receptor signals,” *J. Cell Sci.*, vol. 115, no. 3, pp. 455–465, 2002.

[103] R. M. Richardson, R. J. Marjoram, L. S. Barak, and R. Snyderman, “Role of the Cytoplasmic Tails of CXCR1 and CXCR2 in Mediating Leukocyte Migration, Activation, and Regulation,” *J. Immunol.*, vol. 170, no. 6, pp. 2904–2911, 2003, doi: 10.4049/jimmunol.170.6.2904.

[104] R. M. Richardson, R. A. DuBose, H. Ali, E. D. Tomhave, B. Haribabu, and R. Snyderman, “Regulation of Human Interleukin-8 Receptor A: Identification of a Phosphorylation Site Involved in Modulating Receptor Functions,” *Biochemistry*, vol. 34, no. 43, pp. 14193–14201, 1995, doi: 10.1021/bi00043a025.

[105] S. G. Mueller, J. R. White, W. P. Schraw, V. Lam, and A. Richmond, “Ligand-induced desensitization of the human CXC chemokine receptor-2 is modulated by multiple serine residues in the carboxyl-terminal domain of the receptor,” *J. Biol. Chem.*, vol. 272, no. 13, pp. 8207–8214, 1997, doi: 10.1074/jbc.272.13.8207.

[106] I. Gaidarov, J. G. Krupnick, J. R. Falck, J. L. Benovic, and J. H. Keen, “Arrestin function in G protein-coupled receptor endocytosis requires phosphoinositide binding,” *EMBO J.*, vol. 18, no. 4, pp. 871–881, 1999, doi: 10.1093/emboj/18.4.871.

[107] X. Tian, D. S. Kang, and J. L. Benovic., “β-arrestins and G protein-coupled receptor trafficking,” 2014. doi: 10.1007/978-3-642-41199-1.

[108] M. Azzi *et al.*, “β-arrestin-mediated activation of MAPK by inverse agonists reveals distinct active conformations for G protein-coupled receptors,” *Proc. Natl. Acad. Sci. U. S. A.*, vol. 100, no. 20, pp. 11406–11411, 2003, doi: 10.1073/pnas.1936664100.

[109] K. A. DeFea, J. Zalevsky, M. S. Thoma, O. Dery, R. D. Mullins, and N. W. Bunnett, “β-Arrestin-dependent endocytosis of proteinase-activated receptor 2 is required for intracellular targeting of activated ERK1/2,” *J. Cell Biol.*, vol. 148, no. 6, pp. 1267–1281, 2000, doi: 10.1083/jcb.148.6.1267.

[110] P. H. McDonald, “beta -Arrestin 2: A Receptor-Regulated MAPK Scaffold for the Activation of JNK3,” *Science (80-.).*, vol. 290, no. 5496, pp. 1574–1577, 2000, doi: 10.1126/science.290.5496.1574.

[111] Y. Sun, Z. Cheng, L. Ma, and G. Pei, “β-arrestin2 is critically involved in

CXCR4-mediated chemotaxis, and this is mediated by its enhancement of p38 MAPK activation," *J. Biol. Chem.*, vol. 277, no. 51, pp. 49212–49219, 2002, doi: 10.1074/jbc.M207294200.

[112] L. Ge, S. K. Shenoy, R. J. Lefkowitz, and K. DeFea, "Constitutive protease-activated receptor-2-mediated migration of MDA MB-231 breast cancer cells requires both β-arrestin-1 and -2," *J. Biol. Chem.*, vol. 279, no. 53, pp. 55419–55424, 2004, doi: 10.1074/jbc.M410312200.

[113] M. Zoudilova, J. Min, H. L. Richards, D. Carter, T. Huang, and K. A. DeFea, "B-Arrestins Scaffold Cofilin With Chronophin To Direct Localized Actin Filament Severing and Membrane Protrusions Downstream of Protease-Activated Receptor-2," *J. Biol. Chem.*, vol. 285, no. 19, pp. 14318–14329, 2010, doi: 10.1074/jbc.M109.055806.

[114] L. Ge, Y. Ly, M. Hollenberg, and K. DeFea, "A β-Arrestin-dependent Scaffold Is Associated with Prolonged MAPK Activation in Pseudopodia during Protease-activated Receptor-2-induced Chemotaxis," *J. Biol. Chem.*, vol. 278, no. 36, pp. 34418–34426, 2003, doi: 10.1074/jbc.M300573200.

[115] L. Ma and G. Pei, "B-Arrestin Signaling and Regulation of Transcription," *J. Cell Sci.*, vol. 120, no. 2, pp. 213–218, 2007, doi: 10.1242/jcs.03338.

[116] L. M. Luttrell *et al.*, "β-Arrestin-Dependent Formation of β2 Adrenergic Receptor-Src Protein Kinase Complexes," *Science (80-.).*, vol. 283, no. January, pp. 655–661, 1999.

[117] W. E. Miller, S. Maudsley, S. Ahn, K. D. Khan, L. M. Luttrell, and R. J. Lefkowitz, "β-arrestin1 interacts with the catalytic domain of the tyrosine kinase c-SRC. Role of β-arrestin1-dependent targeting of c-SRC in receptor endocytosis," *J. Biol. Chem.*, vol. 275, no. 15, pp. 11312–11319, 2000, doi: 10.1074/jbc.275.15.11312.

[118] J. Barlic *et al.*, "Regulation of tyrosine kinase activation and granule release through β-arrestin by CXCRI," *Nat. Immunol.*, vol. 1, no. 3, pp. 227–233, 2000, doi: 10.1038/79767.

[119] P. H. Mcdonald *et al.*, "Beta-Arrestin: a receptor-regulated MAPK scaffold for the activation of JNK3," *Science (80-.).*, vol. 290, no. 5496, pp. 1574–1577, 2000.

[120] A. M. Aragay *et al.*, "Monocyte chemoattractant protein-1-induced CCR2B receptor desensitization mediated by the G protein-coupled receptor kinase 2," *Proc. Natl. Acad. Sci. U. S. A.*, vol. 95, no. 6, pp. 2985–2990, 1998, doi: 10.1073/pnas.95.6.2985.

[121] K. A. DeFea, "Stop That Cell! β-Arrestin-Dependent Chemotaxis: A Tale of Localized Actin Assembly and Receptor Desensitization," *Annu. Rev. Physiol.*, vol. 69, no. 1, pp. 535–560, 2007, doi: 10.1146/annurev.physiol.69.022405.154804.

[122] T. J. Povsic, T. A. Kohout, and R. J. Lefkowitz, "β-Arrestin1 Mediates Insulin-like Growth Factor 1 (IGF-1) Activation of Phosphatidylinositol 3-Kinase (PI3K) and Anti-apoptosis," *J. Biol. Chem.*, vol. 278, no. 51, pp. 51334–51339, 2003, doi: 10.1074/jbc.M309968200.

[123] C. M. Revankar, C. M. Vines, D. F. Cimino, and E. R. Prossnitz, "Arrestins block G protein-coupled receptor-mediated apoptosis," *J. Biol. Chem.*, vol. 279, no. 23, pp. 24578–24584, 2004, doi: 10.1074/jbc.M402121200.

[124] D. L. Hunton *et al.*, “β-arrestin 2-dependent angiotensin II type 1A receptor-mediated pathway of chemotaxis,” *Mol. Pharmacol.*, vol. 67, no. 4, pp. 1229–1236, 2005, doi: 10.1124/mol.104.006270.

[125] A. M. Fong, R. T. Premont, R. M. Richardson, Y. R. A. Yu, R. J. Lefkowitz, and D. D. Patel, “Defective lymphocyte chemotaxis in β-arrestin2- and GRK6-deficient mice,” *Proc. Natl. Acad. Sci. U. S. A.*, vol. 99, no. 11, pp. 7478–7483, 2002, doi: 10.1073/pnas.112198299.

[126] K. L. Pierce and R. J. Lefkowitz, “Classical and new roles of β-arrestins in the regulation of G-protein-coupled receptors,” *Nat. Rev. Neurosci.*, vol. 2, no. 10, pp. 727–733, 2001, doi: 10.1038/35094577.

[127] J. p. Paccaud, J. Schifferli, and M. Baggiolini, “NAP-1/IL-8 Induced Up-regulation of CR1 receptors in human neutrophil leukocytes,” *Biochem. Biophys. Res. Commun.*, vol. 166, no. 15, pp. 187–192, 1990.

[128] T. Yoshimura *et al.*, “Purification of a human monocyte-derived neutrophil chemotactic factor that has peptide sequence similarity to other host defense cytokines.,” *Proc. Natl. Acad. Sci. U. S. A.*, vol. 84, no. 24, pp. 9233–9237, 1987, doi: 10.1073/pnas.84.24.9233.

[129] P. Peveri, A. Walz, B. Dewald, and M. Baggiolini, “A novel neutrophil-activating factor produced by human mononucelar phagocytes,” *J. Exp. Med.*, vol. 167, no. 5, pp. 1547–1559, 1988.

[130] P. Peveri, A. Walz, and H. Aschauer, “Purification and amino acid sequencing of naf novel neutrophil-activating factor produced by monocytes,” *Biochem. Biophys. Res. Commun.*, vol. 149, no. 2, pp. 755–761, 1987.

[131] H. Ha, B. Debnath, and N. Neamati, “Role of the CXCL8-CXCR1 / 2 Axis in Cancer and Inflammatory Diseases,” *Theranostics*, vol. 7, no. 6, 2017, doi: 10.7150/thno.15625.

[132] E. Hoffmann, O. Dittrich-Breiholz, H. Holtmann, and M. Kracht, “Multiple control of interleukin-8 gene expression.,” *J. Leukoc. Biol.*, vol. 72, no. 5, pp. 847–55, 2002, [Online]. Available: http://www.ncbi.nlm.nih.gov/pubmed/12429706.

[133] G. Lazennec and A. Richmond, “Chemokines and chemokine receptors: new insights into cancer-related inflammation,” *Trends Mol. Med.*, vol. 16, no. 3, pp. 133–144, 2010, doi: 10.1016/j.molmed.2010.01.003.

[134] L. M. Campbell, P. J. Maxwell, and D. J. J. Waugh, “Rationale and Means to Target Pro-Inflammatory Interleukin-8 (CXCL8) Signaling in Cancer,” *Pharmaceuticals*, pp. 929–959, 2013, doi: 10.3390/ph6080929.

[135] P. J. Maxwell *et al.*, “HIF-1 and NF-κB-mediated upregulation of CXCR1 and CXCR2 expression promotes cell survival in hypoxic prostate cancer cells,” *Oncogene*, vol. 26, no. 52, pp. 7333–7345, 2007, doi: 10.1038/sj.onc.1210536.

[136] T. S. Collins, L. F. Lee, and J. P. Y. Ting, “Paclitaxel up-regulates interleukin-8 synthesis in human lung carcinoma through an NF-κB- and AP-1-dependent mechanism,” *Cancer Immunol. Immunother.*, vol. 49, no. 2, pp. 78–84, 2000, doi: 10.1007/s002620050605.

[137] C. Gabellini *et al.*, “Functional activity of CXCL8 receptors, CXCR1 and CXCR2, on human malignant melanoma progression,” *Eur. J. Cancer*, vol.

45, no. 14, pp. 2618–2627, 2009, doi: 10.1016/j.ejca.2009.07.007.

[138] O. Holz *et al.*, “SCH527123, a novel CXCR2 antagonist, inhibits ozone-induced neutrophilia in healthy subjects,” *Eur. Respir. J.*, vol. 35, no. 3, pp. 564–570, 2010, doi: 10.1183/09031936.00048509.

[139] D. Gales, C. Clark, U. Manne, and T. Samuel, “The Chemokine CXCL8 in Carcinogenesis and Drug Response.,” *ISRN Oncol.*, vol. 2013, p. 859154, 2013, doi: 10.1155/2013/859154.

[140] S. Manna and G. Ramesh, “Interleukin-8 Induces Nuclear Transcription Factor-κB through a TRAF6-dependent Pathway,” *J. Biol. Chem.*, vol. 280, no. 8, pp. 7010–7021, 2005.

[141] M. Karin and F. R. Greten, “NF-κB: Linking inflammation and immunity to cancer development and progression,” *Nat. Rev. Immunol.*, vol. 5, no. 10, pp. 749–759, 2005, doi: 10.1038/nri1703.

[142] A. Li, S. Dubey, M. L. Varney, B. J. Dave, and R. K. Singh, “IL-8 Directly Enhanced Endothelial Cell Survival, Proliferation, and Matrix Metalloproteinases Production and Regulated Angiogenesis,” *J. Immunol.*, vol. 170, no. 6, pp. 3369–3376, 2003, doi: 10.4049/jimmunol.170.6.3369.

[143] D. J. J. Waugh and C. Wilson, “The interleukin-8 pathway in cancer,” *Clin. Cancer Res.*, vol. 14, no. 21, pp. 6735–6741, 2008, doi: 10.1158/1078-0432.CCR-07-4843.

[144] A. Li, M. L. Varney, J. Valasek, M. Godfrey, B. J. Dave, and R. K. Singh, “Autocrine role of interleukin-8 in induction of endothelial cell proliferation, survival, migration and MMP-2 production and angiogenesis,” *Angiogenesis*, vol. 8, no. 1, pp. 63–71, 2005, doi: 10.1007/s10456-005-5208-4.

[145] S. Singh, A. P. Singh, B. Sharma, L. B. Owen, and R. K. Singh, “CXCL8 and its cognate receptors in melanoma progression and metastasis,” *Futur. Oncol.*, vol. 6, no. 1, pp. 111–116, 2010, doi: 10.2217/fon.09.128.

[146] Y. M. Zhu, S. J. Webster, D. Flower, and P. J. Woll, “Interleukin-8/CXCL8 is a growth factor for human lung cancer cells,” *Br. J. Cancer*, vol. 91, no. 11, pp. 1970–1976, 2004, doi: 10.1038/sj.bjc.6602227.

[147] D. Schadendorf, A. Möller, B. Algermissen, M. Worm, M. Sticherling, and B. M. Czarnetzki, “IL-8 produced by human malignant melanoma cells in vitro is an essential autocrine growth factor.,” *J. Immunol.*, vol. 151, no. 5, pp. 2667–75, 1993, [Online]. Available: http://www.ncbi.nlm.nih.gov/pubmed/8360485.

[148] M. Miyamoto, Y. Shimizu, K. Okada, Y. Kashii, K. Higuchi, and A. Watanabe, “Effect of interleukin-8 on production of tumor-associated substances and autocrine growth of human liver and pancreatic cancer cells,” *Cancer Immunol. Immunother.*, vol. 47, no. 1, pp. 47–57, 1998, doi: 10.1007/s002620050503.

[149] R. Brew, J. S. Erikson, D. C. West, A. R. Kinsella, J. Slavin, and S. E. Christmas, “Interleukin-8 as an autocrine growth factor for human colon carcinoma cells in vitro,” *Cytokine*, vol. 12, no. 1, pp. 78–85, 2000, doi: 10.1006/cyto.1999.0518.

[150] O. Oladipo *et al.*, “The expression and prognostic impact of CXC-chemokines in stage II and III colorectal cancer epithelial and stromal tissue,” *Br. J. Cancer*, vol. 104, no. 3, pp. 480–487, 2011, doi: 10.1038/sj.bjc.6606055.

[151] W. E. Holmes *et al.*, “Structure and Functional Expression of a Human Interleukin-8 Receptor,” *Science (80-.).*, vol. 253, no. 5025, pp. 1278–1280, 1991.

[152] P. M. Murphy and H. L. Tiffany, “Cloning of Complementary DNA Encoding a Functional Human Interleukin-8 Receptor,” *Science (80-.).*, vol. 253, no. 5025, pp. 1280–1283, 1991.

[153] P. M. Murphy, “The Molecular Biology of Leukocyte Chemoattractant Receptors,” *Annu. Rev. Immunol.*, vol. 12, no. 1, pp. 593–633, 1994, doi: 10.1146/annurev.iy.12.040194.003113.

[154] S. K. Ahuja, J. C. Lee, and P. M. Murphy, “CXC chemokines bind to unique sets of selectivity determinants that can function independently and are broadly distributed on multiple domains of human interleukin-8 receptor B: Determinants of high affinity binding and receptor activation are distinct,” *J. Biol. Chem.*, vol. 271, no. 1, pp. 225–232, 1996, doi: 10.1074/jbc.271.1.225.

[155] D. J. Brat, A. C. Bellail, and E. G. Van Meir, “The role of interleukin-8 and its receptors in gliomagenesis and tumoral angiogenesis,” *Neuro. Oncol.*, vol. 7, no. 2, pp. 122–133, 2005, doi: 10.1215/s1152851704001061.

[156] S. K. Ahuja and P. M. Murphy, “The CXC chemokines growth-regulated oncogene (GRO) α, GROβ, GROγ, neutrophil-activating peptide-2, and epithelial cell-derived neutrophil- activating peptide-78 are potent agonists for the type B, but not the type A, human interleukin-8 receptor,” *J. Biol. Chem.*, vol. 271, no. 34, pp. 20545–20550, 1996, doi: 10.1074/jbc.271.34.20545.

[157] G. H. Fan, W. Yang, J. Sai, and A. Richmond, “Phosphorylation-independent Association of CXCR2 with the Protein Phosphatase 2A Core Enzyme,” *J. Biol. Chem.*, vol. 276, no. 20, pp. 16960–16968, 2001, doi: 10.1074/jbc.M009292200.

[158] R. M. Richardson, B. C. Pridgen, B. Haribabu, H. Ali, and R. Snyderman, “Differential cross-regulation of the human chemokine receptors CXCR1 and CXCR2. Evidence for time-dependent signal generation,” *J. Biol. Chem.*, vol. 273, no. 37, pp. 23830–23836, 1998, doi: 10.1074/jbc.273.37.23830.

[159] K. Rajarathnam, G. N. Prado, H. Fernando, I. Clark-Lewis, and J. Navarro, “Probing receptor binding activity of interleukin-8 dimer using a disulfide trap,” *Biochemistry*, vol. 45, no. 25, pp. 7882–7888, 2006, doi: 10.1021/bi0605944.

[160] I. Clark-lewis, B. Dewaldn, M. Loetschefl, and B. Mosefl, “Structural Requirements for interleukin-8 Function Identified by Design of Analogs and CXC Chemokine Hybrids,” *J. Biol. Chem.*, vol. 269, no. 23, pp. 16075–16081, 1994.

[161] M. W. Nasser, S. K. Raghuwanshi, D. J. Grant, V. R. Jala, K. Rajarathnam, and R. M. Richardson, “Differential Activation and Regulation of CXCR1 and CXCR2 by CXCL8 Monomer and Dimer,” *J. Immunol.*, vol. 183, no. 5, pp. 3425–3432, 2009, doi: 10.4049/jimmunol.0900305.

[162] R. Bertini *et al.*, “Noncompetitive allosteric inhibitors of the inflammatory chemokine receptors CXCR1 and CXCR2: Prevention of reperfusion injury,” *Proc. Natl. Acad. Sci. U. S. A.*, vol. 101, no. 32, pp. 11791–11796, 2004, doi: 10.1073/pnas.0402090101.

[163] W. Gonsiorek *et al.*, “Pharmacological characterization of Sch527123, a potent allosteric CXCR1/CXCR2 antagonist.,” *J. Pharmacol. Exp. Ther.*, vol.

322, no. 2, pp. 477–85, 2007, doi: 10.1124/jpet.106.118927.

[164] J. M. Wang, G. Taraboletti, K. Matsushima, J. Van Damme, and A. Mantovani, “Induction of haptotactic migration of melanoma cells by neutrophil activating protein/interleukin-8,” *Biochem. Biophys. Res. Commun.*, vol. 169, no. 1, pp. 165–170, 1990, doi: 10.1016/0006-291X(90)91449-3.

[165] G. Venkatakrishnan, R. Salgia, and J. E. Groopman, “Chemokine Receptors CXCR-1/2 Activate Mitogen-activated Protein Kinase via the Epidermal Growth Factor Receptor in Ovarian Cancer Cells,” *J. Biol. Chem.*, vol. 275, no. 10, pp. 6868–6875, 2000, [Online]. Available: http://www.jbc.org/cgi/content/full/275/10/6868.

[166] D. A. P. de C. Zuccari *et al.*, “An immunohistochemical study of interleukin-8 (IL-8) in breast cancer,” *Acta Histochem.*, vol. 114, no. 6, pp. 571–576, 2012, doi: 10.1016/j.acthis.2011.10.007.

[167] N. Todorović-Raković and J. Milovanović, “Interleukin-8 in breast cancer progression,” *J. Interf. Cytokine Res.*, vol. 33, no. 10, pp. 563–570, 2013, doi: 10.1089/jir.2013.0023.

[168] M. Rotondi, F. Coperchini, F. Latrofa, and L. Chiovato, “Role of chemokines in thyroid cancer microenvironment: Is CXCL8 the main player?,” *Front. Endocrinol. (Lausanne).*, vol. 9, no. JUL, pp. 1–14, 2018, doi: 10.3389/fendo.2018.00314.

[169] Y. Kitadai *et al.*, “Expression of interleukin-8 correlates with vascularity in human gastric carcinomas,” *Am. J. Pathol.*, vol. 152, no. 1, pp. 93–100, 1998.

[170] F. A. Ferrer *et al.*, “Angiogenesis and prostate cancer: In vivo and in vitro expression of angiogenesis factors by prostate cancer cells,” *Urology*, vol. 51, no. 1, pp. 161–167, 1998, doi: 10.1016/S0090-4295(97)00491-3.

[171] Y. Lin *et al.*, “Identification of interleukin-8 as estrogen receptor-regulated factor involved in breast cancer invasion and angiogenesis by protein arrays,” *Int. J. Cancer*, vol. 109, no. 4, pp. 507–515, 2004, doi: 10.1002/ijc.11724.

[172] Y. Chen *et al.*, “ERβ and PEA3 co-activate IL-8 expression and promote the invasion of breast cancer cells,” *Cancer Biol. Ther.*, vol. 11, no. 5, pp. 497–511, 2011, doi: 10.4161/cbt.11.5.14667.

[173] J. Folkman, “Angiogenesis in cancer, vascular, rheumatoid and other disease,” *Nat. Med.*, vol. 1, pp. 27–31, 1995.

[174] D. B. Gurevich *et al.*, “Live imaging of wound angiogenesis reveals macrophage orchestrated vessel sprouting and regression,” *EMBO*, vol. 37, no. June, pp. 1–23, 2018, doi: 10.15252/embj.201797786.

[175] D. Hanahan and J. Folkman, “Patterns and Emerging Mechanisms of the Angiogenic Switch during Tumorigenesis,” *Cell*, vol. 86, no. August, pp. 353–364, 1996.

[176] S. Singh, S. Wu, M. Varney, A. P. Singh, and R. K. Singh, “CXCR1 and CXCR2 silencing modulates CXCL8-dependent endothelial cell proliferation, migration and capillary-like structure formation,” *Microvasc. Res.*, vol. 82, no. 3, pp. 318–325, 2011, doi: 10.1016/j.mvr.2011.06.011.

[177] M. L. Petreaca, M. Yao, Y. Liu, D. Kathryn, and M. Martins-Green, “Transactivation of Vascular Endothelial Growth Factor Receptor-2 by Interleukin-8 (IL-8/CXCL8) Is Required for IL-8/CXCL8-induced Endothelial

Permeability," *Mol. Biol. Cell*, vol. 18, no. 12, pp. 5014–5023, 2007.

[178] G. Niu and X. Chen, "Why Integrin as a Primary Target for Imaging and Therapy," *Theranostics*, vol. 1, pp. 30–47, 2012, doi: 10.7150/thno/v01p0030.

[179] M. P. Keane, J. A. Belperio, Y. Y. Xue, M. D. Burdick, and R. M. Strieter, "Depletion of CXCR2 Inhibits Tumor Growth and Angiogenesis in a Murine Model of Lung Cancer," *J. Immunol.*, vol. 172, no. 5, pp. 2853–60, 2004, doi: 10.4049/jimmunol.172.5.2853.

[180] A. Li, X. J. Cheng, A. Moro, R. K. Singh, O. J. Hines, and G. Eibl, "CXCR2-Dependent Endothelial Progenitor Cell Mobilization in Pancreatic Cancer Growth 1," *Transl. Oncol.*, vol. 4, no. 1, pp. 20–28, 2011, doi: 10.1593/tlo.10184.

[181] C. L. Addison *et al.*, " The CXC Chemokine Receptor 2, CXCR2, Is the Putative Receptor for ELR + CXC Chemokine-Induced Angiogenic Activity ," *J. Immunol.*, vol. 165, no. 9, pp. 5269–5277, 2000, doi: 10.4049/jimmunol.165.9.5269.

[182] J. Milovanovic, N. Todorovic-Rakovic, and Z. Abu Rabi, "The prognostic role of interleukin-8 (IL-8) and matrix metalloproteinases -2 and -9 in lymph node-negative untreated breast cancer patients," *J. B.U.ON.*, vol. 18, no. 4, pp. 866–873, 2013.

[183] F. Balkwill and A. Mantovani, "Inflammation and cancer: Back to Virchow?," *Lancet*, vol. 357, no. 9255, pp. 539–545, 2001, doi: 10.1016/S0140-6736(00)04046-0.

[184] Y. Zhang, L. Wang, M. Zhang, M. Jin, C. Bai, and X. Wang, "Potential mechanism of interleukin-8 production from lung cancer cells: An involvement of EGF-EGFR-PI3K-Akt-Erk pathway," *J. Cell. Physiol.*, vol. 227, no. 1, pp. 35–43, 2012, doi: 10.1002/jcp.22722.

[185] J. E. De Larco, B. R. K. Wuertz, and L. T. Furcht, "The potential role of neutrophils in promoting the metastatic phenotype of tumors releasing interleukin-8," *Clin. Cancer Res.*, vol. 10, no. 15, pp. 4895–4900, 2004, doi: 10.1158/1078-0432.CCR-03-0760.

[186] J. J. Christiansen and A. K. Rajasekaran, "Reassessing epithelial to mesenchymal transition as a prerequisite for carcinoma invasion and metastasis," *Cancer Res.*, vol. 66, no. 17, pp. 8319–8326, 2006, doi: 10.1158/0008-5472.CAN-06-0410.

[187] N. Mukaida, "Pathophysiological roles of interleukin-8/CXCL8 in pulmonary diseases," *Am. J. Physiol. Lung Cell. Mol. Physiol.*, vol. 284, no. 4, pp. L566-77, 2003, doi: 10.1152/ajplung.00233.2002.

[188] A. S. Khazali, A. M. Clark, and A. Wells, "Inflammatory cytokine IL-8/CXCL8 promotes tumour escape from hepatocyte-induced dormancy," *Br. J. Cancer*, vol. 118, no. 4, pp. 566–576, 2018, doi: 10.1038/bjc.2017.414.

[189] A. Kamalakar *et al.*, "Circulating Interleukin-8 levels explain breast cancer osteolysis in mice and humans," *Bone*, vol. 61, pp. 176–185, 2015, doi: 10.1016/j.bone.2014.01.015.Circulating.

[190] M. S. Bendre, D. C. Montague, T. Peery, N. S. Akel, D. Gaddy, and L. J. Suva, "Interleukin-8 stimulation of osteoclastogenesis and bone resorption is a mechanism for the increased osteolysis of metastatic bone disease," *Bone*,

vol. 33, no. 1, pp. 28–37, 2003, doi: 10.1016/S8756-3282(03)00086-3.

[191] N. Sunaga *et al.*, “Clinicopathological and prognostic significance of interleukin-8 expression and its relationship to KRAS mutation in lung adenocarcinoma.,” *Br. J. Cancer*, vol. 110, no. 8, pp. 2047–2053, 2014, doi: 10.1038/bjc.2014.110.

[192] A. Yuan, C. J. Yu, K. T. Luh, S. H. Kuo, Y. C. Lee, and P. C. Yang, “Aberrant p53 expression correlates with expression of vascular endothelial growth factor mRNA and interleukin-8 mRNA and neoangiogenesis in non-small-cell lung cancer,” *J. Clin. Oncol.*, vol. 20, no. 4, pp. 900–910, 2002, doi: 10.1200/JCO.20.4.900.

[193] Q. Shi, J. L. Abbruzzese, S. Huang, I. J. Fidler, Q. Xiong, and K. Xie, “Constitutive and inducible interleukin 8 expression by hypoxia and acidosis renders human pancreatic cancer cells more tumorigenic and metastatic,” *Clin. Cancer Res.*, vol. 5, no. 11, pp. 3711–3721, 1999.

[194] I. H. Benoy *et al.*, “Increased serum interleukin-8 in patients with early and metastatic breast cancer correlates with early dissemination and survival,” *Clin. Cancer Res.*, vol. 10, no. 21, pp. 7157–7162, 2004, doi: 10.1158/1078-0432.CCR-04-0812.

[195] J. Heidemann *et al.*, “Angiogenic effects of interleukin 8 (CXCL8) in human intestinal microvascular endothelial cells are mediated by CXCR2,” *J. Biol. Chem.*, vol. 278, no. 10, pp. 8508–8515, 2003, doi: 10.1074/jbc.M208231200.

[196] R. I. Fernando, M. D. Castillo, M. Litzinger, D. H. Hamilton, and C. Palena, “IL-8 signaling plays a critical role in the epithelial-mesenchymal transition of human carcinoma cells,” *Cancer Res.*, vol. 71, no. 15, pp. 5296–5306, 2011, doi: 10.1158/0008-5472.CAN-11-0156.

[197] J. David, C. Dominguez, D. Hamilton, and C. Palena, “The IL-8/IL-8R Axis: A Double Agent in Tumor Immune Resistance,” *Vaccines*, vol. 4, no. 3, p. 22, 2016, doi: 10.3390/vaccines4030022.

[198] B. Y. A. D. Luster and J. V Ravetch, “Biochemical characterization of gamma interferon-inducible cytokine,” *J. Exp. Med.*, vol. 166, no. October, pp. 1084–1097, 1987.

[199] J. A. Belperio *et al.*, “CXC chemokines in angiogenesis,” *J. Leukoc. Biol.*, vol. 68, no. 1, pp. 1–8, 2000, doi: 10.1189/jlb.0805480.

[200] P. Van Den Borne, P. H. A. Quax, I. E. Hoefer, and G. Pasterkamp, “The multifaceted functions of CXCL10 in cardiovascular disease,” *Biomed Res. Int.*, vol. 2014, 2014, doi: 10.1155/2014/893106.

[201] A. Antonelli, S. M. Ferrari, D. Giuggioli, E. Ferrannini, C. Ferri, and P. Fallahi, “Chemokine (C-X-C motif) ligand (CXCL)10 in autoimmune diseases,” *Autoimmun. Rev.*, vol. 13, no. 3, pp. 272–280, 2014, doi: 10.1016/j.autrev.2013.10.010.

[202] A. Pellegrino *et al.*, “CXCR3-binding chemokines in multiple myeloma,” vol. 207, pp. 221–227, 2004, doi: 10.1016/j.canlet.2003.10.036.

[203] B. K. K. Lo, M. Yu, D. Zloty, B. Cowan, J. Shapiro, and K. J. McElwee, “CXCR3/ligands are significantly involved in the tumorigenesis of basal cell carcinomas,” *Am. J. Pathol.*, vol. 176, no. 5, pp. 2435–2446, 2010, doi:

10.2353/ajpath.2010.081059.

[204] J. M. Farber, “A macrophage mRNA selectively induced by y-interferon encodes a member of the platelet factor 4 family of cytokines,” vol. 87, no. July, pp. 5238–5242, 1990.

[205] L. Lasagni *et al.*, “An alternatively spliced variant of CXCR3 mediates the inhibition of endothelial cell growth induced by IP-10, Mig, and I-TAC, and acts as functional receptor for platelet factor 4,” *J. Exp. Med.*, vol. 197, no. 11, pp. 1537–1549, 2003, doi: 10.1084/jem.20021897.

[206] Y. A. Berchiche and T. P. Sakmar, “CXC chemokine receptor 3 alternative splice variants selectively activate different signaling pathways,” *Mol. Pharmacol.*, vol. 90, no. 4, pp. 483–495, 2016, doi: 10.1124/mol.116.105502.

[207] A. Steen, O. Larsen, S. Thiele, and M. M. Rosenkilde, “Biased and G protein-independent signaling of chemokine receptors,” *Front. Immunol.*, vol. 5, no. JUN, pp. 1–13, 2014, doi: 10.3389/fimmu.2014.00277.

[208] M. O. Aksoy *et al.*, “CXCR3 surface expression in human airway epithelial cells: Cell cycle dependence and effect on cell proliferation,” *Am. J. Physiol. - Lung Cell. Mol. Physiol.*, vol. 290, no. 5, pp. 909–919, 2006, doi: 10.1152/ajplung.00430.2005.

[209] A. Korniejewska, A. J. Mcknight, Z. Johnson, M. L. Watson, and S. G. Ward, “Expression and agonist responsiveness of CXCR3 variants in human T lymphocytes,” *Immunology*, vol. 132, no. 4, pp. 503–515, 2011, doi: 10.1111/j.1365-2567.2010.03384.x.

[210] S. Shahabuddin *et al.*, “CXCR3 chemokine receptor-induced chemotaxis in human airway epithelial cells: Role of p38 MAPK and PI3K signaling pathways,” *Am. J. Physiol. - Cell Physiol.*, vol. 291, no. 1, 2006, doi: 10.1152/ajpcell.00441.2005.

[211] A. Bonacchi *et al.*, “Signal transduction by the chemokine receptor CXCR3: Activation of Ras/ERK, Src, and phosphatidylinositol 3-kinase/Akt controls cell migration and proliferation in human vascular pericytes,” *J. Biol. Chem.*, vol. 276, no. 13, pp. 9945–9954, 2001, doi: 10.1074/jbc.M010303200.

[212] R. Ji *et al.*, “Human type II pneumocyte chemotactic responses to CXCR3 activation are mediated by splice variant A,” *Am. J. Physiol. - Lung Cell. Mol. Physiol.*, vol. 294, no. 6, pp. 1187–1197, 2008, doi: 10.1152/ajplung.00388.2007.

[213] P. Méndez-Samperio, A. Pérez, and L. Rivera, “Mycobacterium bovis Bacillus Calmette-Guérin (BCG)-induced activation of PI3K/Akt and NF-kB signaling pathways regulates expression of CXCL10 in epithelial cells,” *Cell. Immunol.*, vol. 256, no. 1–2, pp. 12–18, 2009, doi: 10.1016/j.cellimm.2008.12.002.

[214] Q. Shen, R. Zhang, and N. R. Bhat, “MAP kinase regulation of IP10/CXCL10 chemokine gene expression in microglial cells,” *Brain Res.*, vol. 1086, no. 1, pp. 9–16, 2006, doi: 10.1016/j.brainres.2006.02.116.

[215] S. G. Kelsen *et al.*, “The chemokine receptor CXCR3 and its splice variant are expressed in human airway epithelial cells,” *Am. J. Physiol. - Lung Cell. Mol. Physiol.*, vol. 287, no. 3 31-3, pp. 584–591, 2004, doi: 10.1152/ajplung.00453.2003.

[216] S. V. Maru *et al.*, “Chemokine production and chemokine receptor expression

by human glioma cells: Role of CXCL10 in tumour cell proliferation," *J. Neuroimmunol.*, vol. 199, no. 1–2, pp. 35–45, 2008, doi: 10.1016/j.jneuroim.2008.04.029.

[217] R. A. Colvin, G. S. V. Campanella, J. Sun, and A. D. Luster, "Intracellular domains of CXCR3 that mediate CXCL9, CXCL10, and CXCL11 function," *J. Biol. Chem.*, vol. 279, no. 29, pp. 30219–30227, 2004, doi: 10.1074/jbc.M403595200.

[218] L. Liu, M. K. Callahan, D. R. Huang, and R. M. Ransohoff, "Chemokine Receptor CXCR3: An Unexpected Enigma," *Curr. Top. Dev. Biol.*, vol. 68, no. 05, pp. 149–181, 2005, doi: 10.1016/S0070-2153(05)68006-4.

[219] K. Eichel, D. Jullié, and M. Von Zastrow, "β -Arrestin drives MAP kinase signalling from clathrin-coated structures after GPCR dissociation," no. January, 2016, doi: 10.1038/ncb3307.

[220] P. Van Den Borne, P. H. A. Quax, I. E. Hoefer, and G. Pasterkamp, "The multifaceted functions of CXCL10 in cardiovascular disease," *Biomed Res. Int.*, vol. 2014, no. July, 2014, doi: 10.1155/2014/893106.

[221] P. Sfriso *et al.*, "Epithelial CXCR3-B Regulates Chemokines Bioavailability in Normal, but Not in Sjögren's Syndrome, Salivary Glands," *J. Immunol.*, vol. 176, no. 4, pp. 2581–2589, 2006, doi: 10.4049/jimmunol.176.4.2581.

[222] D. Datta *et al.*, "Ras-induced modulation of CXCL10 and its receptor splice variant CXCR3-B in MDA-MB-435 and MCF-7 cells: Relevance for the development of human breast cancer," *Cancer Res.*, vol. 66, no. 19, pp. 9509–9518, 2006, doi: 10.1158/0008-5472.CAN-05-4345.

[223] N. Giuliani *et al.*, "CXCR3 and its binding chemokines in myeloma cells: expression of isoforms and potential relationships with myeloma cell proliferation and survival," *Haematologica*, vol. 11, no. 91, pp. 1489–1497, 2006.

[224] S. Grethe and M. I. Pörn-Ares, "p38 MAPK regulates phosphorylation of Bad via PP2A-dependent suppression of the MEK1/2-ERK1/2 survival pathway in TNF-α induced endothelial apoptosis," *Cell. Signal.*, vol. 18, no. 4, pp. 531–540, 2006, doi: 10.1016/j.cellsig.2005.05.023.

[225] I. Petrai *et al.*, "Activation of p38MAPK mediates the angiostatic effect of the chemokine receptor CXCR3-B," *Int. J. Biochem. Cell Biol.*, vol. 40, no. 9, pp. 1764–1774, 2008, doi: 10.1016/j.biocel.2008.01.008.

[226] Q. Wu, R. Dhir, and A. Wells, "Altered CXCR3 isoform expression regulates prostate cancer cell migration and invasion," *Mol. Cancer*, vol. 11, pp. 1–16, 2012, doi: 10.1186/1476-4598-11-3.

[227] J. E. Ehlert, C. A. Addison, M. D. Burdick, S. L. Kunkel, and R. M. Strieter, "Identification and Partial Characterization of a Variant of Human CXCR3 Generated by Posttranscriptional Exon Skipping," *J. Immunol.*, vol. 173, no. 10, pp. 6234–6240, 2004, doi: 10.4049/jimmunol.173.10.6234.

[228] M. Furuya, T. Suyama, and H. Usui, "Up-regulation of CXC chemokines and their receptors : implications for proinflammatory microenvironments of ovarian carcinomas and endometriosis B," pp. 1676–1687, 2007, doi: 10.1016/j.humpath.2007.03.023.

[229] V. Booth, D. W. Keizer, M. B. Kamphuis, I. Clark-Lewis, and B. D. Sykes,

"The CXCR3 binding chemokine IP-10/CXCL10: Structure and receptor interactions," *Biochemistry*, vol. 41, no. 33, pp. 10418–10425, 2002, doi: 10.1021/bi026020q.

[230] M. Metzemaekers, V. Vanheule, R. Janssens, S. Struyf, and P. Proost, "Overview of the mechanisms that may contribute to the non-redundant activities of interferon-inducible CXC chemokine receptor 3 ligands," *Front. Immunol.*, vol. 8, no. JAN, 2018, doi: 10.3389/fimmu.2017.01970.

[231] S. Kim, M. Bakre, H. Yin, and J. A. Varner, "Inhibition of endothelial cell survival and angiogenesis by protein kinase A," *J. Clin. Invest.*, vol. 110, no. 7, pp. 933–941, 2002, doi: 10.1172/JCI0214268.

[232] M. K. Tulic *et al.*, "Innate lymphocyte-induced CXCR3B-mediated melanocyte apoptosis is a potential initiator of T-cell autoreactivity in vitiligo," *Nat. Commun.*, vol. 10, no. 1, pp. 1–13, 2019, doi: 10.1038/s41467-019-09963-8.

[233] J. S. Smith *et al.*, "C-X-C Motif Chemokine Receptor 3 Splice Variants Differentially Activate Beta-Arrestins to Regulate Downstream Signaling Pathways s," *Am. Soc. Pharmacol. Exp. Ther.*, vol. 92, no. August, pp. 136–150, 2017.

[234] G. S. V. Campanella, R. A. Colvin, and A. D. Luster, "CXCL10 can inhibit endothelial cell proliferation independently of CXCR3," *PLoS One*, vol. 5, no. 9, pp. 1–10, 2010, doi: 10.1371/journal.pone.0012700.

[235] S. Struyf *et al.*, "Angiostatic and chemotactic activities of the CXC chemokine CXCL4L1 (platelet factor-4 variant) are mediated by CXCR3," *Blood*, vol. 117, no. 2, pp. 480–488, 2011, doi: 10.1182/blood-2009-11-253591.

[236] M. Furuya *et al.*, "Differential expression patterns of CXCR3 variants and corresponding CXC chemokines in clear cell ovarian cancers and endometriosis," *Gynecol. Oncol.*, vol. 122, no. 3, pp. 648–655, 2011, doi: 10.1016/j.ygyno.2011.05.034.

[237] M. Liu, S. Guo, and J. K. Stiles, "The emerging role of CXCL10 in cancer (Review)," *Oncol. Lett.*, vol. 2, no. 4, pp. 583–589, 2011, doi: 10.3892/ol.2011.300.

[238] S. C. Wightman *et al.*, "Oncogenic CXCL10 signalling drives metastasis development and poor clinical outcome," *Br. J. Cancer*, vol. 113, no. 2, pp. 327–335, 2015, doi: 10.1038/bjc.2015.193.

[239] M. Baggiolini, "Chemokines in pathology and medicine," 2001.

[240] K. Kawada *et al.*, "Pivotal role of CXCR3 in melanoma cell metastasis to lymph nodes," *Cancer Res.*, vol. 64, no. 11, pp. 4010–4017, 2004, doi: 10.1158/0008-5472.CAN-03-1757.

[241] M. M. Robledo *et al.*, "Expression of Functional Chemokine Receptors CXCR3 and CXCR4 on Human Melanoma Cells," *J. Biol. Chem.*, vol. 276, no. 48, pp. 45098–45105, 2001, doi: 10.1074/jbc.M106912200.

[242] L. Trentin *et al.*, "The chemokine receptor CXCR3 is expressed on malignant B cells and mediates chemotaxis," *J. Clin. Invest.*, vol. 104, no. 1, pp. 115–121, 1999, doi: 10.1172/JCI7335.

[243] K. A. Norton, A. S. Popel, and N. B. Pandey, "Heterogeneity of chemokine cell-surface receptor expression in triple-negative breast cancer," *Am. J. Cancer Res.*, vol. 5, no. 4, pp. 1295–1307, 2015.

[244] S. Y. Shin, J.-S. Nam, Y. Lim, and Y. H. Lee, “TNFα-exposed Bone Marrow-derived Mesenchymal Stem Cells Promote Locomotion of MDA-MB-231 Breast Cancer Cells through Transcriptional Activation of CXCR3 Ligand Chemokines,” *J. Biol. Chem.*, vol. 285, no. 40, pp. 30731–30740, 2010, doi: 10.1074/jbc.M110.128124.

[245] B. D. A. Arenberg *et al.*, “Interferon-gamma-inducible protein 10 (IP-10) is an angiostatic factor that inhibits human non-small cell lung cancer (NSCLC) tumorigenesis and spontaneous metastases.,” *J. Exp. Med.*, vol. 184, no. September, pp. 981–992, 1996.

[246] C. S. Tannenbaum *et al.*, “The CXC Chemokines IP-10 and Mig Are Necessary for IL-12-Mediated Regression of the Mouse RENCA Tumor,” *J. Immunol.*, vol. 161, no. 2, pp. 927–932, 1998.

[247] M. Teichmann, B. Meyer, A. Beck, and G. Niedobitek, “Expression of the interferon-inducible chemokine IP-10 (CXCL10), a chemokine with proposed anti-neoplastic functions , in Hodgkin lymphoma and nasopharyngeal carcinoma,” *J. Pathol.*, vol. 206, no. March, pp. 68–75, 2005, doi: 10.1002/path.1745.

[248] P. Romagnani *et al.*, “Cell cycle – dependent expression of CXC chemokine receptor 3 by endothelial cells mediates angiostatic activity Find the latest version : Cell cycle – dependent expression of CXC chemokine receptor 3 by endothelial cells mediates angiostatic activity,” *J. Clin. Invest.*, vol. 107, no. 1, pp. 53–63, 2001.

[249] X. Ma *et al.*, “CXCR3 expression is associated with poor survival in breast cancer and promotes metastasis in a murine model,” *Mol. Cancer Ther.*, vol. 8, no. 3, pp. 490–498, 2009, doi: 10.1158/1535-7163.MCT-08-0485.

[250] E. Pradelli *et al.*, “Antagonism of chemokine receptor CXCR3 inhibits osteosarcoma metastasis to lungs,” *Int. J. Cancer*, vol. 125, no. 11, pp. 2586–2594, 2009, doi: 10.1002/ijc.24665.

[251] D. Jones, R. J. Benjamin, A. Shahsafaei, and D. M. Dorfman, “The chemokine receptor CXCR3 is expressed in a subset of B-cell lymphomas and is a marker of B-cell chronic lymphocytic leukemia,” *Blood, J. Am. Soc. Hematol.*, vol. 95, no. 2, pp. 627–632, 2000.

[252] K. Kawada *et al.*, “Chemokine receptor CXCR3 promotes colon cancer metastasis to lymph nodes,” *Oncogene*, vol. 26, no. 32, pp. 4679–4688, 2007, doi: 10.1038/sj.onc.1210267.

[253] B. Cambien *et al.*, “Organ-specific inhibition of metastatic colon carcinoma by CXCR3 antagonism,” *Br. J. Cancer*, vol. 100, no. 11, pp. 1755–1764, 2009, doi: 10.1038/sj.bjc.6605078.

[254] G. Boulday, Z. Haskova, M. E. J. Reinders, S. Pal, and D. M. Briscoe, “Vascular Endothelial Growth Factor-Induced Signaling Pathways in Endothelial Cells That Mediate Overexpression of the Chemokine IFN-γ-Inducible Protein of 10 kDa In Vitro and In Vivo,” *J. Immunol.*, vol. 176, no. 5, pp. 3098–3107, 2006, doi: 10.4049/jimmunol.176.5.3098.

[255] R. M. Strieter, M. D. Burdick, J. Mestas, B. Gomperts, M. P. Keane, and J. A. Belperio, “Cancer CXC chemokine networks and tumour angiogenesis,” *Eur. J. Cancer*, vol. 42, no. 6, pp. 768–778, 2006, doi: 10.1016/j.ejca.2006.01.006.

[256] J. Yang and A. Richmond, “The Angiostatic Activity of Interferon-Inducible

Protein-10/ CXCL10 in Human Melanoma Depends on Binding to CXCR3 but Not to Glycosaminoglycan," *Cancer*, vol. 9, no. 6, pp. 846–855, 2009, doi: 10.1016/j.ymthe.2004.01.010.The.

[257] M. D. Burdick *et al.*, "CXCL11 Attenuates Bleomycin-induced Pulmonary Fibrosis via Inhibition of Vascular Remodeling," *Am. J. Respir. Crit. Care Med.*, vol. 171, no. 3, pp. 261–268, 2005, doi: 10.1164/rccm.200409-1164OC.

[258] S. Mukherjee, *The emperor of all maladies: a biography of cancer.* Simon and Schuster., 2010.

[259] G. M. T. Cheetham, "Novel protein kinases and molecular mechanisms of autoinhibition," *Curr. Opin. Struct. Biol.*, vol. 14, no. November, pp. 700–705, 2004, doi: 10.1016/j.sbi.2004.10.011.

[260] A. Levitzki, "Signal-transduction therapy A novel approach to disease management," *FEBS*, vol. 226, pp. 1–13, 1994.

[261] D. R. Knighton *et al.*, "Crystal Structure of the Catalytic Subunit of Cyclic Adenosine Monophosphate-Dependent Protein Kinase," *Science (80-.).*, vol. 253, no. 5018, pp. 407–414, 1991.

[262] I. Shchemelinin, L. Šefc, and E. Nečas, "Protein kinases, their function and implication in cancer and other diseases," *Folia Biol. (Praha).*, vol. 52, no. 3, pp. 81–101, 2006.

[263] H. D. H. Showalter and A. I. Kraker, "Small Molecule Inhibitors of the Platelet-Derived Growth Factor Receptor , the Fibroblast Growth Factor Receptor , and Src Family Tyrosine Kinases," *Pharmacol. Ther.*, vol. 76, no. 97, pp. 55–71, 1997.

[264] R. R. Jr, "Properties of FDA-approved small molecule protein kinase inhibitors : A 2020 update," *Pharmacol. Res.*, vol. 152, no. December 2019, p. 104609, 2020, doi: 10.1016/j.phrs.2019.104609.

[265] M. Huse and J. Kuriyan, "The Conformational Plasticity of Protein Kinases," *Cell*, vol. 109, no. 3, pp. 275–282, 2002.

[266] A. C. Dar and K. M. Shokat, "The Evolution of Protein Kinase Inhibitors from Antagonists to Agonists of Cellular Signaling," *Annu. Rev. Biochem.*, vol. 80, pp. 769–795, 2011, doi: 10.1146/annurev-biochem-090308-173656.

[267] Z. Zhao and P. E. Bourne, "Overview of Current Type I/II Kinase Inhibitors," 2018. [Online]. Available: http://arxiv.org/abs/1811.09718.

[268] P. Wu, M. H. Clausen, and T. E. Nielsen, "Allosteric small-molecule kinase inhibitors," *Pharmacol. Ther.*, vol. 156, pp. 59–68, 2015, doi: 10.1016/j.pharmthera.2015.10.002.

[269] F. Zuccotto, E. Ardini, E. Casale, and M. Angiolini, "Through the ' Gatekeeper Door ': Exploiting the Active Kinase Conformation," *J. Med. Chem.*, vol. 53, no. 7, pp. 2681–2694, 2010, doi: 10.1021/jm901443h.

[270] Y. Liu and N. S. Gray, "Rational design of inhibitors that bind to inactive kinase conformations," *Nat. Chem. Biol.*, vol. 2, no. 7, pp. 358–364, 2006, doi: 10.1038/nchembio799.

[271] V. Modi and R. L. Dunbrack, "Defining a new nomenclature for the structures of active and inactive kinases," *Proc. Natl. Acad. Sci.*, vol. 116, no. 14, pp.

6818–6827, 2019, doi: 10.1073/pnas.1814279116.

[272] O. Chahrour, D. Cairns, Z. Omran, and N. Ng, “Small Molecule Kinase Inhibitors as Anti-Cancer Therapeutics,” *Mini-Reviews Med. Chem.*, vol. 12, pp. 399–411, 2012.

[273] L. Munoz, “Non-kinase targets of protein kinase inhibitors,” *Nat. Publ. Gr.*, vol. 16, no. 6, pp. 424–440, 2017, doi: 10.1038/nrd.2016.266.

[274] R. Thaimattam, R. Banerjee, R. Miglani, and J. Iqbal, “Protein Kinase Inhibitors : Structural Insights Into Selectivity,” *Curr. Pharm. Des.*, vol. 13, no. 27, pp. 2751–2765, 2007.

[275] L. Debakey and N. Lydon, “Attacking cancer at its foundation,” *Nat. Med.*, vol. 15, no. 10, pp. 1153–1157, 2009, doi: 10.1038/nm1009-1153.

[276] W. M. Oldham and H. E. Hamm, “Heterotrimeric G protein activation by G-protein-coupled receptors,” *Nat. Rev. Mol. Cell Biol.*, vol. 9, no. 1, pp. 60–71, 2008, doi: 10.1038/nrm2299.

[277] M. I. Simon, M. P. Strathmann, and N. Gautam, “Diversity of G proteins in signal transduction,” *Science (80-.).*, vol. 252, no. 1971, pp. 802–808, 1991, doi: 10.1126/science.1902986.

[278] Y. Sun, D. McGarrigle, and X. Y. Huang, “When a G protein-coupled receptor does not couple to a G protein,” *Mol. Biosyst.*, vol. 3, no. 12, pp. 849–854, 2007, doi: 10.1039/b706343a.

[279] D. C. New, K. Wu, A. W. S. Kwok, and Y. H. Wong, “G protein-coupled receptor-induced Akt activity in cellular proliferation and apoptosis,” *FEBS J.*, vol. 274, no. 23, pp. 6025–6036, 2007, doi: 10.1111/j.1742-4658.2007.06116.x.

[280] R. C. Russo, C. C. Garcia, M. M. Teixeira, and F. A. Amaral, “The CXCL8/IL-8 chemokine family and its receptors in inflammatory diseases,” *Expert Rev. Clin. Immunol.*, vol. 10, no. 5, pp. 593–619, 2014, doi: 10.1586/1744666X.2014.894886.

[281] G. Xue and B. A. Hemmings, “PKB/akt-dependent regulation of cell motility,” *J. Natl. Cancer Inst.*, vol. 105, no. 6, pp. 393–404, 2013, doi: 10.1093/jnci/djs648.

[282] C. Knall, G. S. Worthen, and G. L. Johnson, “Interleukin 8-stimulated phosphatidylinositol-3-kinase activity regulates the migration of human neutrophils independent of extracellular signal-regulated kinase and p38 mitogen-activated protein kinases.,” *Proc. Natl. Acad. Sci. U. S. A.*, vol. 94, no. 7, pp. 3052–7, 1997, doi: 10.1073/pnas.94.7.3052.

[283] L.-H. Wang *et al.*, “Advances of AKT Pathway in Human Oncogenesis and as a Target for Anti-Cancer Drug Discovery,” *Curr. Cancer Drug Targets*, vol. 8, no. 1, pp. 2–6, 2008, doi: 10.2174/156800908783497159.

[284] H. Jiang, X. Wang, W. Miao, B. Wang, and Y. Qiu, “CXCL8 promotes the invasion of human osteosarcoma cells by regulation of PI3K/Akt signaling pathway,” *Apmis*, vol. 125, no. 9, pp. 773–780, 2017, doi: 10.1111/apm.12721.

[285] C. Y. Lee, C. Y. Huang, M. Y. Chen, C. Y. Lin, H. C. Hsu, and C. H. Tang, “IL-8 increases integrin expression and cell motility in human chondrosarcoma cells,” *J. Cell. Biochem.*, vol. 112, no. 9, pp. 2549–2557,

2011, doi: 10.1002/jcb.23179.

[286] L. Wang *et al.*, “Activation of IL-8 via PI3K/AKT-dependent pathway is involved in leptin-mediated epithelial-mesenchymal transition in human breast cancer cells,” *Cancer Biol. Ther.*, vol. 16, no. 8, pp. 1220–1230, 2015, doi: 10.1080/15384047.2015.1056409.

[287] C. H. Lin, H. W. Cheng, H. P. Ma, C. H. Wu, C. Y. Hong, and B. C. Chen, “Thrombin induces NF-κB activation and IL-8/CXCL8 expression in lung epithelial cells by a Rac1-dependent PI3K/Akt pathway,” *J. Biol. Chem.*, vol. 286, no. 12, pp. 10483–10494, 2011, doi: 10.1074/jbc.M110.112433.

[288] Y. L. Dong, S. M. Kabir, E. S. Lee, and D. S. Son, “CXCR2-driven ovarian cancer progression involves upregulation of proinflammatory chemokines by potentiating NF-κB activation via EGFR-transactivated Akt signaling,” *PLoS One*, vol. 8, no. 12, pp. 16–20, 2013, doi: 10.1371/journal.pone.0083789.

[289] L. Shi *et al.*, “Regulatory mechanisms of betacellulin in CXCL8 production from lung cancer cells,” *J. Transl. Med.*, vol. 12, no. 1, pp. 1–11, 2014, doi: 10.1186/1479-5876-12-70.

[290] Y. Wang *et al.*, “PI3K inhibitor LY294002, as opposed to wortmannin, enhances AKT phosphorylation in gemcitabine-resistant pancreatic cancer cells,” *Int. J. Oncol.*, vol. 50, no. 2, pp. 606–612, 2017, doi: 10.3892/ijo.2016.3804.

[291] E. Zhang, X. Feng, F. Liu, P. Zhang, J. Liang, and X. Tang, “Roles of PI3K/Akt and c-Jun signaling pathways in human papillomavirus type 16 oncoprotein-induced HIF-1α, VEGF, and IL-8 expression and in vitro angiogenesis in non-small cell lung cancer cells,” *PLoS One*, vol. 9, no. 7, pp. 1–13, 2014, doi: 10.1371/journal.pone.0103440.

[292] S. Kim, M. Jeon, J. E. Lee, and S. J. Nam, “MEK activity controls IL-8 expression in tamoxifen-resistant MCF-7 breast cancer cells,” *Oncology Reports*, vol. 35, no. 4. pp. 2398–2404, 2016, doi: 10.3892/or.2016.4557.

[293] H. C. Lane, A. R. Anand, and R. K. Ganju, “Cbl and Akt regulate CXCL8-induced and CXCR1- and CXCR2-mediated chemotaxis,” *Int. Immunol.*, vol. 18, no. 8, pp. 1315–1325, 2006, doi: 10.1093/intimm/dxl064.

[294] C. F. MacManus *et al.*, “Interleukin-8 Signaling Promotes Translational Regulation of Cyclin D in Androgen-Independent Prostate Cancer Cells,” *Mol. Cancer Res.*, vol. 5, no. 7, pp. 737–748, 2007, doi: 10.1158/1541-7786.MCR-07-0032.

[295] L. Snoeks, C. R. Weber, J. R. Turner, M. Bhattacharyya, K. Wasland, and S. D. Savkovic, “Tumor suppressor Foxo3a is involved in the regulation of lipopolysaccharide-induced interleukin-8 in intestinal HT-29 cells,” *Infect. Immun.*, vol. 76, no. 10, pp. 4677–4685, 2008, doi: 10.1128/IAI.00227-08.

[296] M. Takami, V. Terry, and L. Petruzzelli, “Signaling Pathways Involved in IL-8-Dependent Activation of Adhesion Through Mac-1,” *J. Immunol.*, vol. 168, no. 9, pp. 4559–4566, 2002, doi: 10.4049/jimmunol.168.9.4559.

[297] D. Chelouche-Lev, C. P. Miller, C. Tellez, M. Ruiz, M. Bar-Eli, and J. E. Price, “Different signalling pathways regulate VEGF and IL-8 expression in breast cancer: Implications for therapy,” *Eur. J. Cancer*, vol. 40, no. 16, pp. 2509–2518, 2004, doi: 10.1016/j.ejca.2004.05.024.

[298] K. I. Amiri and A. Richmond, “Role of NF-kB in melanoma,” *Cancer Res.*, vol. 24, no. 2, pp. 301–313, 2009, doi: 10.1007/s10555-005-1579-7.Role.

[299] A. Sparmann and D. Bar-Sagi, “Ras-induced interleukin-8 expression plays a critical role in tumor growth and angiogenesis,” *Cancer Cell*, vol. 6, no. 5, pp. 447–458, 2004, doi: 10.1016/j.ccr.2004.09.028.

[300] J. Fang, M. Ding, L. Yang, L. Z. Liu, and B. H. Jiang, “PI3K/PTEN/AKT signaling regulates prostate tumor angiogenesis,” *Cell. Signal.*, vol. 19, no. 12, pp. 2487–2497, 2007, doi: 10.1016/j.cellsig.2007.07.025.

[301] L. Hu, J. Hofmann, and R. B. Jaffe, “Phosphatidylinostol 3-kinase mediates angiogenesis and vascular permeability associated with ovarian carcinoma,” *Clin. Cancer Res.*, vol. 11, no. 22, pp. 8208–8212, 2005, doi: 10.1158/1078-0432.CCR-05-0206.

[302] D. Trisciuoglio, A. Iervolino, G. Zupi, and D. Del Bufalo, “Involvement of PI3K and MAPK Signaling in bcl-2- induced Vascular Endothelial Growth Factor Expression in Melanoma Cells,” *Mol Biol Cell*, vol. 16, no. September, pp. 4153–4162, 2005, doi: 10.1091/mbc.E04.

[303] P. J. Maxwell *et al.*, “Potentiation of inflammatory CXCL8 signalling sustains cell survival in pten-deficient prostate carcinoma,” *Eur. Urol.*, vol. 64, no. 2, pp. 177–188, 2013, doi: 10.1016/j.eururo.2012.08.032.

[304] A. S. Dhillon, S. Hagan, O. Rath, and W. Kolch, “MAP kinase signalling pathways in cancer,” *Oncogene*, vol. 26, no. 22, pp. 3279–3290, 2007, doi: 10.1038/sj.onc.1210421.

[305] S. Kostenko, “Physiological roles of mitogen-activated-protein-kinase-activated p38-regulated/activated protein kinase,” *World J. Biol. Chem.*, vol. 2, no. 5, p. 73, 2011, doi: 10.4331/wjbc.v2.i5.73.

[306] W. Kolch, “Coordinating ERK/MAPK signalling through scaffolds and inhibitors,” *Nat. Rev. Mol. Cell Biol.*, vol. 6, no. 11, pp. 827–837, 2005, doi: 10.1038/nrm1743.

[307] H. K. Koul, M. Pal, and S. Koul, “Role of p38 MAP Kinase Signal Transduction in Solid Tumors,” *Genes and Cancer*, vol. 4, no. 9–10, pp. 342–359, 2013, doi: 10.1177/1947601913507951.

[308] J. Downward, “Targeting RAS signalling pathways in cancer therapy,” *Nat. Rev. Cancer*, vol. 3, no. 1, pp. 11–22, 2003, doi: 10.1038/nrc969.

[309] C. Knall, S. Young, J. A. Nick, A. M. Buhl, G. S. Worthen, and G. L. Johnson, “Interleukin-8 Regulation of the Ras/Raf/Mitogen-activated Protein Kinase Pathway in Human Neutrophils,” *J. Biol. Chem.*, vol. 271, no. 5, pp. 2832–2838, 1996, doi: 10.1074/jbc.271.5.2832.

[310] J. A. McCubrey *et al.*, “Roles of the Raf/MEK/ERK pathway in cell growth, malignant transformation and drug resistance,” *Biochim. Biophys. Acta - Mol. Cell Res.*, vol. 1773, no. 8, pp. 1263–1284, 2007, doi: 10.1016/j.bbamcr.2006.10.001.

[311] F. Chang *et al.*, “Signal transduction mediated by the Ras/Raf/MEK/ERK pathway from cytokine receptors to transcription factors: Potential targeting for therapeutic intervention,” *Leukemia*, vol. 17, no. 7, pp. 1263–1293, 2003, doi: 10.1038/sj.leu.2402945.

[312] L. S. Steelman, S. C. Pohnert, J. G. Shelton, R. A. Franklin, F. E. Bertrand,

and J. A. McCubrey, “JAK/STAT, Raf/MEK/ERK, PI3K/Akt and BCR-ABL in cell cycle progression and leukemogenesis,” *Leukemia*, vol. 18, no. 2, pp. 189–218, 2004, doi: 10.1038/sj.leu.2403241.

[313] W. L. Blalock *et al.*, “Signal transduction, cell cycle regulatory, and anti-apoptotic pathways regulated by IL-3 in hematopoietic cells: Possible sites for intervention with anti-neoplastic drugs,” *Leukemia*, vol. 13, no. 8, pp. 1109–1166, 1999, doi: 10.1038/sj.leu.2401493.

[314] K. E. Mercer and C. A. Pritchard, “Raf proteins and cancer: B-Raf is identified as a mutational target,” *Biochim. Biophys. Acta - Rev. Cancer*, vol. 1653, no. 1, pp. 25–40, 2003, doi: 10.1016/S0304-419X(03)00016-7.

[315] U. Naumann, I. Eisenmann-Tappe, and U. R. Rapp, “The role of Raf kinases in development and growth of tumors.,” *Recent Results Cancer Res.*, vol. 143, pp. 237–244, 1997, doi: 10.1007/978-3-642-60393-8_16.

[316] K. Mercer, A. Chiloeches, M. Hüser, M. Kiernan, R. Marais, and C. Pritchard, “ERK signalling and oncogene transformation are not impaired in cells lacking A-Raf,” *Oncogene*, vol. 21, no. 3, pp. 347–355, 2002, doi: 10.1038/sj.onc.1205101.

[317] T. Brummer, P. E. Shaw, M. Reth, and Y. Misawa, “Inducible gene deletion reveals different roles for B-Raf and Raf-1 in B-cell antigen receptor signalling,” *EMBO J.*, vol. 21, no. 21, pp. 5611–5622, 2002, doi: 10.1093/emboj/cdf588.

[318] M. J. Garnett and R. Marais, “Guilty as charged: B-RAF is a human oncogene,” *Cancer Cell*, vol. 6, no. 4, pp. 313–319, 2004, doi: 10.1016/j.ccr.2004.09.022.

[319] S. R. Hingorani, M. A. Jacobetz, G. P. Robertson, M. Herlyn, and D. A. Tuveson, “Suppression of BRAFV599E in human melanoma abrogates transformation,” *Cancer Res.*, vol. 63, no. 17, pp. 5198–5202, 2003.

[320] M. Karasarides *et al.*, “B-RAF is a therapeutic target in melanoma,” *Oncogene*, vol. 23, no. 37, pp. 6292–6298, 2004, doi: 10.1038/sj.onc.1207785.

[321] K.-L. Guan *et al.*, “Negative regulation of the serine/threonine kinase B-Raf by Akt,” *J. Biol. Chem.*, vol. 275, no. 35, pp. 27354–27359, 2000.

[322] P. M. Navolanic, J. T. Lee, and J. A. McCubrey, “Docetaxel cytotoxicity is enhanced by inhibition of the Raf/MEK/ERK signal transduction pathway,” *Cancer Biol. Ther.*, vol. 2, no. 6, pp. 677–678, 2003, doi: 10.4161/cbt.2.6.535.

[323] R. Roskoski, “ERK1/2 MAP kinases: Structure, function, and regulation,” *Pharmacol. Res.*, vol. 66, no. 2, pp. 105–143, 2012, doi: 10.1016/j.phrs.2012.04.005.

[324] D. Xythalis, M. B. Frewin, and P. W. Gudewicz, “Inhibition of IL-8-mediated MAPK activation in human neutrophils by beta1 integrin ligands.,” *Inflammation*, vol. 26, no. 2, pp. 83–8, 2002.

[325] F. Luppi, A. M. Longo, W. I. de Boer, K. F. Rabe, and P. S. Hiemstra, “Interleukin-8 stimulates cell proliferation in non-small cell lung cancer through epidermal growth factor receptor transactivation,” *Lung Cancer*, vol. 56, no. 1, pp. 25–33, 2007, doi: 10.1016/j.lungcan.2006.11.014.

[326] H. Takamori, Z. G. Oades, R. C. Hoch, M. Burger, and I. U. Schraufstatter,

"Autocrine growth effect of IL-8 and GROα on a human pancreatic cancer cell line, Capan-1," *Pancreas*, vol. 21, no. 1, pp. 52–56, 2000, doi: 10.1097/00006676-200007000-00051.

[327] B. B. Aggarwal and B. Sung, "NF-κB in cancer: A matter of life and death," *Cancer Discov.*, vol. 1, no. 6, pp. 469–471, 2011, doi: 10.1158/2159-8290.CD-11-0260.

[328] R. M. Richardson, H. Ail, B. C. Pridgen, B. Haribabu, and R. Snyderman, "Multiple signaling pathways of human interleukin-8 receptor A.," *J. Biol. Chem.*, vol. 273, no. 17, pp. 10690–10695, 1998.

[329] P. Rafiee *et al.*, "Effect of curcumin on acidic pH-induced expression of IL-6 and IL-8 in human esophageal epithelial cells (HET-1A): Role of PKC, MAPKs, and NF-κB," *Am. J. Physiol. - Gastrointest. Liver Physiol.*, vol. 296, no. 2, pp. 388–398, 2009, doi: 10.1152/ajpgi.90428.2008.

[330] Y. Chen, X. Rao, K. Huang, X. Jiang, H. Wang, and L. Teng, "FH535 inhibits proliferation and motility of colon cancer cells by targeting Wnt/ß-catenin signaling pathway," *J. Cancer*, vol. 8, no. 16, pp. 3142–3153, 2017, doi: 10.7150/jca.19273.

[331] C. Murphy *et al.*, "Nonapical and cytoplasmic expression of interleukin-8, CXCR1, and CXCR2 correlates with cell proliferation and microvessel density in prostate cancer," *Clin. Cancer Res.*, vol. 11, no. 11, pp. 4117–4127, 2005, doi: 10.1158/1078-0432.CCR-04-1518.

[332] S. H. Ridley *et al.*, "Actions of IL-1 are selectively controlled by p38 mitogen-activated protein kinase: regulation of prostaglandin H synthase-2, metalloproteinases, and IL-6 at different levels," *J. Immunol.*, vol. 158, no. 7, pp. 3165–3173, 1997.

[333] C. L. Manthey, S. W. Wang, S. D. Kinney, and Z. Yao, "SB202190, a selective inhibitor of p38 mitogen-activated protein kinase, is a powerful regulator of LPS-induced mRNAs in monocytes," *J. Leukoc. Biol.*, vol. 64, no. 3, pp. 409–417, 1998, doi: 10.1002/jlb.64.3.409.

[334] J. Westra, B. Doornbos-van der Meer, P. de Boer, M. A. van Leeuwen, M. H. van Rijswijk, and P. C. Limburg, "Strong inhibition of TNF-alpha production and inhibition of IL-8 and COX-2 mRNA expression in monocyte-derived macrophages by RWJ 67657, a p38 mitogen-activated protein kinase (MAPK) inhibitor.," *Arthritis Res. Ther.*, vol. 6, no. 4, 2004, doi: 10.1186/ar1204.

[335] L. P. Chan *et al.*, "IL-8 promotes inflammatory mediators and stimulates activation of p38 MAPK/ERK-NF-κB pathway and reduction of JNK in HNSCC," *Oncotarget*, vol. 8, no. 34, pp. 56375–56388, 2017, doi: 10.18632/oncotarget.16914.

[336] Q. Liu *et al.*, "The CXCL8-CXCR1/2 pathways in cancer," *Cytokine Growth Factor Rev.*, vol. 31, pp. 61–71, 2016, doi: 10.1016/j.cytogfr.2016.08.002.

[337] F. M. Vega and A. J. Ridley, "Rho GTPases in cancer cell biology," *FEBS Lett.*, vol. 582, no. 14, pp. 2093–2101, 2008, doi: 10.1016/j.febslet.2008.04.039.

[338] A. J. Ridley, "Rho GTPases and actin dynamics in membrane protrusions and vesicle trafficking," *Trends Cell Biol.*, vol. 16, no. 10, pp. 522–529, 2006, doi: 10.1016/j.tcb.2006.08.006.

[339] W. E. Allen, G. E. Jones, J. W. Pollard, and A. J. Ridley, “Rho, Rac and Cdc42 regulate actin organization and cell adhesion in macrophages,” *J. Cell Sci.*, vol. 110, no. 6, pp. 707–720, 1997.

[340] A. J. Ridley, “Rho GTPase signalling in cell migration,” *Curr. Opin. Cell Biol.*, vol. 36, pp. 103–112, 2015, doi: 10.1016/j.ceb.2015.08.005.

[341] A. L. Bishop and A. Hall, “Rho GTPases and their effector proteins.,” *Biochem. J.*, vol. 348 Pt 2, pp. 241–55, 2000, doi: 10.1042/0264-6021:3480241.

[342] I. U. Schraufstatter, J. Chung, and M. Burger, “IL-8 activates endothelial cell CXCR1 and CXCR2 through Rho and Rac signaling pathways.,” *Am. J. Physiol. Lung Cell. Mol. Physiol.*, vol. 280, no. 6, pp. L1094–L1103, 2000.

[343] Y. Lai, X. H. Liu, Y. Zeng, Y. Zhang, and Y. Shen, “Interleukin-8 induces the endothelial cell migration through the Rac1 / RhoA-p38MAPK pathway,” *Eur. Rev. Med. Pharmacol. Sci.*, pp. 630–638, 2012, doi: 10.7150/ijbs.7.782.

[344] G. Fritz, I. Just, and B. Kaina, “Rho GTPases are over-expressed in human tumors,” *Int. J. Cancer*, vol. 81, no. 5, pp. 682–687, 1999, doi: 10.1002/(SICI)1097-0215(19990531)81:5<682::AID-IJC2>3.0.CO;2-B.

[345] S. A. Benitah, P. F. Valerón, L. Van Aelst, C. J. Marshall, and J. C. Lacal, “Rho GTPases in human cancer: An unresolved link to upstream and downstream transcriptional regulation,” *Biochim. Biophys. Acta - Rev. Cancer*, vol. 1705, no. 2, pp. 121–132, 2004, doi: 10.1016/j.bbcan.2004.10.002.

[346] S. D. Merajver and S. Z. Usmani, “Multifaceted role of Rho proteins in angiogenesis,” *J. Mammary Gland Biol. Neoplasia*, vol. 10, no. 4, pp. 291–298, 2005, doi: 10.1007/s10911-006-9002-8.

[347] E. A. Cox and A. Huttenlocher, “Regulation of integrin-mediated adhesion during cell migration,” *Microsc. Res. Tech.*, vol. 43, no. 5, pp. 412–419, 1998, doi: 10.1002/(SICI)1097-0029(19981201)43:5<412::AID-JEMT7>3.0.CO;2-F.

[348] G. A. Wildenberg *et al.*, “p120-Catenin and p190RhoGAP Regulate Cell-Cell Adhesion by Coordinating Antagonism between Rac and Rho,” *Cell*, vol. 127, no. 5, pp. 1027–1039, 2006, doi: 10.1016/j.cell.2006.09.046.

[349] T. Gómez Del Pulgar, S. A. Benitah, P. F. Valerón, C. Espina, and J. C. Lacal, “Rho GTPase expression in tumourigenesis: Evidence for a significant link,” *BioEssays*, vol. 27, no. 6, pp. 602–613, 2005, doi: 10.1002/bies.20238.

[350] A. B. Jaffe and A. Hall, “RHO GTPASES: Biochemistry and Biology,” *Annu. Rev. Cell Dev. Biol.*, vol. 21, no. 1, pp. 247–269, 2005, doi: 10.1146/annurev.cellbio.21.020604.150721.

[351] P. Friedl and K. Wolf, “Tumour-cell invasion and migration: diversity and escape mechanisms,” *Nat. Rev. Cancer*, vol. 3, no. 5, pp. 362–374, 2003, doi: 10.1038/nrc1075.

[352] F. L. Miles, F. L. Pruitt, K. L. Van Golen, and C. R. Cooper, “Stepping out of the flow: Capillary extravasation in cancer metastasis,” *Clin. Exp. Metastasis*, vol. 25, no. 4, pp. 305–324, 2008, doi: 10.1007/s10585-007-9098-2.

[353] S. L. Hwang *et al.*, “Rac1 gene mutations in human brain tumours,” *Eur. J. Surg. Oncol.*, vol. 30, no. 1, pp. 68–72, 2004, doi: 10.1016/j.ejso.2003.10.018.

[354] D. Joyce *et al.*, “Integration of Rac-dependent regulation of cyclin D1 transcription through a nuclear factor-κB-dependent pathway,” *J. Biol. Chem.*, vol. 274, no. 36, pp. 25245–25249, 1999, doi: 10.1074/jbc.274.36.25245.

[355] M. Watanabe *et al.*, “DOCK2 and DOCK5 Act Additively in Neutrophils To Regulate Chemotaxis, Superoxide Production, and Extracellular Trap Formation,” *J. Immunol.*, vol. 193, no. 11, pp. 5660–5667, 2014, doi: 10.4049/jimmunol.1400885.

[356] Y. Chen, F. Meng, B. Wang, L. He, Y. Liu, and Z. Liu, “Dock2 in the development of inflammation and cancer,” *Eur. J. Immunol.*, vol. 48, no. 6, pp. 915–922, 2018, doi: 10.1002/eji.201747157.

[357] F. M. Vega and A. J. Ridley, “Rho GTPases in cancer cell biology,” *FEBS Lett.*, vol. 582, no. 14, pp. 2093–2101, 2008, doi: 10.1016/j.febslet.2008.04.039.

[358] O. C. Rodriguez, W. S. Andrew, C. A. Mandato, P. Forscher, W. M. Bement, and C. M. Waterman-Storer, “Conserved microtubule–actin interactions in cell movement and morphogenesis,” *Nat. cell*, vol. 5, no. 7, pp. 599–609, 2003.

[359] B. Bouzahzah *et al.*, “Rho family GTPases regulate mammary epithelium cell growth and metastasis through distinguishable pathways,” *Mol. Med.*, vol. 7, no. 12, pp. 816–830, 2001, doi: 10.1007/bf03401974.

[360] J. van Hengel *et al.*, “Continuous Cell Injury Promotes Hepatic Tumorigenesis in Cdc42-Deficient Mouse Liver,” *Gastroenterology*, vol. 134, no. 3, pp. 781–792, 2008, doi: 10.1053/j.gastro.2008.01.002.

[361] S. Lee, B. T. Craig, C. V. Romain, J. Qiao, and D. H. Chung, “Silencing of CDC42 inhibits neuroblastoma cell proliferation and transformation,” *Cancer Lett.*, vol. 355, no. 2, pp. 210–216, 2014, doi: 10.1016/j.canlet.2014.08.033.

[362] A. Friesland, Y. Zhao, Y. H. Chen, L. Wang, H. Zhou, and Q. Lu, “Small molecule targeting Cdc42-intersectin interaction disrupts Golgi organization and suppresses cell motility,” *Proc. Natl. Acad. Sci. U. S. A.*, vol. 110, no. 4, pp. 1261–1266, 2013, doi: 10.1073/pnas.1116051110.

[363] R. Sorber *et al.*, “Whole genome sequencing of newly established pancreatic cancer lines identifies novel somatic mutation (c.2587G>A) in axon guidance receptor plexin A1 as enhancer of proliferation and invasion,” *PLoS One*, vol. 11, no. 3, 2016, doi: 10.1371/journal.pone.0149833.

[364] A. M. Labrousse *et al.*, “Cell Migration : Integrating Signals from Front to Back,” vol. 302, no. December, pp. 1704–1710, 2003.

[365] G. O. C. Cory and A. J. Ridley, “Braking WAVEs,” *Nature*, vol. 418, no. 6899, pp. 732–733, 2002, doi: 10.1038/418732a.

[366] M. D. Welch and R. D. Mullins, “Cellular Control of Actin Nucleation,” *Annu. Rev. Cell Dev. Biol.*, vol. 18, no. 1, pp. 247–288, 2002, doi: 10.1146/annurev.cellbio.18.040202.112133.

[367] L. F. Lee *et al.*, “Interleukin-8 confers androgen-independent growth and migration of LNCaP: Differential effects of tyrosine kinases Src and FAK,” *Oncogene*, vol. 23, no. 12, pp. 2197–2205, 2004, doi: 10.1038/sj.onc.1207344.

[368] P. M. F. Siesser and S. K. Hanks, “The signaling and biological implications of FAK overexpression in cancer,” *Clin. Cancer Res.*, vol. 12, no. 11 I, pp.

3233–3237, 2006, doi: 10.1158/1078-0432.CCR-06-0456.

[369] I. RB and Y. TJ, “Role of Src expression and activation in human cancer,” *Oncogene*, vol. 19, pp. 5636–5642, 2000, [Online]. Available: http://dx.doi.org/10.1038/sj.onc.1203912.

[370] J. T. Parsons, K. H. Martin, J. K. Slack, J. M. Taylor, and S. A. Weed, “Focal Adhesion Kinase: A regulator of focal adhesion dynamics and cell movement,” *Oncogene*, vol. 19, no. 49, pp. 5606–5613, 2000, doi: 10.1038/sj.onc.1203877.

[371] V. Bolós, J. M. Gasent, S. Lopez-Tarruella, and E. Grande, “The dual kinase complex FAK-Src as a promising therapeutic target in cancer,” *Onco. Targets. Ther.*, vol. 3, pp. 83–97, 2010.

[372] D. J. Webb, J. T. Parsons, and A. F. Horwitz, “Adhesion assembly, disassembly and turnover in migrating cells - Over and over and over again,” *Nat. Cell Biol.*, vol. 4, no. 4, 2002, doi: 10.1038/ncb0402-e97.

[373] D. Ilić *et al.*, “Reduced cell motility and enhanced focal adhesion contact formation in cells from FAK-deficient mice,” *Nature*, vol. 377, no. 6549, pp. 539–544, 1995, doi: 10.1038/377539a0.

[374] R. A. Klinghoffer, C. Sachsenmaier, J. A. Cooper, and P. Soriano, “Src family kinases are required for integrin but not PDGFR signal transduction,” *EMBO J.*, vol. 18, no. 9, pp. 2459–2471, 1999, doi: 10.1093/emboj/18.9.2459.

[375] R. Feniger-Barish, I. Yron, T. Meshel, E. Matityahu, and A. Ben-Baruch, “IL-8-induced migratory responses through CXCR1 and CXCR2: Association with phosphorylation and cellular redistribution of focal adhesion kinase,” *Biochemistry*, vol. 42, no. 10, pp. 2874–2886, 2003, doi: 10.1021/bi026783d.

[376] E. Cohen-Hillel, I. Yron, T. Meshel, G. Soria, H. Attal, and A. Ben-Baruch, “CXCL8-induced FAK phosphorylation via CXCR1 and CXCR2: Cytoskeleton- and integrin-related mechanisms converge with FAK regulatory pathways in a receptor-specific manner,” *Cytokine*, vol. 33, no. 1, pp. 1–16, 2006, doi: 10.1016/j.cyto.2005.11.006.

[377] W. -T Chen, “Proteolytic activity of specialized surface protrusions formed at rosette contact sites of transformed cells,” *J. Exp. Zool.*, vol. 251, no. 2, pp. 167–185, 1989, doi: 10.1002/jez.1402510206.

[378] Sue Goo Rhee and Yun Soo Bae, “Regulation of phosphoinositide-specific phospholipase C isozymes,” *J. Biol. Chem.*, vol. 272, no. 24, pp. 15045–15048, 1997, doi: 10.1074/jbc.272.24.15045.

[379] E. G. Lapetina, B. Reep, B. R. Ganong, and R. M. Bell, “Exogenous sn-1,2-diacylglycerols containing saturated fatty acids function as bioregulators of protein kinase C in human platelets,” *J. Biol. Chem.*, vol. 260, no. 3, pp. 1358–1361, 1985.

[380] L. F. Brass and S. K. Joseph, “A role for inositol triphosphate in intracellular Ca2+ mobilization and granule secretion in platelets,” *J. Biol. Chem.*, vol. 260, no. 28, pp. 15172–15179, 1985.

[381] S. F. Steingerg, “Structural basis of protein kinase C isoform function,” *Physi*, vol. 88, no. 4, pp. 1341–137, 2008, doi: 10.1038/jid.2014.371.

[382] H. Nakanishi, K. A. Brewer, and J. H. Exton, “Activation of the ζ isozyme of protein kinase C by phosphatidylinositol 3,4,5-trisphosphate,” *J. Biol. Chem.*,

vol. 268, no. 1, pp. 13–16, 1993.

[383] C. Limatola, D. Schaap, W. H. Moolenaar, and W. J. Van Blitterswijk, “Phosphatidic acid activation of protein kinase C-ζ overexpressed in COS cells. Comparison with other protein kinase C isotypes and other acidic lipids,” *Biochem. J.*, vol. 304, no. 3, pp. 1001–1008, 1994, doi: 10.1042/bj3041001.

[384] G. Müller, M. Ayoub, P. Storz, J. Rennecke, D. Fabbro, and K. Pfizenmaier, “PKC zeta is a molecular switch in signal transduction of TNF-alpha, bifunctionally regulated by ceramide and arachidonic acid.,” *EMBO J.*, vol. 14, no. 9, pp. 1961–1969, 1995, doi: 10.1002/j.1460-2075.1995.tb07188.x.

[385] H. Xiao and M. Liu, “Atypical protein kinase C in cell motility,” *Cell. Mol. Life Sci.*, vol. 70, no. 17, pp. 3057–3066, 2013, doi: 10.1007/s00018-012-1192-1.

[386] C. Larsson, “Protein kinase C and the regulation of the actin cytoskeleton,” *Cell. Signal.*, vol. 18, no. 3, pp. 276–284, 2006, doi: 10.1016/j.cellsig.2005.07.010.

[387] M. C. Cardaba *et al.*, “CCL3 induced migration occurs independently of intracellular calcium release,” *Biochem. Biophys. Res. Commun.*, vol. 418, no. 1, pp. 17–21, 2012, doi: 10.1016/j.bbrc.2011.12.081.

[388] S. C. Mills *et al.*, “Cell migration towards CXCL12 in leukemic cells compared to breast cancer cells,” *Cell. Signal.*, vol. 28, no. 4, pp. 316–324, 2016, doi: 10.1016/j.cellsig.2016.01.006.

[389] I. Hamshaw, M. Ajdarirad, and A. Mueller, “The role of PKC and PKD in CXCL12 directed prostate cancer migration,” *Biochem. Biophys. Res. Commun.*, vol. 519, no. 1, pp. 86–92, 2019, doi: 10.1016/j.bbrc.2019.08.134.

[390] Y. Fu and C. S. Rubin, “Protein kinase D: Coupling extracellular stimuli to the regulation of cell physiology,” *EMBO Rep.*, vol. 12, no. 8, pp. 785–796, 2011, doi: 10.1038/embor.2011.139.

[391] X. Xu and T. Jin, “The novel functions of the PLC/PKC/PKD signaling axis in G protein-coupled receptor-mediated chemotaxis of neutrophils,” *J. Immunol. Res.*, vol. 2015, pp. 14–19, 2015, doi: 10.1155/2015/817604.

[392] Z. G. Goldsmith and D. N. Dhanasekaran, “G Protein regulation of MAPK networks,” *Oncogene*, vol. 26, no. 22, pp. 3122–3142, 2007, doi: 10.1038/sj.onc.1210407.

[393] S. Rieken *et al.*, “ G 12 /G 13 Family G Proteins Regulate Marginal Zone B Cell Maturation, Migration, and Polarization ,” *J. Immunol.*, vol. 177, no. 5, pp. 2985–2993, 2006, doi: 10.4049/jimmunol.177.5.2985.

[394] A. M. Buhl, N. L. Johnson, N. Dhanasekaran, and G. L. Johnson, “Gα12 and Gα13 stimulate Rho-dependent stress fiber formation and focal adhesion assembly,” *J. Biol. Chem.*, vol. 270, no. 42, pp. 24631–24634, 1995, doi: 10.1074/jbc.270.42.24631.

[395] G. Soldevila and E. A. García-Zepeda, “The role of the Jak-Stat pathway in chemokine-mediated signaling in T lymphocytes,” *Signal Transduct.*, vol. 7, no. 5–6, pp. 427–438, 2007, doi: 10.1002/sita.200700144.

[396] R. I. Susana R. Neves, Prahlad T. Ram, “G Protein Pathways,” *Science (80-.).*, vol. 296, no. 5573, pp. 1636–1639, 2002, doi: 10.1126/science.1071550.

[397] S. Kopetz, A. N. Shah, and G. E. Gallick, “Src continues aging: Current and future clinical directions,” *Clin. Cancer Res.*, vol. 13, no. 24, pp. 7232–7236, 2007, doi: 10.1158/1078-0432.CCR-07-1902.

[398] A. C. Newton, “Protein kinase C: Structure, function, and regulation,” *J. Biol. Chem.*, vol. 270, no. 48, pp. 28495–28498, 1995, doi: 10.1074/jbc.270.48.28495.

[399] M. G. Kazanietz, *Protein Kinase C in cancer signaling and therapy*. 2010.

[400] X. Xu and T. Jin, “The novel functions of the PLC/PKC/PKD signaling axis in G protein-coupled receptor-mediated chemotaxis of neutrophils,” *J. Immunol. Res.*, vol. 2015, pp. 14–19, 2015, doi: 10.1155/2015/817604.

[401] R. T. Waldron and E. Rozengurt, “Oxidative stress induces protein kinase D activation in intact cells: Involvement of Src and dependence on protein kinase C,” *J. Biol. Chem.*, vol. 275, no. 22, pp. 17114–17121, 2000, doi: 10.1074/jbc.M908959199.

[402] M. Cobbaut and J. Van Lint, “Function and regulation of protein kinase d in oxidative stress: A tale of isoforms,” *Oxid. Med. Cell. Longev.*, vol. 2018, pp. 28–30, 2018, doi: 10.1155/2018/2138502.

[403] Q. J. Wang, “PKD at the crossroads of DAG and PKC signaling,” *Trends Pharmacol. Sci.*, vol. 27, no. 6, pp. 317–323, 2006.

[404] X. Xu *et al.*, “GPCR-Mediated PLCβγ/PKCβ/PKD Signaling Pathway Regulates the Cofilin Phosphatase Slingshot 2 in Neutrophil Chemotaxis,” *Mol. Biol. Cell*, vol. 26, no. 5, pp. 874–886, 2015, doi: 10.1534/g3.120.401131.

[405] E. R. Sharlow *et al.*, “Potent and selective disruption of protein kinase D functionality by a benzoxoloazepinolone,” *J. Biol. Chem.*, vol. 283, no. 48, pp. 33516–33526, 2008, doi: 10.1074/jbc.M805358200.

[406] N. Nagarsheth, M. S. Wicha, and W. Zou, “Chemokines in the cancer microenvironment and their relevance in cancer immunotherapy,” *Nat. Rev. Immunol.*, vol. 17, no. 9, pp. 559–572, 2017, doi: 10.1038/nri.2017.49.

[407] A. Klarenbeek *et al.*, “Targeting chemokines and chemokine receptors with antibodies,” *Drug Discov. Today Technol.*, vol. 9, no. 4, pp. e237–e244, 2012, doi: 10.1016/j.ddtec.2012.05.003.

[408] Y. M. Zhu and P. J. Woll, “Mitogenic effects of interleukin-8/CXCL8 on cancer cells.,” *Future Oncol.*, vol. 1, no. 5, pp. 699–704, 2005, doi: 10.2217/14796694.1.5.699.

[409] I. Roy, D. B. Evans, and M. B. Dwinell, “Chemokines and chemokine receptors: Update on utility and challenges for the clinician,” *Surgery*, vol. 155, no. 6, pp. 961–973, 2014.

[410] Ş. Comsa, A. M. Cimpean, and M. Raica, “The story of MCF-7 breast cancer cell line: 40 years of experience in research,” *Anticancer Res.*, vol. 35, no. 6, pp. 3147–3154, 2015, doi: 10.1038/430021a.

[411] F. Alimirah, J. Chen, Z. Basrawala, H. Xin, and D. Choubey, “DU-145 and PC-3 human prostate cancer cell lines express androgen receptor: Implications for the androgen receptor functions and regulation,” *FEBS Lett.*, vol. 580, no. 9, pp. 2294–2300, 2006, doi: 10.1016/j.febslet.2006.03.041.

[412] P. N. Procma, “Oris TM Pro Cell Migration Assay Tissue Culture Treated Cell Migration of Adherent Cell Lines Table of Contents ORIS ™ PRO CELL MIGRATION ASSAY.”

[413] D. Helmer *et al.*, “Rational design of a peptide capture agent for CXCL8 based on a model of the CXCL8:CXCR1 complex,” *RSC Adv.*, vol. 5, no. 33, pp. 25657–25668, 2015, doi: 10.1039/C4RA13749C.

[414] P. J. Polverini and D. A. Arenberg, “The role of cxc chemokines as regulators of angiogenesis,” *Shock*, vol. 4, no. 3. pp. 155–160, 1995, doi: 10.1097/00024382-199509000-00001.

[415] R. Bertini *et al.*, “Receptor binding mode and pharmacological characterization of a potent and selective dual CXCR1/CXCR2 non-competitive allosteric inhibitor,” *Br. J. Pharmacol.*, vol. 165, no. 2, pp. 436–454, 2012, doi: 10.1111/j.1476-5381.2011.01566.x.

[416] M. Liu *et al.*, “CXCL10/IP-10 in infectious diseases pathogenesis and potential therapeutic implications,” *Cytokine Growth Factor Rev.*, vol. 22, no. 3, pp. 121–130, 2011, doi: 10.1016/j.cytogfr.2011.06.001.

[417] R. Tokunaga *et al.*, “CXCL9, CXCL10, CXCL11/CXCR3 axis for immune activation – A target for novel cancer therapy,” *Cancer Treat. Rev.*, vol. 63, pp. 40–47, 2018, doi: 10.1016/j.ctrv.2017.11.007.

[418] S. Singh, A. Sadanandam, and R. K. Singh, “Chemokines in tumor angiogenesis and metastasis,” *Cancer Metastasis Rev.*, vol. 26, no. 3–4, pp. 453–467, 2007, doi: 10.1007/s10555-007-9068-9.

[419] W. Chanput, J. J. Mes, and H. J. Wichers, “THP-1 cell line: An in vitro cell model for immune modulation approach,” *International Immunopharmacology*, vol. 23, no. 1. Elsevier, pp. 37–45, 2014, doi: 10.1016/j.intimp.2014.08.002.

[420] S. Tsuchiya, M. Yamabe, Y. Yamaguchi, Y. Kobayashi, T. Konno, and K. Tada, “Establishment and characterization of a human acute monocytic leukemia cell line (THP-1). Int J Cancer. 1980; 26:171–176. DOI: 10.1002/ijc.2910260208,” *Int. J. Cancer*, vol. 176, no. 2, pp. 171–176, 1980.

[421] R. J. Phillips, M. Lutz, and B. Premack, “Differential signaling mechanisms regulate expression of CC chemokine receptor-2 during monocyte maturation,” *J. Inflamm.*, vol. 2, pp. 1–14, 2005, doi: 10.1186/1476-9255-2-14.

[422] D. G. Souza *et al.*, “Repertaxin, a novel inhibitor of rat CXCR2 function, inhibits inflammatory responses that follow intestinal ischaemia and reperfusion injury,” *Br. J. Pharmacol.*, vol. 143, no. 1, pp. 132–142, 2004, doi: 10.1038/sj.bjp.0705862.

[423] M. L. Varney, S. Singh, A. Li, R. Mayer-Ezell, R. Bond, and R. K. Singh, “Small molecule antagonists for CXCR2 and CXCR1 inhibit human colon cancer liver metastases,” *Cancer Lett.*, vol. 300, no. 2, pp. 180–188, 2011, doi: 10.1016/j.canlet.2010.10.004.

[424] C. Ginestier *et al.*, “CXCR1 blockade selectively targets human breast cancer stem cells in vitro and in xenografts,” *J. Clin. Invest.*, vol. 120, no. 2, pp. 485–497, 2010, doi: 10.1172/JCI39397.One.

[425] Y. Ning *et al.*, “The CXCR2 Antagonist, SCH-527123, Shows Antitumor

Activity and Sensitizes Cells to Oxaliplatin in Preclinical Colon Cancer Models," *Mol. Cancer Ther.*, vol. 11, no. 6, pp. 1353–1364, 2012, doi: 10.1158/1535-7163.MCT-11-0915.

[426] A. F. Schott *et al.*, "Phase Ib pilot study to evaluate reparixin in combination with weekly paclitaxel in patients with HER-2–negative metastatic breast cancer," *Clin. Cancer Res.*, vol. 23, no. 18, pp. 5358–5365, 2017, doi: 10.1158/1078-0432.CCR-16-2748.

[427] J. R. White *et al.*, "Identification of a potent, selective non-peptide CXCR2 antagonist that inhibits interleukin-8-induced neutrophil migration," *J. Biol. Chem.*, vol. 273, no. 17, pp. 10095–10098, 1998, doi: 10.1074/jbc.273.17.10095.

[428] F. Liotti, M. De Pizzol, M. Allegretti, N. Prevete, and R. M. Melillo, "Multiple anti-tumor effects of Reparixin on thyroid cancer," *Oncotarget*, vol. 8, no. 22, pp. 35946–35961, 2017, doi: 10.18632/oncotarget.16412.

[429] M. Xu, H. Jiang, H. Wang, J. Liu, B. Liu, and Z. Guo, "SB225002 inhibits prostate cancer invasion and attenuates the expression of BSP, OPN and MMP-2," *Oncol. Rep.*, vol. 40, no. 2, pp. 726–736, 2018, doi: 10.3892/or.2018.6504.

[430] M. Montano, "Model Systems," in *Translational Biology in Medicine*, 2014, pp. 9–33.

[431] R. L. Contento *et al.*, "CXCR4-CCR5: A couple modulating T cell functions," *Proc. Natl. Acad. Sci. U. S. A.*, vol. 105, no. 29, pp. 10101–10106, 2008, doi: 10.1073/pnas.0804286105.

[432] A. Mueller, N. G. Mahmoud, and P. G. Strange, "Diverse signalling by different chemokines through the chemokine receptor CCR5," *Biochem. Pharmacol.*, vol. 72, no. 6, pp. 739–748, 2006, doi: 10.1016/j.bcp.2006.06.001.

[433] R. O. Jacques *et al.*, "Dynamin function is important for chemokine receptor-induced cell migration," *Cell Biochem. Funct.*, vol. 33, no. 6, pp. 407–414, 2015, doi: 10.1002/cbf.3131.

[434] P. H. Goh, "Roles of protein kinase C and arrestin in migration of cells via CXCR4/CXCL12 signalling axis," Doctoral Dissertation, University of East Anglia, 2018.

[435] S. C. Mills, L. Howell, A. Beekman, L. Stokes, and A. Mueller, "Rac1 plays a role in CXCL12 but not CCL3-induced chemotaxis and Rac1 GEF inhibitor NSC23766 has off target effects on CXCR4.," *Cell. Signal.*, vol. 42, no. May 2017, pp. 88–96, 2017, doi: 10.1016/j.cellsig.2017.10.006.

[436] M. Wolf, M. B. Delgado, S. A. Jones, B. Dewald, I. Clark-Lewis, and M. Baggiolini, "Granulocyte chemotactic protein 2 acts via both IL-8 receptors, CXCR1 and CXCR2," *Eur. J. Immunol.*, vol. 28, no. 1, pp. 164–170, 1998, doi: 10.1002/(SICI)1521-4141(199801)28:01<164::AID-IMMU164>3.0.CO;2-S.

[437] C. Giagulli *et al.*, "HIV-1 matrix protein p17 binds to the IL-8 receptor CXCR1 and shows IL-8-like chemokine activity on monocytes through Rho/ROCK activation," *Blood*, vol. 119, no. 10, pp. 2274–2283, 2012, doi: 10.1182/blood-2011-06-364083.

[438] R. T. Abraham and A. Weiss, “Jurkat T cells and development of the T-cell receptor signalling paradigm,” *Nat. Rev. Immunol.*, vol. 4, no. 4, pp. 301–308, 2004, doi: 10.1038/nri1330.

[439] A. Freund *et al.*, “IL-8 expression and its possible relationship with estrogen-receptor-negative status of breast cancer cells,” *Oncogene*, vol. 22, no. 2, pp. 256–265, 2003, doi: 10.1038/sj.onc.1206113.

[440] K. J. Chavez, S. V. Garimella, and S. Lipkowitz, “Triple negative breast cancer cell lines: One tool in the search for better treatment of triple negative breast cancer,” *Breast Dis.*, vol. 32, no. 1–2, pp. 35–48, 2010, doi: 10.3233/BD-2010-0307.

[441] V. Vinader *et al.*, “An agarose spot chemotaxis assay for chemokine receptor antagonists,” *J. Pharmacol. Toxicol. Methods*, vol. 64, no. 3, pp. 213–216, 2011, doi: 10.1016/j.vascn.2011.01.004.

[442] M. Ahmed *et al.*, “Agarose Spot as a Comparative Method for in situ Analysis of Simultaneous Chemotactic Responses to Multiple Chemokines,” *Sci. Rep.*, vol. 7, no. 1, pp. 1–11, 2017, doi: 10.1038/s41598-017-00949-4.

[443] S. Fu and J. Lin, “Blocking interleukin-6 and interleukin-8 signaling inhibits cell viability, colony-forming activity, and cell migration in human triple-negative breast cancer and pancreatic cancer cells,” *Anticancer Res.*, vol. 38, no. 11, pp. 6271–6279, 2018, doi: 10.21873/anticanres.12983.

[444] B. Sharma, K. C. Nannuru, M. L. Varney, and R. K. Singh, “Host Cxcr2-dependent regulation of mammary tumor growth and metastasis,” *Clin. Exp. Metastasis*, vol. 32, no. 1, pp. 65–72, 2015, doi: 10.1007/s10585-014-9691-0.

[445] L. Brandolini *et al.*, “Targeting CXCR1 on breast cancer stem cells: Signaling pathways and clinical application modelling,” *Oncotarget*, vol. 6, no. 41, pp. 43375–43394, 2015, doi: 10.18632/oncotarget.6234.

[446] H. Xu *et al.*, “CXCR2 promotes breast cancer metastasis and chemoresistance via suppression of AKT1 and activation of COX2,” *Cancer Lett.*, vol. 412, pp. 69–80, 2018, doi: 10.1016/j.canlet.2017.09.030.

[447] A. Muller *et al.*, “Involvement of chemokine receptors in breast cancer metastasis,” *Nature*, vol. 410, no. 6824, pp. 50–56, 2001.

[448] A. S. L. Chan, W. W. I. Lau, A. C. H. Szeto, J. Wang, and Y. H. Wong, “Differential Regulation of CXCL8 Production by Different G Protein Subunits with Synergistic Stimulation by Gi- and Gq-Regulated Pathways,” *J. Mol. Biol.*, vol. 428, no. 19, pp. 3869–3884, 2016, doi: 10.1016/j.jmb.2016.03.026.

[449] S. Tai *et al.*, “PC3 is a cell line characteristic of prostatic small cell carcinoma,” *Prostate*, vol. 71, no. 15, pp. 1668–1679, 2011, doi: 10.1002/pros.21383.

[450] J. Reiland, L. T. Furcht, and J. B. McCarthy, “CXC-chemokines stimulate invasion and chemotaxis in prostate carcinoma cells through the CXCR2 receptor,” *Prostate*, vol. 41, no. 2, pp. 78–88, 1999, doi: 10.1002/(SICI)1097-0045(19991001)41:2<78::AID-PROS2>3.0.CO;2-P.

[451] Sun Jin Kim, H. Uehara, T. Karashima, M. Mccarty, N. Shih, and I. J. Fidler, “Expression of interleukin-8 correlates with angiogenesis, tumorigenicity, and metastasis of human prostate cancer cells implanted orthotopically in nude mice,” *Neoplasia*, vol. 3, no. 1, pp. 33–42, 2001, doi:

10.1038/sj.neo.7900124.

[452] A. Seaton *et al.*, “Interleukin-8 signaling promotes androgen-independent proliferation of prostate cancer cells via induction of androgen receptor expression and activation,” *Carcinogenesis*, vol. 29, no. 6, pp. 1148–1156, 2008, doi: 10.1093/carcin/bgn109.

[453] A. D. Luster and P. Leder, “IP-10, a -C-X-C- chemokine, elicits a potent thymus-dependent antitumor response in vivo,” *J. Exp. Med.*, vol. 178, no. 3, pp. 1057–1065, 1993, doi: 10.1084/jem.178.3.1057.

[454] D. D. Taub, D. L. Longo, and W. J. Murphy, “Human interferon-inducible protein-10 induces mononuclear cell infiltration in mice and promotes the migration of human T lymphocytes into the peripheral tissues of human peripheral blood lymphocytes-SCID mice,” *Blood*, vol. 87, no. 4, pp. 1423–1431, 1996, doi: 10.1182/blood.v87.4.1423.bloodjournal8741423.

[455] D. Petrovic-Djergovic, M. Popovic, S. Chittiprol, H. Cortado, R. F. Ransom, and S. Partida-Sánchez, “CXCL10 induces the recruitment of monocyte-derived macrophages into kidney, which aggravate puromycin aminonucleoside nephrosis,” *Clin. Exp. Immunol.*, vol. 180, no. 2, pp. 305–315, 2015, doi: 10.1111/cei.12579.

[456] D. A. Lauffenburger and A. F. Horwitz, “Cell migration: A physically integrated molecular process,” *Cell*, vol. 84, no. 3, pp. 359–369, 1996, doi: 10.1016/S0092-8674(00)81280-5.

[457] R. J. Bodnar, C. C. Yates, and A. Wells, “IP-10 blocks vascular endothelial growth factor-induced endothelial cell motility and tube formation via inhibition of calpain,” *Circ. Res.*, vol. 98, no. 5, pp. 617–625, 2006, doi: 10.1161/01.RES.0000209968.66606.10.

[458] H. Shiraha, A. Glading, K. Gupta, and A. Wells, “IP-10 inhibits epidermal growth factor-induced motility by decreasing epidermal growth factor receptor-mediated calpain activity,” *J. Cell Biol.*, vol. 146, no. 1, pp. 243–253, 1999, doi: 10.1083/jcb.146.1.243.

[459] A. Antonosante *et al.*, “Autocrine CXCL8-dependent invasiveness triggers modulation of actin cytoskeletal network and cell dynamics,” *Aging (Albany. NY).*, vol. 12, no. 2, pp. 1928–1951, 2020, doi: 10.18632/aging.102733.

[460] S. A. Jones, B. Moser, and M. Thelen, “A comparison of post-receptor signal transduction events in Jurkat cells transfected with either IL-8R1 or IL-8R2 Chemokine mediated activation of p42/p44 MAP-kinase (ERK-2),” *FEBS Lett.*, vol. 364, no. 2, pp. 211–214, 1995, doi: 10.1016/0014-5793(95)00397-R.

[461] M. Veenstra and R. Ransohoff, “Chemokine receptor CXCR2: physiology regulator and neuroinflammation controller?,” *J. Neuroimmunol.*, vol. 246, no. 1–2, pp. 1–9, 2012, doi: 10.1038/jid.2014.371.

[462] A. Stadtmann and A. Zarbock, “CXCR2: From bench to bedside,” *Front. Immunol.*, vol. 3, no. AUG, pp. 1–12, 2012, doi: 10.3389/fimmu.2012.00263.

[463] K. Liu *et al.*, “A multiplex calcium assay for identification of GPCR agonists and antagonists.,” *Assay Drug Dev. Technol.*, vol. 8, no. 3, pp. 367–379, 2010, doi: 10.1089/adt.2009.0245.

[464] K. Kiselyov, D. M. Shin, and S. Muallem, “Signalling specificity in GPCR-

dependent Ca2+ signalling," *Cell. Signal.*, vol. 15, no. 3, pp. 243–253, 2003, doi: 10.1016/S0898-6568(02)00074-8.

[465] J. M. Planesas, V. I. Pérez-Nueno, J. I. Borrell, and J. Teixidó, "Studying the binding interactions of allosteric agonists and antagonists of the CXCR4 receptor," *J. Mol. Graph. Model.*, vol. 60, pp. 1–14, 2015, doi: 10.1016/j.jmgm.2015.05.004.

[466] N. Tuteja, "Signaling through G protein coupled receptors," *Plant Signal. Behav.*, vol. 4, no. 10, pp. 942–947, 2009, doi: 10.4161/psb.4.10.9530.

[467] R. Bertini *et al.*, "Noncompetitive allosteric inhibitors of the inflammatory chemokine receptors CXCR1 and CXCR2: Prevention of reperfusion injury," *Proc. Natl. Acad. Sci.*, vol. 101, no. 32, pp. 11791–11796, 2004, doi: 10.1073/pnas.0402090101.

[468] D. L. Miller, L. J., Kurtzman, S. H., Wang, Y. A. N. P. I. N. G., Anderson, K. H., Lindquist, R. R., & Kreutzer, "Expression of interleukin-8 receptors on tumor cells and vascular endothelial cells in human breast cancer tissue," *Anticancer Res.*, vol. 18, no. 1A, pp. 77–81, 1998.

[469] L. Skoog *et al.*, "Estrogen receptor levels and survival of breast cancer patients: A study on patients participating in randomized trials of adjuvant therapy," *Acta Oncol. (Madr).*, vol. 26, no. 2, pp. 95–100, 1987, doi: 10.3109/02841868709091747.

[470] J. E. De Larco *et al.*, "A potential role for interleukin-8 in the metastatic phenotype of breast carcinoma cells.," *Am. J. Pathol.*, vol. 158, no. 2, pp. 639–646, 2001, doi: 10.1016/S0002-9440(10)64005-9.

[471] J. Sharma *et al.*, "Elevated IL-8, TNF-alpha, and MCP-1 in men with metastatic prostate cancer starting androgen-deprivation therapy (ADT) are associated with shorter time to castration-resistance and overall survival," *Prostate*, vol. 74, no. 8, pp. 820–828, 2014.

[472] S. Araki *et al.*, "Interleukin-8 is a molecular determinant of androgen independence and progression in prostate cancer," *Cancer Res.*, vol. 67, no. 14, pp. 6854–6862, 2007, doi: 10.1158/0008-5472.CAN-07-1162.

[473] K. Xie, "Interleukin-8 and human cancer biology," *Cytokine Growth Factor Rev.*, vol. 12, no. 4, pp. 375–391, 2001, doi: 10.1016/S1359-6101(01)00016-8.

[474] M. L. G. Lamm, D. D. Long, S. M. Goodwin, and C. Lee, "Transforming growth factor-β1 inhibits membrane association of protein kinase Cα in a human prostate cancer cell line, PC3," *Endocrinology*, vol. 138, no. 11, pp. 4657–4664, 1997, doi: 10.1210/endo.138.11.5531.

[475] R. Aalinkeel *et al.*, "Nanotherapy silencing the interleukin-8 gene produces regression of prostate cancer by inhibition of angiogenesis," *Immunology*, vol. 148, no. 4, pp. 387–406, 2016, doi: 10.1111/imm.12618.

[476] L. J. Goldstein *et al.*, "A window-of-opportunity trial of the CXCR1/2 inhibitor reparixin in operable HER-2-negative breast cancer," *Breast Cancer Res.*, vol. 22, no. 1, pp. 1–9, 2020, doi: 10.1186/s13058-019-1243-8.

[477] F. Casilli *et al.*, "Inhibition of interleukin-8 (CXCL8/IL-8) responses by repertaxin, a new inhibitor of the chemokine receptors CXCR1 and CXCR2," *Biochem. Pharmacol.*, vol. 69, no. 3, pp. 385–394, 2005, doi:

10.1016/j.bcp.2004.10.007.

[478] S. Singh *et al.*, “Small-molecule antagonists for CXCR2 and CXCR1 inhibit human melanoma growth by decreasing tumor cell proliferation, survival, and angiogenesis,” *Clin. Cancer Res.*, vol. 15, no. 7, pp. 2380–2386, 2009, doi: 10.1158/1078-0432.CCR-08-2387.

[479] J. F. De Vasconcellos *et al.*, “SB225002 induces cell death and cell cycle arrest in acute lymphoblastic leukemia cells through the activation of GLIPR1,” *PLoS One*, vol. 10, no. 8, pp. 1–19, 2015, doi: 10.1371/journal.pone.0134783.

[480] M. Du *et al.*, “SB225002 Promotes Mitotic Catastrophe in Chemo-Sensitive and -Resistant Ovarian Cancer Cells Independent of p53 Status In Vitro,” *PLoS One*, vol. 8, no. 1, 2013, doi: 10.1371/journal.pone.0054572.

[481] V. Das, S. Bhattacharya, C. Chikkaputtaiah, S. Hazra, and M. Pal, “The basics of epithelial–mesenchymal transition (EMT): A study from a structure, dynamics, and functional perspective,” *J. Cell. Physiol.*, vol. 234, no. 9, pp. 14535–14555, 2019, doi: 10.1002/jcp.28160.

[482] M. N. Khan *et al.*, “CXCR1 / 2 antagonism with CXCL8 / Interleukin-8 analogue tumor cell proliferation and suppressing angiogenesis,” *Oncotarget*, vol. 6, no. 25, 2015.

[483] M. Wendel, I. E. Galani, E. Suri-Payer, and A. Cerwenka, “Natural killer cell accumulation in tumors is dependent on IFN-γ and CXCR3 ligands,” *Cancer Res.*, vol. 68, no. 20, pp. 8437–8445, 2008, doi: 10.1158/0008-5472.CAN-08-1440.

[484] D. S. Chen and I. Mellman, “Oncology meets immunology: The cancer-immunity cycle,” *Immunity*, vol. 39, no. 1, pp. 1–10, 2013, doi: 10.1016/j.immuni.2013.07.012.

[485] H. Bronger, V. Magdolen, P. Goettig, and T. Dreyer, “Proteolytic chemokine cleavage as a regulator of lymphocytic infiltration in solid tumors,” *Cancer Metastasis Rev.*, vol. 38, no. 3, pp. 417–430, 2019, doi: 10.1007/s10555-019-09807-3.

[486] N. Redjimi *et al.*, “CXCR3+ T regulatory cells selectively accumulate in human ovarian carcinomas to limit type I immunity,” *Cancer Res.*, vol. 72, no. 17, pp. 4351–4360, 2012, doi: 10.1158/0008-5472.CAN-12-0579.

[487] C. Billottet, C. Quemener, and A. Bikfalvi, “CXCR3, a double-edged sword in tumor progression and angiogenesis,” *Biochim. Biophys. Acta - Rev. Cancer*, vol. 1836, no. 2, pp. 287–295, 2013, doi: 10.1016/j.bbcan.2013.08.002.

[488] D. Venkatasubbu G, “Drugging Protein Kinases in Cancer: from Small Molecules to Nanoparticles,” *MOJ Proteomics Bioinforma.*, vol. 5, no. 5, pp. 154–156, 2017, doi: 10.15406/mojpb.2017.05.00173.

[489] L. Kondapalli, K. Soltani, and M. E. Lacouture, “The promise of molecular targeted therapies: Protein kinase inhibitors in the treatment of cutaneous malignancies,” *J. Am. Acad. Dermatol.*, vol. 53, no. 2, pp. 291–302, 2005, doi: 10.1016/j.jaad.2005.02.011.

[490] J. Zhang, P. L. Yang, and N. S. Gray, “Targeting cancer with small molecule kinase inhibitors,” *Nat. Rev. Cancer*, vol. 9, no. 1, pp. 28–39, 2009, doi: 10.1038/nrc2559.

[491] L. Lamalice, F. Le Boeuf, and J. Huot, “Endothelial cell migration during angiogenesis,” *Circ. Res.*, vol. 100, no. 6, pp. 782–794, 2007, doi: 10.1161/01.RES.0000259593.07661.1e.

[492] B. Vanhaesebroeck *et al.*, “Synthesis and function of 3-phosphorylated inositol lipids,” *Annu. Rev. Biochem.*, vol. 70, no. 1, pp. 535–602, 2001.

[493] L. Yang *et al.*, “Akt/protein kinase B signaling inhibitor-2, a selective small molecule inhibitor of Akt signaling with antitumor activity in cancer cells overexpressing Akt,” *Cancer Res.*, vol. 64, no. 13, pp. 4394–4399, 2004, doi: 10.1158/0008-5472.CAN-04-0343.

[494] L. M. Ooms *et al.*, “The Inositol Polyphosphate 5-Phosphatase PIPP Regulates AKT1-Dependent Breast Cancer Growth and Metastasis,” *Cancer Cell*, vol. 28, no. 2, pp. 155–169, 2015, doi: 10.1016/j.ccell.2015.07.003.

[495] S. Ghosh *et al.*, “Inhibition of SHIP2 activity inhibits cell migration and could prevent metastasis in breast cancer cells,” *J. Cell Sci.*, vol. 131, no. 16, 2018, doi: 10.1242/jcs.216408.

[496] B. H. T. Vo, D. Morton, S. Komaragiri, A. C. Millena, C. Leath, and S. A. Khan, “TGF-β effects on prostate cancer cell migration and invasion are mediated by PGE2 through activation of PI3K/AKT/mTOR pathway,” *Endocrinology*, vol. 154, no. 5, pp. 1768–1779, 2013, doi: 10.1210/en.2012-2074.

[497] G. M. Fuhler, G. J. Knol, A. L. Drayer, and E. Vellenga, “Impaired interleukin-8- and GROα-induced phosphorylation of extracellular signal-regulated kinase result in decreased migration of neutrophils from patients with myelodysplasia,” *J. Leukoc. Biol.*, vol. 77, no. 2, pp. 257–266, 2005, doi: 10.1189/jlb.0504306.

[498] S. C. Mills, “Chemokine Signalling in Malignant Cell Migration,” no. May, 2018.

[499] S. Merlot and R. A. Firtel, “Leading the way: Directional sensing through phosphatidylinositol 3-kinase and other signaling pathways,” *J. Cell Sci.*, vol. 116, no. 17, pp. 3471–3478, 2003, doi: 10.1242/jcs.00703.

[500] I. Vivanco and C. L. Sawyers, “The phosphatidylinositol 3-kinase-AKT pathway in humancancer,” *Nat. Rev. Cancer*, vol. 2, no. 7, pp. 489–501, 2002, doi: 10.1038/nrc839.

[501] A. Enomoto *et al.*, “Akt/PKB regulates actin organization and cell motility via girdin/APE,” *Dev. Cell*, vol. 9, no. 3, pp. 389–402, 2005, doi: 10.1016/j.devcel.2005.08.001.

[502] D. Huang, T. Zhou, K. Lafleur, C. Nevado, and A. Caflisch, “Kinase selectivity potential for inhibitors targeting the ATP binding site: A network analysis,” *Bioinformatics*, vol. 26, no. 2, pp. 198–204, 2010, doi: 10.1093/bioinformatics/btp650.

[503] G. Cheng and K. Zygourakis, “Cell migration,” *Tissue Eng.*, vol. 2, no. 4, pp. 77–98, 2007, doi: 10.1201/9781420008333.ch6.

[504] K. Ono and J. Han, “The p38 signal transduction pathway Activation and function,” *Cell. Signal.*, vol. 12, no. 1, pp. 1–13, 2000, doi: 10.1016/S0898-6568(99)00071-6.

[505] G. Keil, “Mapping the intracellular molecular mechanisms of chemokine

signalling within cancer," Doctoral Dissertation, University of East Anglia, 2019.

[506] J. S. Kerr, R. O. Jacques, C. Moyano Cardaba, T. Tse, D. Sexton, and A. Mueller, "Differential regulation of chemotaxis: Role of Gβγ in chemokine receptor-induced cell migration," *Cell. Signal.*, vol. 25, no. 4, pp. 729–735, 2013, doi: 10.1016/j.cellsig.2012.12.015.

[507] S. Liu, R. H. Goldstein, E. M. Scepansky, and M. Rosenblatt, "Inhibition of Rho-associated kinase signaling prevents breast cancer metastasis to human bone," *Cancer Res.*, vol. 69, no. 22, pp. 8742–8751, 2009, doi: 10.1158/0008-5472.CAN-09-1541.

[508] N. Watanabe, T. Kato, A. Fujita, T. Ishizaki, and S. Narumiya, "Cooperation between mDia1 and ROCK in Rho-induced actin reorganization," *Nat. Cell Biol.*, vol. 1, no. 3, pp. 136–143, 1999, doi: 10.1038/11056.

[509] A. Mueller and P. G. Strange, "Mechanisms of internalization and recycling of the chemokine receptor, CCR5," *Eur. J. Biochem.*, vol. 271, no. 2, pp. 243–252, 2004, doi: 10.1046/j.1432-1033.2003.03918.x.

[510] C. M. Ryan *et al.*, "ROCK activity and the Gβγ complex mediate chemotactic migration of mouse bone marrow-derived stromal cells," *Stem Cell Res. Ther.*, vol. 6, no. 1, 2015, doi: 10.1186/s13287-015-0125-y.

[511] A. K. Cross, V. Richardson, S. A. Ali, I. Palmer, D. D. Taub, and R. C. Rees, "Migration responses of human monocytic cell lines to α- and β-chemokines," *Cytokine*, vol. 9, no. 7, pp. 521–528, 1997, doi: 10.1006/cyto.1996.0196.

[512] S. M. Jay, E. Skokos, F. Laiwalla, M. M. Krady, and T. R. Kyriakides, "Foreign body giant cell formation is preceded by lamellipodia formation and can be attenuated by inhibition of Rac1 activation," *Am. J. Pathol.*, vol. 171, no. 2, pp. 632–640, 2007, doi: 10.2353/ajpath.2007.061213.

[513] I. M. Berenjeno, F. Núñez, and X. R. Bustelo, "Transcriptomal profiling of the cellular transformation induced by Rho subfamily GTPases," *Oncogene*, vol. 26, no. 29, pp. 4295–4305, 2007, doi: 10.1038/sj.onc.1210194.

[514] C. Zhang, S. Zhang, Z. Zhang, J. He, Y. Xu, and S. Liu, "ROCK has a crucial role in regulating prostate tumor growth through interaction with c-Myc," *Oncogene*, vol. 33, no. 49, pp. 5582–5591, 2014, doi: 10.1038/onc.2013.505.

[515] K. Riento and A. J. Ridley, "Rocks: Multifunctional kinases in cell behaviour," *Nat. Rev. Mol. Cell Biol.*, vol. 4, no. 6, pp. 446–456, 2003, doi: 10.1038/nrm1128.

[516] W. G. Roberts *et al.*, "Antitumor activity and pharmacology of a selective focal adhesion kinase inhibitor, PF-562,271," *Cancer Res.*, vol. 68, no. 6, pp. 1935–1944, 2008, doi: 10.1158/0008-5472.CAN-07-5155.

[517] K. M. Yamada and S. Even-Ram, "Integrin regulation of growth factor receptors," *Nat. Cell Biol.*, vol. 4, no. 4, 2002, doi: 10.1038/ncb0402-e75.

[518] L. L. Remsing Rix *et al.*, "Global target profile of the kinase inhibitor bosutinib in primary chronic myeloid leukemia cells," *Leukemia*, vol. 23, no. 3, pp. 477–485, 2009, doi: 10.1038/leu.2008.334.

[519] R. O. Jacques, "Pharmacological insights into C-C motif chemokine receptor 5 mediated chemotaxis," *Univ. East Angl.*, 2013, [Online]. Available: https://ueaeprints.uea.ac.uk/42415/1/2013JacquesROPhD.pdf.

[520] S. Bieerkehazhi *et al.*, “Novel Src/Abl tyrosine kinase inhibitor bosutinib suppresses neuroblastoma growth via inhibiting Src/Abl signaling,” *Oncotarget*, vol. 8, no. 1, pp. 1469–1480, 2017, doi: 10.18632/oncotarget.13643.

[521] L. Yu *et al.*, “Bosutinib Acts as a Tumor Inhibitor via Downregulating Src/NF-κB/Survivin Expression in HeLa Cells,” *Anat. Rec.*, vol. 302, no. 12, pp. 2193–2200, 2019, doi: 10.1002/ar.24269.

[522] S. J. Humphrey, D. E. James, and M. Mann, “Protein Phosphorylation: A Major Switch Mechanism for Metabolic Regulation,” *Trends Endocrinol. Metab.*, vol. 26, no. 12, pp. 676–687, 2015, doi: 10.1016/j.tem.2015.09.013.

[523] J. S. Lee, W. S. Kwon, M. S. Rahman, S. J. Yoon, Y. J. Park, and M. G. Pang, “Actin-related protein 2/3 complex-based actin polymerization is critical for male fertility,” *Andrology*, vol. 3, no. 5, pp. 937–946, 2015, doi: 10.1111/andr.12076.

[524] T. Eiseler, A. Hausser, L. De Kimpe, J. Van Lint, and K. Pfizenmaier, “Protein kinase D controls actin polymerization and cell motility through phosphorylation of cortactin,” *J. Biol. Chem.*, vol. 285, no. 24, pp. 18672–18683, 2010, doi: 10.1074/jbc.M109.093880.

[525] J. Chen, F. Deng, S. V. Singh, and Q. J. Wang, “Protein kinase D3 (PKD3) contributes to prostate cancer cell growth and survival through a PKCε/PKD3 pathway downstream of Akt and ERK 1/2,” *Cancer Res.*, vol. 68, no. 10, pp. 3844–3853, 2008, doi: 10.1158/0008-5472.CAN-07-5156.

[526] Z. Liu *et al.*, “Expression of the Arp2/3 complex in human gliomas and its role in the migration and invasion of glioma cells,” *Oncol. Rep.*, vol. 30, no. 5, pp. 2127–2136, 2013, doi: 10.3892/or.2013.2669.

[527] F. Wang, P. Herzmark, O. D. Weiner, S. Srinivasan, G. Servant, and H. R. Bourne, “Lipid products of PI(3)Ks maintain persistent cell polarity and directed motility in neutrophils,” *Nat. Cell Biol.*, vol. 4, no. 7, pp. 513–518, 2002, doi: 10.1038/ncb810.

[528] C. Y. Chung, S. Funamoto, and R. A. Firtel, “Signaling pathways controlling cell polarity and chemotaxis,” *Trends Biochem. Sci.*, vol. 26, no. 9, pp. 557–566, 2001, doi: 10.1016/S0968-0004(01)01934-X.

[529] D. Chodniewicz and D. V. Zhelev, “Chemoattractant receptor-stimulated F-actin polymerization in the human neutrophil is signaled by 2 distinct pathways,” *Blood*, vol. 101, no. 3, pp. 1181–1184, 2003, doi: 10.1182/blood-2002-05-1435.

[530] J.-A. Montero, B. Kilian, J. Chan, P. E. Bayliss, and C.-P. Heisenberg, “Phosphoinositide 3-Kinase Is Required for Process Outgrowth and Cell Polarization of Gastrulating Mesendodermal Cells,” *Curr. Biol.*, vol. 13, no. August, pp. 1279–1289, 2003, doi: 10.1016/S.

[531] S. Wennström *et al.*, “Activation of phosphoinositide 3-kinase is required for PDGF-stimulated membrane ruffling,” *Curr. Biol.*, vol. 4, no. 5, pp. 385–393, 1994, doi: 10.1016/S0960-9822(00)00087-7.

[532] Y. Lai, Y. Shen, X. H. Liu, Y. Zhang, Y. Zeng, and Y. F. Liu, “Interleukin-8 induces the endothelial cell migration through the activation of phosphoinositide 3-kinase-Rac1/RhoA pathway,” *Int. J. Biol. Sci.*, vol. 7, no. 6, pp. 782–791, 2011, doi: 10.7150/ijbs.7.782.

[533] Y. Qian *et al.*, “PI3K induced actin filament remodeling through Akt and p70S6K1: Implication of essential role in cell migration,” *Am. J. Physiol. - Cell Physiol.*, vol. 286, no. 1 55-1, pp. 153–163, 2004, doi: 10.1152/ajpcell.00142.2003.

[534] M. Morales-Ruiz *et al.*, “Vascular endothelial growth factor-stimulated actin reorganization and migration of endothelial cells is regulated via the serine/threonine kinase Akt,” *Circ. Res.*, vol. 86, no. 8, pp. 892–896, 2000, doi: 10.1161/01.RES.86.8.892.

[535] M. Higuchi, N. Masuyama, Y. Fukui, A. Suzuki, and Y. Gotoh, “Akt mediates Rac/Cdc42-regulated cell motility in growth factor-stimulated cells and in invasive PTEN knockout cells,” *Curr. Biol.*, vol. 11, no. 24, pp. 1958–1962, 2001, doi: 10.1016/S0960-9822(01)00599-1.

[536] V. Kansra, C. Groves, J. C. Gutierrez-Ramos, and R. D. Polakiewicz, “Phosphatidylinositol 3-Kinase-dependent Extracellular Calcium Influx Is Essential for CX3CR1-mediated Activation of the Mitogen-activated Protein Kinase Cascade,” *J. Biol. Chem.*, vol. 276, no. 34, pp. 31831–31838, 2001, doi: 10.1074/jbc.M009374200.

[537] D. F. Heigener, D. R. Gandara, and M. Reck, “Targeting of MEK in lung cancer therapeutics,” *Lancet Respir. Med.*, vol. 3, no. 4, pp. 319–327, 2015, doi: 10.1016/S2213-2600(15)00026-0.

[538] C. Neuzillet, A. Tijeras-Raballand, L. De Mestier, J. Cros, S. Faivre, and E. Raymond, “MEK in cancer and cancer therapy,” *Pharmacol. Ther.*, vol. 141, no. 2, pp. 160–171, 2014, doi: 10.1016/j.pharmthera.2013.10.001.

[539] K. P. Hoeflich *et al.*, “Oncogenic BRAF is required for tumor growth and maintenance in melanoma models,” *Cancer Res.*, vol. 66, no. 2, pp. 999–1006, 2006, doi: 10.1158/0008-5472.CAN-05-2720.

[540] H. Davies *et al.*, “Mutations of the BRAF gene in human cancer,” *Nature*, vol. 417, no. 6892, pp. 949–954, 2002, doi: 10.1038/nature00766.

[541] S. Lourenco, V. H. Teixeira, T. Kalber, R. J. Jose, R. A. Floto, and S. M. Janes, “Macrophage Migration Inhibitory Factor–CXCR4 Is the Dominant Chemotactic Axis in Human Mesenchymal Stem Cell Recruitment to Tumors,” *J. Immunol.*, vol. 194, no. 7, pp. 3463–3474, 2015, doi: 10.4049/jimmunol.1402097.

[542] Y. Zhou *et al.*, “MEK inhibitor effective against proliferation in breast cancer cell,” *Tumor Biol.*, vol. 35, no. 9, pp. 9269–9279, 2014, doi: 10.1007/s13277-014-1901-5.

[543] J. Ye, A. Li, Q. Liu, X. Wang, and J. Zhou, “Inhibition of mitogen-activated protein kinase kinase enhances apoptosis induced by arsenic trioxide in human breast cancer MCF-7 cells,” *Clin. Exp. Pharmacol. Physiol.*, vol. 32, no. 12, pp. 1042–1048, 2005, doi: 10.1111/j.1440-1681.2005.04302.x.

[544] Y. Zhao *et al.*, “MEK inhibitor, PD98059, promotes breast cancer cell migrationby inducing β-catenin nuclear accumulation,” *Oncol. Rep.*, vol. 38, no. 5, pp. 3055–3063, 2017, doi: 10.3892/or.2017.5955.

[545] H. J. Bian *et al.*, “MAPK/p38 regulation of cytoskeleton rearrangement accelerates induction of macrophage activation by TLR4, but not TLR3,” *Int. J. Mol. Med.*, vol. 40, no. 5, pp. 1495–1503, 2017, doi: 10.3892/ijmm.2017.3143.

[546] A. J. Ridley, “Rho GTPases and cell migration,” *J Cell Sci*, vol. 114, no. Pt 15, pp. 2713–2722, 2001, doi: 10.1083/jcb.150.4.807.

[547] D. Bar-Sagi and A. Hall, “Ras and Rho GTPases: A family reunion,” *Cell*, vol. 103, no. 2, pp. 227–238, 2000, doi: 10.1016/S0092-8674(00)00115-X.

[548] B. Boettner and L. Van Aelst, “The role of Rho GTPases in disease development,” *Gene*, vol. 286, no. 2, pp. 155–174, 2002, doi: 10.1016/S0378-1119(02)00426-2.

[549] J. Monypenny, D. Zicha, C. Higashida, F. Oceguera-Yanez, S. Narumiya, and N. Watanabe, “Cdc42 and Rac Family GTPases Regulate Mode and Speed but Not Direction of Primary Fibroblast Migration during Platelet-Derived Growth Factor-Dependent Chemotaxis,” *Mol. Cell. Biol.*, vol. 29, no. 10, pp. 2730–2747, 2009, doi: 10.1128/mcb.01285-08.

[550] A. J. Ridley, “Membrane ruffling and signal transduction.,” *BioEssays*, vol. 16, no. 5, pp. 321–327, 1994.

[551] Y. Gao, J. B. Dickerson, F. Guo, J. Zheng, and Y. Zheng, “Rational design and characterization of a Rac GTPase-specific small molecule inhibitor,” *Proc. Natl. Acad. Sci.*, vol. 101, no. 20, pp. 7618–7623, 2004, doi: 10.1073/pnas.0307512101.

[552] E. Hernández, A. De La Mota-Peynado, S. Dharmawardhane, and C. Vlaar, “Novel inhibitors of Rac1 in metastatic breast cancer,” *P. R. Health Sci. J.*, vol. 29, no. 4, pp. 348–356, 2010.

[553] A. Baier, V. N. E. Ndoh, P. Lacy, and G. Eitzen, “Rac1 and Rac2 control distinct events during antigen-stimulated mast cell exocytosis,” *J. Leukoc. Biol.*, vol. 95, no. 5, pp. 763–774, 2014, doi: 10.1189/jlb.0513281.

[554] T. J. Mitchison and L. P. Cramer, “Actin-based cell motility and cell locomotion,” *Cell*, vol. 84, no. 3, pp. 371–379, 1996, doi: 10.1016/S0092-8674(00)81281-7.

[555] Y. Fallah, J. Brundage, P. Allegakoen, and A. N. Shajahan-Haq, “MYC-Driven pathways in breast cancer subtypes,” *Biomolecules*, vol. 7, no. 3, pp. 1–6, 2017, doi: 10.3390/biom7030053.

[556] A. V. Somlyo, D. Bradshaw, S. Ramos, C. Murphy, C. E. Myers, and A. P. Somlyo, “Rho-kinase inhibitor retards migration and in vivo dissemination of human prostate cancer cells,” *Biochem. Biophys. Res. Commun.*, vol. 269, no. 3, pp. 652–659, 2000, doi: 10.1006/bbrc.2000.2343.

[557] C. R. Evelyn *et al.*, “CCG-1423: A small-molecule inhibitor of RhoA transcriptional signaling,” *Mol. Cancer Ther.*, vol. 6, no. 8, pp. 2249–2260, 2007, doi: 10.1158/1535-7163.MCT-06-0782.

[558] A. Nishikimi *et al.*, “Blockade of inflammatory responses by a small-molecule inhibitor of the Rac activator DOCK2,” *Chem. Biol.*, vol. 19, no. 4, pp. 488–497, 2012, doi: 10.1016/j.chembiol.2012.03.008.

[559] J. B. Stokes *et al.*, “Inhibition of focal adhesion kinase by PF-562,271 inhibits the growth and metastasis of pancreatic cancer concomitant with altering the tumor microenvironment,” *Mol. Cancer Ther.*, vol. 10, no. 11, pp. 2135–2145, 2011, doi: 10.1158/1535-7163.MCT-11-0261.

[560] C. Hu *et al.*, “Antitumor effect of focal adhesion kinase inhibitor PF562271 against human osteosarcoma in vitro and in vivo,” *Cancer Sci.*, vol. 108, no.

7, pp. 1347–1356, 2017, doi: 10.1111/cas.13256.

[561] S. Tehrani, N. Tomasevic, S. Weed, R. Sakowicz, and J. A. Cooper, “Src phosphorylation of cortactin enhances actin assembly,” *Proc. Natl. Acad. Sci. U. S. A.*, vol. 104, no. 29, pp. 11933–11938, 2007, doi: 10.1073/pnas.0701077104.

[562] A. Lochner and J. A. Moolman, “The many faces of H89: A review,” *Cardiovasc. Drug Rev.*, vol. 24, no. 3–4, pp. 261–274, 2006, doi: 10.1111/j.1527-3466.2006.00261.x.

[563] K. Limbutara, A. Kelleher, C. R. Yang, V. Raghuram, and M. A. Knepper, “Phosphorylation Changes in Response to Kinase Inhibitor H89 in PKA-Null Cells,” *Sci. Rep.*, vol. 9, no. 1, pp. 1–10, 2019, doi: 10.1038/s41598-019-39116-2.

[564] S. P. Davies, H. Reddy, M. Caivano, and P. Cohen, “Specificity and mechanism of action of some commonly used protein kinase inhibitors,” *Biochem. J.*, vol. 351, no. 1, pp. 95–105, 2000, doi: 10.1517/13543776.11.3.405.

[565] J. Leemhuis, S. Boutillier, G. Schmidt, and D. K. Meyer, “The protein kinase A inhibitor H89 acts on cell morphology by inhibiting Rho kinase,” *J. Pharmacol. Exp. Ther.*, vol. 300, no. 3, pp. 1000–1007, 2002, doi: 10.1124/jpet.300.3.1000.

[566] L. Zhang, Y. Xu, J. Xu, Y. Wei, and X. Xu, “Protein kinase A inhibitor, H89, enhances survival and clonogenicity of dissociated human embryonic stem cells through Rho-associated coiled-coil containing protein kinase (ROCK) inhibition,” *Hum. Reprod.*, vol. 31, no. 4, pp. 832–843, 2016, doi: 10.1093/humrep/dew011.

[567] Y. Gao and Y. Gao, “Cyclic AMP Signaling,” *Biol. Vasc. Smooth Muscle Vasoconstriction Dilatation*, pp. 169–180, 2017, doi: 10.1007/978-981-10-4810-4_13.

[568] A. J. Murray, “Pharmacological PKA inhibition: All may not be what it seems,” *Sci. Signal.*, vol. 1, no. 22, pp. 1–7, 2008, doi: 10.1126/scisignal.122re4.

[569] J. H. Iwasa and R. D. Mullins, “Spatial and Temporal Relationships between Actin-Filament Nucleation, Capping, and Disassembly,” *Curr. Biol.*, vol. 17, no. 5, pp. 395–406, 2007, doi: 10.1016/j.cub.2007.02.012.

[570] D. V. Ilatovskaya *et al.*, “Arp2/3 complex inhibitors adversely affect actin cytoskeleton remodeling in the cultured murine kidney collecting duct M-1 cells,” *Cell Tissue Res.*, vol. 354, no. 3, pp. 783–792, 2013, doi: 10.1161/CIRCULATIONAHA.110.956839.

[571] A. Tarafdar and A. M. Michie, “Protein kinase C in cellular transformation: A valid target for therapy?,” *Biochem. Soc. Trans.*, vol. 42, no. 6, pp. 1556–1562, 2014, doi: 10.1042/BST20140255.

[572] N. Bacher, Y. Zisman, E. Berent, and E. Livneh, “Isolation and characterization of PKC-L, a new member of the protein kinase C-related gene family specifically expressed in lung, skin, and heart.:,” *Mol. Cell. Biol.*, vol. 12, no. 3, p. 1404.1, 1992, doi: 10.1128/mcb.12.3.1404-a.

[573] W. S. Liu and C. A. Heckman, “The sevenfold way of PKC regulation,” *Cell. Signal.*, vol. 10, no. 8, pp. 529–542, 1998, doi: 10.1016/S0898-

6568(98)00012-6.

[574] N. Thuille *et al.*, “PKCθ/β and CYLD Are Antagonistic Partners in the NFκB and NFAT Transactivation Pathways in Primary Mouse CD3+ T Lymphocytes,” *PLoS One*, vol. 8, no. 1, pp. 1–13, 2013, doi: 10.1371/journal.pone.0053709.

[575] L. N. Christina, T. Nikolaus, W. Katarzyna, G. Thomas, L. Michael, and B. Gottfried, “PKCα and PKCβ cooperate functionally in CD3-induced de novo IL-2 mRNA transcription,” *Immunol. Lett.*, vol. 151, no. 1–2, pp. 31–38, 2013, doi: 10.1016/j.imlet.2013.02.002.

[576] J.-H. Kang, “Protein Kinase C (PKC) Isozymes and Cancer,” *New J. Sci.*, vol. 2014, pp. 1–36, 2014, doi: 10.1155/2014/231418.

[577] A. X. Wu-Zhang and A. C. Newton, “Protein kinase C pharmacology: Refining the toolbox,” *Biochem. J.*, vol. 452, no. 2, pp. 195–209, 2013, doi: 10.1042/BJ20130220.

[578] L. Goldberg-Bittman *et al.*, “The expression of the chemokine receptor CXCR3 and its ligand, CXCL10, in human breast adenocarcinoma cell lines,” *Immunol. Lett.*, vol. 92, no. 1–2, pp. 171–178, 2004, doi: 10.1016/j.imlet.2003.10.020.

[579] S. Tavares *et al.*, “Actin stress fiber organization promotes cell stiffening and proliferation of pre-invasive breast cancer cells,” *Nat. Commun.*, vol. 8, no. May, 2017, doi: 10.1038/ncomms15237.

[580] T. Togo, J. M. Alderton, and R. A. Steinhardt, “The mechanism of cell membrane repair,” *Zygote*, vol. 8, no. S1, pp. S31–S32, 1999, doi: 10.1017/s096719940013014x.

[581] M. Furuya *et al.*, “Differential expression patterns of CXCR3 variants and corresponding CXC chemokines in clear cell ovarian cancers and endometriosis,” *Gynecol. Oncol.*, vol. 122, no. 3, pp. 648–655, 2011, doi: 10.1016/j.ygyno.2011.05.034.

[582] R. Singh, J. W. Lilladr, and S. Singh, “Chemokines: Key players in cancer progression and metastasis,” *Front. Biosci. - Sch.*, vol. 3 S, no. 4, pp. 1569–1582, 2011, doi: 10.2741/s246.

[583] T. Suyama *et al.*, “Up-regulation of the interferon γ (IFN-γ)-inducible chemokines IFN-inducible T-cell α chemoattractant and monokine induced by IFN-γ and of their receptor CXC receptor 3 in human renal cell carcinoma,” *Cancer*, vol. 103, no. 2, pp. 258–267, 2005, doi: 10.1002/cncr.20747.

[584] H. Guo *et al.*, “Pivotal Advance: PKCζ is required for migration of macrophages,” *J. Leukoc. Biol.*, vol. 85, no. 6, pp. 911–918, Jun. 2009, doi: 10.1189/jlb.0708429.

[585] Y. Liu *et al.*, “Down-regulation of PKCζ expression inhibits chemotaxis signal transduction in human lung cancer cells,” *Lung Cancer*, vol. 63, no. 2, pp. 210–218, 2009, doi: 10.1016/j.lungcan.2008.05.010.

[586] W. Brenner *et al.*, “Migration of renal carcinoma cells is dependent on protein kinase Cδ via β1 integrin and focal adhesion kinase,” *Int. J. Oncol.*, vol. 32, no. 5, pp. 1125–1131, 2008, doi: 10.3892/ijo.32.5.1125.

[587] J.-Y. Chuang *et al.*, “CCL5/CCR5 axis promotes the motility of human oral cancer cells,” *J. Cell. Physiol.*, vol. 220, no. 2, pp. 418–426, Aug. 2009, doi:

10.1002/jcp.21783.

[588] Q. Pan *et al.*, “Protein kinase Cε is a predictive biomarker of aggressive breast cancer and a validated target for RNA interference anticancer therapy,” *Cancer Res.*, vol. 65, no. 18, pp. 8366–8371, 2005, doi: 10.1158/0008-5472.CAN-05-0553.

[589] K. Jain and A. Basu, “Protein kinase C-ε promotes EMT in breast cancer,” *Breast Cancer Basic Clin. Res.*, vol. 8, no. 1, pp. 61–67, 2014, doi: 10.4137/BCBCR.S13640.

[590] C. Keenan and D. Kelleher, “Protein kinase C and the cytoskeleton,” *Cell. Signal.*, vol. 10, no. 4, pp. 225–232, 1998, doi: 10.1016/S0898-6568(97)00121-6.

[591] E. J. Quann, X. Liu, G. Altan-Bonnet, and M. Huse, “A Cascade of Protein Kinase C Isozymes Promotes Cytoskeletal Polarization in T Cells,” *Nat. Immunol.*, vol. 176, no. 5, pp. 139–148, 2011, doi: 10.1016/j.physbeh.2017.03.040.

[592] S. D. Tachado *et al.*, “Regulation of tumor invasion and metastasis in protein kinase C epsilon-transformed NIH3T3 fibroblasts,” *J. Cell. Biochem.*, vol. 85, no. 4, pp. 785–797, 2002, doi: 10.1002/jcb.10164.

[593] D. Brandt, M. Gimona, M. Hillmann, H. Haller, and H. Mischak, “Protein kinase C induces actin reorganization via a Src- and Rho-dependent pathway,” *J. Biol. Chem.*, vol. 277, no. 23, pp. 20903–20910, 2002, doi: 10.1074/jbc.M200946200.

[594] M. H. Aziz *et al.*, “Protein kinase C mediates Stat3Ser727 phosphorylation, Stat3-regulated gene expression, and cell invasion in various human cancer cell lines through integration with MAPK cascade (RAF-1, MEK1/2, and ERK1/2),” *Oncogene*, vol. 29, no. 21, pp. 3100–3109, 2010, doi: 10.1038/onc.2010.63.

[595] M. Nakanishi, R. Teshima, H. Ikebuchi, and T. Terao, “The Effect of Staurosporine on Ca2+ Signals in Rat Basophilic Leukemia (RBL-2H3) Cells,” *Chem. Pharm. Bull.*, vol. 39, no. 3, pp. 747–751, 1991, doi: 10.1248/cpb.39.747.

[596] H. Sipma, L. Van Der Zee, J. Van Den Akker, A. Den Hertog, and A. Nelemans, “The effect of the PKC inhibitor GF109203X on the release of Ca2+ from internal stores and Ca2+ entry in DDT1 MF-2 cells,” *Br. J. Pharmacol.*, vol. 119, no. 4, pp. 730–736, 1996, doi: 10.1111/j.1476-5381.1996.tb15733.x.

[597] M. Holinstat, D. Mehta, T. Kozasa, R. D. Minshall, and A. B. Malik, “Protein kinase Cα-induced p115RhoGEF phosphorylation signals endothelial cytoskeletal rearrangement,” *J. Biol. Chem.*, vol. 278, no. 31, pp. 28793–28798, 2003, doi: 10.1074/jbc.M303900200.

[598] M. Rumsby, J. Schmitt, M. Sharrard, G. Rodrigues, M. Stower, and N. Maitland, “Human prostate cell lines from normal and tumourigenic epithelia differ in the pattern and control of choline lipid headgroups released into the medium on stimulation of protein kinase C,” *Br. J. Cancer*, vol. 104, no. 4, pp. 673–684, 2011, doi: 10.1038/sj.bjc.6606077.

[599] C. A. O’Brian, N. E. Ward, V. G. Vogel, and S. E. Singletary, “Elevated Protein Kinase C Expression in Human Breast Tumor Biopsies Relative to

Normal Breast Tissue," *Cancer Res.*, vol. 49, no. 12, pp. 3215–3217, 1989.

[600] M. Olguín-Albuerne, G. Domínguez, and J. Morán, "Effect of staurosporine in the morphology and viability of cerebellar astrocytes: Role of reactive oxygen species and NADPH oxidase," *Oxid. Med. Cell. Longev.*, vol. 2014, 2014, doi: 10.1155/2014/678371.

[601] K. Abe, M. Yoshida, T. Usui, S. Horinouchi, and T. Beppu, "Highly synchronous culture of fibroblasts from G2 block caused by staurosporine, a potent inhibitor of protein kinases," *Exp. Cell Res.*, vol. 192, no. 1, pp. 122–127, 1991, doi: 10.1016/0014-4827(91)90166-R.

[602] T. Oikawa *et al.*, "Inhibition of angiogenesis by staurosporine, a potent protein kinase inhibitor," *J. Antibiot. (Tokyo).*, vol. 45, no. 7, pp. 1155–1160, 1992, doi: 10.7164/antibiotics.45.1155.

[603] K. K. Hedberg, G. B. Birrell, D. L. Habliston, and O. H. Griffith, "Staurosporine induces dissolution of microfilament bundles by a protein kinase C-independent pathway," *Exp. Cell Res.*, vol. 188, no. 2, pp. 199–208, 1990, doi: 10.1016/0014-4827(90)90160-C.

[604] P. Cornford *et al.*, "Protein kinase C isoenzyme patterns characteristically modulated in early prostate cancer," *Am. J. Pathol.*, vol. 154, no. 1, pp. 137–144, 1999, doi: 10.1016/S0002-9440(10)65260-1.

[605] A. F. Schott *et al.*, "A phase Ib study of the CXCR1/2 inhibitor Reparixin in combination with weekly paclitaxel in metastatic HER2 negative breast cancer - final analysis," in *Molecular Cancer Therapeutics*, 2015, vol. TARG-15-C2.

[606] P. A. Ruffini, "The CXCL8-CXCR1/2 Axis as a Therapeutic Target in Breast Cancer Stem-Like Cells," *Front. Oncol.*, vol. 9, no. February, pp. 1–4, 2019, doi: 10.3389/fonc.2019.00040.

[607] M. J. Smit *et al.*, "CXCR3-mediated chemotaxis of human T cells is regulated by a G i-and phospholipase C-dependent pathway and not via activation of MEK/p44/p42 MAPK nor Akt/PI-3 kinase," *Blood*, vol. 102, no. 6, pp. 1959–1965, 2003, doi: 10.1182/blood-2002-12-3945.

[608] A. P. Curnock, Y. Sotsios, K. L. Wright, and S. G. Ward, "Optimal Chemotactic Responses of Leukemic T Cells to Stromal Cell-Derived Factor-1 Requires the Activation of Both Class IA and IB Phosphoinositide 3-Kinases," *J. Immunol.*, vol. 170, no. 8, pp. 4021–4030, 2003, doi: 10.4049/jimmunol.170.8.4021.

[609] D. Mochly-rosen, K. Das, and K. V Grimes, "Protein kinase C , an elusive therapeutic target ?," *Nat. Rev. Drug Discov.*, vol. 11, no. December, 2012, doi: 10.1038/nrd3871.

[610] Y. Mu, G. Zang, U. Engström, C. Busch, and M. Landström, "TGFβ-induced phosphorylation of Par6 promotes migration and invasion in prostate cancer cells," *Br. J. Cancer*, vol. 112, no. 7, pp. 1223–1231, 2015, doi: 10.1038/bjc.2015.71.

[611] S. Kuroda, N. Nakagawa, C. Tokunaga, K. Tatematsu, and K. Tanizawa, "Mammalian Homologue of the Caenorhabditis elegans UNC-76 Protein Involved in Axonal Outgrowth Is a Protein Kinase C zeta –interacting Protein," *J. Cell Biol.*, vol. 144, no. 3, pp. 403–412, 1999.

[612] G. Zang, Y. Mu, L. Gao, A. Bergh, and M. Landström, “PKCζ facilitates lymphatic metastatic spread of prostate cancer cells in a mice xenograft model,” *Oncogene*, vol. 38, no. 22, pp. 4215–4231, 2019, doi: 10.1038/s41388-019-0722-9.

[613] S. Yao *et al.*, “Prkc-ζ expression promotes the aggressive phenotype of human prostate cancer cells and is a novel target for therapeutic intervention,” *Genes and Cancer*, vol. 1, no. 5, pp. 444–464, 2010, doi: 10.1177/1947601910376079.

[614] R. Sun *et al.*, “Protein kinase C ζ is required for epidermal growth factor-induced chemotaxis of human breast cancer cells,” *Cancer Res.*, vol. 65, no. 4, pp. 1433–1441, 2005, doi: 10.1158/0008-5472.CAN-04-1163.

[615] S. Huang *et al.*, “HGF-induced PKCζ activation increases functional CXCR4 expression in human breast cancer cells,” *PLoS One*, vol. 7, no. 1, 2012, doi: 10.1371/journal.pone.0029124.

[616] A. Kuett *et al.*, “IL-8 as mediator in the microenvironment-leukaemia network in acute myeloid leukaemia,” *Sci. Rep.*, vol. 5, no. November, pp. 1–11, 2015, doi: 10.1038/srep18411.

[617] C. Yao *et al.*, “Interleukin-8 modulates growth and invasiveness of estrogen receptor-negative breast cancer cells,” *Int. J. Cancer*, vol. 121, no. 9, pp. 1949–1957, 2007, doi: 10.1002/ijc.22930.

[618] L.-F. Lee *et al.*, “IL-8 Reduced Tumorigenicity of Human Ovarian Cancer In Vivo Due to Neutrophil Infiltration,” *J. Immunol.*, vol. 164, no. 5, pp. 2769–2775, 2000, doi: 10.4049/jimmunol.164.5.2769.